Photoinduced Electron Transfer: Synthetic Models of the Primary Processes in Photosynthesis

Thesis by

Burton Alan Leland

In Partial Fulfillment of the Requirements

for the Degree of

Doctor of Philosophy

California Institute of Technology

Pasadena, California

1987

(submitted November 12, 1986)

In Memory of
Jeffrey Scott

Acknowledgments

It is a pleasure to acknowledge the abounding support and enthusiasm of my advisors Peter Dervan, and John Hopfield. Their interest in the field provided the impetus for this research, and it was an enjoyable experience to collaborate with them.

I would like to acknowledge Alvin Joran, without whose synthetic tenacity might have terminated this research before its full fruition. I am especially grateful to Al Sylwester for his eagerness and curiosity for science. He was always a source of encouragement when nothing seemed to work. Special thanks go to my bioorganic tutor, Scott Youngquist, for helpful discussions, critical distractions, and unique perspective on life that helped me through many a trying time. I am also indebted to Jim Sluka for programming consultations, TEXpert aid, and a car loan at a critical time during interview season. Thanks also to Dave Beratan and Jose Onuchic for helpful theory consultations. I would also pay particular thanks to Jim Hanson for boldly going where no man has gone before with this research (live long and prosper). Many other individuals both within and beyond the Dervan group unknowingly helped me through many a dark time and for that I am grateful.

Thanks go to Peter Felker, Spencer Baskin, and Marcos Dantus who lended expert technical assistance in the picosecond fluorescence lifetime studies in the

laboratories of A.H. Zewail. The assistance of Janet Marshall and Andy Axup of the H.B. Gray group for help in the steady–state emission, and the phosphorescence lifetime investigations was much appreciated. Thanks also to members of the F.C. Anson group for electrochemical consultations. Special thanks for the unpleasant proofreading task and critical improvements go to Scott Youngquist, Dave Beratan, Jose Onuchic, and Warren Wade. The help and encouragment from my wife, Pam, are greatly appreciated during these times in which I was so difficult to tolerate. We are especially grateful to all of our Caltech friends for their thoughts and prayers as a result of our unfortunate loss.

This research was supported by the National Science Foundation.

Abstract

A general synthetic method is presented for the preparation of a series of *meso*–phenyloctamethylporphyrin–linker–quinone compounds for investigation of intramolecular photoinduced electron transfer rates by picosecond fluorescence spectroscopy. Distance effects were investigated through the incorporation of zero, one, or two bicyclo[2.2.2]octyl linker units separating the porphyrin and quinone. Addition of one bicyclo[2.2.2]octyl linker decreases k_{ET} by at least a full order of magnitude. The addition of a second bicyclo[2.2.2]octyl linker unit decreases the electron transfer rate by 500 to $\geq$1700. Investigation of solvent effects on the electron transfer rate, as obtained from the picosecond fluorescence lifetimes of the compounds, indicate weak solvent dependencies as expected for electron transfer from a neutral initial state. Conversely, dramatic solvent dependencies are expected for the back transfer rates in these compounds. Investigation of temperature effects on the electron transfer rate revealed a relatively temperature insensitive electron transfer rate (nuclear tunneling). This is the first synthetic porphyrin–quinone compound to date to exhibit electron transfer quenching at low temperatures. The nonexponential emission decays of samples at 77K in frozen solvent matrices are proposed to arise from an ensemble of rotational conformations between the porphyrin donor and the benzoquinone acceptor, which is well described by an angle–modulated decay analysis. The dependence of k_{ET} on

the precise geometric orientation of the donor and acceptor reinforces the nonadiabatic nature of these transfers. Exothermicity effects for a structurally homologous series of porphyrin–benzoquinones prepared by the general synthetic method in four solvents of varying polarity indicate large changes in the electron transfer rate with small changes in the driving force at low exothermicities, followed by a relatively ΔG° insensitive region. At the highest exothermicity case studied, a modest decrease in the electron transfer rate was observed. No dramatic evidence for the inverted region was observed for the photoinduced electron transfer from the porphyrin excited singlet transfer to the quinone acceptor over the range of exothermicity studied ($0.5 \leq \Delta G^\circ_{rel} \leq 1.1$ eV (benzene)). A comparison of the results with classical and semiclassical theories is presented.

Table of Contents *page*

List of Figures *page*

Chapter 1

Chapter 2

Chapter 3

Chapter 7

List of Schemes *page*

Chapter 1

Chapter 3

Chapter 4

List of Tables *page*

Chapter 4

Chapter 5

Chapter 1

Introduction

Introduction

The conversion of solar energy to chemical energy is an exceedingly critical electron transfer (ET) pathway which is the major input of energy into the biosphere. The process of photosynthesis requires the input of light–energy, carbon dioxide, and an oxidizable substrate. Green plants, algae, and cyanobacteria utilize water as the oxidizable substrate producing oxygen and reducing carbon dioxide to carbohydrates in the presence of chlorophyll and light.[1, 2]

$$CO_2 + 2H_2O \xrightarrow[\text{chlorophyll}]{h\nu} (CH_2O) + O_2 + H_2O + 112 \text{ kcal/mole}$$

Other bacteria capable of photosynthesis substitute sources other than water for their reducing equivalents, such as hydrogen sulfide, various other sulfur compounds, or organic compounds.[2] The general requirement of an alternative substrate to water distinguishes the bacterial photosynthetic process from the higher plants.

The functional apparatus of a photosynthetic organism, collectively called the photosystem (PS), consists of light harvesting components, specialized assemblies of proteins and prosthetic groups called reaction centers (RCs), a host of chemical intermediates, and the structural protein and membrane components and is shown

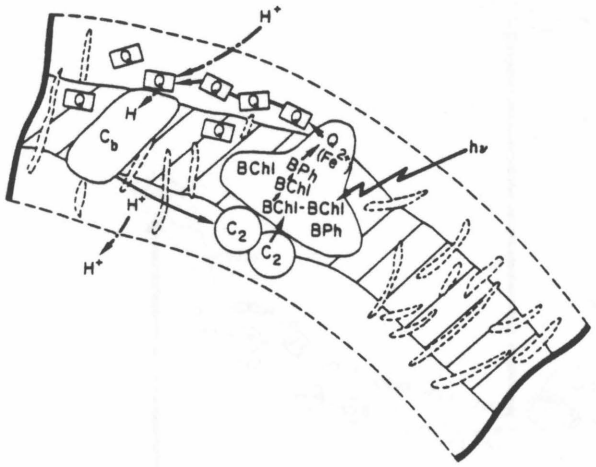

Figure 1. Schematic representation of *in vivo* bacterial reaction centers (from reference 1, p. 86, Figure 4).

schematically in Figure 1. The higher plants utilize a coupled dual photosystem arrangement termed photosystem I (PS I) and photosystem II (PS II). The general scheme for this arrangement (Figure 2) is called the Z scheme.[3,4] Photosystem I is designated as P700, indicating light–induced absorbance changes at 700 nm, and the analogous designation of PS II is P680. P700 is the primary electron donor in the photochemical activity of PS I,[5] and shows reversible photooxidation behavior upon red light exposure. Excitation of PS II (P680) reaction center yields the oxidized $P680^+$, which is subsequently reduced by electrons from water oxidation. Similarly, excitation of PS I (P700) gives rise to $P700^+$ which is reduced via an intersystem electron transport chain from PS II.[6]

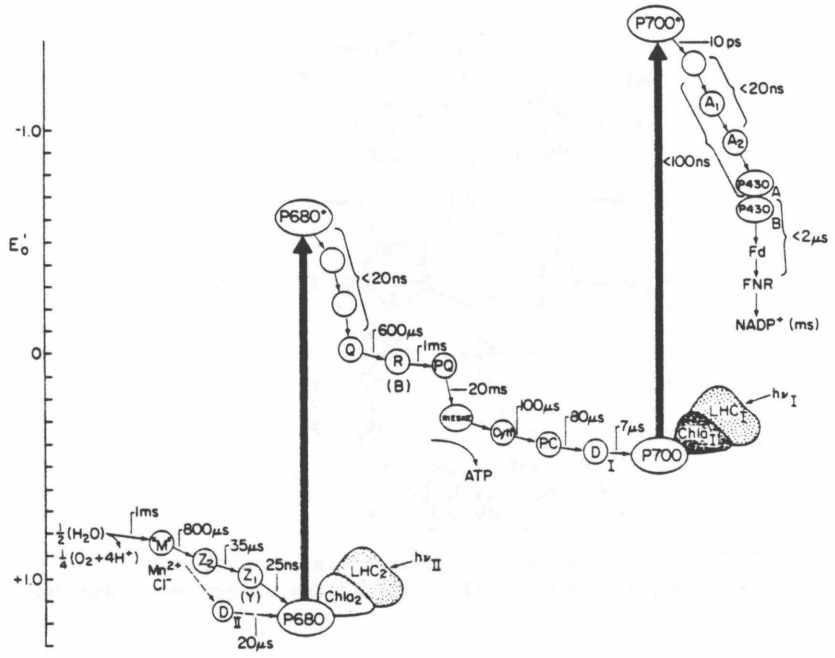

Figure 2. Z scheme of photosynthetic electron transport (from reference 1, p. 13, Figure 3).

It has long been known that the reactions of oxygen–evolving photosystems have been of two types, those activated by photons (light reactions) and those which occur in the absence of light (dark reactions).[6] The light reactions involve the intermediacy of a series of oxidation–reduction components forming the electron–transport chain, and occur in the RCs of PS I and PS II. The primary events of the light reactions occur in the femto– to nanosecond regime, consisting of the absorption of light, transfer of excitation energy to the RCs, and photo–induced charge separation within the RC by the excitation energy. A vectoral arrange-

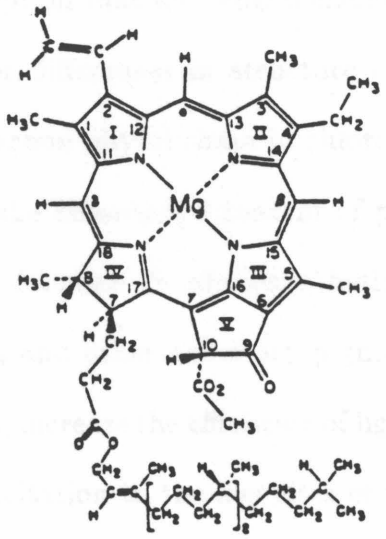

Molecular structure of chlorophyll *a*. Replacement of CH_3 by CHO in ring II gives chlorophyll *b*. and replacement of $CHCH_2$ by O—CHO in ring I gives chlorophyll *d*.

Figure 3. Molecular structure of chlorophyll derivatives.

ment of electron acceptors allows an extremely efficient transfer of electrons to secondary acceptors resulting in an electrical and proton gradient across a membrane. Secondary events, occurring in the nanosecond to second timescale, couple these potentials[7-9] to the production of high–energy intermediates (ATP),[10,11] evolution of oxygen, and the transport of ions across membranes. Finally, dark reactions occurring on longer timescales utilize the chemical energy stored in high–energy intermediates (ATP, NADH, NADPH) to drive enzymatic reactions that ultimately lead to the reduction of carbon dioxide to carbohydrates.[2]

The possession of at least one of the eight types of chlorophylls appears to be universal in photosynthetic organisms. The chlorophylls all have a similar molecular structure (Figure 3) and are closely related both structurally and biosyntheti-

cally to hemes, with the exception that the central chelated metal is magnesium[12] instead of iron. Some minor differences in structure include the exocyclic ring structure and a long hydrocarbon phytol chain in chlorophyll derivatives.

A major proportion of the chlorophyll content of photosyntheic membranes (~99%) serves an antennae function in photosynthetic systems.[2] A battery of light–harvesting chlorophylls and other accessory pigments, the chemical nature of which is species dependent, increase the efficiency of light collection by absorbing light and transferring the excitation to the key sites of photochemistry, the reaction centers (RCs).[13] The higher plants rely largely on the chlorophylls for their light harvesting function which absorb in the blue and red portions of the visible spectrum. Additional pigments also aid in this function including carotenoids[14, 15] (long chain polyunsaturated hydrocarbons), and in some species of bacteria and algae, phycobiliproteins[16] (proteins containing linear tetrapyrrols). The organized antennae maximize their functional capabilities by exploiting the differing absorption characteristics of the various chromophores resulting in the ability to utilize virtually the entire solar spectrum in some organisms. Energy transfer between the antennae chromophores ultimately results in the transfer of excitation to the RCs.

Oxygen–evolving photosynthetic systems consist of two principle sites of photochemical activity known as the reaction centers. Evidence from a number of sources including circular dichroism[17] (CD), electron paramagntic resonance [18, 19] (EPR), electron nuclear double resonance [19] (ENDOR), and other physical methods lend support to the theory that the PS I reaction center is a chlorophyll–*a*

dimer. However, some sources claim that a monomer in a special environment more adequately explains linewidths from magnetic resonance experiments.[20] Extensive physical study of P680 has also been underway.[6] The input of excitation energy into the reaction center either directly or via the antennae complex results in the photooxidation of the primary donor. The vectoral arrangement of electron acceptors in the RC then yields a fast and extremely efficient manifold for the separation of charge.

The details of the operation of RCs from photosynthetic bacteria are understood in greater detail than those of plants. The bacterial systems are substantially reduced in complexity, the coupled dual photosystem arrangement of green plants being replaced by a single photosystem in bacteria, but the functional similarities are surprising. The more exhaustive study of bacterial systems is largely due to technical difficulties in obtaining biochemically well–defined preparations of RCs from green plants. The study of plant photosynthetic systems is generally performed on subchloroplast fractions enriched in one or the other of the RCs. The simpler bacterial systems, however, lend themselves well to purification procedures allowing the associated antennae pigments to be stripped off of the bacterial reaction centers, hence removing complications due to the spectral signatures of these chromophores. It is these bacterial systems which have yielded the greatest insight into the inner workings of the photosynthetic electron–transfer chain.[21]

The critical components in a bacterial RC[22,23] are four BChl molecules, two bacteriopheophytins (BPheo is a metal–free BChl), and a nonheme ferroquinone complex [$Q(Fe^{2+})$]. The primary electron donor is a so–called special pair[24,25] of

BChl molecules, (P, or $BChl_2$), absorbing at 865 and 605 nm in *Rhodopsuedomonas sphaeroides.* In other species of bacteria the absorption shifts slightly: 883 nm in *Chromatium vinosum* and 960 nm in *Rhodopsuedomonas viridis.* The nature of the iron–quinone complex and the role of the iron is not well understood, but is under active investigation. A recent study[26] indicated that removal of the iron slows the electron transfer from the primary quinone (Q_A) to the secondary quinone (Q_B) by only a factor of two in the reaction centers from *R. sphaeroides.* Reconstitution with other divalent metals (*e.g.*, Mn^{2+}, Co^{2+}, Ni^{2+}, Cu^{2+}, Zn^{2+}) restores the native kinetics for this transfer. The formation and decay of P^+I^- in RCs from *R. sphearoides* exhibited identical yields (100%) of $P^+Q_A^-$ for native and Zn^{2+} reconstituted RCs,[27] while in the absence of a metal the yield drops to ~47%, implicating a critical role for the metal in the electron transfer step $P^+I^-Q_A \longrightarrow P^+IQ_A^-$. The possible role of the Fe^{2+} ion suggested by these authors[27] includes (a) preservation of the structural integrity of the RC, (b) spin or magnetic field effects, (c) alteration of the Q_A reduction potential by electrostatic interaction, or (d) changes in the reorganization energies governing the transfer.

Analysis of the temperature dependence of the primary reactions in RCs continues to accumulate. While several electron transfer steps appear to show classical activation parameters, as in the oxidation of the high potential cytochromes in *R. sphaeroides,*[28] other transfers have been observed to occur at temperatures as low as 4K. A key study by DeVault and Chance[29] investigated the oxidation of the low potential *c*–type cytochromes in *Chromatium vinosum* responsible for the reduction of the photooxidized special pair $(BChl)_2$, which shows a temperature

independent rate below ~100K (Figure 4). Further studies determined that the photooxidation of $(BChl)_2$ has been observed to be temperature independent over the full temperature range of 4–300K.[31,32] Some of the back transfer steps in the electron transfer pathway, normally discriminated against in native RCs (*e.g.*, $(BChl)_2^{+\cdot}IQ_A^{-\cdot} \rightarrow (BChl)_2IQ_A$) show curious negative activation energies, *i.e.*, the rate actually decreases with increasing temperature above 100K.[33,34] Bacterial systems tend to display negative temperature coefficients for the reverse primary reactions, while those of green plants have positive coefficients in the high temperature regions.[35] A comprehensive summary of RC temperature effects can be found in a recent review.[36]

Historically, the identity of the primary electron acceptor of the RCs was linked to technical advances in fast spectroscopy.[21] Early work identified the $Q(Fe^{2+})$ complex as the primary acceptor.[37,38] The reduced quinone was stable on the millisecond time scale, and nanosecond laser pulses were unable to detect an earlier intermediate. The first indications that other chromophores were involved was the detection of a new transient with a 10 nsec lifetime at room temperature[39] observed when normal photosynthetic electron transfers were blocked, as in the prior reduction of the $Q(Fe^{2+})$ center to $Q^{-\cdot}(Fe^{2+})$. This transient showed absorbance bleaching in the BPheo absorbing regions, and was the first indication of a prior step in the electron transfer chain. However, to prove this intermediate was not an artifact, it had to be detected under conditions where normal photosynthetic electron transfer processes were viable.

Subsequent studies using picosecond spectroscopic techniques identified a new

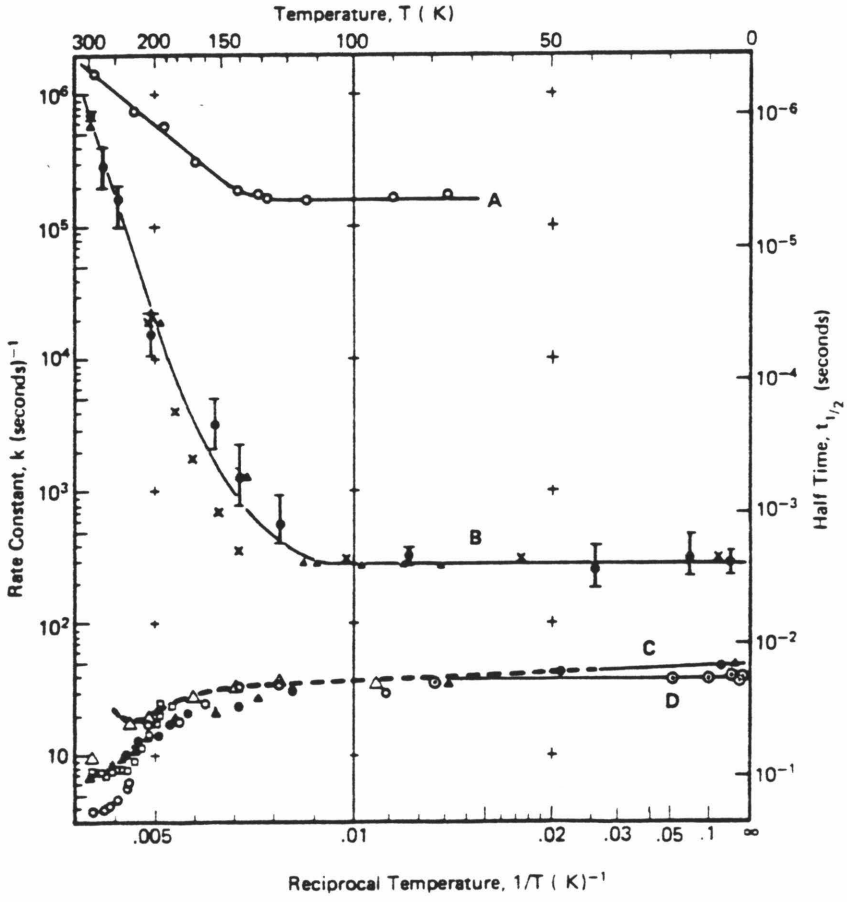

Figure 4. Temperature dependence of bacterial photosynthetic electron transfers. Curves A and B: photoinduced cytochrome oxidation. Curves C and D: reversed primary reactions (from reference 30, p. 3, Figure 1.1).

intermediate 10 psec after excitation which did not decay between 10–200 psec after illumination even when the $Q(Fe^{2+})$ center was reduced prior to excitation.[40] A diagnostic 1250 nm absorption band was experimentally observed when $(BChl)_2^{+\cdot}$ was formed either chemically by the addition of oxidants, or photochemically by the illumination of the RCs with 865 nm light, and a key picosecond measurement[41] demonstrated that the rate of formation of this infrared absorption was <10 psec. Even the removal of the $Q(Fe^{2+})$ center did not effect the 1250 nm kinetics.[42] Another intermediate was clearly implicated in the ET pathway.

$$(BChl)_2IQ(Fe^{2+}) \xrightarrow[k > 10^{11}sec^{-1}]{h\nu} (BChl)_2^{+\cdot}I^{-\cdot}Q(Fe^{2+}) \xrightarrow[k = 6.7x10^{9}sec^{-1}]{} (BChl)_2^{+\cdot}IQ^{-\cdot}(Fe^{2+})$$

Numerous investigations[40–45] on the picosecond time scale implicated the involvement of BPheo or possibly the monomeric BChl as intermediate acceptors enroute to the primary quinone acceptor. The role of the monomeric BChl is not well understood, and its implication as an intermediate acceptor is still controversial. A recent report[46] argues that no picosecond study to date has demonstrated convincingly that $P^{+\cdot}BChl^{-\cdot}$ is a kinetically or spectrally resolved intermediate state. The specific spectral features which implicate the monomeric BChl as an intermediate acceptor appear to be highly dependent upon excitation flash duration, intensity, and polarization, as well as other experimental parameters such as temperature and even medium.[47] Some of these spectral features implicating the monomeric BChl in the ET pathway may well be due to the influences of protein conforma-

tions or other environmental factors.[48] A summary of the kinetic scheme for the photosynthetic electron transfer pathway in RCs is shown in Scheme I.

Our understanding of the function of RCs has been obtained largely from a myriad of physical techniques which have allowed the identification of key events in the electron transfer sequence. Fast spectroscopic techniques have identified the intermediates in the ET sequence. The presence of magnetic interactions between the oxidized or reduced chromophores have led to the estimation of separation distances between the components of the RC.[21,36] While the significance of these studies should not be underestimated, crystallographic analysis will ultimately provide the definitive insights into the function of the RC.

A crystal structure[49,50] of the RC of *R. viridis* at 3Å resolution has been reported which allows the visualization of the chromophores at the atomic level. While significant refinements in the structure remain to be completed, this is the first detailed look at the orientations and interactions of the RC components, and is a key breakthrough toward increasing our understanding of the enormous functional success of the photosynthetic unit.

The crystals are reported to be photochemically active in the crystalline state[51,52] suggesting only minor perturbations have been introduced by extraction of the RCs from the membrane and the crystallization process. These reaction centers crystallize with the attendant *c*–type cytochrome still attached, allowing the orientation of the cytochrome hemes to be determined as well (Figure 5). There is an approximate 2–fold rotation symmetry axis relating the two groups of chromophores within the RC, one BChl–*b* of the special pair, one monomeric

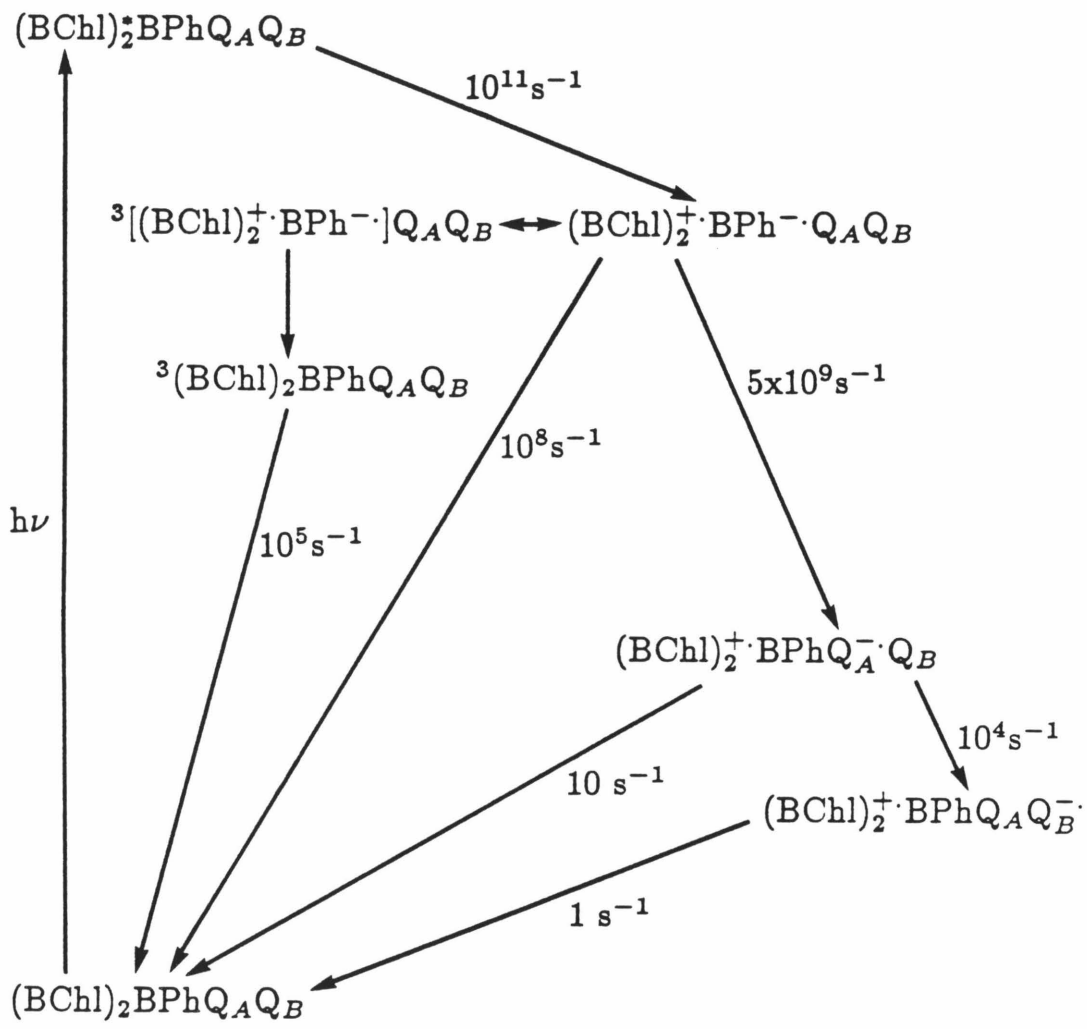

Scheme I. Kinetic scheme for photosynthetic electron transfer reactions.

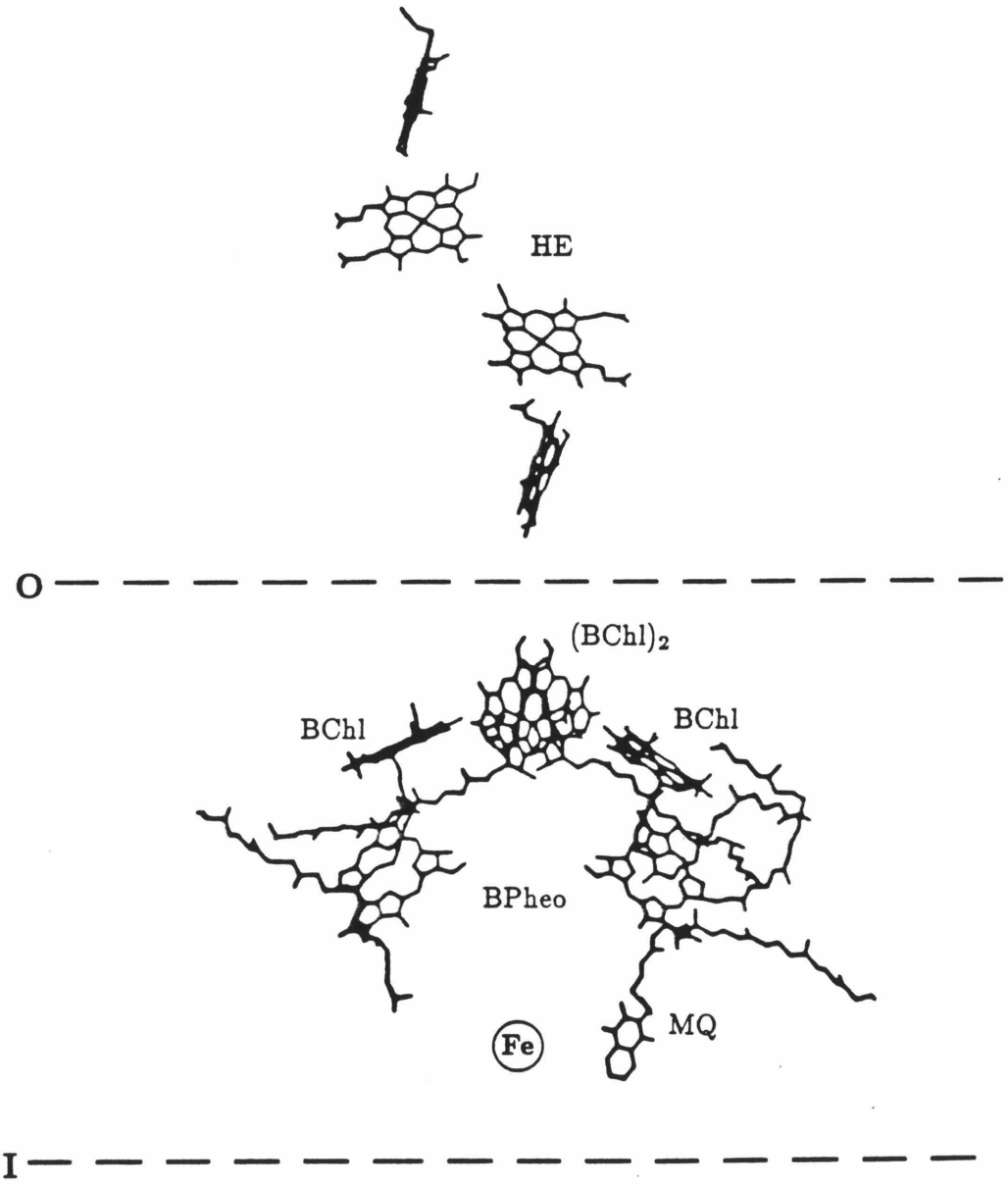

Figure 5. Crystal structure of the reaction center complex from *R. viridus* (from reference 49).

BChl–*b*, and one BPheo–*b*. The position of the non–heme iron is on or very close to this symmetry axis. The planes containing the BChl–*b*s of the special pair are approximately 3Å apart and tipped at ~15°. In close proximity to the special pair is another monomeric BChl–*b*, with a center–to–center distance (Mg to Mg) of ~13Å and an angle between planes of ~70°. Each of these monomeric BChl–*b* molecules are adjacent to a BPheo–*b* with a distance between ring centers of ~11Å and an angle between ring planes of ~64°. While the tetrapyrrole rings of the monomeric BChl and BPheo obey the 2–fold rotation symmetry, parts of the phytol side chains do not, and there appear to be significant contacts between the BChl–*b* and BPheo–*b* via the phytol side chains. The only quinone in the structure is located ~7Å from the non–heme iron, consistent with recent EPR studies.[53] The absence of a second quinone in the structure suggests a strict inequivalence in the two otherwise identical electron transfer pathways. As yet this inequivalence has not been shown to extend to any asymmetry in the protein backbone of the structure.[50] The possibility that one quinone was lost in the preparation of the crystals, or that the quinone is disordered can not yet be excluded by the authors. The heme groups in the cytochrome subunit are vectorally arranged on an axis at ~60° to the 2–fold symmetry axis of the RC core. Only the heme closest to the special pair lies on this axis with a (heme) Fe–Mg (BChl–*b*) distance of ~21Å. Analysis of the protein backbone[51] has located a tyrosine residue between the closest heme group and the special pair which may implicate the involvement of the protein side chains in the electron transfer pathway, and may call for closer scrutiny of the amino acid side chains in the structure once the full

protein sequence is known and these residues can be pinpointed. The remaining heme Fe–Fe distances in the cytochrome subunit as they extend away from the special pair are ~14Å, ~16Å, and ~14Å. Recent progress has also been made on the crystal structure of the RC from R. sphaeroides at 3Å resolution, and results will soon be available for comparison of the two structures.[54]

The photosynthetic reaction center is a unique assembly competent at extremely efficient charge–separation in high yield (the quantum yield for the photooxidation of $(BChl)_2$ is 1.02 ± 0.04 in *R. sphaeroides*[55]). The extraordinary functional success has prompted the development of a number of synthetic model systems which have enjoyed only moderate success at reproducing various aspects of the RC function. Clearly our success for adequate modeling of the biological process requires a fundamental understanding of how key parameters affect electron transfer rates. Nature has shown us a remarkable example of the efficient use of photochemical energy, incorporating a given set of driving forces, donor–acceptor distances and orientations into a protein framework. Ideally, if one understood the fundamental dependencies of electron transfer rates on these variables, one might be able to successfully mimic the biological system.

Sparked in part by the increasing understanding of electron transfer in biological systems, the theoretical underpinning of electron transfer reactions in general continues to develop. Initial theoretical treatments of ET reactions treated nuclear motion in a classical framework.[30, 36] Subsequent work has investigated the problem in a semi–classical,[56] as well as quantum mechanical[30, 57-60] framework, and are reviewed extensively elsewhere.[36, 61] The classical treatment originally

proposed by Marcus[62] was developed over 30 years ago and has been immensely successful at predicting ET rate constants in self–exchange and electrode reactions, and is briefly discussed below.

The potential energy surface for a reaction is a function of all relevant nuclear coordinates coupled to the reaction. Such a surface would include coordinates for all degrees of vibrational, translational, and rotational motion. In addition, orientational coordinates of the surrounding medium are also included since the averaged equilibrium orientations of solvent molecules may differ for reactants and products in an electron transfer reaction due to the transfer of charge, especially when the surrounding medium involves an appreciable solvent dipole. A cross–section of this surface in many–dimensional coordinate space along an "effective nuclear coordinate" reduces the complexity of a multi–dimensional surface to a single coordinate analysis. If the reactant and product are considered to be harmonic oscillators, the potential energy curves can be described as intersecting parabola (Figure 6) along this effective coordinate. In the classical analysis, a reaction is only possible if the curves intersect, and a transition from the reactant (R) surface to the product (P) surface can be discussed. Two limiting cases exist, one in which strong mixing is present between the R and P curves resulting in a large splitting between the potential energy curves, and is called the adiabatic limit. In the nonadiabatic limit, the reactant and product only weakly interact, and the crossing point must be traversed many times before crossing to the P surface. The application of the Frank–Condon principle would then require that the transfer of an electron is instantaneous, *i.e.*, that the nuclei in the "activated complex" do not

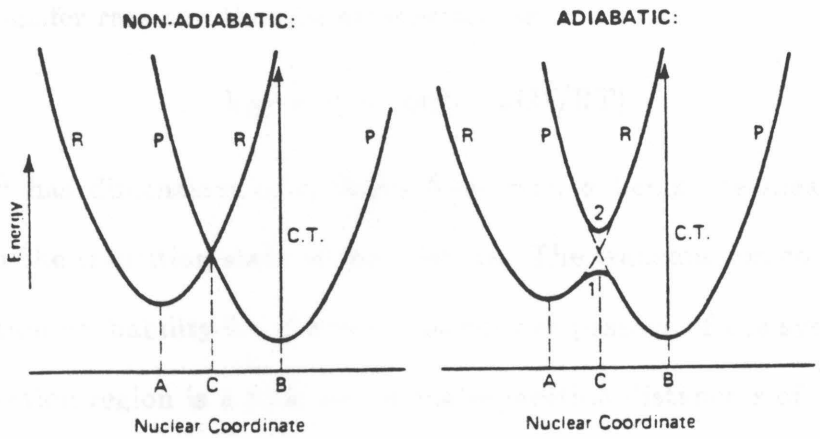

Figure 6. Nuclear potential energy curves in the adiabatic and nonadiabatic limit.

have time to change either their positions or their momenta during the electron transfer event. To conserve energy in the transfer, ET must occur at configurations where the potential energy of the reactant equals that of the product, or at the intersection region in Figure 6.

The calculation of the rate constant for electron transfer is then reduced to quantifying the probability of reaching the intersection region and of staying on the lower surface. Thermal and vibrational fluctuations result in the system being displaced from the equilbrium energy minimum of the R curve to that of the intersection region. Once the system has reached the intersection point, the probability of transfer is related to the extent of the coupling of the electronic orbitals of the two reactants (*i.e.*, adiabatic or nonadiabatic) which in turn is

related to parameters such as separation distance and orientation effects. The electron transfer rate can then be expressed[61] as

$$k_{ET} = \kappa A\sigma^2 \exp(-\Delta G^{\ddagger}/RT) \qquad [1.1]$$

where $A\sigma^2$ has dimensions of collision frequency, σ being the mean separation distance in the transition state of the reaction. The transmission coefficient κ, or the transition probability for electron transfer per passage of the system through the intersection region is a function of the separation distance r of the reactants and is generally assumed to vary at large r approximately as $\exp(-\beta r)$.[61] For adiabatic reactions, $\kappa \approx 1$, and for nonadiabatic reactions, $\kappa \ll 1$. Finally, the rate is dependent on the free energy of activation for the reaction, $\Delta G^{\ddagger}$, expressed as[61]

$$\Delta G^{\ddagger} = w^{r} + \frac{\lambda}{4}\left(1 + \frac{\Delta G^{\circ\prime}}{\lambda}\right)^2 \qquad [1.2]$$

$$\Delta G^{\circ\prime} = \Delta G^{\circ} + w^{p} - w^{r} \qquad [1.3]$$

which relates $\Delta G^{\ddagger}$ to the "standard" free energy of reaction in the prevailing medium, ΔG°, the work terms for bringing the reactants (w^{r}) or products (w^{p}) to the mean separation distance σ, (or r), and the reorganization energy (λ) coupled to the transfer. The quantity $\Delta G^{\circ\prime}$ thus corresponds to the free energy of the reaction when the reactants are at separation distance r. The λ term is composed of an inner sphere component, related to changes in bond lengths, and an outer sphere component, related to bulk changes in solvent orientations.[61]

$$\lambda = \lambda_i + \lambda_o \qquad [1.4]$$

$$\lambda_i = \Sigma_j \frac{f_j^{\mathrm{r}} f_j^{\mathrm{p}}}{f_j^{\mathrm{r}} + f_j^{\mathrm{p}}} (\Delta \mathrm{q}_j)^2 \qquad [1.5]$$

$$\lambda_o = (\Delta \mathrm{e})^2 \left[\frac{1}{2a_1} + \frac{1}{2a_2} - \frac{1}{r} \right] \left[\frac{1}{n^2} - \frac{1}{\epsilon_{\mathrm{s}}} \right] \qquad [1.6]$$

The paramenters f_j^{r} and f_j^{p} are the jth normal mode force constants in the reactants and products, respectively, $\Delta \mathrm{q}_j$ is the change in equilibrium value of the jth normal coordinate, Δe is the charge transferred from one reactant to the other, a_1 and a_2 are the radii of the (spherical) reactants, r is the separation distance, n is the solvent index of refraction, and ϵ_s is the solvent dielectric constant. This treatment assumes the vibrations within the reactants can be treated as harmonic oscillators, and the derivation of the outer sphere component of the reorganization energy is based on the dielectric unsaturation approximation[61, 63, 64] which assumes that the dielectric polarizations around the reactants responds linearly to any changes in charge.

Quantum–mechanical treatments express the nonadiabatic electron transfer rate as[36]

$$\mathrm{k}_{ET} = \frac{2\pi}{\hbar} \mid H_{\mathrm{ab}} \mid^2 (\mathrm{FC}) \qquad [1.7]$$

where H_{ab} is the electronic matrix element for the electronic coupling of the reactant and product states, and is equal to one–half the separation of the R and P curves (Figure 6) for a purely adiabatic description. The quantity (FC) is the Frank–Condon factor, a sum of overlap integrals for the vibrational and solvational wavefunctions for the reactants with those of the products weighted by suitable

Boltzmann factors. In the harmonic approximation and the high temperature limit, this results in a rate expressed[61] as

$$k_{ET} = \frac{2\pi}{\hbar} \mid H_{ab} \mid^2 \frac{1}{\sqrt{4\pi\lambda kT}} \exp\left(\frac{-(\Delta G^{\circ\prime} + \lambda)^2}{4\lambda kT}\right) \qquad [1.8]$$

The implications of equation [1.8] have sparked extensive experimental investigations of exothermicity effects on electron transfer rates. Shown in Figure 7 is a plot of k_{ET} as a function of driving force ($\Delta G^{\circ\prime}$) for an electron transfer reaction. The electron transfer rate is predicted to increase until $\Delta G^{\circ\prime}$ equals the reorganization energy (λ) coupled to the transfer, and further increases in exothermicity are predicted to result in a decrease in k_{ET}. Superimposed on the curve is a diffusion limited rate plateau which can mask the results from intermolecular investigations (see below). The existence of the inverted region has been invoked to explain the efficiency of the forward transfers in photosynthetic RCs. If the forward transfers are optimized at a driving force equal to the reorganization energy, the back transfers would fall in the highly exothermic region, and the expression [1.8] above would predict these rates would be slower, although the driving force is considerably greater. Thus, the forward transfers could compete effectively with deletarious back transfers.

Because the nuclear motion is treated classically in equations [1.8] and [1.2], this derivation assumes kT is much larger than the relevant nuclear frequency coupled to the transfer, thus presenting a problem in treating low–temperature kinetic data. An alternative theoretical approach by Hopfield[56] sought to specifically treat the possibility of nuclear tunneling at low temperature. This derivation pointed

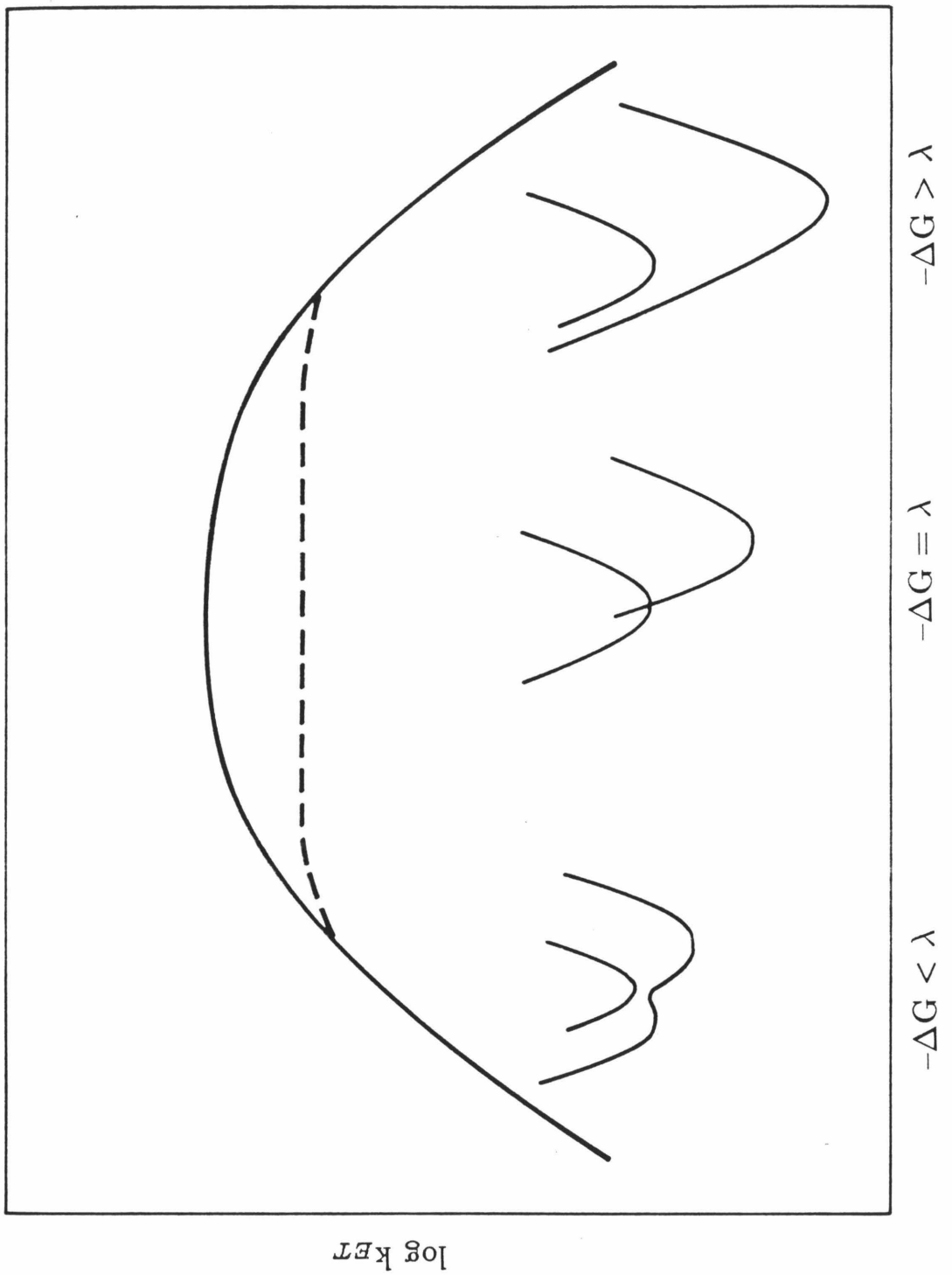

Figure 7. Dependence of the electron transfer rate constant on reaction exothermicity.

out that electron transfer between fixed sites (as in most biological transfers) is analogous to energy transfer by the Förster–Dexter mechanism[65,66] and that the rate of electron transfer could be described by

$$k = \frac{2\pi}{\hbar} \mid T_{ab} \mid^2 \int D_a(E) D_b(E) dE \qquad [1.9]$$

where D_a and D_b are the 'electron removal' and 'electron insertion' spectra, respectively, and are analogous to Förster's optical emission and absorption spectra. Assuming these spectra could be approximated by Gaussian distributions, a semiclassical expression for k_{ET} was derived[56] as

$$k_{ET} = \frac{2\pi}{\hbar} \mid T_{ab} \mid^2 \frac{1}{\sqrt{4\pi\lambda T_{eff}}} \exp\left(\frac{-(\Delta G^{\circ\prime} + \lambda)^2}{4\lambda T_{eff}}\right) \qquad [1.10]$$

$$T_{eff} = \frac{\hbar\omega}{2} \coth\left(\frac{\hbar\omega}{2k_B T}\right) \qquad [1.11]$$

Low–temperature effects could then be treated with an 'effective' temperature, T_{eff}, in the calculation of the Frank–Condon factor. This effective temperature has the behavior of approaching $k_B T$ at high temperature, and $\hbar\omega/2$ (temperature independent) at low temperatures. Equation [1.10] was the first to give reasonable quantitative agreement with the low–temperature data of DeVault and Chance on cytochrome *c* oxidation in *Chromatium vinosum*.[56]

Extensive effort has been underway to develop the theoretical framework necessary to quanitatively predict electron transfer rates. The ultimate success will require an intimate knowledge of the effects of key parameters such a exothermicity, donor–acceptor separation distance and orientations, bridging medium,

solvent, temperature, and reorganization energies coupled to electron tranfer reactions. All of these effects have been dealt with extensively in numerous theoretical treatments of the electron transfer problem. What remains is to develop experimental systems which can investigate these parameters systematically for future refinements of theoretical treatments.

Chapter 2

Previous Studies

Intermolecular Studies

Early attempts to confirm the predictions of electron transfer theory involved the study of intermolecular quenching of various donors and acceptors. One of the classic studies in this regard was the work of Rehm and Weller[67] who studied the fluorescence quenching of a large number of donors and acceptors in fluid solution. At low driving forces the electron transfer rates increased considerably, and then a plateau was observed. No evidence for the inverted region was observed (Figure 1). A later pulse radiolysis study by Beitz and Miller[68,69] sought to control the diffusion aspect of the problem by studying the electron transfer rates in a rigid solvent matrix at low temperature. The extraction of k_{ET} values required significant deconvolutions, and assumptions of randomly distributed donors and acceptors. This approach was moderately successful, and hinted at inverted region effects in the high exothermicity cases studied.

The intermolecular approach is plagued with problems of distributions of donor–acceptor distances, orientations and diffusion limited rates. These and other studies[70] suggested the optimum approach for investigations of electron transfer parameters is the explicit control of all aspects which govern electron transfer. Such unambiguous control of electron transfer parameters is exceedingly important for comparison with theoretical developments of the last three decades. The rigorous experimental control of these parameters in precisely defined synthetic

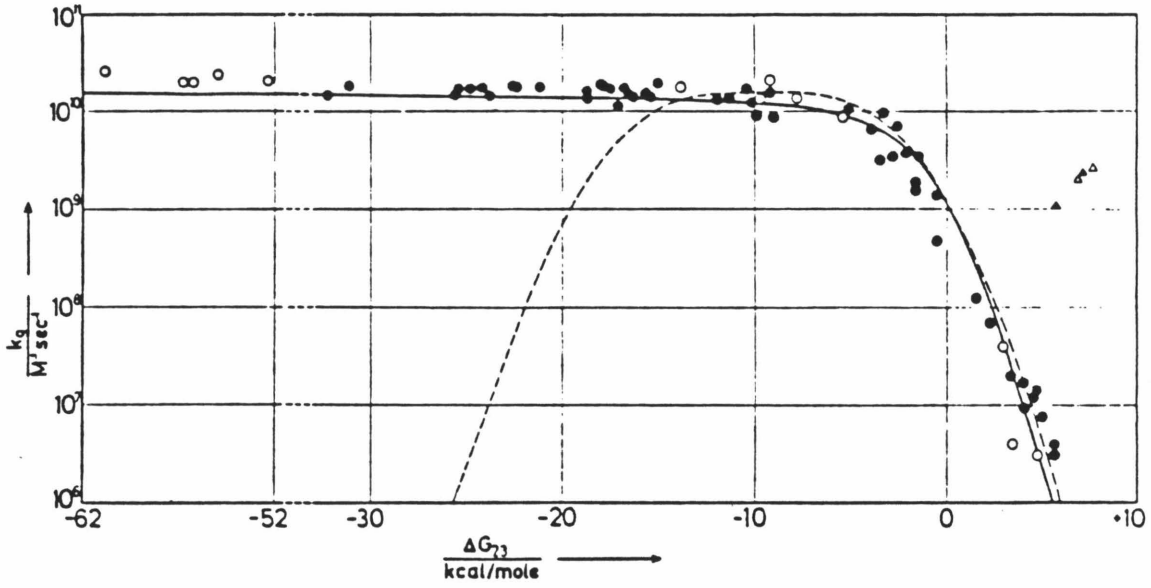

Figure 1. Intermolecular fluorescence quenching study of donors and acceptors (from reference 67).

systems has become available only recently. In analogy with biological donors and acceptors, the focus of discussion in the next section will be on porphyrin–quinone model systems.

Intramolecular Bichromophoric Studies

The first model system reported in the literature incorporating a linked porphyrin–quinone system was that of Tabushi[71] (see below).

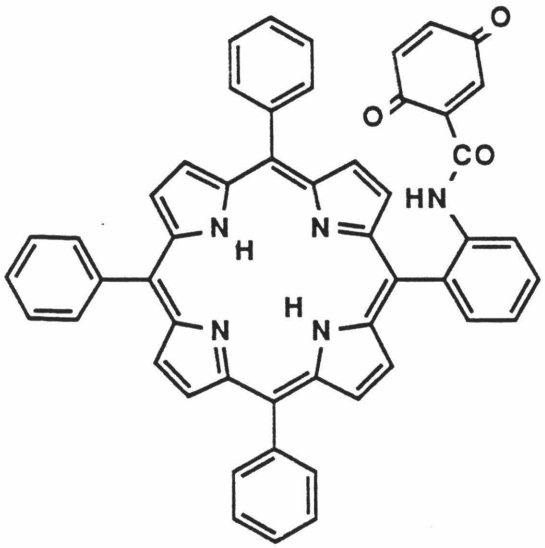

I

^{1}H NMR clearly indicated the close proximity of the quinone to the tetraphenylporphyrin ring system. The fluorescence from **I** was observed to be of "very low intensity," demonstrating that an efficient quenching pathway for the porphyrin excited singlet was available, and was presumed to indicate electron transfer quenching. Comparison with previous studies of intermolecular quenching of TPP fluorescence by *p*–benzoquinone indicated the "effective" quinone concentration

of **I** was $\sim 4 \times 10^{-2}$M pointing to the advantagous use of an intramolecular system to achieve high effective acceptor concentrations in an attempt to circumvent diffusion limited rates.

This study was the first in a long series of intramolecular porphyrin systems subsequently prepared for the investigation electron transfer rates. The list includes porphyrins linked to quinones or other acceptors,[72-85] face–to–face porphyrin–quinones,[86-92] porphyrin dimers or trimers,[93-101] and a porphyrin dimer linked to a quinone.[102, 103] Much of the early work on porphyrin oligomers was devoted to the spectral characterization of such species for comparison with emerging spectroscopic and EPR studies on photosynthetic reaction centers. Later studies probed the electron transfer capabilities of such systems. The wealth of porphyrin–acceptor (generally quinone) systems which followed sought to mimic various aspects of the primary events in RCs, and to study the effects of various parameters on ET rates, such as distance or orientation effects. While these systems had succeeded in overcoming diffusion limited rates which can mask the results from intermolecular studies, there remained significant problems to overcome. In particular, systems which link an acceptor to a porphyrin via flexible hydrocarbon linkers for the analysis of distance effects are plagued with conformational dynamics resulting in ill–defined donor–acceptor separation distances and orientations. These sytems are characterized by complex emission behavior, often requiring multiexponential analyses to fit the emission data. The ensemble of donor–acceptor distances gives rise to a distribution of electron transfer rates which is difficult to deconvolute without prior knowledge of the accessible donor–acceptor conforma-

tions. While these studies are significant in establishing the existence of efficient electron transfer quenching pathways from the porphyrin excited state, it is unlikely that quantitative data for comparison with theory will ever be obtained from this approach. Only systems which seek to unambiguously control distance and/or orientations will be discussed in detail here.

A number of systems which followed were successful at limiting the complications of conformational flexibility. Shown below are two such systems. The di-

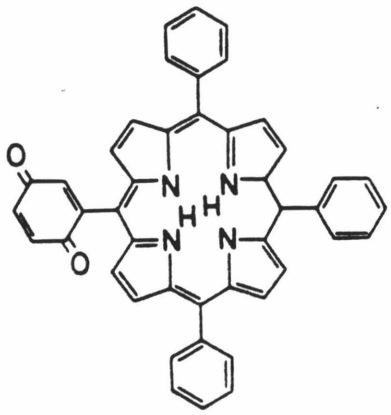

II

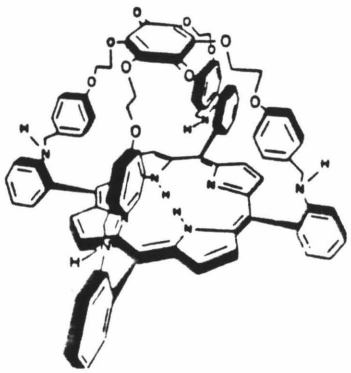

III

rectly coupled porphyrin–quinone system **II** studied by Netzel[80] showed extremely fast ($>10^{11}$ s^{-1}) electron transfer quenching attributable to the close proximity of the quinone acceptor and is likely an example of an adiabatic transfer. The face–to–face porphyrin–quinone system[87,88] will provide an interesting orientation study on electron transfer rates. Preliminary studies indicate biexponential fluo-

rescence behavior for **III**, possibly the result of two stable conformations. While an orientation study will be significant, the systems does not easily lend itself to exothermicity investigations.

Bichromophoric Systems

Recent work investigating photoinduced electron transfer rates in a rigid bichromophoric system have been reported.[104,105] The molecules shown below were prepared and solvent effects on long distance (5.8 Å edge–to–edge separation)

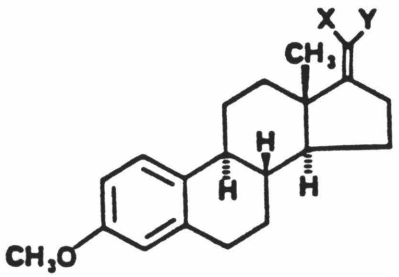

1a X=H ; Y=$COOC_2H_5$
1b X=Y=CN

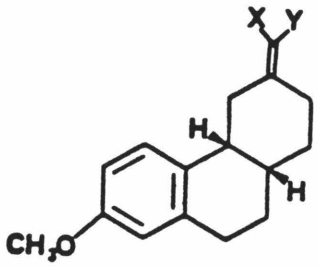

2a X=$COOCH_3$; Y=H
2b X=Y=CN

ET have been investigated. These molecules show the advantagous behavior of an emissive charge–transfer state under certain conditions, allowing a direct probe of the energy of the CT state via the solvatochromism of the CT band. The compounds exhibit highly quenched fluorescence from the photoexcited anisole donor.

The absorption spectra preclude energy transfer from the anisole excited singlet to the substituted ethylene group, implying that electron transfer is the additional decay channel responsible for the observed singlet quenching. The molecules are so strongly quenched that only limits on the electron transfer rates are available for compounds **1b**, **2a**, and **2b** making the quantification of the change in k_{ET} with an increase in the driving force from the alkoxycarbonylethylene to the cyanoethylene acceptor difficult. The molecules have the advantage of a fixed donor–acceptor separation with a minor complication of a slow (on the ET timescale) conformational changes, and hence donor–acceptor distances, available with this hydrocarbon skeleton. A comparison of electron transfer rates was experimentally possible for **1a** in acetonitrile and **1b** in hexane. Unfortunately, the ambiguity in estimating the driving force for the electron transfer in hexane is problematic.

Electrochemical measurement of the driving for for the reaction in acetonitrile coupled with the excitation energy resulted in an estimate of ~1 eV for the driving force for electron transfer. A change of solvent to hexane, for which no electrochemical measurements are presently available, results in significant complications. These authors (and others, see below) utilize a theoretical treatment to estimate the driving force for the reaction in solvents of different dielectric constant based on redox values for the chromophores in solvents which exhibit well–behaved electrochemical behavior (*e.g.*, acetonitrile or dimethylformamide). This theoretical treatment is based on the Onsager field model[106] to estimate the solvation energy of the charge transfer state. The orientation polarization of the

solvent in response to the CT dipole was calculated from

$$E_{op} = \frac{-\mu_{ct}^2}{\rho^3}\left[\left(\frac{\epsilon - 1}{2\epsilon + 1}\right) - \left(\frac{n^2 - 1}{2n^2 + 1}\right)\right] \qquad [3.1]$$

where ρ denotes the radius of the solvation cavity surrounding the molecule, μ_{ct} is the dipole moment of the CT state, ϵ is the solvent dielectric constant, and n is the refractive index of the solvent.

A number of implicit assumptions in this derivation suggest that the use of such a model to calculate driving forces for the electron transfer where very large dipole moments are involved (the authors estimate the dipole moment of **2b** to be ~23D in the CT state) extend the theory beyond its useful limits (molecules of 0-4D dipole moments). The large dipole moments involved in compounds of this type certainly calls into question the applicability of the dielectric unsaturation approximation in any solvent discussions. Clearly one would prefer better estimates of the energies of the CT state, ideally where the redox values can be experimentally determined in the solvents used in the photochemical studies. In the absence of such information, it would be preferable to quantitate changes in k_{ET} within a single solvent if experimentally attainable. Extensions of this work to incremental distance effects are currently in progress,[107-109] and will be discussed in Chapter 5.

Of the few synthetic porphyrin–quinone sytems designed with well–defined donor–acceptor separation distances is the molecule prepared by Wasielewski and coworkers[110, 111] shown below. This system is one of the first to demonstrate single exponential emission lifetimes characteristic of systems having an unambigu-

ous donor–acceptor separation distance. This allows quantitative determination of k_{ET} and allows investigation of solvent and exothermicity effects. The quinones are linked to the porphyrin via a rigid triptycyl linker which has only limited rotational flexibility about the single bond at the porphyrin *meso*–carbon (the barrier to phenyl rotation in tetraphenyl porphyrins is ~18 kcal/mole).[112] Three different porphyrin–quinones were prepared with the acceptor ranging from benzoquinone to anthroquinone, allowing the investigation of exothermicity effects over a driving force range of 0.45 eV. Electron transfer occurs from the photoexcited porphyrin singlet to the quinone with k_{ET} as high as 2.5×10^{11} s^{-1} in some cases. Measurements of fluorescence lifetimes for the three compounds in both the free–base and zinc–porphyrin allowed determination of the forward driving force for this system. In addition, transient spectroscopy was employed to quantitate the rates of back transfer, *i.e.*, from the non–emissive $P^{+\cdot}Q^{-\cdot}$ state returning to ground state products for the same series. The k_{ET} values determined are shown in Figure 2, plotted as a function of the driving force for the reaction ($P^*Q \longrightarrow P^{+\cdot}Q^{-\cdot}$ plotted as •, $P^{+\cdot}Q^{-\cdot} \rightarrow P–Q$ plotted as ▪).

A number of points may cloud the apparent observation of the long–sought demostration of a decrease in k_{ET} with increasing exothermicity for photoinduced transfer originally proposed by Marcus[62] some 30 years ago. In particular, the authors propose that the exothermicity of the electron transfer reaction can be altered by a change in the solvent. The only redox values experimentally measured were for the isolated chromophores in butyronitrile. The values for toluene were calculated based on the method of Weller[113] for estimating the $\Delta G°$ by a change

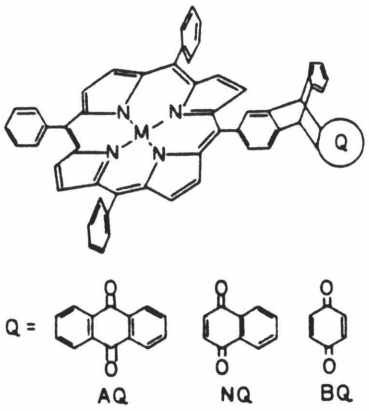

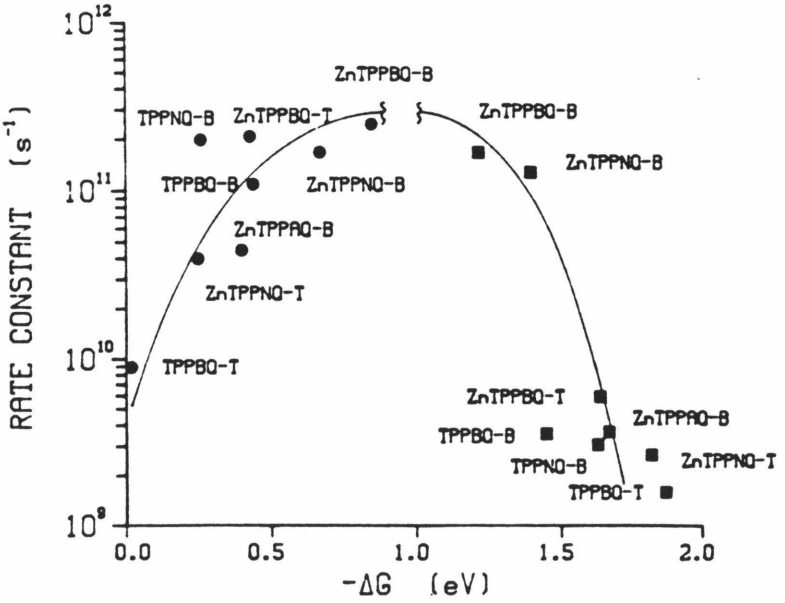

Figure 2. Photoinduced electron transfer rates in porphyrin–triptycyl–quinones: effect of exothermicity.

in the solvent polarity. This procedure requires a number of basic assumptions, namely that the chromophores can be reasonably approximated by point charges in a spherical solvent cavity. While this method has proven successful with a number of small molecules, the large delocalized porphyrin cation is not likely to be as dramatically affected by changes in the solvent polarity as the more localized systems conventionally treated with the Weller method. Classical Marcus theory clearly predicts an increase in λ_o with increases in solvent polarity, thus only compounds within a given solvent can readily be compared. In addition to the changes in solvent, one notices that both free–base and zinc derivatives are presented. To include these data within a reaction series, one would be forced to accept a constant degree of vibronic coupling for both metallo and free base derivatives. The comparison of the forward transfers ($P^*Q \rightarrow P^{+\cdot}Q^{-\cdot}$) is undoubtedly a different reaction series than the reverse reaction in which a CT state returns to the neutral ground state species. Recent theoretical calculations[114] proposed different distance dependencies for T_{ab} with changes in the energy of the transferring state, as is the case for forward and back transfers. As a result, the forward and back transfers cannot be considered as part of the same Marcus plot (note the curves connecting the data are not, and should not be connected). Within the series, however, the choice of acceptors of varying aromaticity may well call the homology of the reaction series into question. One is left to wonder whether the slowness of the back electron transfer from, for example $ZnTPP^{+\cdot}AQ^{-\cdot}$ returning to ground state, merely reflects the increased delocalization of the anthroquinone anion stabilizing the CT state. While this system has some clear advantages over

previous flexibly coupled donors and acceptors, a number of questions remain as to the applicability of the Weller treatment to porphyrin systems, and to the homology of the reaction series. Similar problems exist for data interpretation in a recently reported system claiming to observe the inverted region for photoinduced electron transfer in a capped porphyrin–acceptor.[91] Again, changes in the solvent polarity were employed to alter the reaction driving force. This system has already been demonstrated to have conformational problems in which the quinone oxygen was shown to provide a fifth ligand to the metallo–porphyrin.[89, 90]

A donor–acceptor system rigidly incorporating a rigid steroid spacer is shown below. The electron transfer in this system was studied by pulse radiolysis.[115, 116] The compounds were dissolved in methyltetrahydrofuran and subjected to a high energy pulse of electrons. Secondary electrons are then trapped on both the biphenyl and acceptor ends of the molecule with equal probability. The transfer of the electron from the biphenyl anion to the various acceptors can be followed spectroscopically. After correction for intermolecular events, k_{ET} for the reaction can be quantitated. By studying various acceptors k_{ET} can be investigated as a function of ΔG° (Figure 3). This is the best evidence to date for the existence of the inverted region. The question of reaction homology does appear to remain in the series, however. One notices the acceptors are all fused aromatics on the "normal" region, and quinones comprise the acceptors on the inverted side. Irrespective of whether these two classes of compounds are homologous, analysis of the quinone data alone clearly shows a one order of magnitude decrease in k_{ET} with increasing exothermicity. The data also points to the disturbing possibility that

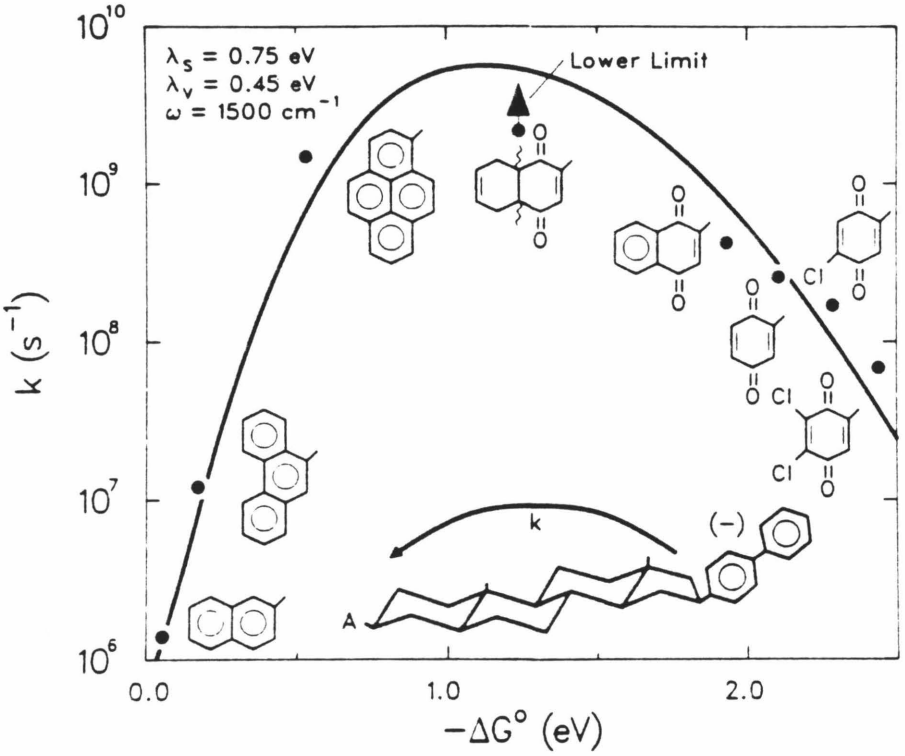

Figure 3. Effect of exothermicity on electron transfer rates in steriod linked donor–acceptor molecules.

very high driving force reactions (~2 eV) may need to be considered to observe the inverted region in this particular case. Clear evidence of the inverted region remains to be demonstrated for photoinduced transfers.

Following publication of the current research,[117] work by Bolton and coworkers examined solvent effects in linked porphyrin–quinones characterized by moderate[85] to maximal[118] control of donor–acceptor separation distance, and indicated correlations of k_{ET} with the solvent index of refraction. Results from these studies will be discussed in comparison with this research later in this manuscript. Other notable systems investigating distance dependencies include electron transfer through aromatic spacers,[119] inorganic systems incorporating distance changes through dithiospirocyclobutane oligomers,[120] peptide linkers,[121] and protein based systems.[122-131]

Triad Systems

Recently, systems have been prepared[132-134] to investigate methods of controlling back transfer rates through the use of a molecular triad approach. Two such systems are shown below. These systems clearly demonstrate the effectiveness of this strategy which results in significant stabilization of the charge–separated state and high yield (τ_{CT} = 2.5 μsec, Φ_{CT} ~70% for **IV**).[133] Similar studies on **V** demonstrated an enhanced yield of the CT state with added electrolyte, increasing the yield from 4% to 25%, and the authors suggest that charged sites in the protein backbone of the RCs may be responsible for optimizing forward electron transfers.[134] This proposal will be directly addressed as refinements in the RC crystal structure discussed previously become available.[49, 50] These re-

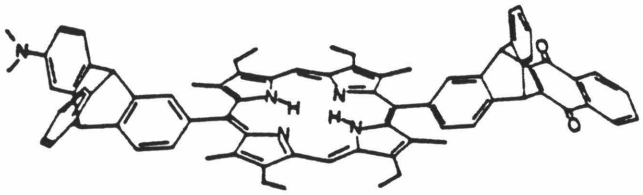

IV

Figure 4a. Dimethylaniline–porphyrin–quinone.[133]

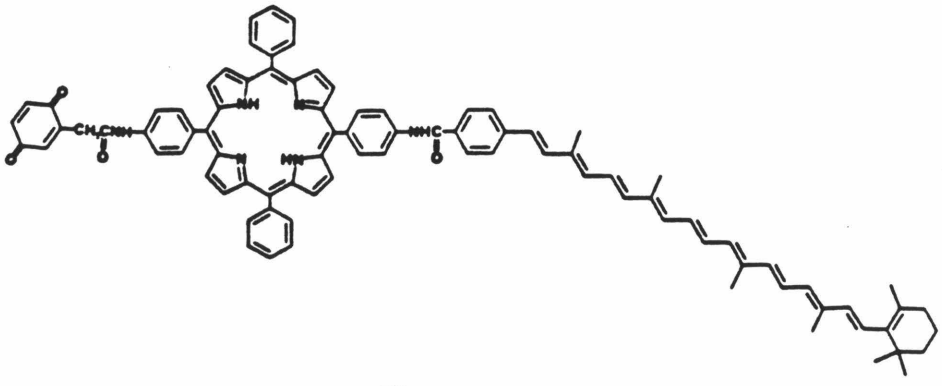

V

Figure 4b. Carotenoid–porphyrin–quinone.[134]

sults imply that carefully constructed systems will ultimately be capable of efficient photoinduced electron transfer, allowing the storage of most of the incident photon energy in the charge–separated state (1.39 eV of the 1.95 eV excitation in **IV**, >1 eV of the 1.8 eV excitation in **V**). The carotenoid–porphyrin–quinone system **V** demonstrates the added advantage of an inherent mechanism for protection of the system from singlet oxygen. The carotenoid component of the molecule has been shown to be capable of rapidly quenching the porphyrin triplet state by energy transfer such that the yield of singlet oxygen in the presence of the carotenoid is substantially reduced.[135] This photoprotection mechanism is important *in vivo*,[136, 137] and will certainly be important for synthetic sytems to minimize the deletarious effects of such a reactive species. This type of system appears to be an effective prototype for a robust synthetic light harvesting system. A derivative of **V** has been shown to be effective for photoexcited transmembrane electron transfer, providing light–driven catalysis of the thermodynamically spontaneous oxidation of ascorbate by ferricyanide ion via electron transfer through a bilayer lipid membrane.[138] The remaining problems to be overcome include the ability to utilize the energy stored in the CT state to drive nonspontaneous chemical reactions.

Experimental Goals

The goals of this research are the design and synthesis of molecular models which allow the investigation of such key electron transfer parameters as (a) distance (b) solvent (c) temperature and (d) exothermicity. A successful intramolecular system will link the donor and acceptor such that minimal chromophore inter-

actions are present to allow individual parameters to be examined with minimal electronic perturbations.

Chapter 3

Synthesis

Design and Synthesis of Rigidly Linked Porphyrin–Quinones

The progress in understanding the enormous success of the photosynthetic unit will undoubtedly be aided by an increased understanding of the fundamental parameters which control electron transfer reactions in general. Intramolecular systems offer distinct advantages to their intermolecular counterparts if unambiguous control of aspects such as donor–acceptor separation distance can be achieved by rational synthetic design. Further insights may well be gained in investigations employing chromophores of direct analogy to photosynthetic RCs. The porphyrin chromophore, of which the natural photosynthetic chromophores are directly related, offers numerous experimental advantages over other donor systems. Not the least of these are the numerous synthetic routes which have been developed over the last century.[139] The large delocalized nature of the porphyrin aromatic system is expected to contribute negligibly to the total reorganization energy (λ) coupled to the electron transfer due to minimal bond length changes associated with oxidation of the porphyrin ring system.[140] Other experimental advantages include large absorption extinction coefficients, and respectable emission quantum yields, facilitating spectroscopic investigations at the low concentrations required to minimize intermolecular events. The porphyrin ring system is an extremely versatile chelator, and virtually every element in the periodic table has been coordinated in the central core,[141] allowing extreme flexiblity for the choice of donor

characteristics. The quinone acceptor was chosen for its importance in the biological realm as the ultimate acceptor in the photosynthetic units. Additionally, the reduction potential of the quinone is readily tunable by synthetic introduction of various substituents.

The choice of an intramolecular donor–acceptor target was an effort to avoid many of the complications of intermolecular systems previously discussed in Chapter 2. The inadequate success of flexibly coupled intramolecular systems for comparison with theory prompted our initial efforts for incorporation of a spacer unit having the characteristics of minimal flexibility and an incremental nature. The bicyclo[2.2.2]octane unit appeared to be the ideal linking unit. Extensive study of energy transfer in systems linked by one and two bicyclo[2.2.2]octyl linkers[142-144] suggested this molecular unit would be ideally suited for investigations of photoinduced electron transfer. The hydrocarbon nature of this linker would additionally offer the advantages of high chemical stability and superior "insulating" characteristics to minimize direct interactions of the donor and acceptor chromophores. The requirement of minimal chromophore interaction is important for maximal relevancy to photosynthetic RCs where the key chromophores are separated by large (~10 Å) distances.[49] The symmetrical nature of the bicyclo[2.2.2]octane unit is highly advantagous in the preparation of oligomers of this linker. The colinear arrangement of single bonds attached to the bridgehead carbons insures identical geometrical orientations between chromophores as a function of repeating linker units in the absence of rotomeric effects.

The synthetic targets for the study of electron transfer are shown below and

consist of an octaalkyl porphyrin linked to a *para*–benzoquinone via zero, one, or two bicyclo[2.2.2]octyl linking units. The bicyclo[2.2.2]octane was chosen as the molecular ruler for investigation of incremental 4 Å changes (per linker unit) in distance on the electron transfer from the photoexcited porphyrin to the quinone. The design and synthesis of the single bicyclo[2.2.2]octane linked system was championed by A.D. Joran, and full characterization of this compound can be found elsewhere.[145] The zero and two linker homologs are described herein.

The octaalkyl porphyrin unit was chosen largely for its superior excited state energetics and reasonable synthetic achievability. While a statistical synthetic approach is feasible, in which the requisite bicyclo[2.2.2]octyl substituted benzaldehyde, benzaldehyde (or tolylaldehyde), and pyrrole are combined to yield a tetraphenyl porphyrin analog, the generally low yields for this reaction prompted the alternative synthetic approach used here. Tetraphenyl porphyrins have the added disadvantage of a higher oxidation potential and lower singlet excitation energies[141] which could hamper investigations of highly exothermic reactions for probing the existence of the inverted region for photoinduced electron transfers.

Initial targets in this research were aimed at direct coupling of the bicyclo[2.2.2]octyl unit to the porphyrin ring, and are briefly described here for the benefit of future workers in the field. The steric constraints at the *meso*–position of the porphyrin thwarted several alternative approaches to such a direct coupling. The statistical approach described above in which a bicyclo[2.2.2]octane substituted at the bridgehead carbon with an aldehyde functionality proved unsuccessful at competing with the more reactive benzaldehyde reagent, resulting in

the exclusive isolation of tetraphenyl porphyrin. Even the reaction of this aldehydic bicyclo[2.2.2]octane, pyrrole, and the substantially less reactive aliphatic butyraldehyde resulted only in the isolation tetra–propyl porphyrin and no evidence for incorporation of the bicyclo[2.2.2]octyl linker unit. Numerous alternative approaches via synthesis of bicyclo[2.2.2]octyl substituted dipyrrylmethanes were also unsuccessful.[145] It is noteworthy that no porphyrins with tertiary substituents at the *meso*–position have been reported in the literature either natural or synthetic. A closely related porphodimethene structure has been reported[146] which could not be oxidized to the corresponding porphyrin, presumably due to the steric bulk of the *meso*–*tert*–butyl groups.

The first system successfully prepared in this research[145] incorporated a phenyl spacer unit to reduce steric constraints at the porphyrin *meso*–position. The general synthetic approach[147] involves the preparation of a substituted benzaldehyde derivative for condensation with a tetra–pyrrolic *ac*–biladiene[148] (see below). The condensation of aromatic and aliphatic aldehydes with *ac*–biladienes had been shown to give reasonable yields of *meso*–substituted porphyrins[149] and suggested this approach would be viable.

While the presence of the phenyl ring results in an ambiguous coupling with the porphyrin π–system, it has been held constant throughout the series and will allow the investigation of the incremental distance effects on electron transfer irrespective of this complication. It should be noted that although the phenyl ring is presented coplanar with the porphyrin ring in Figure 1, it is quite rigidly perpendicular to the π–system due to the presence of the flanking methyl groups.

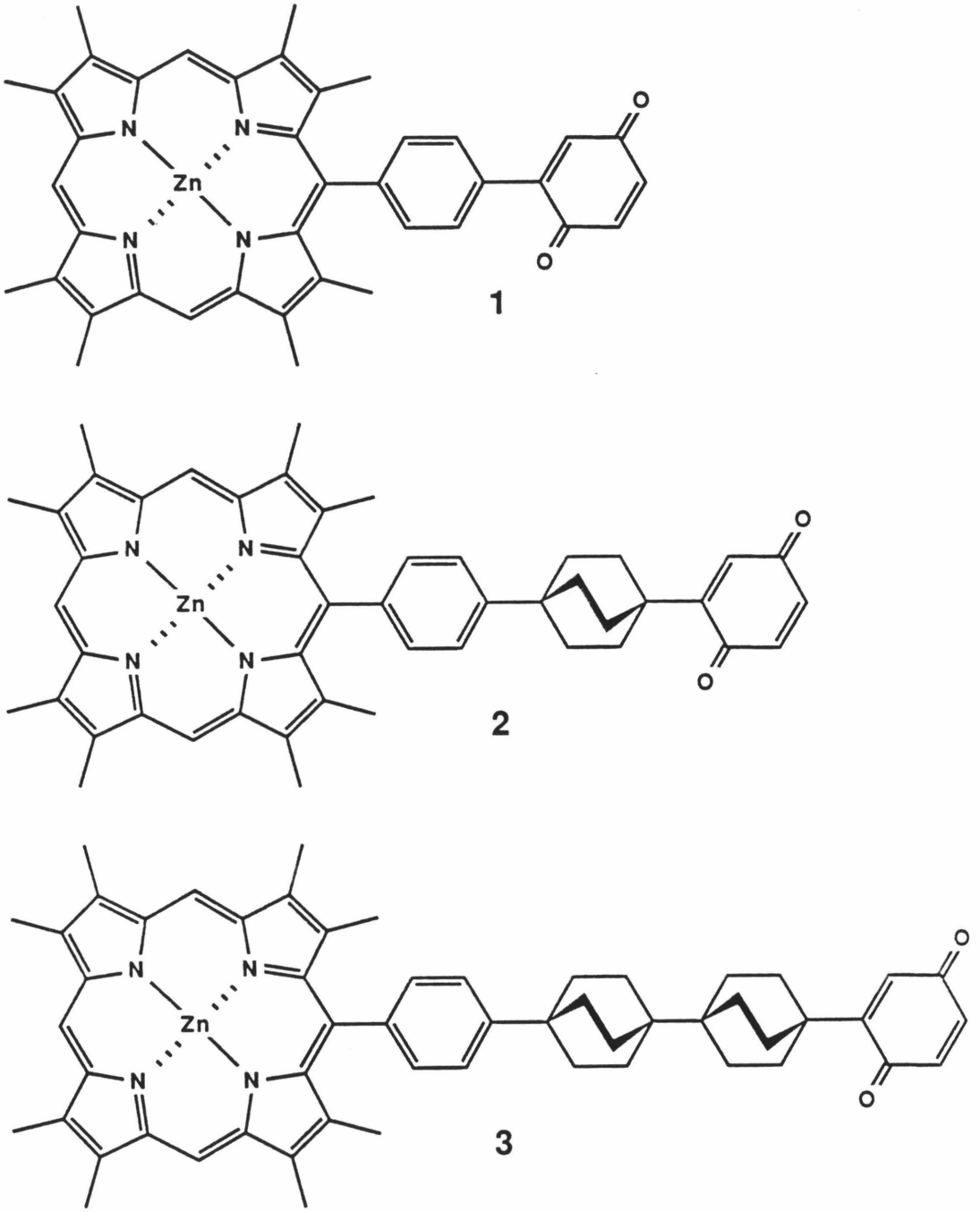

Figure 1. Porphyrin–quinone series for investigation of incremental distance effects on electron transfer rates. Edge–to–edge separation distances (based on Dreiding models) are 6, 10, and 14 Å for **1**–**3**, respectively.

The barrier to phenyl rotation in tetraphenyl porphyrins ranges from ~18 kcal/mol in the absence of flanking groups at the β positions of the pyrrole rings,[112] to $\geq$26 kcal/mol for ortho substituted *meso*–phenyl groups,[150] and is expected to be a very large barrier in the systems under investigation here. The only rotational freedom of the *meso*–phenyl ring in the compounds under investigation here is a "wobble" frequency of undetermined magnitude.

The synthesis of the requisite bibicyclo[2.2.2]octane precursor is shown in Scheme I. The first six steps were known and are a modification of the original approach used by Brown.[151] Minor modifications of the original procedure included the use of an alternative decarboxylation procedure[152] for substantially increased yields of olefin **9**. The synthesis of compounds **12–16** followed the original procedures of Zimmerman, *et al.*[142,143] The conversion of **16** to the required bibicyclo[2.2.2]octyl benzaldehyde derivative **20** (Scheme II) represent new chemistry and full characterization of the intermediates can be found in Chapter 7.

Heterofunctionality of the bicyclo[2.2.2]octyl unit is achieved by reaction of the key diiodobicyclo[2.2.2]octyl derivative **11** with one equivalent of silver acetate. Subsequent steps in the synthesis exploit the reaction characteristics of the differentiated ends of the bicyclo[2.2.2]octane unit. A key step in the reaction scheme is the conversion of the dimethoxy–bibicyclo[2.2.2]octyl derivative **15** to the iodo–alcohol derivative **16**. This is a curiously successful reaction that presumably is a consequence of the differing solubility characteristics of the dimethoxy–bibicyclo[2.2.2]octane starting material and the iodo–alcohol product in the benzene–HI emulsion as originally proposed by Zimmerman, *et al.*[143] This reaction was un-

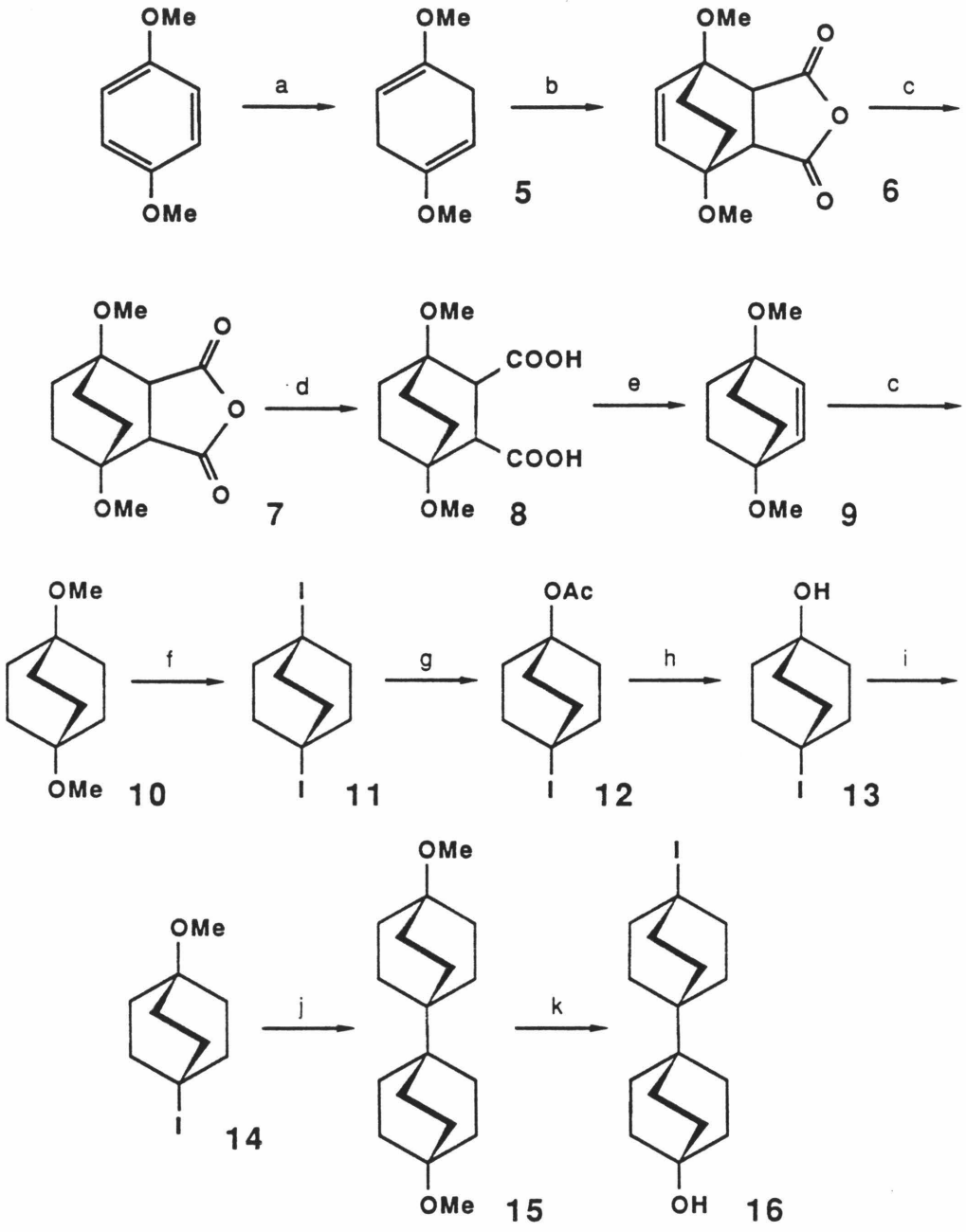

Scheme I. Synthesis of bibicyclo[2.2.2]octyl precursors.

Notes for Scheme I: a) Li/NH_3. b) Maleic anhydride, $CHCl_3$, Δ. c) H_2, Pd catalyst. d) H_2O, 1,2 dimethoxyethane, Δ. e) Cu_2O, 2, 2′ dipyridyl, quinoline, Δ. f) 57% HI, Δ. g) AgOAc, HOAc, Δ. h) KOH, EtOH, Δ. i) CH_3I, NaH, 1,2 dimethoxyethane. j) Mg, Et_2O, $NiCl_2$, Δ. k) C_6H_6, HI, Δ.

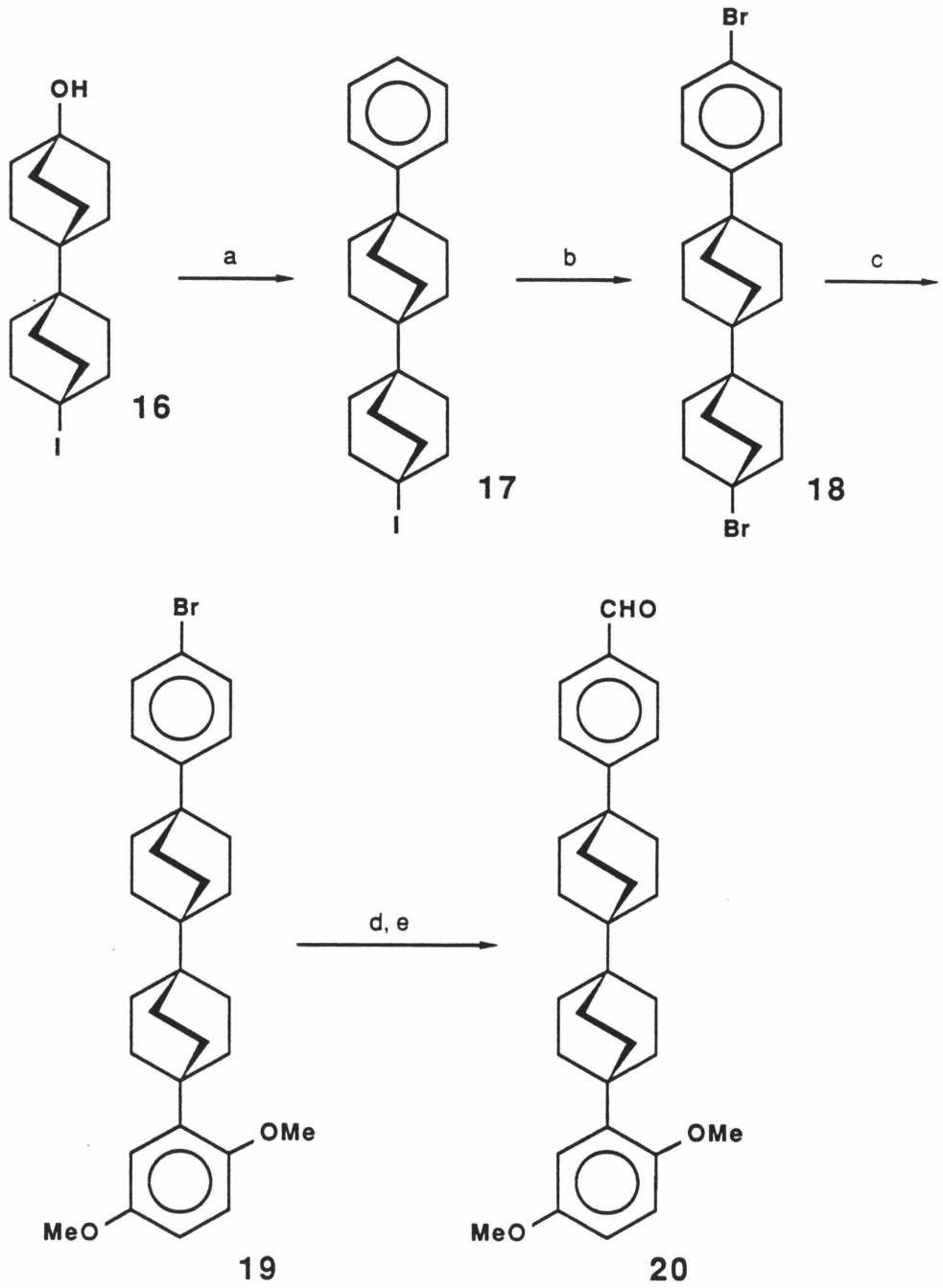

Scheme II. Synthesis of bibicyclo[2.2.2]octyl substituted benzaldehyde **20**.

Notes for Scheme II: a) C_6H_6, BF_3, *p*–TsOH, Δ. b) Fe, Br_2, CCl_4, Δ. c) Dimethoxybenzene, 1,2 dichloroethane, $AlBr_3$, Δ. d) *n*–BuLi, THF, –78° C. e) DMF, –78° C.

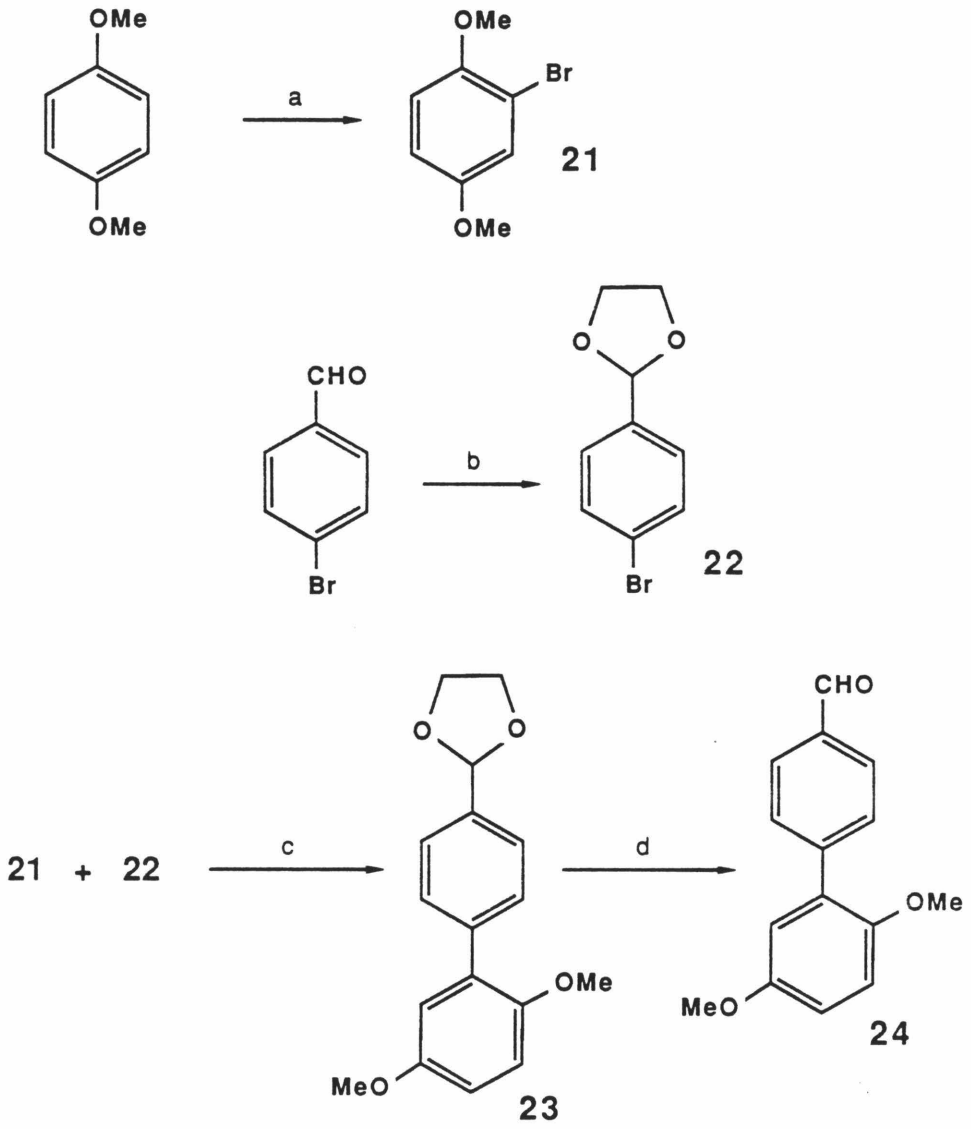

Scheme III. Synthesis of biphenyl aldehyde **24**.

Notes for Scheme III: a) KBr, EtOH, H_2SO_4, H_2O_2, Δ. b) Ethylene glycol, *p*–TsOH, toluene, azeotrope. c) Mg, THF, $Ni(P\emptyset_3)_2Cl_2$, Δ. d) H^+, Δ.

successful on the single bicyclo[2.2.2]octane derivative in our hands, but preparation of the diiodo derivative **11** was achieved by treatment of **10** with 57% HI at elevated temperatures. The iodo–alcohol derivative **16** could likely have been prepared analogously to the single linker derivative by conversion of dimethoxy–bibicyclo[2.2.2]octyl derivative **15** to a diiodo derivative and subsequent treatment with silver acetate, but the pioneering work by Zimmerman[143] resulted in a savings of two steps in the synthetic sequence.

Subsequent steps make extensive use of Friedel–Crafts chemistry to sequentially functionalize the ends of the bibicyclo[2.2.2]octyl linker with the phenyl and dimethoxybenzene groups (Scheme II). The dimethoxybenzene group selected as a robust protecting group readily transformed to the quinone functionality. While the current synthetic sequence involves a Friedel–Crafts alkylation of dimethoxybenzene by the bromo–bibicyclo[2.2.2]octyl derivative **18** using aluminum bromide as the catalyst, it is generally preferable to use the superior BF_3 catalyzed alkylation using bridgehead alcohol derivatives when available. Conversion of the bridgehead bromide to the alcohol proved troublesome, and the current synthetic sequence relies on the less superior aluminum bromide catalyzed alkylation. Conversion of the bromophenyl derivative **19** to the required benzaldehyde derivative **20** was achieved by standard metal–halogen exchange conditions and formylation with *N,N*–dimethylformamide.[153]

Initial synthetic efforts examined the possibility of cross–coupling reactions involving Grignard reagents or organolithiums to couple the bicyclo[2.2.2]octyl unit to aromatic residues following the procedures of Kumada, *et al.*[154] If a suc-

cessful coupling had been achieved, this may have allowed a direct coupling of the bicyclo[2.2.2]octyl unit to the porphyrin (*e.g.*, at a β position as opposed to the *meso*–carbon). This organometallic coupling procedure was demonstrated to be extremely efficient for coupling aromatics with alkenyl reactants or other aromatics, but the coupling of tertiary reagents enjoyed considerably less success. Further refinements in the Friedel–Crafts reaction conditions and successes in the preparation of the *meso*–phenyl porphyrins led to the abandonment of this approach. The organometallic coupling techniques were successfully employed in the preparation of the biphenyl aldehyde intermediate **24** for the preparation of **1**, however, and the synthetic route is shown in Scheme III.

The highly convergent syntheses of compounds **1–3** make use of a modified Woodward[155] approach to synthesize the key *ac*–biladiene used in the synthesis. The full synthesis is shown in Scheme IV. Significant synthetic improvements on the original literature procedures were accomplished by A.D. Joran, resulting in a high yielding route which is discussed in detail elsewhere.[145]

The final step in the synthesis is the condensation of the benzaldehyde derivatives with the *ac*–biladiene (Scheme V). The biladiene has only limited stability and was never stored for long periods of time. The best results were obtained by preparation of the biladiene immediately before condensation with the benzaldehyde derivatives (*e.g.*, **20** or **24**) and discarding any unused material. The biladiene condensation is a general reaction for the preparation of *meso*–substituted porphyrins[149] and resulted a highly convergent overall synthesis. Solubility problems in the bis–linker series resulted in substantially reduced, but tolerable yields

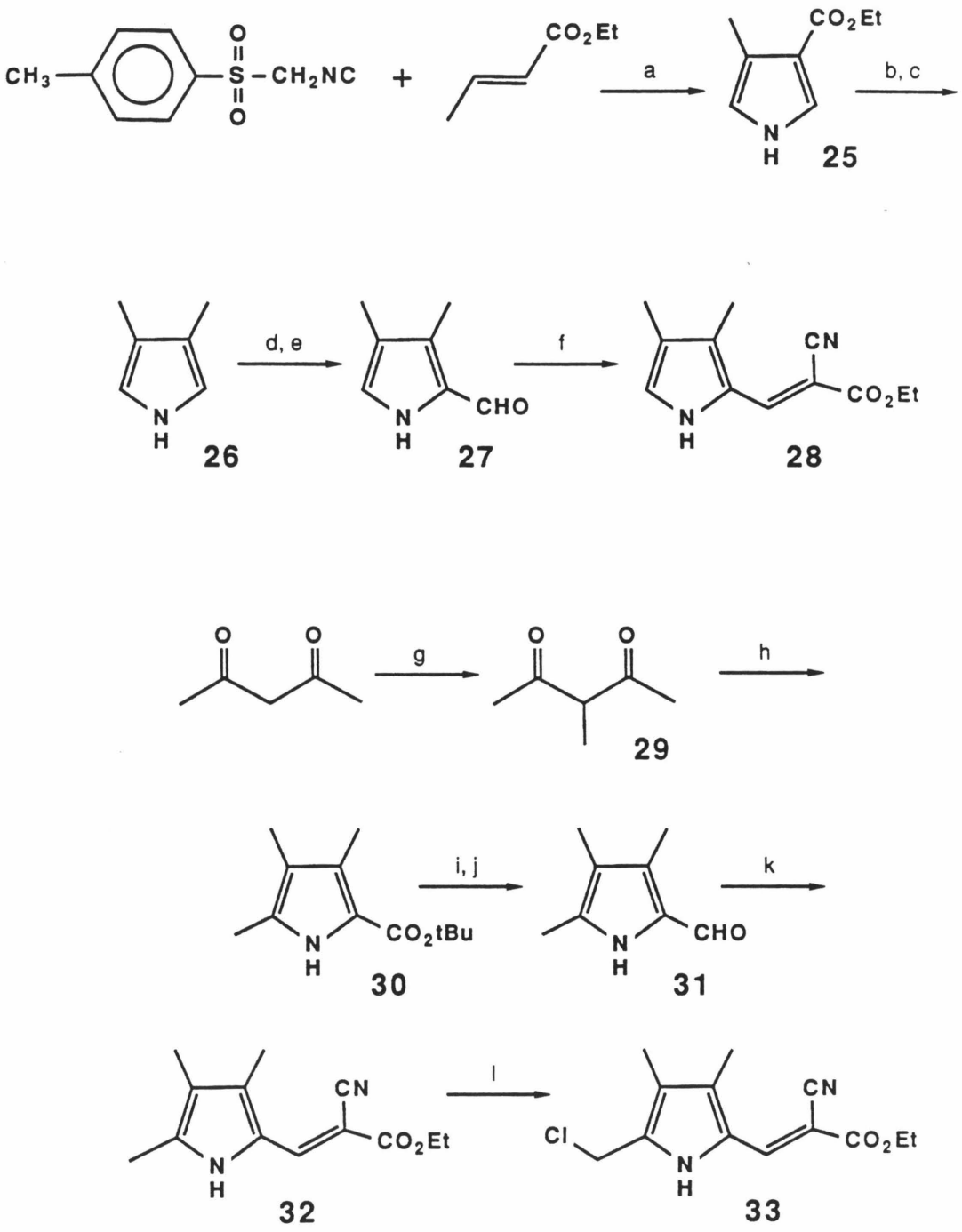

Scheme IV. Synthesis of *ac*–biladiene.

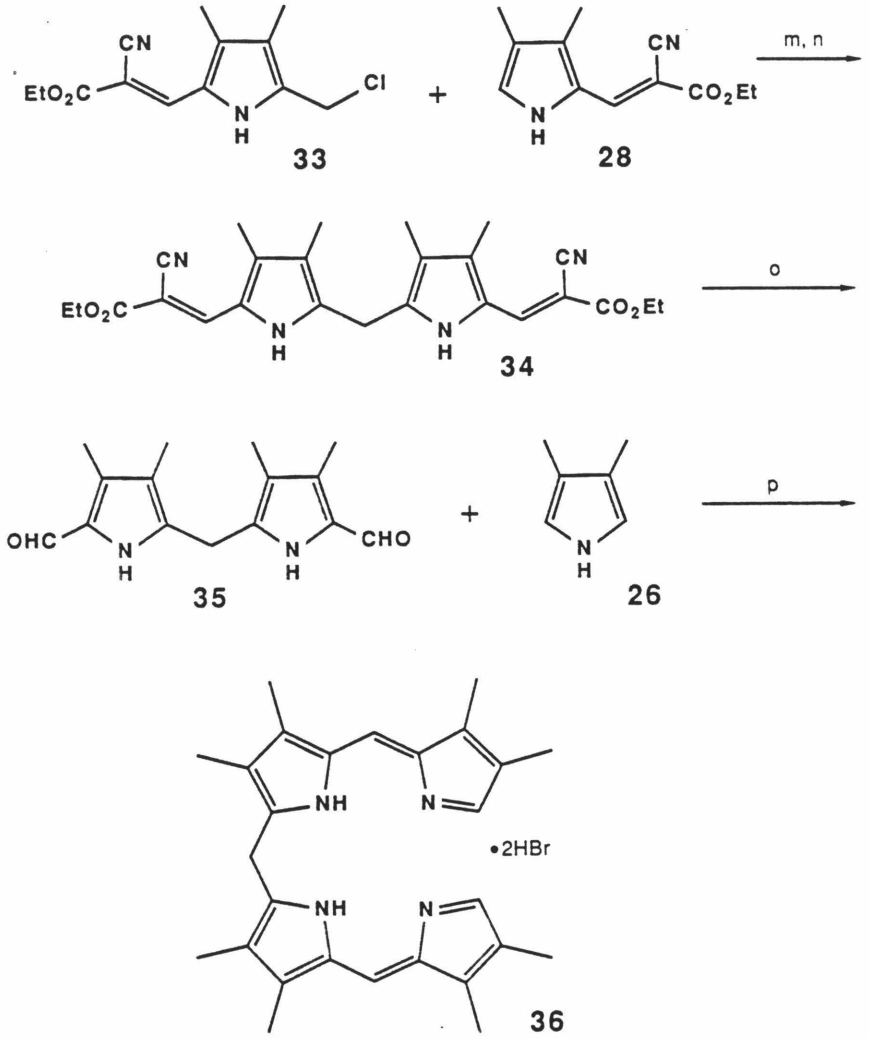

Notes for Scheme IV: a) NaH, DMSO, Et_2O. b) Sodium bis(methoxyethoxy)aluminumhydride, toluene, 25°. c) HCl, H_2O. d) DMF, benzoyl chloride. e) Sodium carbonate, H_2O. f) Ethyl cyanoacetoacetate, diethylamine, benzene, azeotrope. g) CH_3I, K_2CO_3, Δ. h) *t*–Butyl acetate, sodium nitrite, acetic acid → Zn, Δ. i) DMF, benzoyl chloride. j) Ammonium hydroxide. k) Ethyl cyanoacetoacetate, diethylamine, benzene. l) SO_2Cl_2, CH_2Cl_2. m) $SnCl_4$. n) HCl, H_2O. o) NaOH, MeOH, Δ. p) HBr, MeOH, Δ.

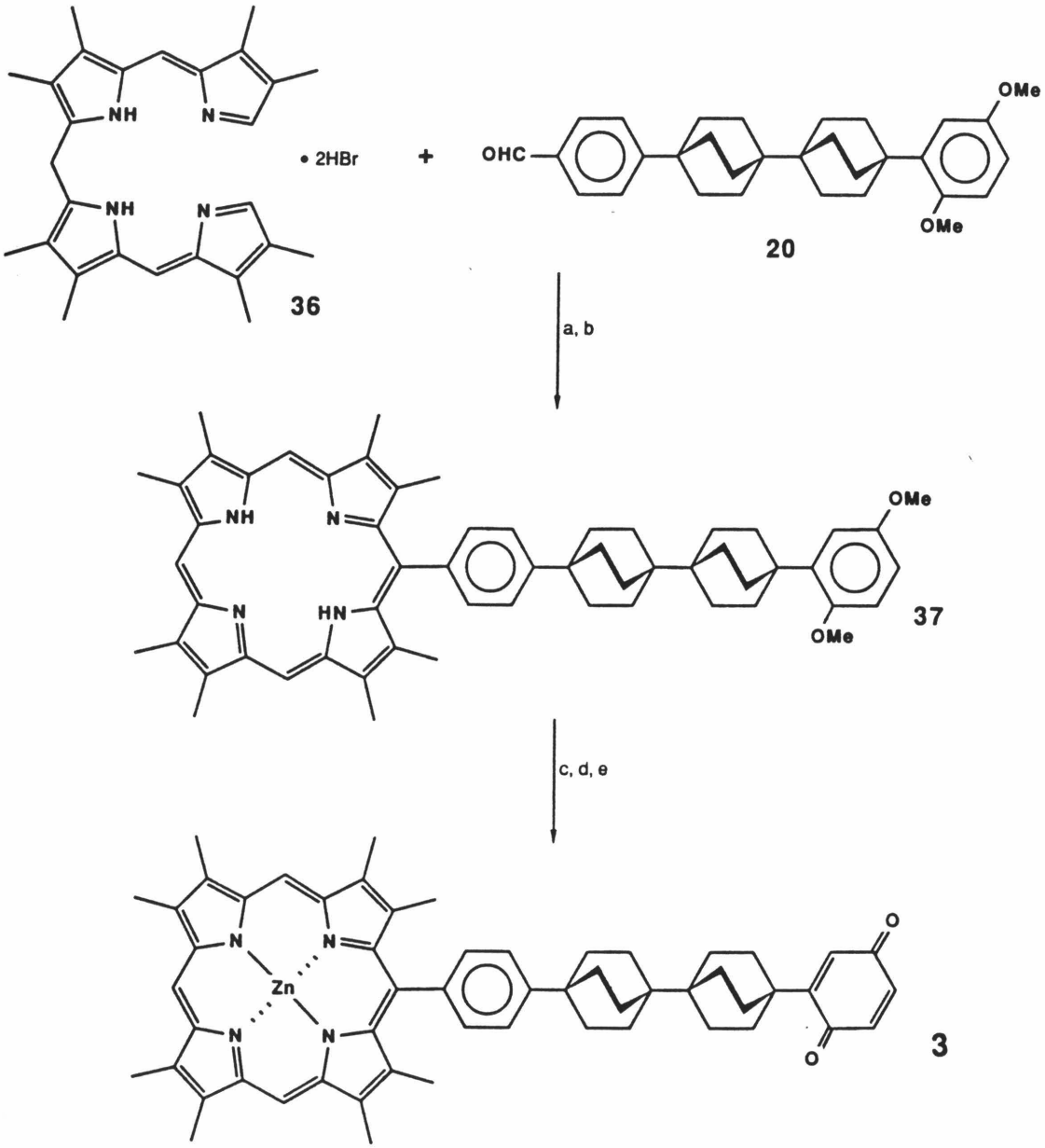

Scheme V. Synthesis of porphyrin–bibicyclo[2.2.2]octyl–quinone **3**.

Notes for Scheme V: a) HBr, HOAc, MeOH, Δ, air. b) $NaHCO_3$. c) BI_3, CH_2Cl_2. d) $Zn(OAc)_2 \bullet 2H_2O$, MeOH, CH_2Cl_2 e) PbO_2, CH_2Cl_2.

of the bis–linked porphyrin derivative **3** compared to the zero or mono–linked compounds.

Flash chromatographic purification[156] of the porphyrin was employed to separate unreacted aldehyde (recovered as the dimethylacetal), and biladiene starting materials, as well as bilatriene and corrole (from oxidative closure of the biladiene) side products. The methyl ethers were then deprotected with boron triiodide to yield the porphyrin–hydroquinone. Boron triiodide[157] proved superior to the earlier reaction conditions employing boron tribromide due to increased yields and reduced reaction times. Generally 25–50 equivalents of a freshly–prepared solution of BI_3 in dry methylene chloride were required for complete deprotection. The use of BBr_3 usually required at least 100 equivalents and a 12–hour reaction time, and was accompanied by increased porphyrin degradation and lower overall yields. The porphyrin–hydroquinone was metallated by standard metallation conditions ($Zn(OAc)_2 \bullet 2H_2O/CH_3OH/CH_2Cl_2$), oxidized to the quinone with lead dioxide in CH_2Cl_2, and subjected to the final purification by flash chromatography to yield the zinc metallo–porphyrin–quinones **1–3**.

Synthesis of Porphyrin–Quinones for Exothermicity Investigations

To investigate the dependence of k_{ET} on reaction exothermicity (ΔG°) a series of porphyrin–quinones were prepared by the general route described in detail above and elsewhere.[145] Dynamic fluorescence lifetime measurements (discussed in Chapter 5) revealed that the single bicyclo[2.2.2]octyl linked derivative exhibited a highly quenched emission lifetime corresponding to a fast electron transfer

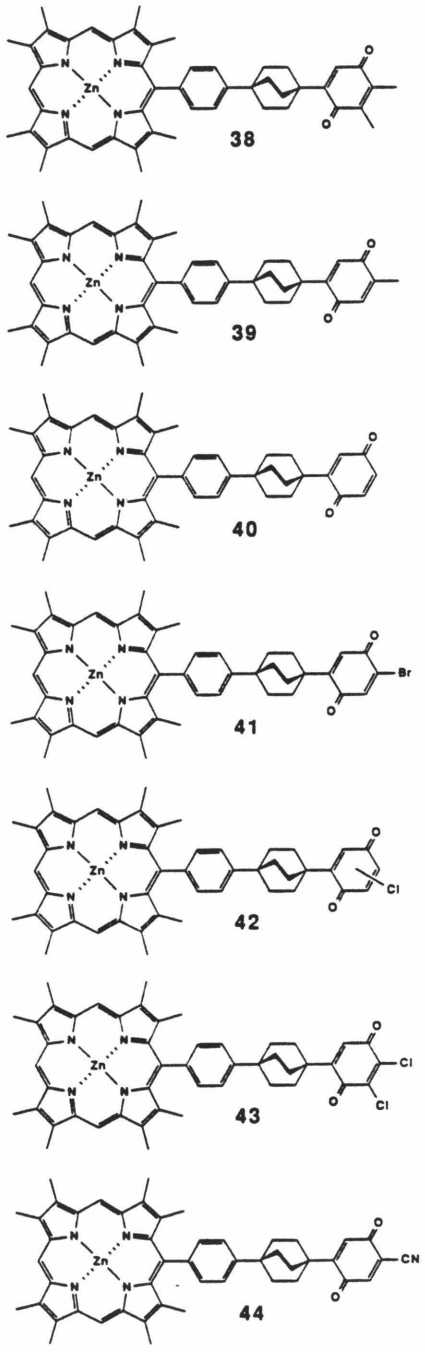

Figure 2. Synthetic porphyrin–quinones for investigation of exothermicity effects on photoinduced electron transfer rates.

deactivation pathway which can effectively compete with the natural deactivation pathways for the porphyrin excited singlet. A series of derivatives based on the single bicyclo[2.2.2]octyl linked compound was then designed to probe the changes in k_{ET} as a function of of reaction exothermicity. The complete series of porphyrin–quinones are shown in Figure 2. To minimize ambiguities in reaction series homology, our goal was to maintain the *p*–benzoquinone functionality throughout the series. Reasonable modulation of the quinone reduction potential was achievable by preparation of variously substituted quinones. The derivatives synthesized were mono– or di–subsituted *p*–benzoquinones, with substitutents of methyl, halogen, or cyano groups. The *structurally* homologous series was prepared by modifications to the highly general route discussed above. The key intermediates required in all cases were the bicyclo[2.2.2]octyl substituted benzaldehydes. The methyl–, dimethyl– and cyano–quinone, and unsubstituted derivatives (**38**, **39**, **44**, and **2** or **40**, respectively) were prepared by A.D. Joran and are described elsewhere.[145]

The synthesis of the bromo–derivative is shown in Scheme VI. The starting material for the sequence was the key benzaldehyde intermediate used in the preparation of **2**.[145] Bromination of this material was accomplished by treatment of the aldehyde with bromine in the absence of light. The electrophylic bromination of the dimethoxybenzene group of the molecule proceeded quantitatively. NMR analysis of the product indicated the bromine was exclusively *para* to the bicyclo[2.2.2]octyl linker. The purified aldehyde was then condensed with the *ac*–biladiene to generate the porphyrin–bromodimethoxybenzene derivative. Standard

deprotection, metallation, and oxidation conditions yielded the porphyrin–bicyclo[2.2.2]octyl–bromoquinone **41**.

The chloro–derivatives were prepared in a slight modification of the above sequence. Extensive investigations encountered substantial difficulties in regioisomeric control of the direct chlorination of *tert*–butyl–2,5–dimethoxybenzene as a model compound.[158] Exhaustive chlorination in an effort to prepare a tri–choro derivative was also unsuccessful. Presumably the position α to the *tert*–butyl was protected by the steric bulk of this group. An alternate procedure used in the preparation of the chloro–quinone derivatives in a synthetic steriod system[115] was investigated.[148] Addition of HCl to methyl–2,5–benzoquinone as a model compound indicated that maximal control of the regiochemistry of the addition was possible with tetrahydrofuran as the reaction solvent. Previous investigations in the literature[159] suggested minimal regiocontrol with other reaction solvents. Analysis of the HCl addition product to methyl–benzoquinone indicated that the chlorine was quantitatively incorporated *para* to the methyl group within the NMR detection limits. This approach appeared to offer the distinct advantage of sequential chlorination of the quinone functionality. This high degree of regioselectivity could not be reproduced under identical reaction conditions with the bicyclo[2.2.2]octyl derivative, however, resulting in the isolation of a 3:2 ratio of the *para*– to *meta*–chloro derivatives. While this may change the vibronics governing the electron transfer for this derivative, it was included in the series for direct comparison with the bromo–derivative discussed above. Consistent with the model chlorinations, conversion of the monochloro to the dichloro derivative was

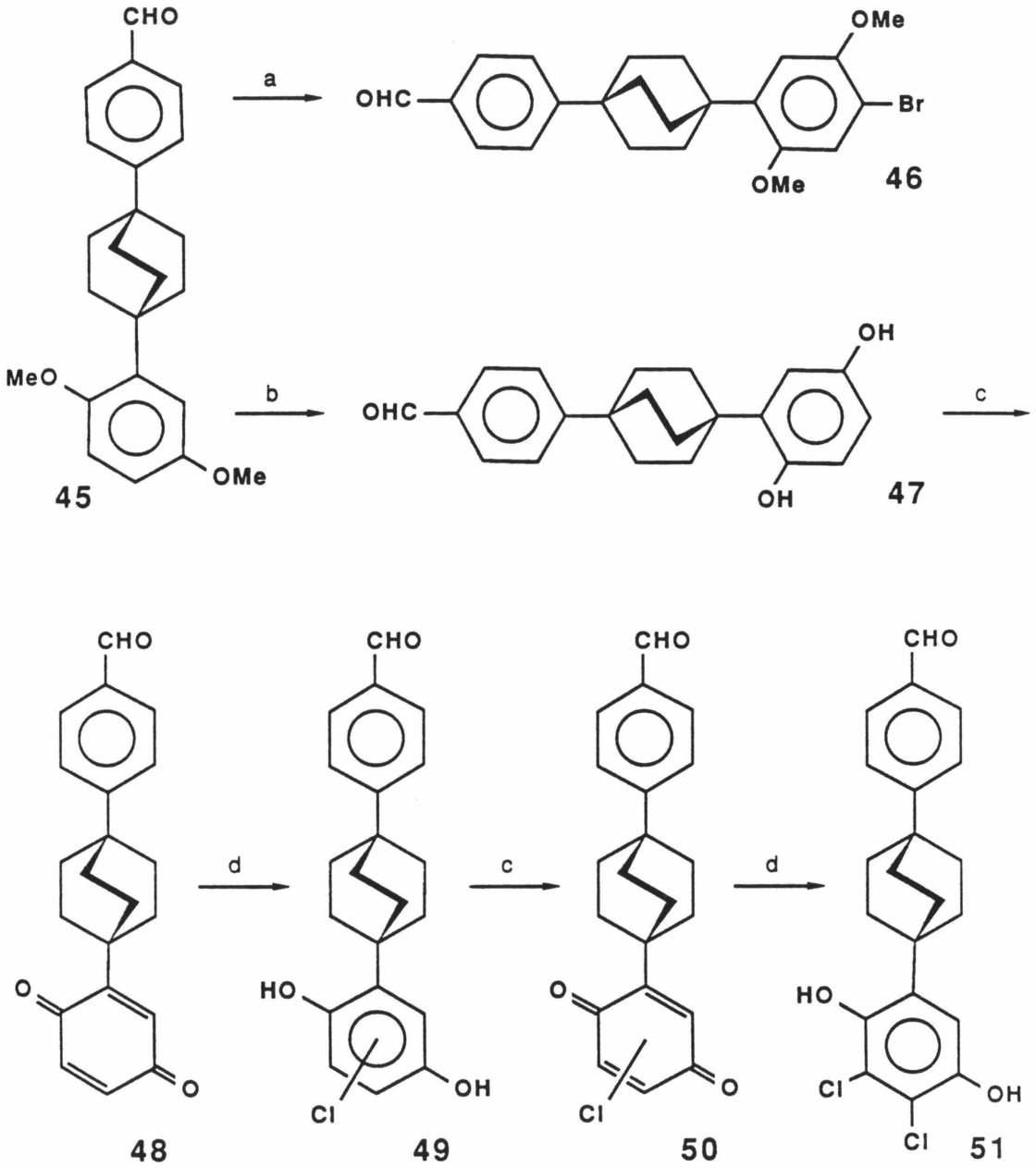

Scheme VI. Synthesis of benzaldehyde derivatives for modified quinone compounds.

Notes for Scheme VI: a) Br_2, 1,2–dichloroethane, 0°C. b) BI_3, CH_2Cl_2, 0°C. c) PbO_2, CH_2Cl_2, Δ. d) HCl(g), THF, 0°C.

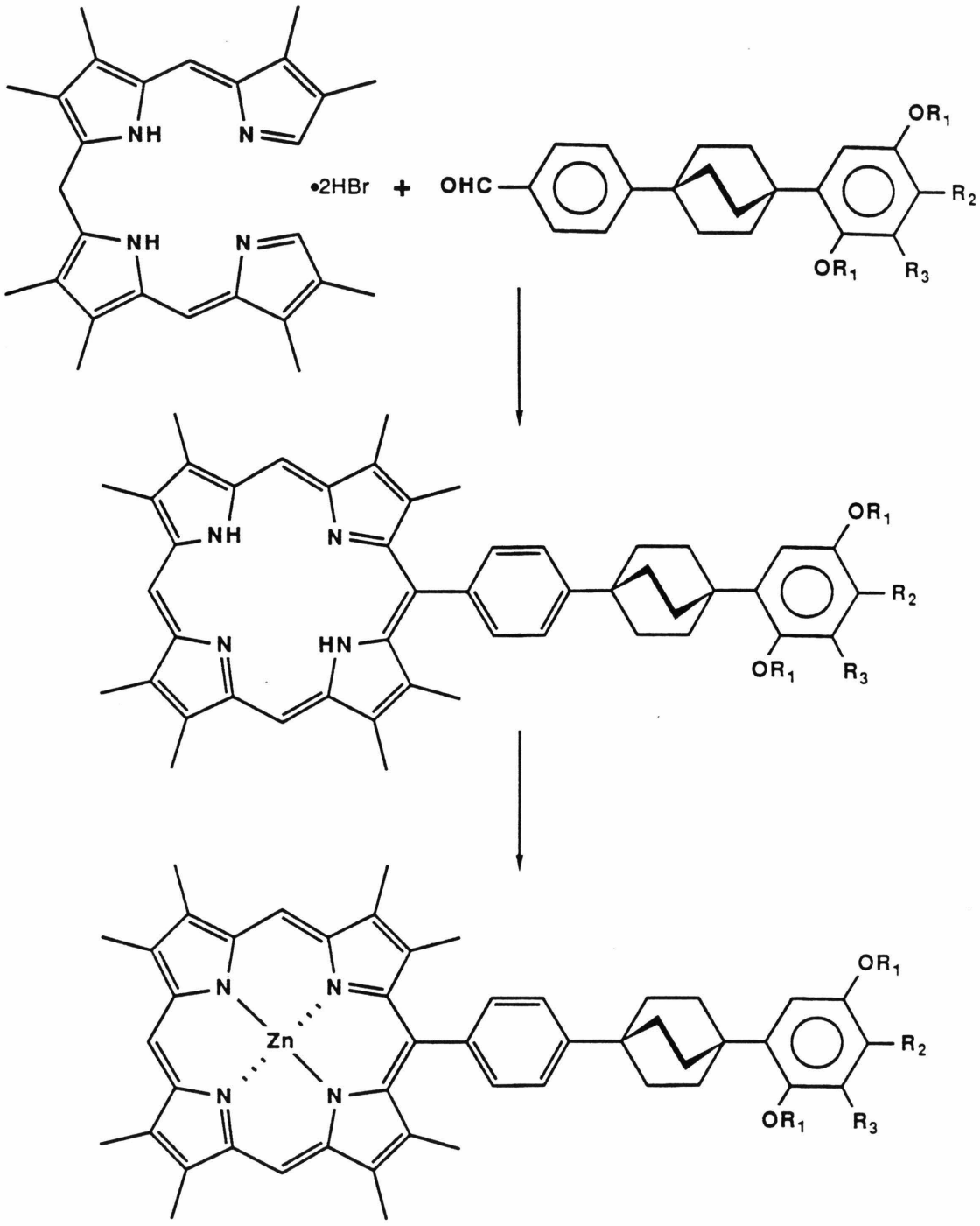

Scheme VII. Synthesis of modified porphyrin–bicyclo[2.2.2]octyl–quinones.

Notes for Scheme VII: $\mathbf{R}_1$ = –Me, $\mathbf{R}_2$ = –Br, $\mathbf{R}_3$ = –H. $\mathbf{R}_1$ = $\mathbf{R}_3$ = –H, $\mathbf{R}_2$= –Cl. $\mathbf{R}_1$ = –H, $\mathbf{R}_2$ = $\mathbf{R}_3$ = –Cl.

straightforward, and no evidence for scrambling of the chlorine between the two remaining ring positions was observed. The full synthetic approach is outlined in Scheme VI and VII.

Electronic Spectra

The absorption spectra of several of the metallo and free–base porphyrin derivatives are presented in Figures 3–13. The spectrum of the [5–(*p–tert*–butylphenyl)–2, 3, 7, 8, 12, 13, 17, 18–octamethylporphyrinato] zinc(II) reference compound[145] (*ZnP^{t}Bu*) is shown in Figure 8 for comparison with the quinone–linked compounds. The spectra are well described by the sum of the individual chromophores and indicate minimal interactions between the porphyrin and the quinone. A possible exception may be the directly linked quinone derivative shown in Figure 3. The visible bands of the porphyrin appear to have slightly broadened and may indicate some interaction is possible in the absence of the bicyclo[2.2.2]octyl linker. If the *meso*–phenyl ring is not rigidly perpendicular to the porphyrin π–system, it will no longer act as a σ–insulating framework, and direct interactions through the π–system may well be possible. The changes in the visible bands for this compound are considerably weaker than those observed for a directly coupled (*i.e.*, lacking the phenylbicyclo[2.2.2]octyl unit) quinone system prepared by A.D. Joran[145] which demonstrated dramatic broadening of the porphyrin visible bands. The porphyrin–quinones incorporating the bicyclo[2.2.2]octyl linker(s) are free of this behavior, and the spectra are virtually superimposable, with the exception of the UV band at approximately 250 nm attributed to the quinone absorption. The

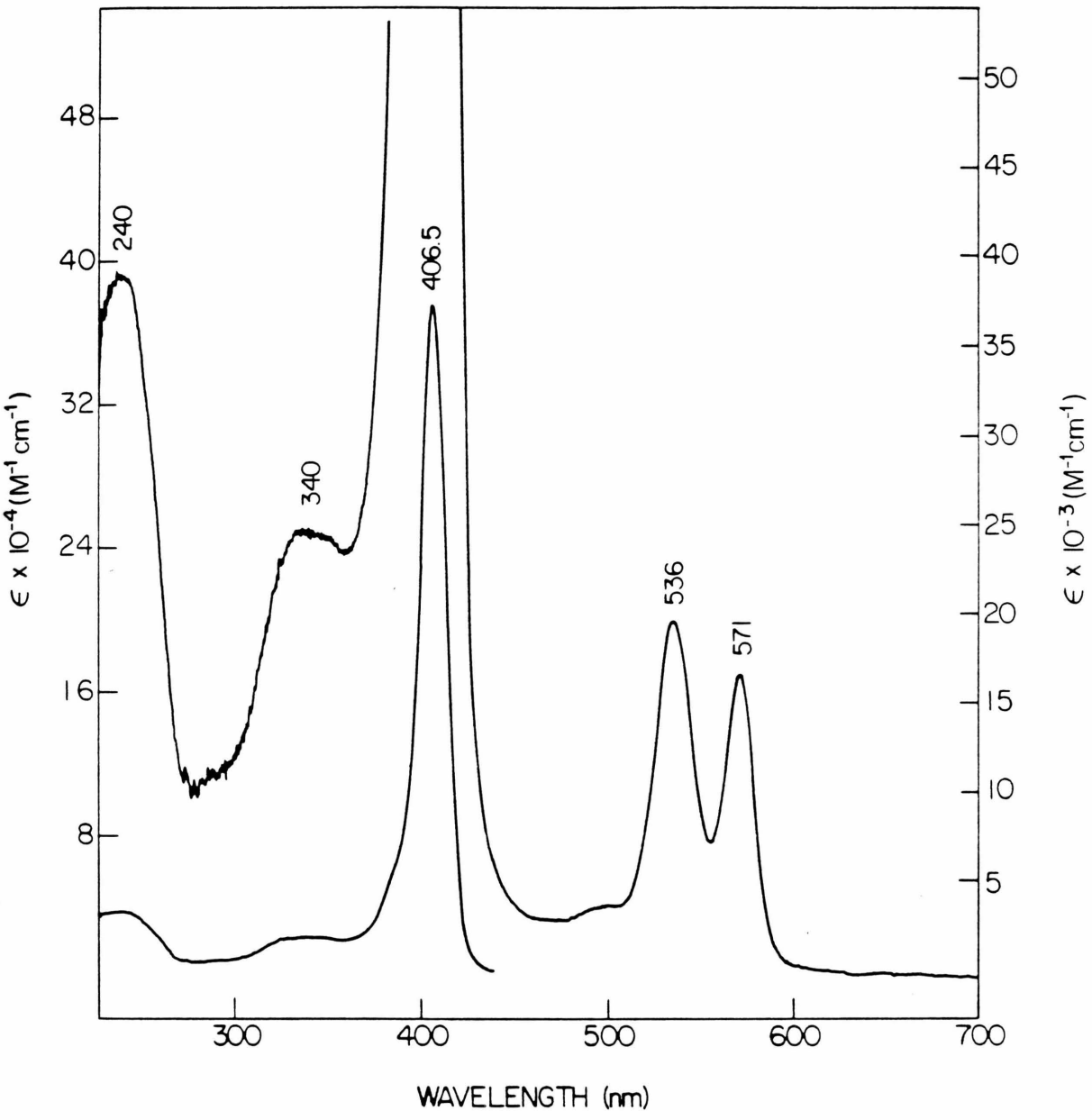

Figure 3. Electronic spectrum of *ZnP0Q* in $CHCl_3$.

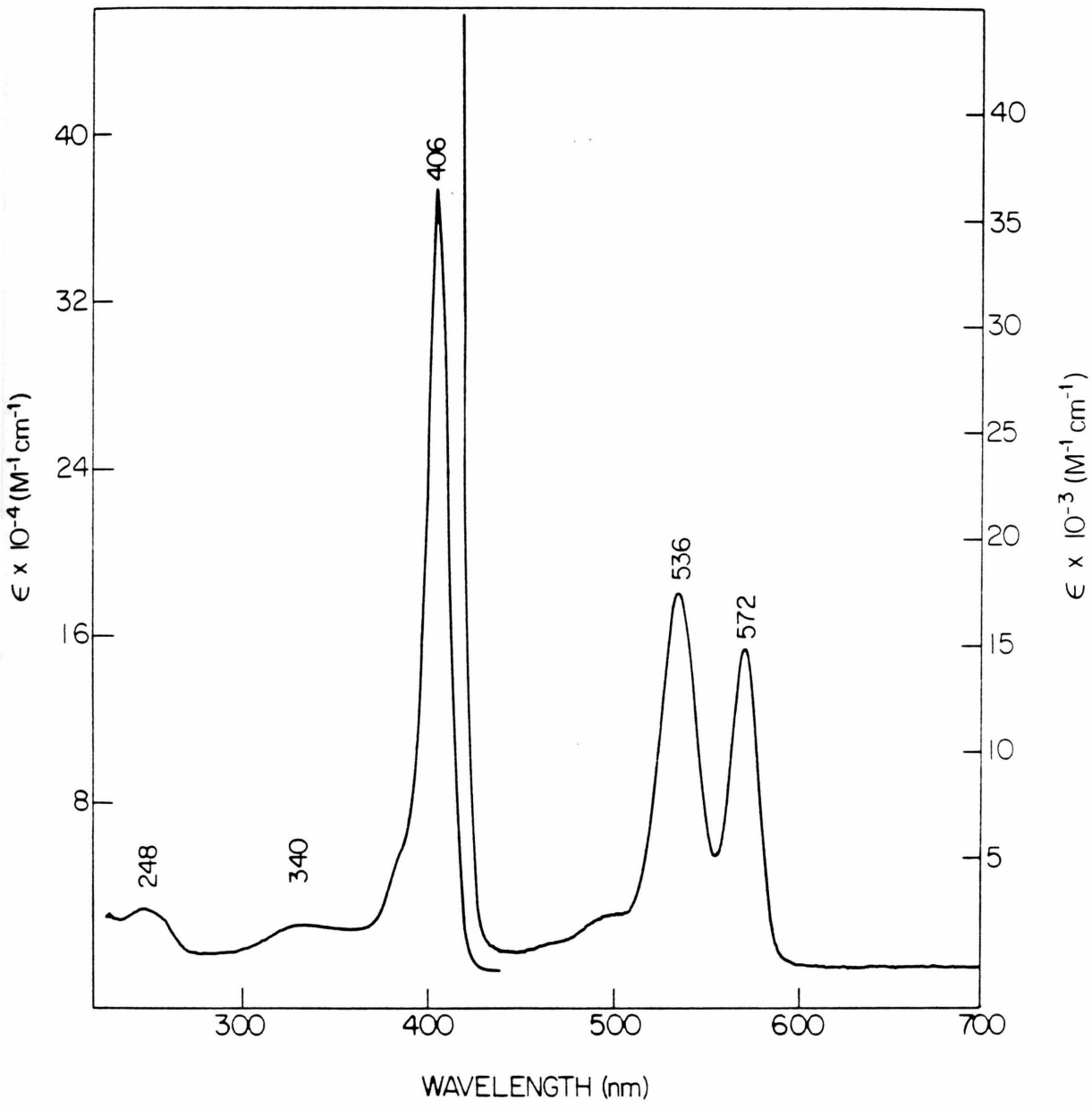

Figure 4. Electronic spectrum of *ZnP2Q* in $CHCl_3$.

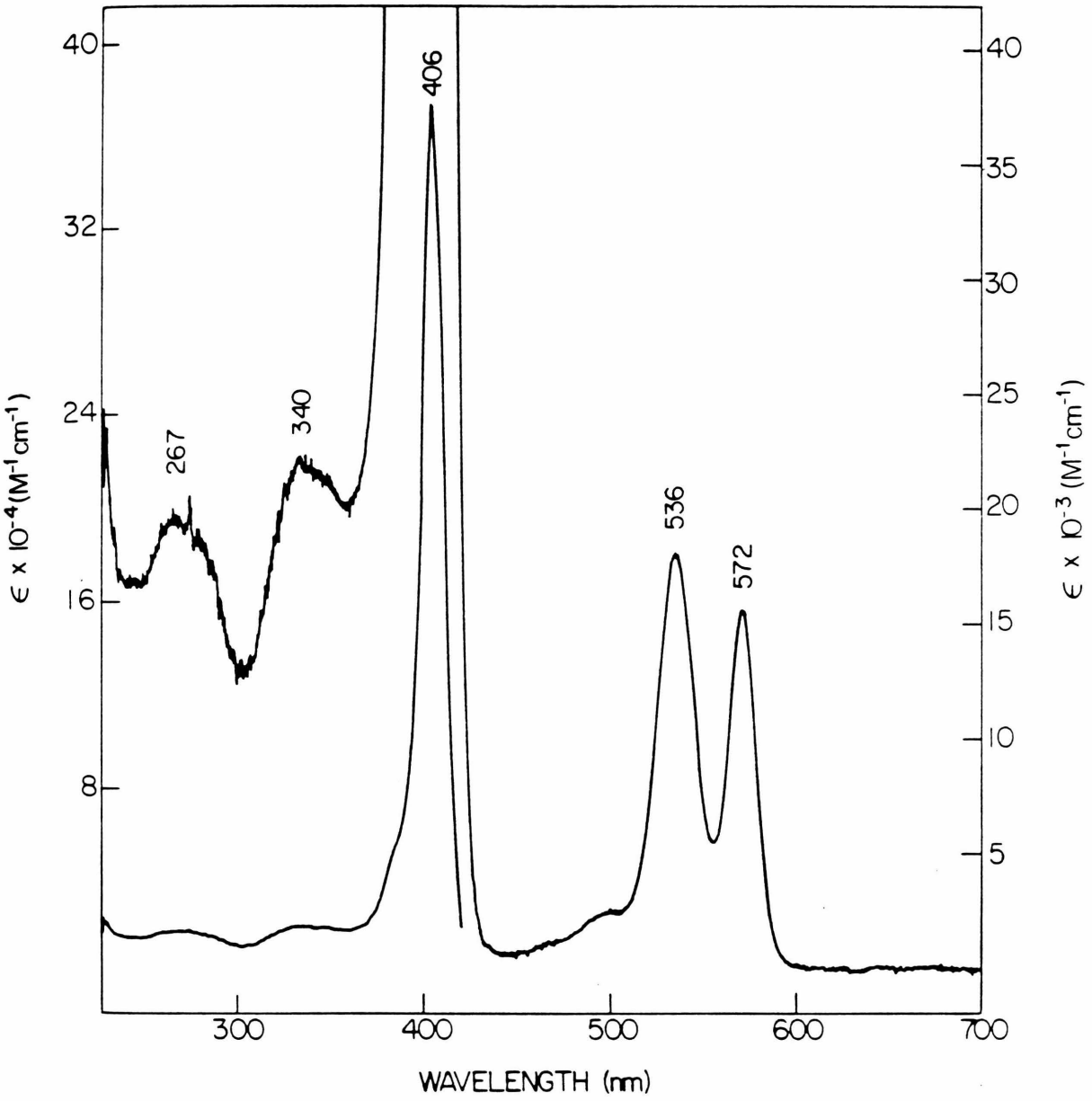

Figure 5. Electronic spectrum of *ZnP1QBr* in $CHCl_3$.

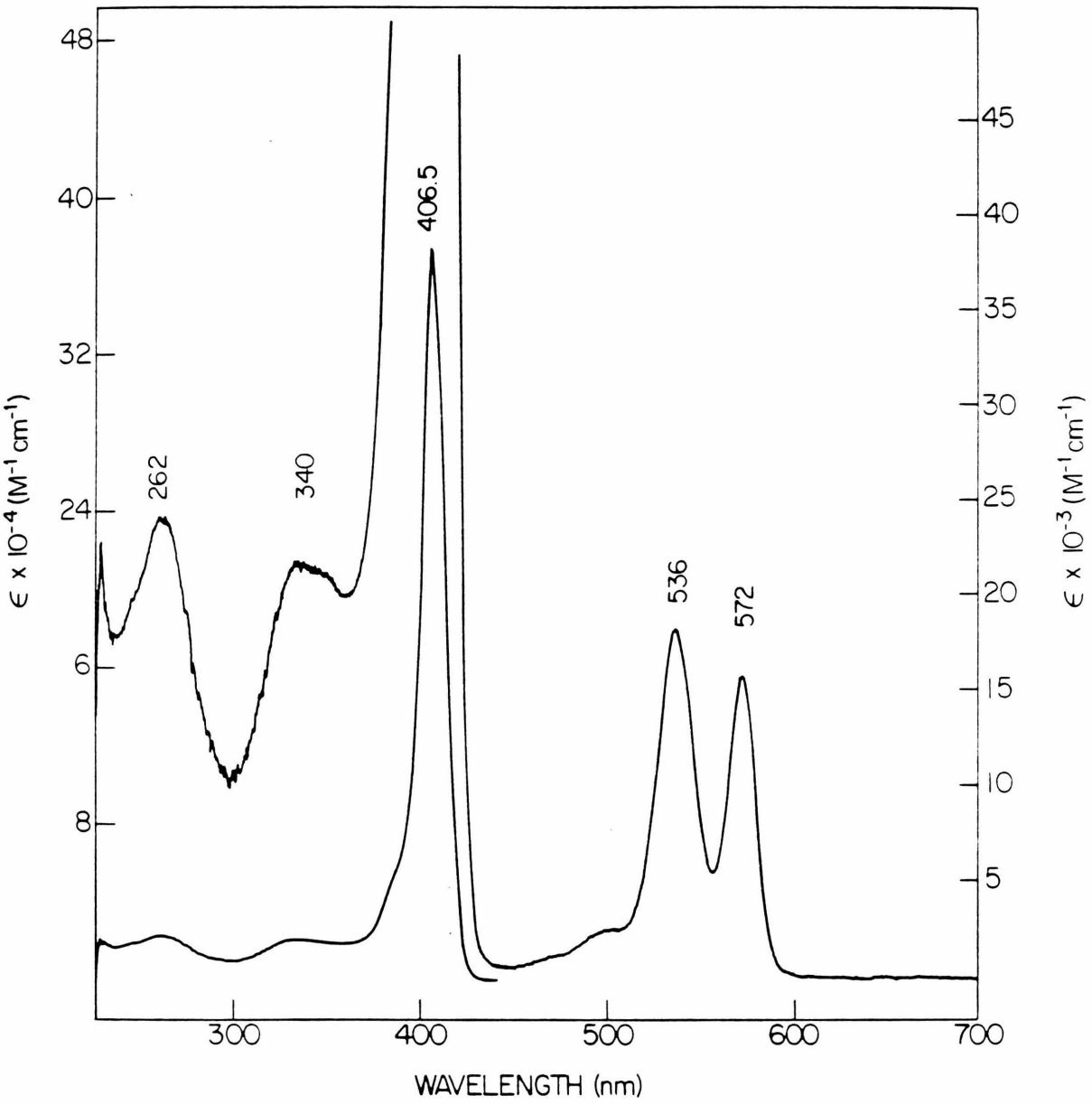

Figure 6. Electronic spectrum of *ZnP1QCl* in $CHCl_3$.

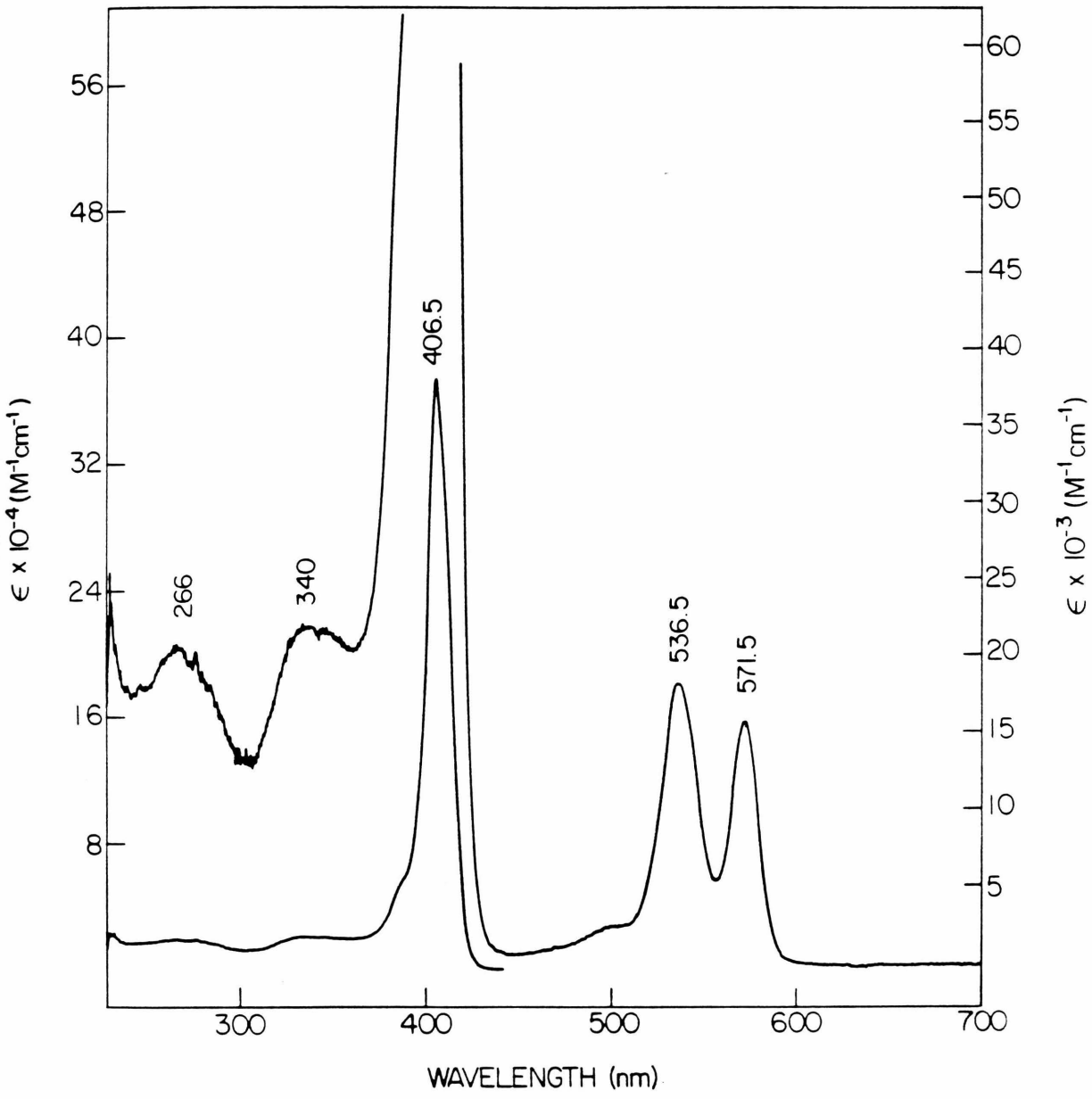

Figure 7. Electronic spectrum of *ZnP1QCl*$_2$ in $CHCl_3$.

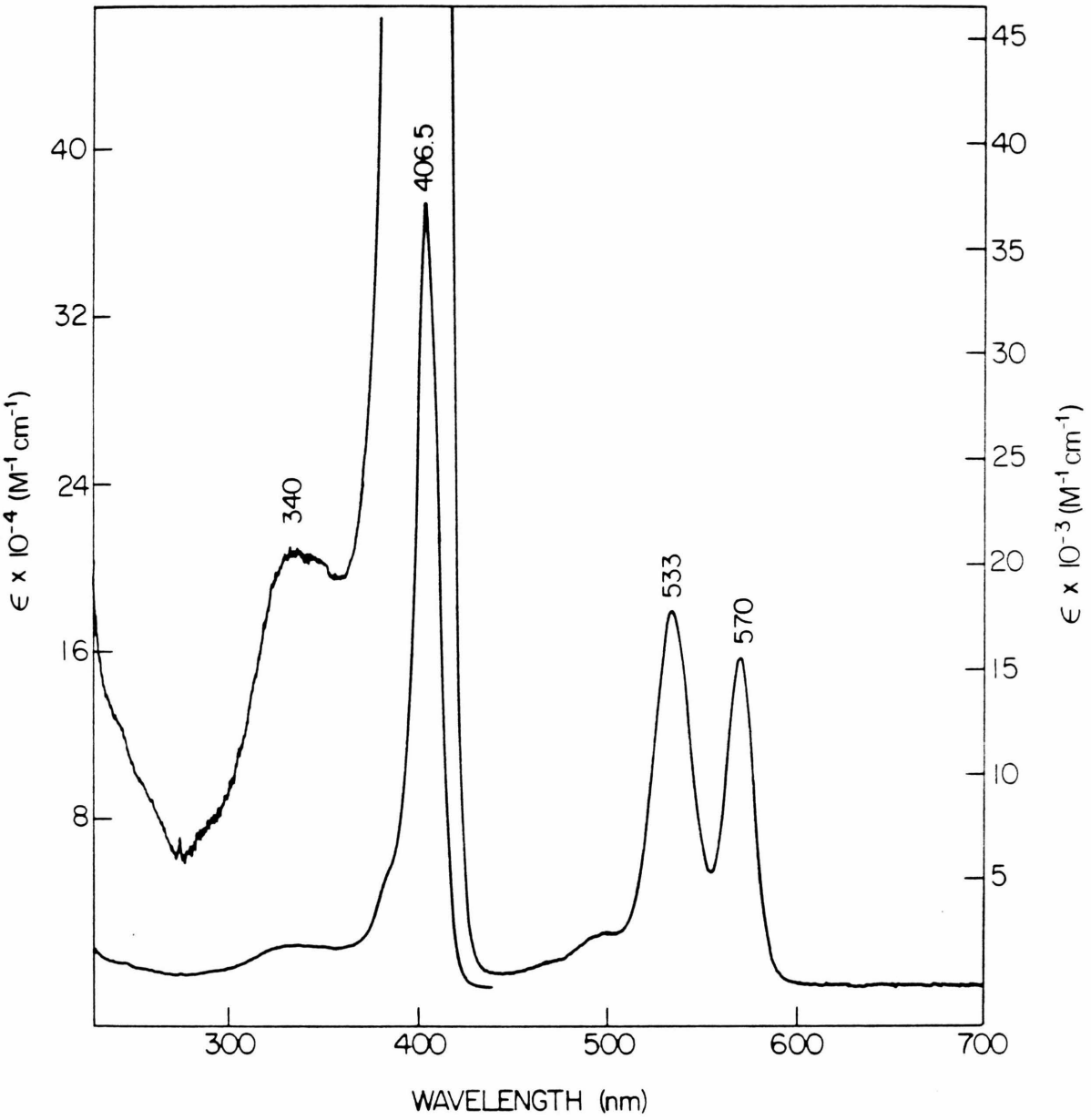

Figure 8. Electronic spectrum of ZnP^tBu in $CHCl_3$.

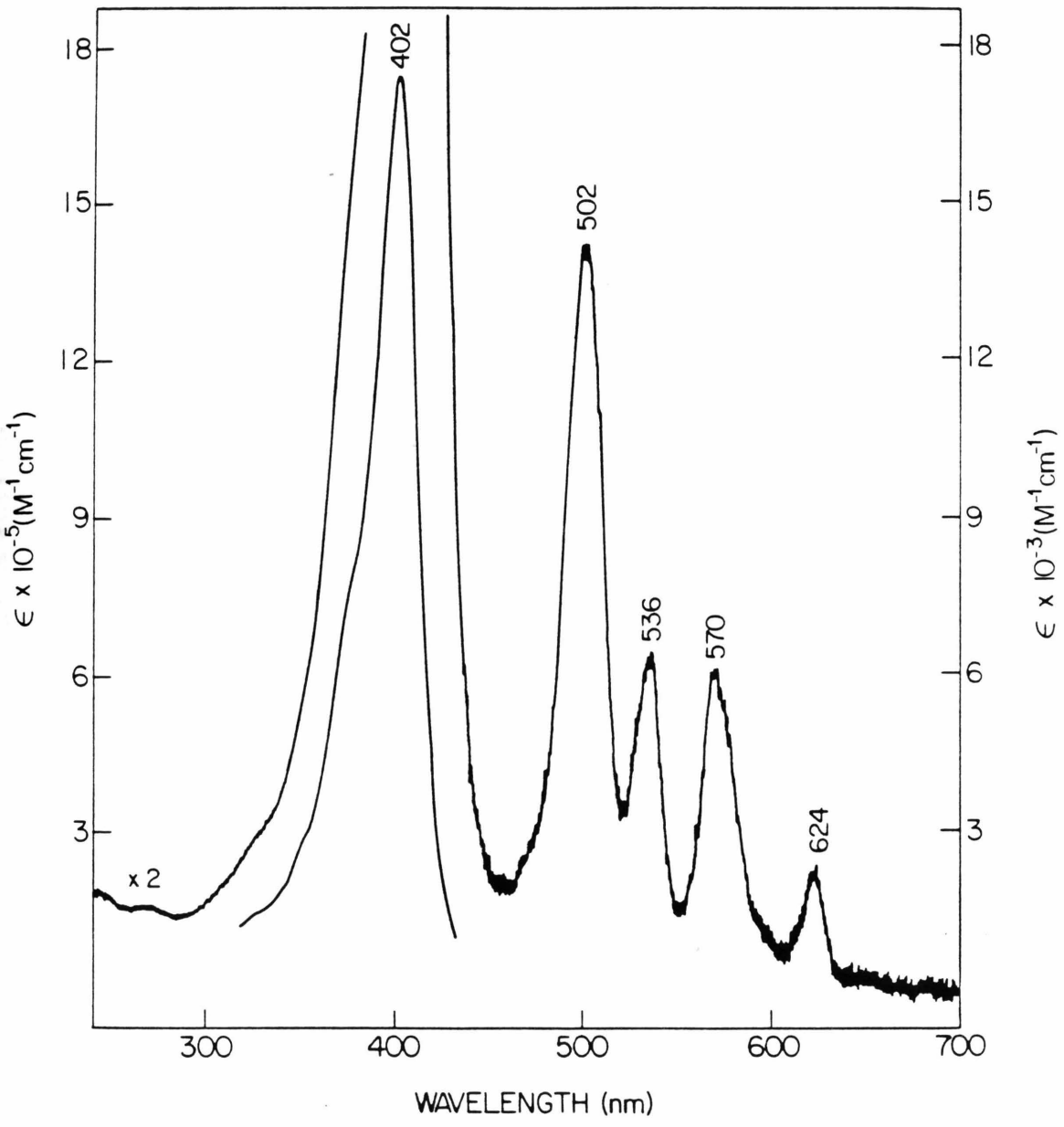

Figure 9. Electronic spectrum of H_2P^tBu in $CHCl_3$.

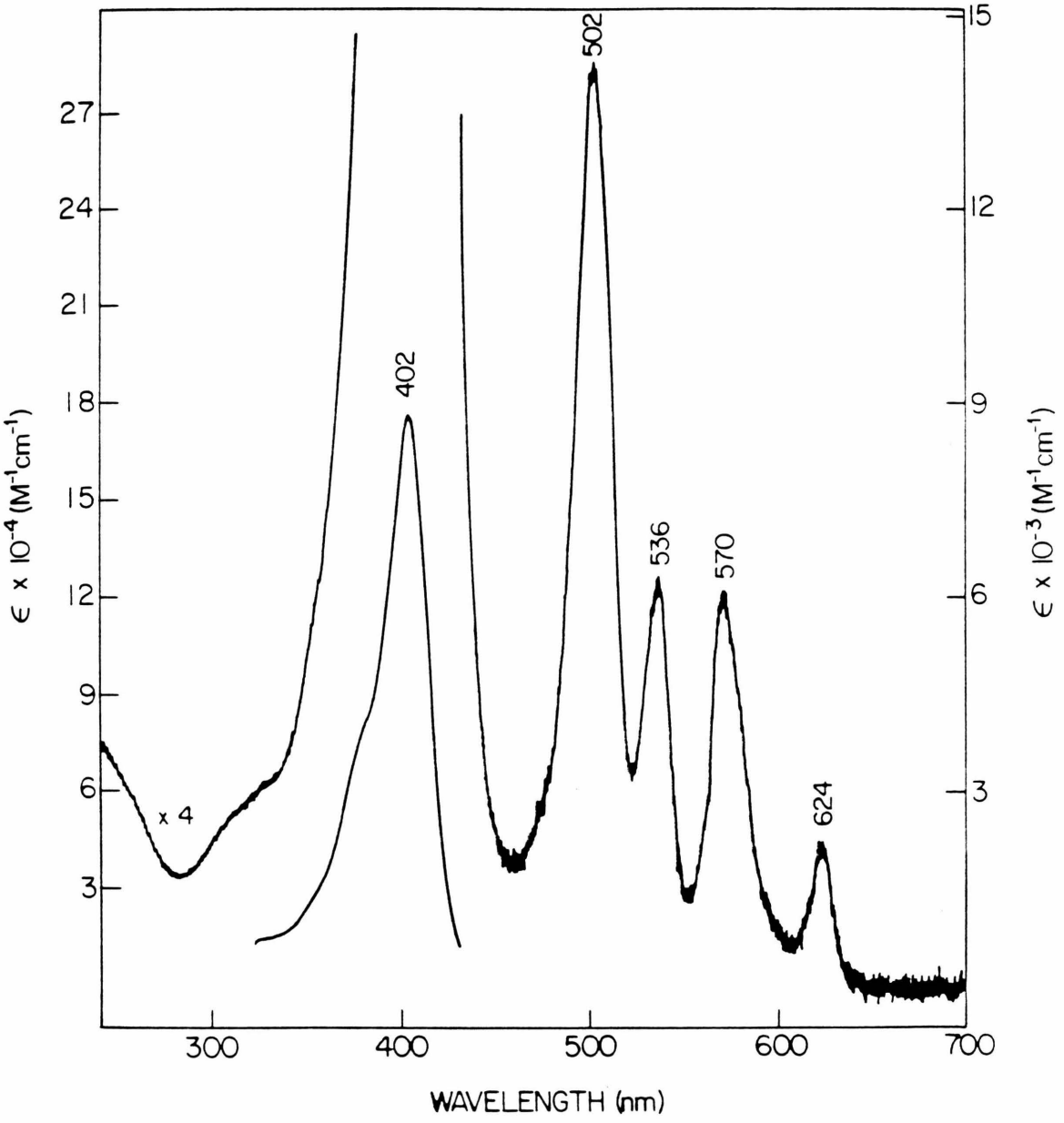

Figure 10. Electronic spectrum of *H_2P0DMB* in $CHCl_3$.

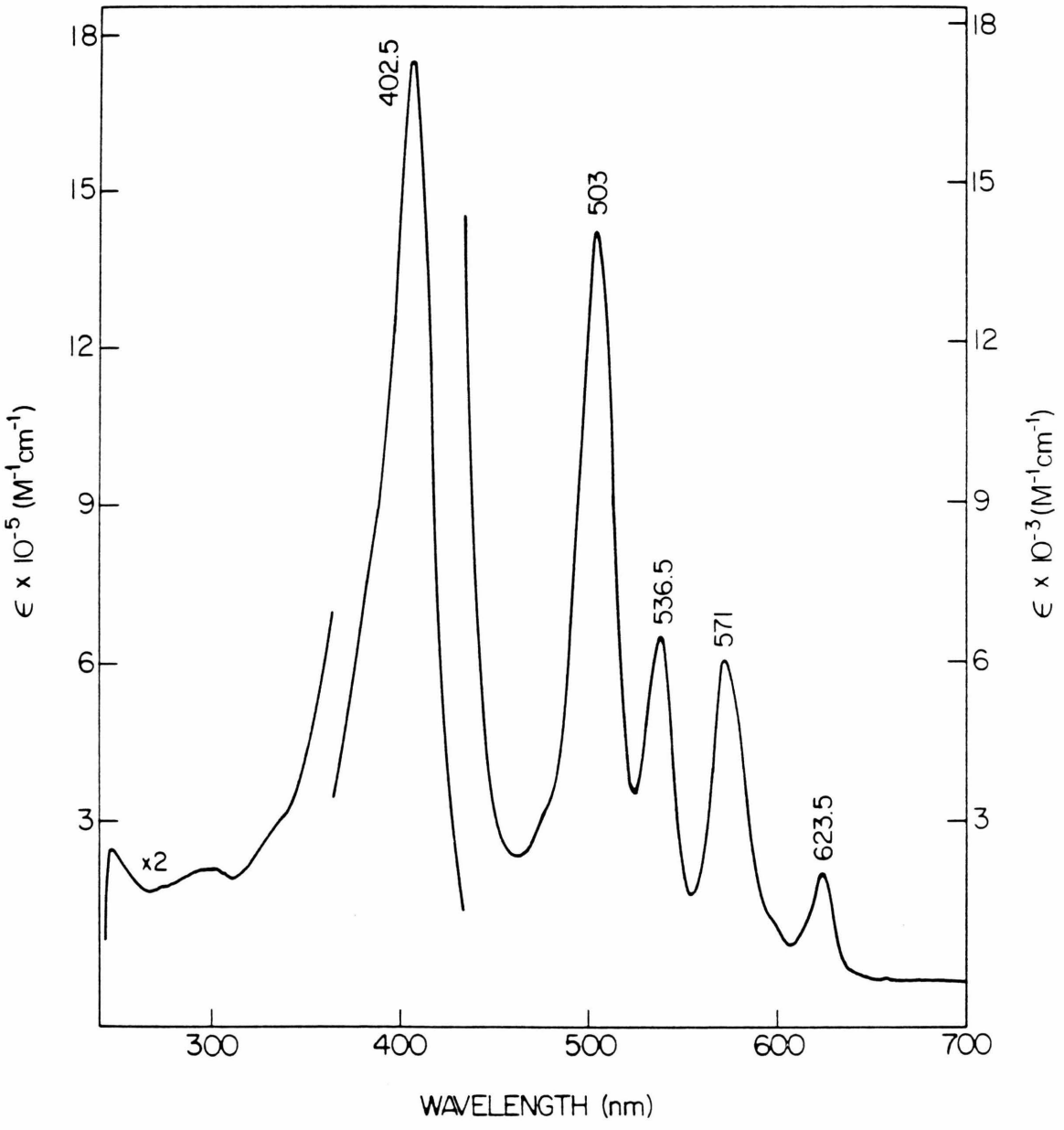

Figure 11. Electronic spectrum of H_2P2DMB in $CHCl_3$.

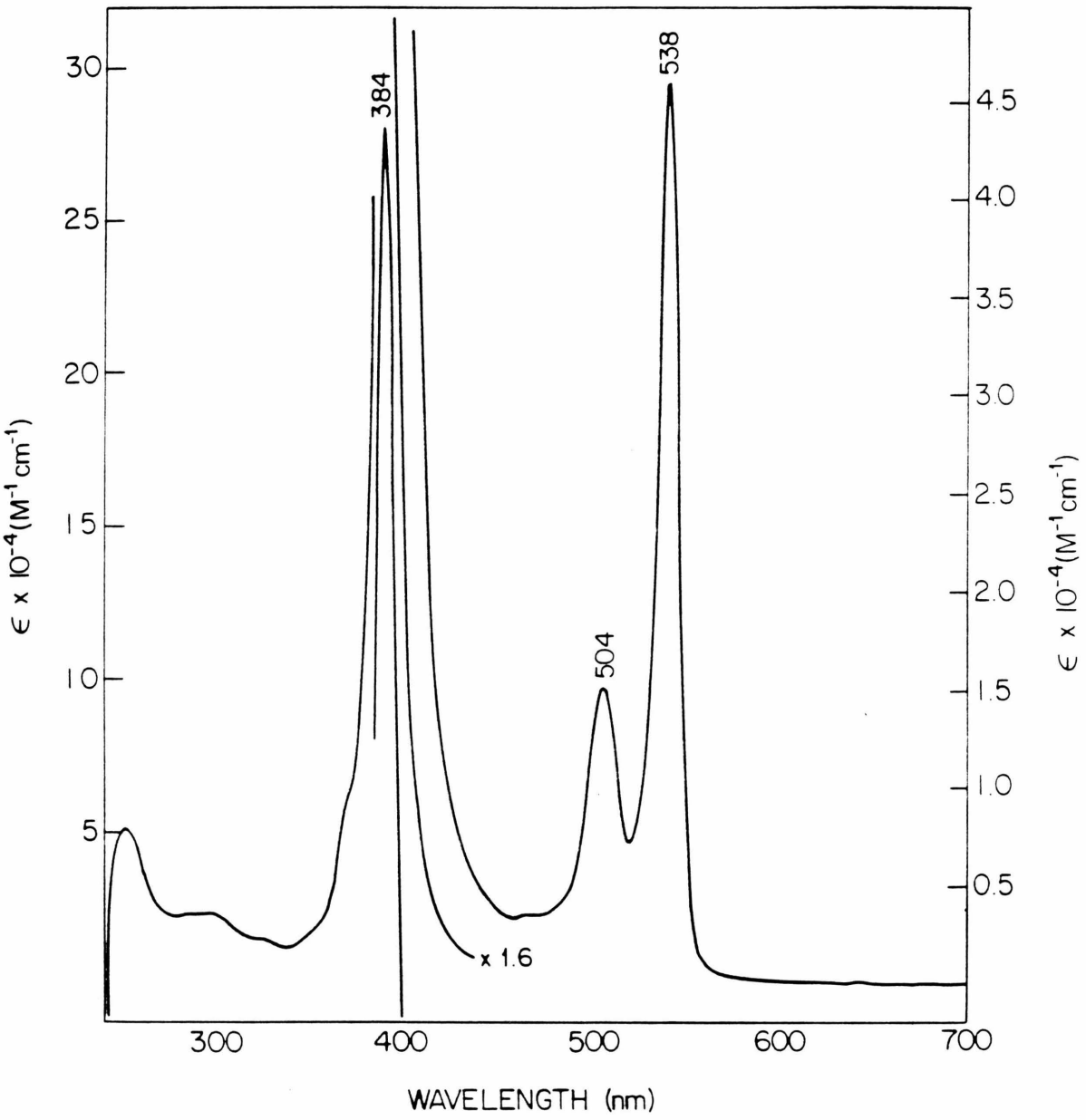

Figure 12. Electronic spectrum of PtP^tBu in $CHCl_3$.

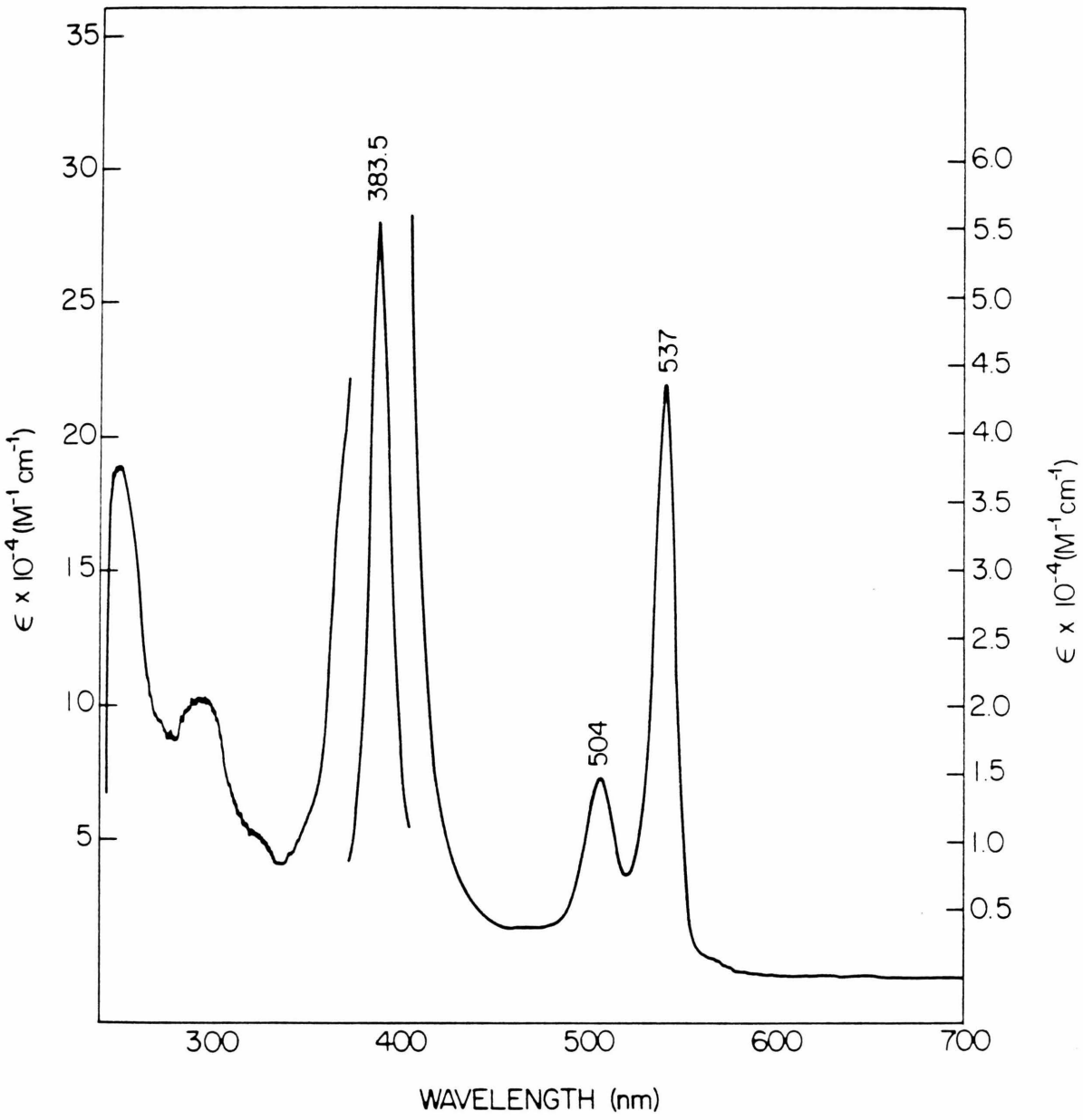

Figure 13. Electronic spectrum of *PtP2DMB* in $CHCl_3$.

minor wavelength changes in this band can be directly attributed to the changes in the quinone substituents. Not shown are the effects of increases in solvent polarity on the absorption bands in which shifts to longer wavelengths are observed, indicative of the π–π^* nature of the transitions. These effects are fully documented elsewhere.[145]

Nuclear Magnetic Resonance Spectra

Representative ^{1}H NMR spectra are shown in Figure 14–18 for the zinc metalloporphyrins **1**, **3**, and **41–43**. The spectra demonstrate the high symmetry in the structures, and the large anisotropic porphyrin and phenyl ring currents spread the proton resonances over a full 10 ppm. The porphyrin *meso*–protons are observed at ~10 ppm in a 2:1 ratio. The *meso*–proton opposite the *meso*–phenyl substituent is shifted upfield from the remaining two *meso*–protons which has been attributed to a buckling of the porphyrin macrocycle induced by increased steric bulk at the *meso* position.[160] The AA′BB′ pattern of the *meso*–phenyl substituent is observable centered at ~7.9 ppm in the bicyclo[2.2.2]octyl substituted derivatives, and downfield in compound **1** which lacks the bicyclo[2.2.2]octyl linker unit. The quinone resonances are observed in their normal region for isolated quinones (6.8–7.4 ppm) and indicated little perturbation by the porphyrin situated some 10 Å away (edge–to–edge). The methyl groups on the porphyrin ring are located at ~3.6 ppm with the exception of the set of methyl groups which flank the *meso*–phenyl group which are shifted upfield to 2.5 ppm due to close proximity to the phenyl ring currents. The AA′BB′ doublet of multiplets for the linker protons are observed

in the 2–2.4 ppm region indicative of the quinone oxidation state. The hydroquinone and dimethoxybenzene derivatives of the singly linked bicyclo[2.2.2]octyl porphyrin compounds exhibit a broad singlet for the linker protons.[145] This behavior is not observed in the bibicyclo[2.2.2]octyl linked derivative **3**, where a quartet of multiplets for the four sets of linker protons are observed for all of the porphyrin derivatives (*e.g.*, Figure 19).

The bromo–quinone derivative **41** (Figure 16) shows two lone singlets for the quinone protons consistent with the assignment of the bromine *para* to the bicyclo[2.2.2]octyl linker. The spectrum shown is from a repurified sample that had been stored for >6 months in the dark, yet the integration of the quinone peaks is clearly not the expected 1:1 pattern as is observed in freshly prepared material. This compound should be routinely oxidized to the quinone immediately prior to use, as was the case in the photochemical investigations, to minimize problems with possible addition–elimination reactions at the bromo–quinone functionality. The monochloro–quinone derivative **42** (Figure 17) shows the quinone pattern expected for the mixture of regioisomers discussed above. The dichloro–quinone derivative **43** (Figure 18) also shows the expected lone singlet for the quinone proton resonance. Finally in Figure 19 a spectrum of the platinum derivative of the bis–linked dimethoxybenzene derivative **60** is shown. Note the differences in the shifts of the *meso*–protons compared to the zinc metallo derivatives (Figures 14–18). The only new proton resonances compared to the compounds discussed above are the two methoxy groups observed at ~3.8 ppm. All four sets of linker protons can be observed in the 1.5–2.2 ppm region after treatment of the sample

with D_2O to reduce the water peak which obscures this region. ^{195}Pt–^{1}H couplings of 10–15 Hz have been observed[161, 162] in platinum porphyrins, but were probably not observed here due to the poor signal to noise of the spectrum as a result of the limited solubility of this derivative.

The ^{1}H NMR data confirm the expected molecular structures. Full characterization of these derivatives and all synthetic intermediates can be found in Chapter 7.

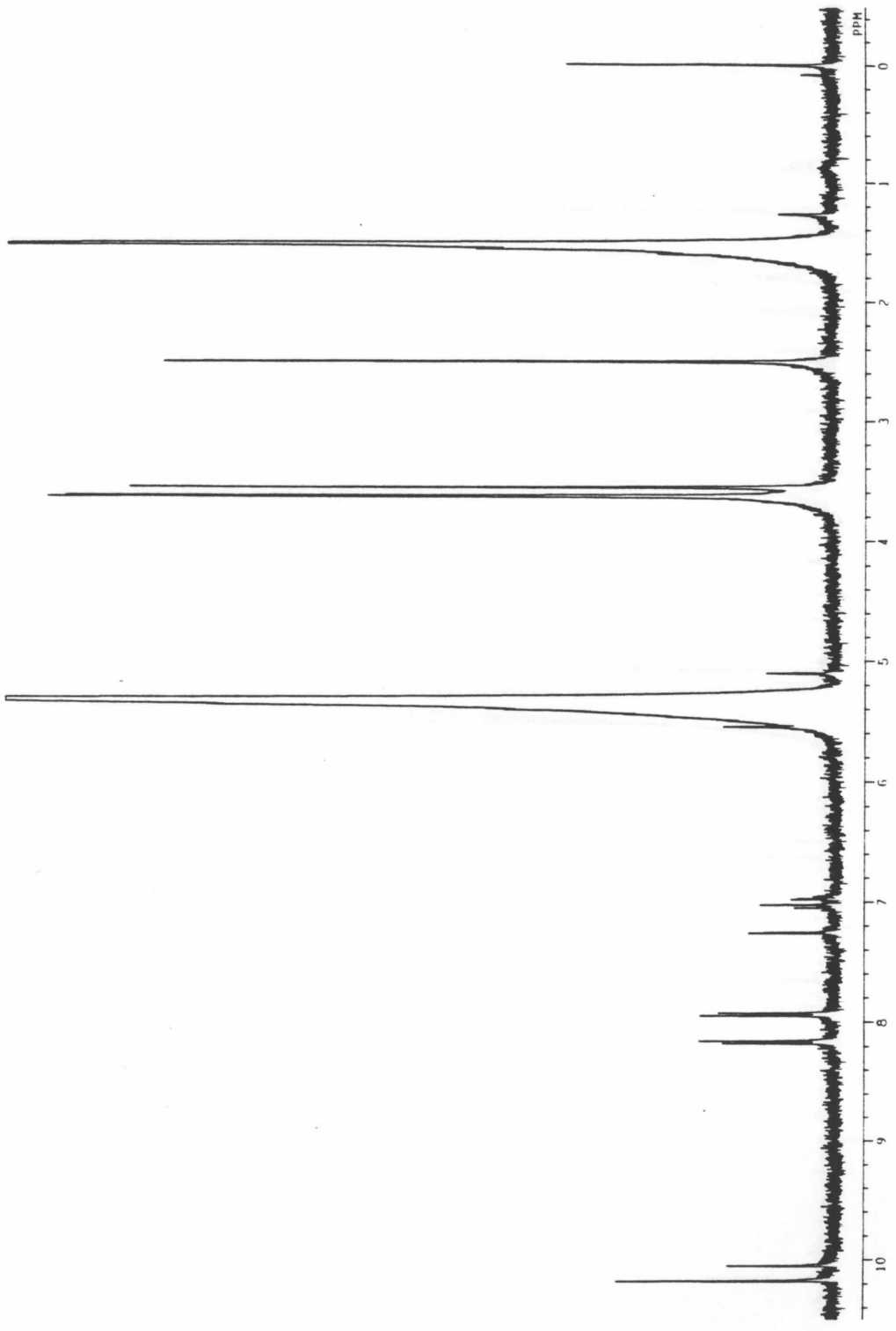

Figure 14. 400MHz ^{1}H NMR spectrum of *ZnP0Q* in CD_2Cl_2.

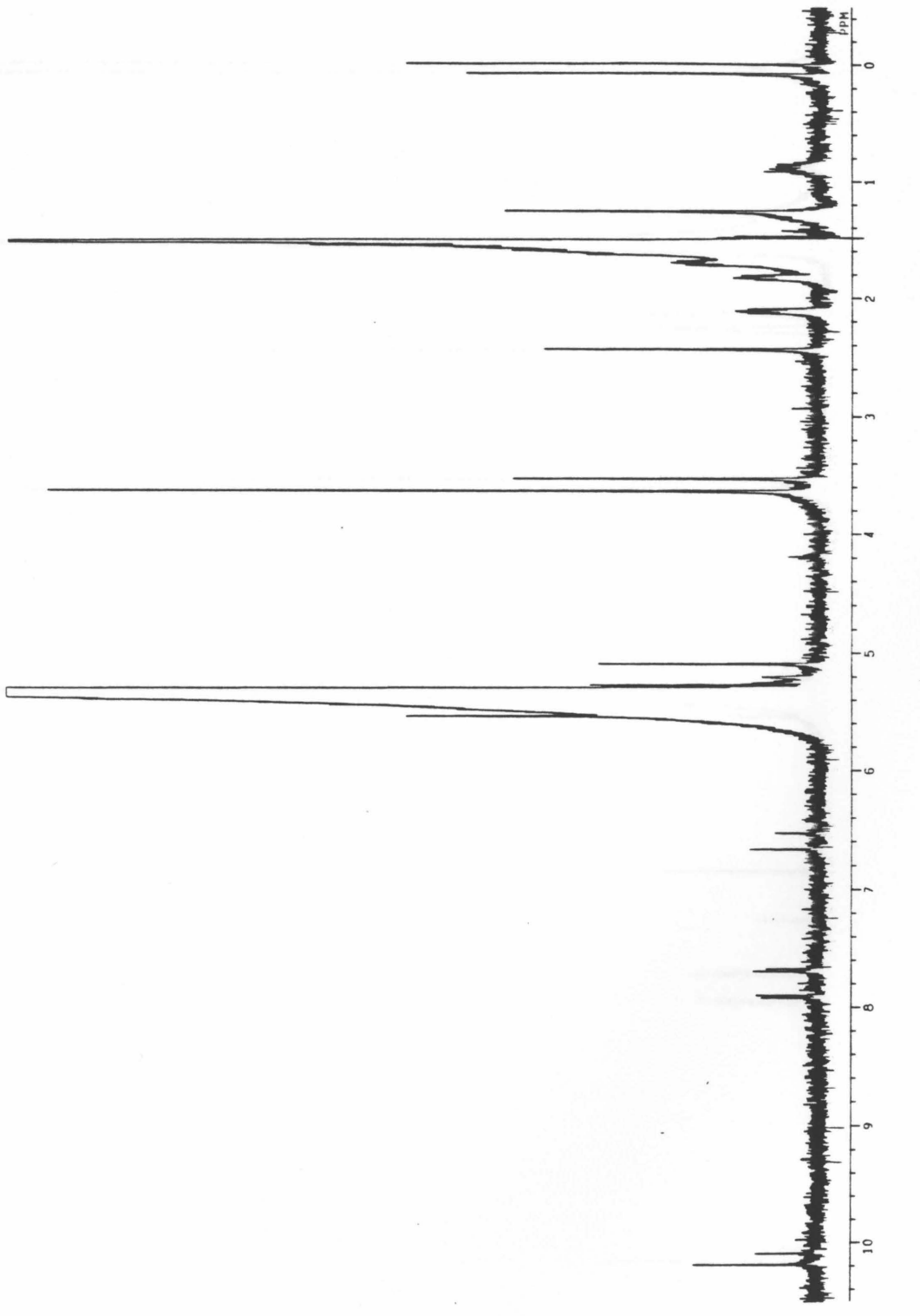

Figure 15. 400MHz ^{1}H NMR spectrum of *ZnP2Q* in CD_2Cl_2.

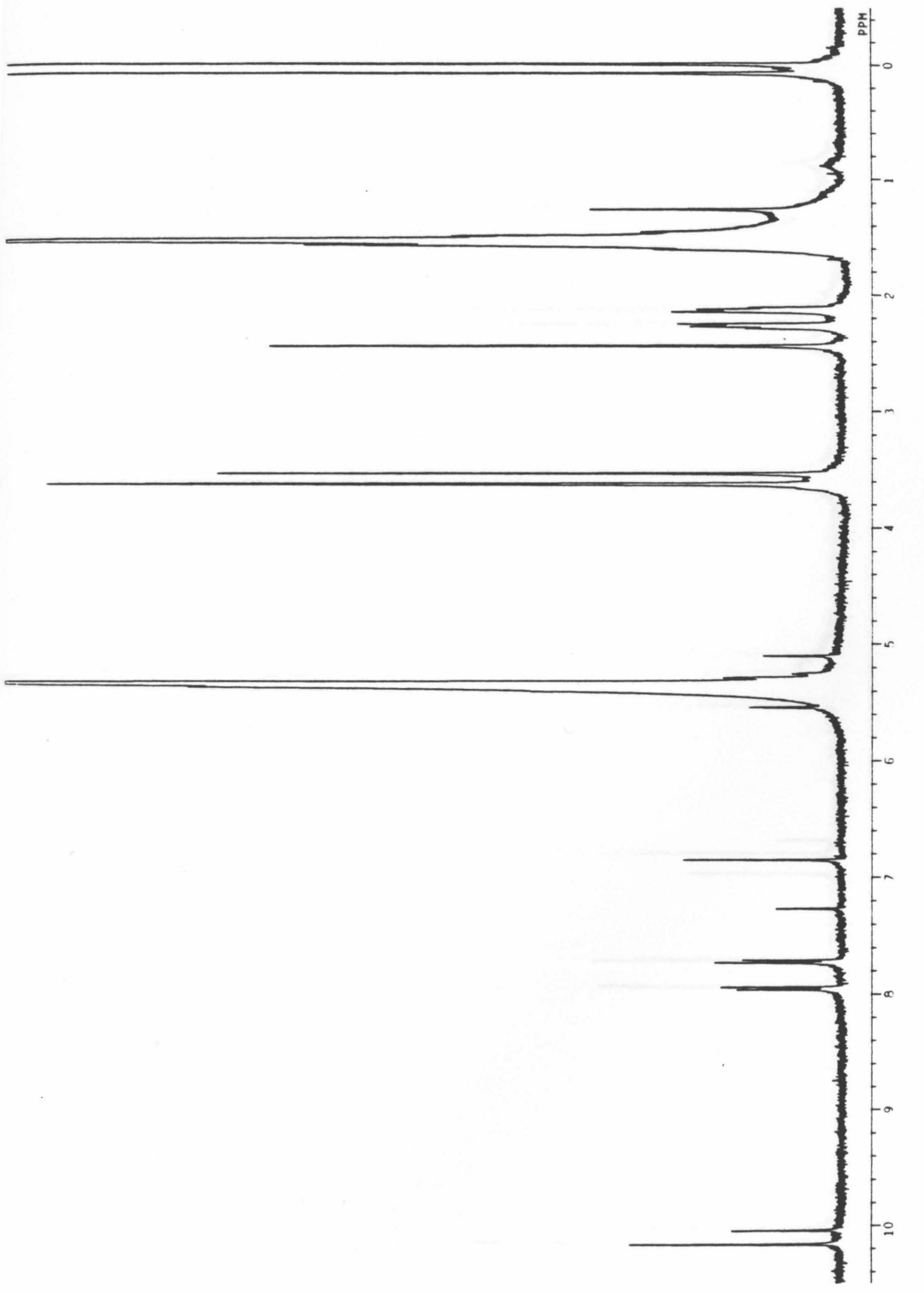

Figure 16. 400MHz ^{1}H NMR spectrum of *ZnP1QBr* in CD_2Cl_2.

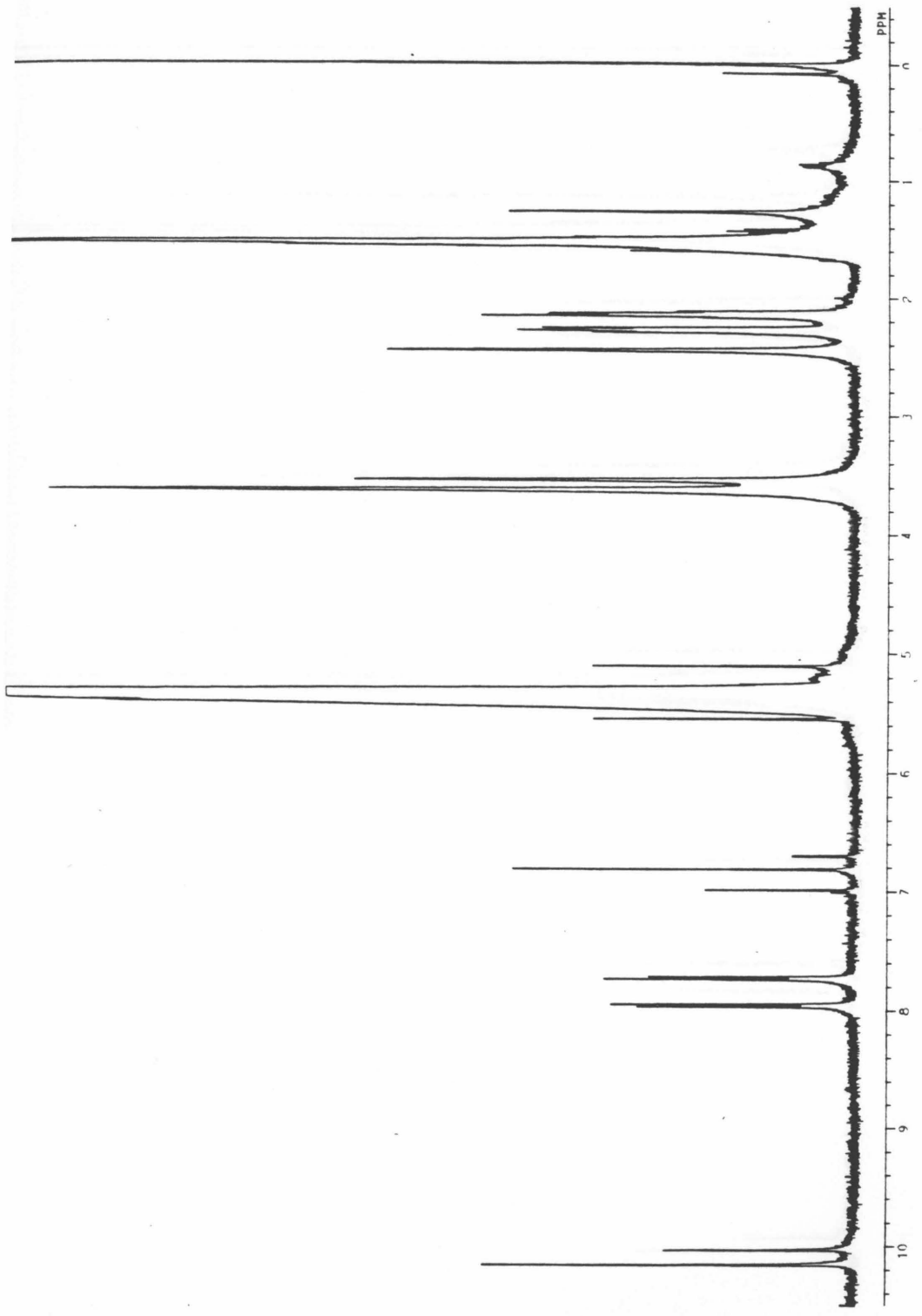

Figure 17. 400MHz ^{1}H NMR spectrum of *ZnP1QCl* in CD_2Cl_2.

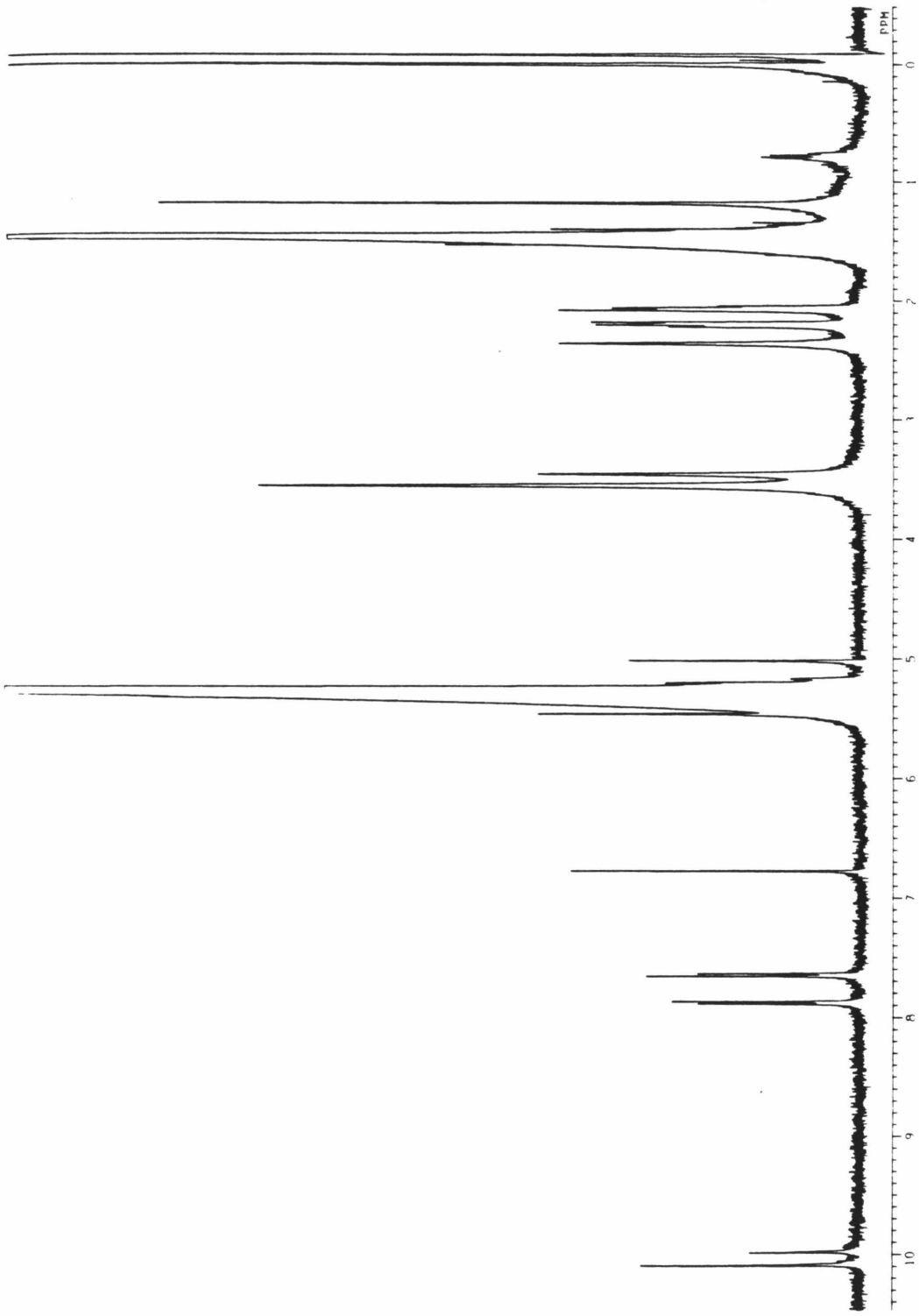

Figure 18. 400MHz ^{1}H NMR spectrum of *ZnP1QCl*$_2$ in CD_2Cl_2.

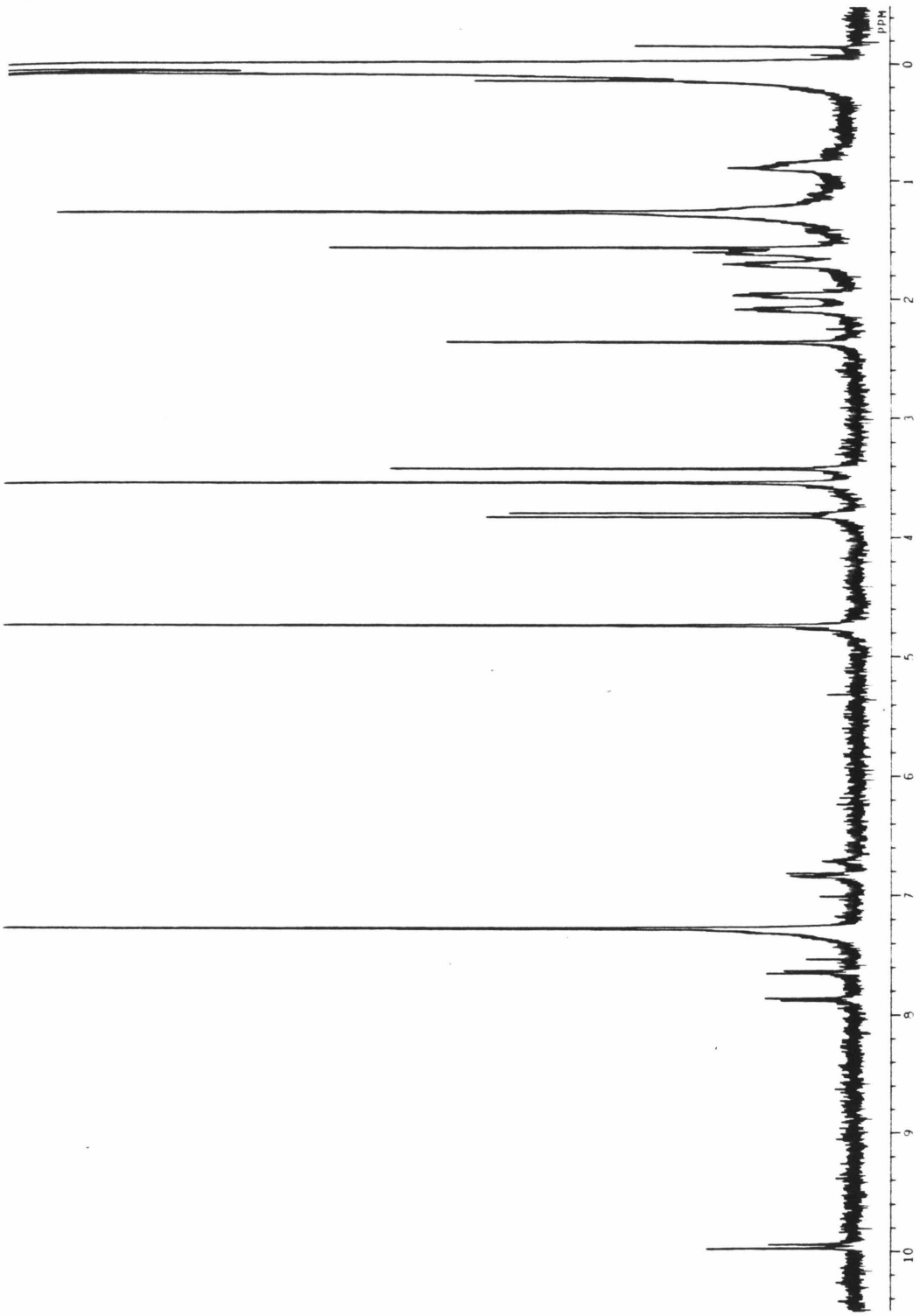

Figure 19. 400MHz ^{1}H NMR spectrum of *Pt2DMB* in $CDCl_3/D_2O$.

Chapter 4

Steady–State Methods

Steady–State Fluorescence Spectroscopy

Preliminary studies of the porphyrin–quinones **1–3** designed to probe the incremental distance effects on k_{ET} were undertaken by investigation of the fluorescence emission behavior of the compounds. Steady–state comparisons between the three quinone substituted porphyrins and a reference porphyrin are discussed here. The reference porphyrin chosen was that of a *meso*–(*p*–*tert*–butylphenyl)octamethyl-porphyrin (H_2P^tBu or ZnP^tBu) prepared via the general synthetic scheme discussed in Chapter 3. Full characterization of this material can be found in reference 145. The kinetic scheme for the deactivation of the photoexcited porphyrin is shown in Scheme I. The reference porphyrin provides the critical data for all the normal deactivation processes in the particular porphyrin skeleton under study. Investigation of the emission characteristics of the compounds **1–3** relative to the reference porphyrin will provide extraction of the electron transfer rate constant.

Superimposed fluorescence emission spectra of the quinone linked derivatives **1–3** and the reference porphyrin are shown in Figure 1 for the zinc metallo–porphyrin derivatives. Clearly there is a substantial effect on the emission intensity relative to the reference porphyrin for the quinone linked derivatives as a function of porphyrin–quinone separation distance. Significantly, however, the fluorescence emission wavelengths for the bicyclo[2.2.2]octyl linked derivatives are unperturbed by the presence of the quinone and only the fluorescence yield is af-

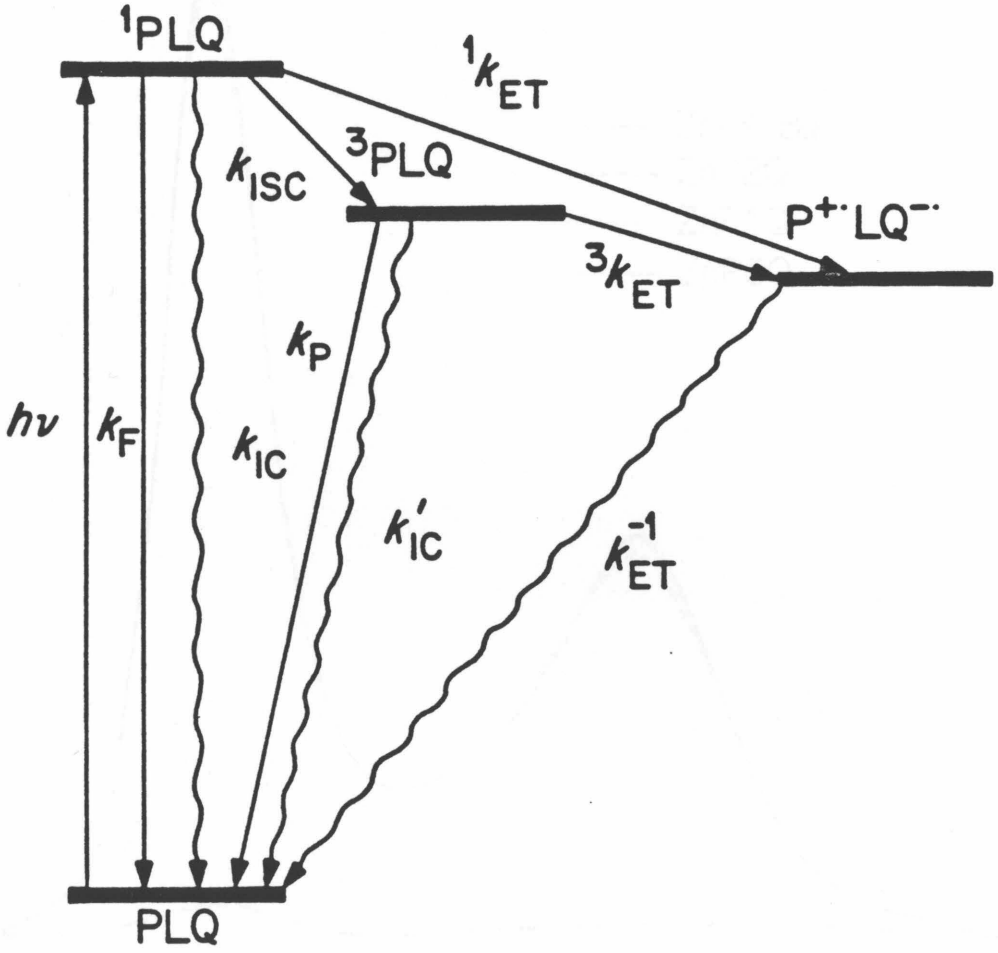

Scheme I. Photochemical kinetic scheme.

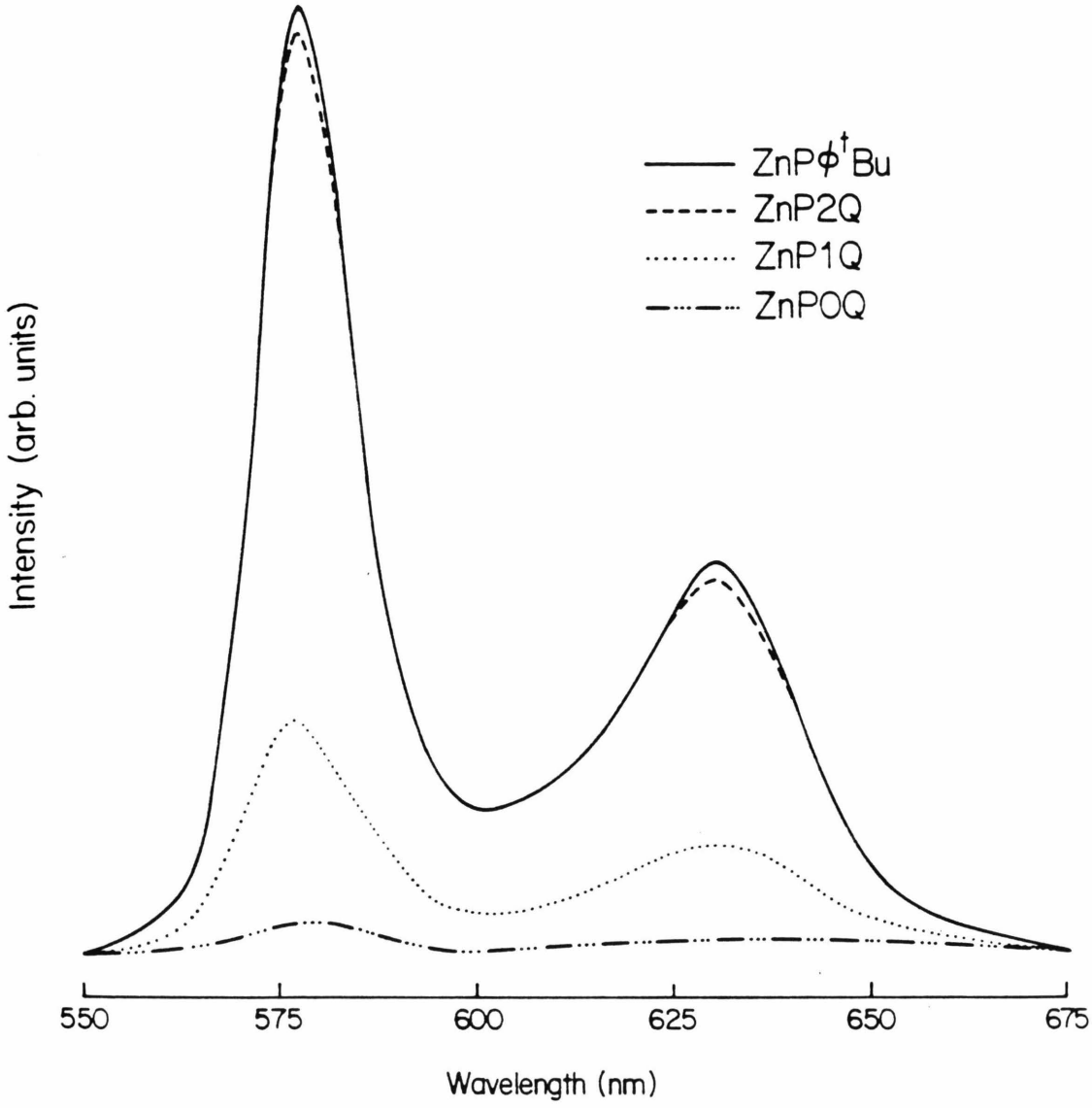

Figure 1. Steady–state fluorescence emission spectra of *ZnP^{t}Bu*, *ZnP0Q*, *ZnP1Q*, *ZnP2Q* in benzene.

fected. This is in striking contrast to previous reports in the literature of flexibly coupled porphyrin–quinone derivatives which the emission spectra show marked dependence on excitation wavelength.[77] Compound **1** (*ZnP0Q*) exhibits virtually complete deactivation of the porphyrin fluorescence. The single bicyclo[2.2.2]octyl linked derivative **2** (*ZnP1Q*) shows considerably more fluorescence than **1**, but highly quenched relative to the reference porphyrin. The porphyrin–quinone separated by two bicyclo[2.2.2]octyl linkers (*ZnP2Q*) exhibits a virtually identical emission yield as the reference ZnP^tBu. The edge–to–edge separation distances between the porphyrin–quinones for **1–3** are 6, 10, and 14 Å, and dramatic differences between the fluorescence yields of the compounds are observed.

The inherent problems associated with a steady–state analysis include difficulties in obtaining exactly matched solutions of the reference porphyrin and the porphyrin–quinones. In addition, the only experimental discrimination of competing processes is based on emission or excitation wavelength, and one must assume that the sample is quantitatively present in the quinone oxidation state. The presence of any porphyrin–hydroquinone, which exhibits an identical emission spectrum and similar fluorescence yield as the reference porphyrin, results in an underestimation of the extracted k_{ET} values. While extreme care was taken to purify the porphyrin–quinones prior to the analyses to minimize this material, it is difficult to rigorously insure the samples are free of this background emissive component (see discussion of dynamic lifetime measurements below).

A Stern–Volmer analysis[163] under steady–state conditions for the kinetic scheme of Scheme 1 in the absence of an electron transfer deactivation pathway

leads to

$$I_f = \mathrm{I}^\circ \Phi_f \qquad [4.1]$$

$$I_f^\circ = \mathrm{I}^\circ \left(\frac{\mathrm{k_f}}{\mathrm{k_f} + \mathrm{k_{isc}} + \mathrm{k_{ic}}} \right) \qquad [4.2]$$

where I_f° is the fluorescence intensity of the reference porphyrin, I° is the excitation lamp intensity, Φ_f° is the fluorescence quantum yield, and $\mathrm{k_f}$, $\mathrm{k_{isc}}$, and $\mathrm{k_{ic}}$ are the rate constants for fluorescence, intersystem crossing, and non–radiative internal conversion, respectively. For the porphyrin–quinone compounds,

$$I_f = \mathrm{I}^\circ \left(\frac{\mathrm{k_f}}{\mathrm{k_f} + \mathrm{k_{isc}} + \mathrm{k_{ic}} + \mathrm{k}_{ET}} \right) \qquad [4.3]$$

where I_f is the fluorescence intensity of the quinone–linked compounds. Assuming the rate constants for all other deactivation pathways are constant in the porphyrin–quinones relative to the reference porphyrin, and the only new deactivation pathway available for the quinone derivatives is electron transfer, the ratio of equation [4.2] to [4.3] yields

$$\frac{I_f^\circ}{I_f} = 1 + \left(\frac{\mathrm{k}_{ET}}{\mathrm{k_f} + \mathrm{k_{isc}} + \mathrm{k_{ic}}} \right) \qquad [4.4]$$

Since

$$\tau_\circ = \frac{1}{(\mathrm{k_f} + \mathrm{k_{isc}} + \mathrm{k_{ic}})} \qquad [4.5]$$

where $\tau_\circ$ is the fluorescence lifetime of the reference porphyrin, substitution into equation [4.4] yields

$$\frac{I_f^\circ}{I_f} = 1 + \mathrm{k}_{ET}\tau_\circ \qquad [4.6]$$

Independent measurements of τ_o for the reference free–base and zinc metallo–porphyrins[117] allows extraction of k_{ET} from the ratio of the fluorescence intensities of the quinone derivatives. The assumptions underlying this kinetic analysis include that (a) the radiative and non–radiative rate constants for the reference porphyrin are identical to the porphyrin–quinone compounds, and (b) electron transfer is the sole additional deactivation pathway available to the quinone derivatives. Assumption (a) was the impetus for the synthesis of the reference porphyrin of identical skeletal framework as the porphyrin–quinones. Clearly, comparisons with other porphyrin skeletons would call this assumption into question or require that these rate constants be explicitly determined. Assumption (b) should also be valid at concentrations low enough to minimize intermolecular complications. The fluorescence intensities were found to be independent of excitation wavelength and concentration (10^{-6}–10^{-7} M). Absorption spectra taken before and after emission measurements confirmed the absence of photochemical degradation. Degradation was observed, however, in methylene chloride and other chlorinated solvents which prohibited their use in these investigations. Fluorescence intensity measurements for solutions of the reference porphyrin and the quinone derivatives were compared back–to–back to insure minimal changes in the excitation lamp intensity (I°) during the course of the experiments. The results presented in Table I for the zinc and free–base porphyrin derivatives.

The extracted k_{ET} values presented in Table I should be considered as approximated values only. More quantitative determinations of the electron transfer rate constants will discussed in the next chapter. Qualitatively, however, a number

Table I. Relative fluorescence yields for H_2PLQ and $ZnPLQ$[a]

Compound	Solvent[b]	I_f/I_f°[c]	k_{ET}[d]
H_2P0Q	C_6H_6	0.01	$6x10^9$
H_2P1Q	C_6H_6	0.80	$1x10^7$
H_2P2Q	C_6H_6	0.94	$4x10^6$
$ZnP0Q$	C_6H_6	0.003	$2x10^{11}$
$ZnP1Q$	C_6H_6	0.27	$2x10^9$
$ZnP2Q$	C_6H_6	0.97	$2x10^7$
H_2P0Q	*n*PrCN	0.02	$3x10^9$
H_2P1Q	*n*PrCN	0.63	$3x10^7$
H_2P2Q	*n*PrCN	0.90	$6x10^6$
$ZnP0Q$	*n*PrCN	0.035	$2x10^{10}$
$ZnP1Q$	*n*PrCN	0.26	$2x10^9$
$ZnP2Q$	*n*PrCN	0.95	$3x10^7$

[a] where the L number indicates the number of intervening bicyclo[2.2.2]octyl units

[b] Benzene was distilled from CaH_2 prior to use. Butyronitrile was distilled from $K_2CO_3/KMnO_4$ and then from P_2O_5.

[c] Fluorescence yields measured under aerobic conditions relative to the reference porphyrin (see text). The estimated uncertainty in these values is ±10%.

[d] Estimated values calculated from $I_\circ/I = 1 + k_{ET}\tau_\circ$ where $\tau_\circ$ (C_6H_6) = $17.5x10^{-9}$ s, $\tau_\circ$ (*n*PrCN) = $18.1x10^{-9}$ s for H_2P^tBu and $\tau_\circ$ (C_6H_6) = $1.45x10^{-9}$ s, $\tau_\circ$ (*n*PrCN) = $1.59x10^{-9}$ s for ZnP^tBu.

of trends can be obtained from these data. In all cases, an ~100–fold increase in the extracted k_{ET} values are observed for the zinc metallo–porphyrin derivatives relative to the metal–free compounds. This is consistent with the changes in the oxidation potentials and singlet energies which results in an increase in exothermicity for the electron transfer reaction by ~0.5 eV for the metallo–derivatives.[117] Clear decreases in rates are observed by the addition of successive bicyclo[2.2.2]octyl linker units. The addition of the first linker results in a decrease in k_{ET} by one to two orders of magnitude. This may reflect a change in mechanism from an adiabatic to nonadiabatic transfer. The addition of the second linker unit results in a further decrease in the electron transfer rate constant by at least another order of magnitude. It should be noted that based on the picosecond fluorescence measurements discussed in the following section, the rates for the bis–linked system must be considered as upper bounds.

The data obtained in the steady–state emission studies demonstrate that minimal interactions between the chromophores are possible due to the enforced spatial separation by the linker units as indicated by the unperturbed emission spectra relative to the reference porphyrin. This result is consistent with previous discussions of the NMR and absorption spectra which also indicate minimal chromophore interactions with the possible exception of the zero–linked compound. The presence of the quinone functionality has dramatically affected the fluorescence emission yield of the porphyrin. Since energy transfer is precluded based on analysis of the absorption data, the additional deactivation pathway responsible for the observed quenching is presumed to be electron transfer. Modulation of the

exothermicity of the electron transfer reaction by comparison of zinc metallo and free–base porphyrins also is consistent with this proposal. Further quantitative determinations of k_{ET} for this series is presented in the next section. These results support the design criteria for a successful intramolecular system, *i.e.*, rigidly linked porphyrin–quinones held at relatively large separation distances (6, 10, and 14 Å edge–to–edge) can exhibit an efficient ET pathway which will allow the investigation of k_{ET} as a function of the various critical parameters with minimal electronic perturbations.

Chapter 5

Dynamic Methods

Picosecond Fluorescence Measurements

The encouraging results from static emission measurements discussed in the previous section prompted the investigation of the time–resolved fluorescence behavior of the rigidly linked porphyrin–quinones. While the static experiments could analyze the sample based on emission and excitation wavelengths, the added time discrimination component allows for a more quantitative investigation of the electron transfer rates in the series. The general approach is similar to the previous studies in that the emission behavior of each of the quinone derivatives is directly compared to the *tert*–butyl reference porphyrin which lacks the electron transfer deactivation pathway but exhibits all other natural deactivation pathways (fluorescence, intersystem crossing, and internal conversion). As discussed elsewhere,[145, 164] complications in the emission of the free base porphyrin due to the scavenging of adventitious metals as a result of the superior chelation ability of the porphyrin macrocycle resulted in the focus of these studies on the zinc metallo–porphyrins.

Porphyrin samples were chromatographed just prior to the picosecond fluorescence lifetime experiments and checked by NMR for purity. Solutions of the porphyrins (10^{-5}–10^{-7} M) in rigorously purified solvents were degassed with 4–5 freeze–thaw degassing cycles at $\leq 10^{-4}$ torr. The samples were excited with the output from a synchronously pumped, cavity dumped dye laser (Rhodamine 6G).

The laser pulses were typically ~15 psec in duration and the full output power was ~20 mW. The samples were excited at 570 nm and the emission was observed at 580 and/or 630 nm. Filtered emission was detected at a right angle to the excitation pulse through a monochrometer and detected with a fast photomultiplier using time–correlated single–photon counting techniques. The overall system response time is largely limited by the photomultiplier rise time resulting in a system response of ~40 psec. Care was taken to insure the transients observed are due to excited state fluorescence and not filter fluorescence. Analysis of the emission with a polarizer at 54.7° to the excitation polarization confirmed that the observed lifetimes are not due to depolarization effects and were independent of concentration in the range of 10^{-5}–10^{-7} M. Individual fluorescence decays were collected on a Tracor Northern (TN–1706) digitizer and transferred to a Compaq© personal computer for data analysis. The system response function was obtained from the scattered laser excitation pulse of a colloidal solution. The fitting routine deconvolutes the system response function, and allows the fit of up to three exponential decays. The complete source code for the analysis routine is available in Appendix A. No more than two exponentials (see below) were ever required to fit the observed decays, and the quality of the fits were excellent as judged by the χ^2 criterion,[165] which were consistently less than 1.2. A complete description of the experimental apparatus is available elsewhere.[166, 167]

In all cases studied, the reference ZnP^tBu porphyrin exhibited monoexponential decay kinetics. The porphyrin–quinone linked by a single bicyclo[2.2.2]octyl spacer (**2**, *ZnP1Q*) routinely exhibited biexponential kinetics. The lifetime of the

second component was similar to the reference ZnP^tBu porphyrin within the relatively large uncertainties in the lifetime for such a minor component, and the amount of this component was observed to increase in solvents which were difficult to obtain rigorously dry. Control experiments[145] suggest that the second minor component was the porphyrin–hydroquinone derivative, most likely formed from the porphyrin sensitized photoreduction of the quinone.[168] Preparation of the porphyrin–hydroquinone via borohydride reduction of the porphyrin–quinone derivative and chromatographic purification resulted in a fluorescence decay enriched in the long lifetime component with a lifetime identical to the reference porphyrin.[145] Since the reduction potential of the hydroquinone precludes electron transfer, one would expect to observe a similar lifetime as the reference compound which also lacks an ET deactivation pathway. The major component of the biexponential fit of the fluorescence emission is a highly quenched material ascribed to the fluorescence lifetime of the porphyrin–quinone derivative.

Time–resolved studies on the porphyrin–quinone lacking the bicyclo[2.2.2]octyl spacer unit (**1**, *ZnP0Q*) revealed an extremely weak emissive component. This emissive component grows in with time upon extended irradiation, and exhibited a lifetime similar to the reference porphyrin. The probable assignment based on the control experiments discussed above is that extended irradiation results in the conversion of a small fraction of the sample to the porphyrin–hydroquinone via porphyrin sensitized photoreduction of the quinone[168] in the presence of adventitious water in the sample. This material then fluoresces with a lifetime easily detected by the experimental apparatus. This suggests that the fluorescence lifetime of the

porphyrin–quinone derivative (*ZnP0Q*) was less than the system response limits, and would require a significantly faster time base to detect emission from this material. The emission observed in the steady–state experiments discussed in the previous chapter can likely be attributed to this minor porphyrin–hydroquinone contaminant, and these results indicate that the electron transfer rate for this material is $\geq 10^{11} s^{-1}$, and may reflect an adiabatic limit to the transfer.

The fluorescence decays of *ZnP2Q* were adequately described by single exponential decays. This may reflect the inability of a slow electron transfer pathway to compete with the other natural decay processes of the excited singlet state. For example, the intersystem crossing rate for zinc octaethylporphyrin (*ZnOEP*) has been reported as $4x10^{8} s^{-1}$.[169] If the inherent electron transfer rate is well below this value, the predominant decay pathway will be via the triplet (see Scheme I, Chapter 4). While the observed fluorescence lifetime was always less than the reference *ZnP^{t}Bu* porphyrin, the experimental uncertainty in these values does not conclusively support the assignment of a quenched lifetime, and as such only limits on the electron transfer rate can be ascertained for this compound. An alternative possibility is that the decay can be described by a biexponential decay (as above) with two components of very similar lifetime, and the monoexponetial lifetime observed is in fact the weighted average of these two lifetimes. This possibility would require an modified fitting algorithm which would analyze the lifetimes of the two components based on the results from the monoexponential fit. As this procedure would introduce two additional free parameters in the fit, a minor improvement in the χ^2 would not likely be significant, and the uncertainties

in the obtained lifetimes would still only allow limits to be placed on the derived k_{ET} values. Investigations of the electron transfer from the excited triplet state for this compound is discussed later in this chapter.

The fluorescence decays of the *ZnP^{t}Bu*, *ZnP1Q*, and *ZnP2Q* are superimposed for comparison in Figure 1, individual decays are shown in Figures 2–4, and the results are tabulated in Table I. Considering the previously presented kinetic scheme (Chapter 4, Scheme I), the extraction of k_{ET} from the observed fluorescence lifetimes is straightforward. Since

$$\tau_\circ = \frac{1}{k_f + k_{isc} + k_{ic}} \qquad [5.1]$$

$$\tau = \frac{1}{k_f + k_{isc} + k_{ic} + k_{ET}} \qquad [5.2]$$

the electron transfer rate constant (k_{ET}) can be obtained from

$$k_{ET} = \frac{1}{\tau} - \frac{1}{\tau_\circ} \qquad [5.3]$$

where $\tau_\circ$ and τ are the fluorescence lifetimes for the reference porphyrin (*ZnP^{t}Bu*) and porphyrin–quinone derivatives (*ZnPLQ*), respectively (other rate constants as previously defined).

The comparison of the mono– and bis–linked porphyrin–quinones allows the determination of the decrease in k_{ET} with the incremental change in distance of 4 Å through the identical hydrocarbon framework. The matrix element governing the electron transfer is generally assumed to decrease exponentially with distance[56] resulting in a distance dependence for the electron transfer rate[61] such that

$$k(r) = k_\circ e^{-\beta(r-r_\circ)} \qquad [5.4]$$

Table I. Fluorescence Lifetimes for Zinc Porphyrins

compound	solvent	χ^2_R	τ, nsec	k_{ET}, s^{-1}	$k_{ET}^{mono}/k_{ET}^{bis}$ †
ZnP^{t}Bu	C_6H_6	1.02	1.47		
ZnP1Q	C_6H_6	1.02	0.064, 1.51 (100:1)	$1.5x10^{10}$	
ZnP2Q	C_6H_6	0.93	1.45	$\leq 9x10^6$	≥ 1700
ZnP^{t}Bu	MTHF	1.04	1.66		
ZnP1Q	MTHF	1.14	0.090, 1.42 (50:1)	$1.0x10^{10}$	
ZnP2Q	MTHF	1.02	1.61	$\leq 2x10^7$	≥ 500
ZnP^{t}Bu	*n*PrCN	1.03	1.59		
ZnP1Q	*n*PrCN	1.16	0.120, 1.64 (10:1)	$7.7x10^9$	
ZnP2Q	*n*PrCN	0.99	1.54	$\leq 2x10^7$	≥ 390
ZnP^{t}Bu	CH_3CN	1.03	1.62		
ZnP1Q	CH_3CN	0.98	0.178, 1.60 (20:1)	$5.0x10^9$	
ZnP2Q	CH_3CN	0.99	1.60	$\leq 8x10^6$	≥ 630

† Ratio of electron transfer rates for mono– (*ZnP1Q*) to bis–linked (*ZnP2Q*) bicyclo[2.2.2]octyl porphyrin–quinones.

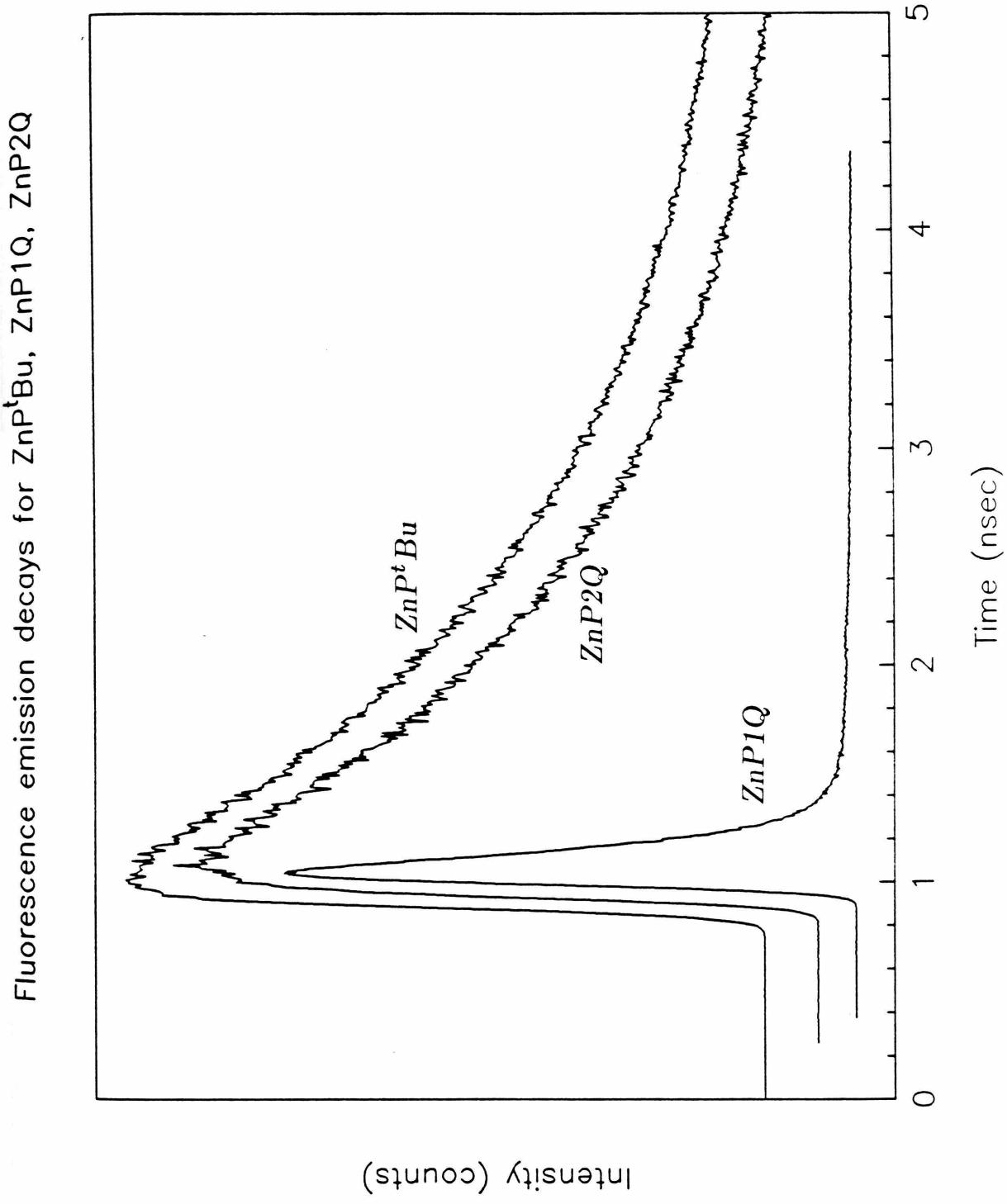

Figure 1. Time–resolved fluorescence decays of *ZnP^{t}Bu*, *ZnP1Q*, *ZnP2Q* in benzene at 298K.

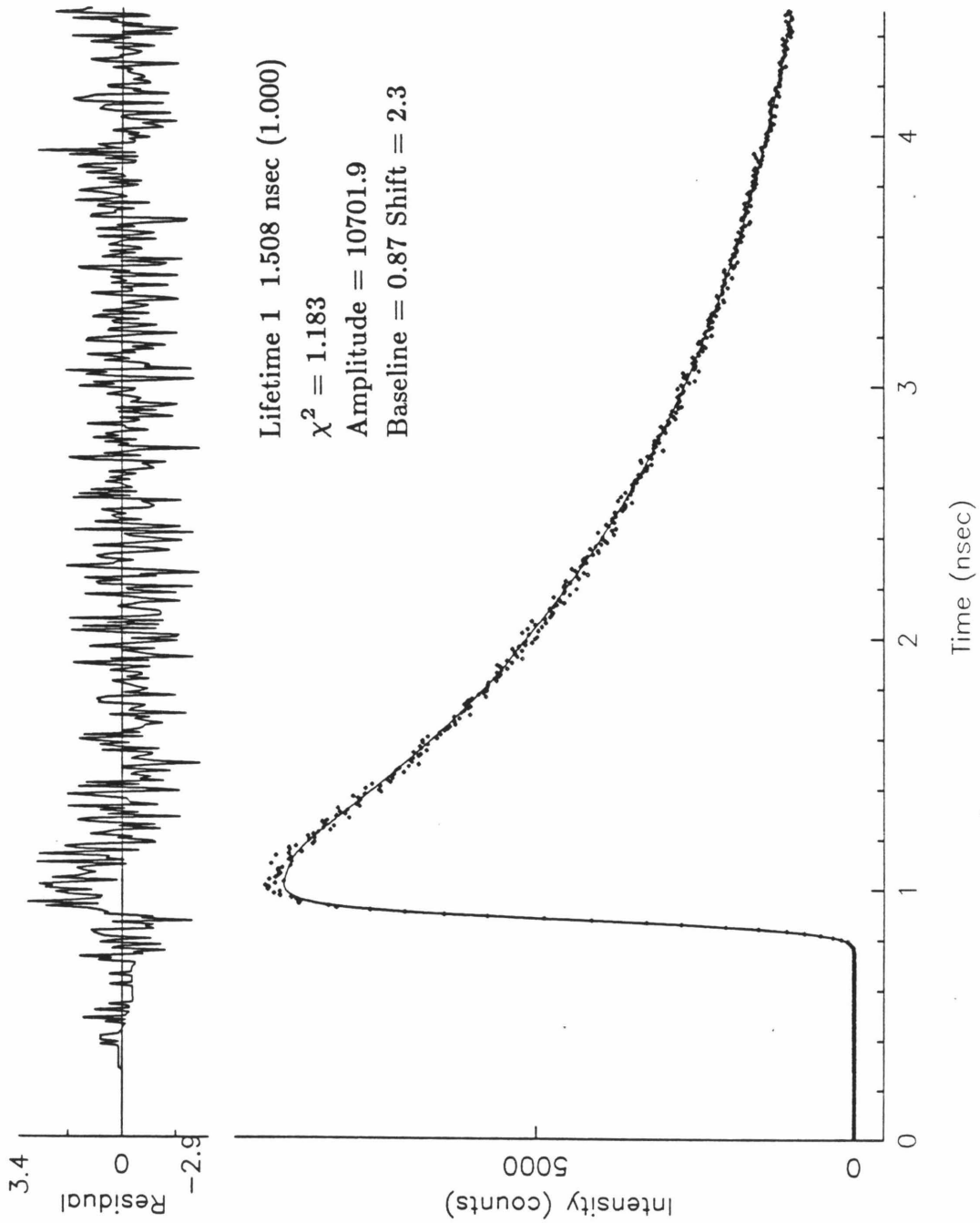

Figure 2. Monoexponential decay analysis of ZnP^tBu in benzene.

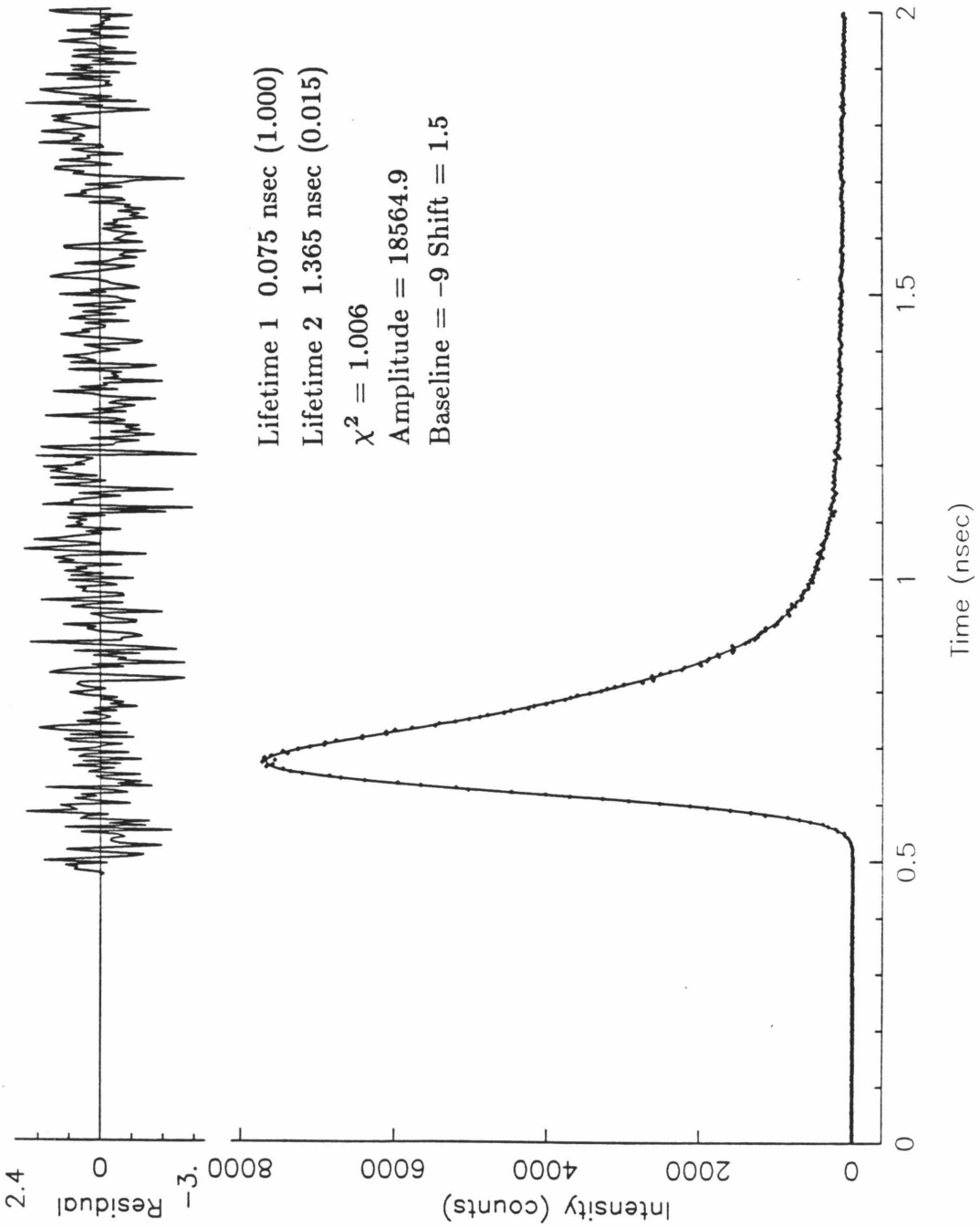

Figure 3. Biexponential decay analysis of *ZnP1Q* in benzene.

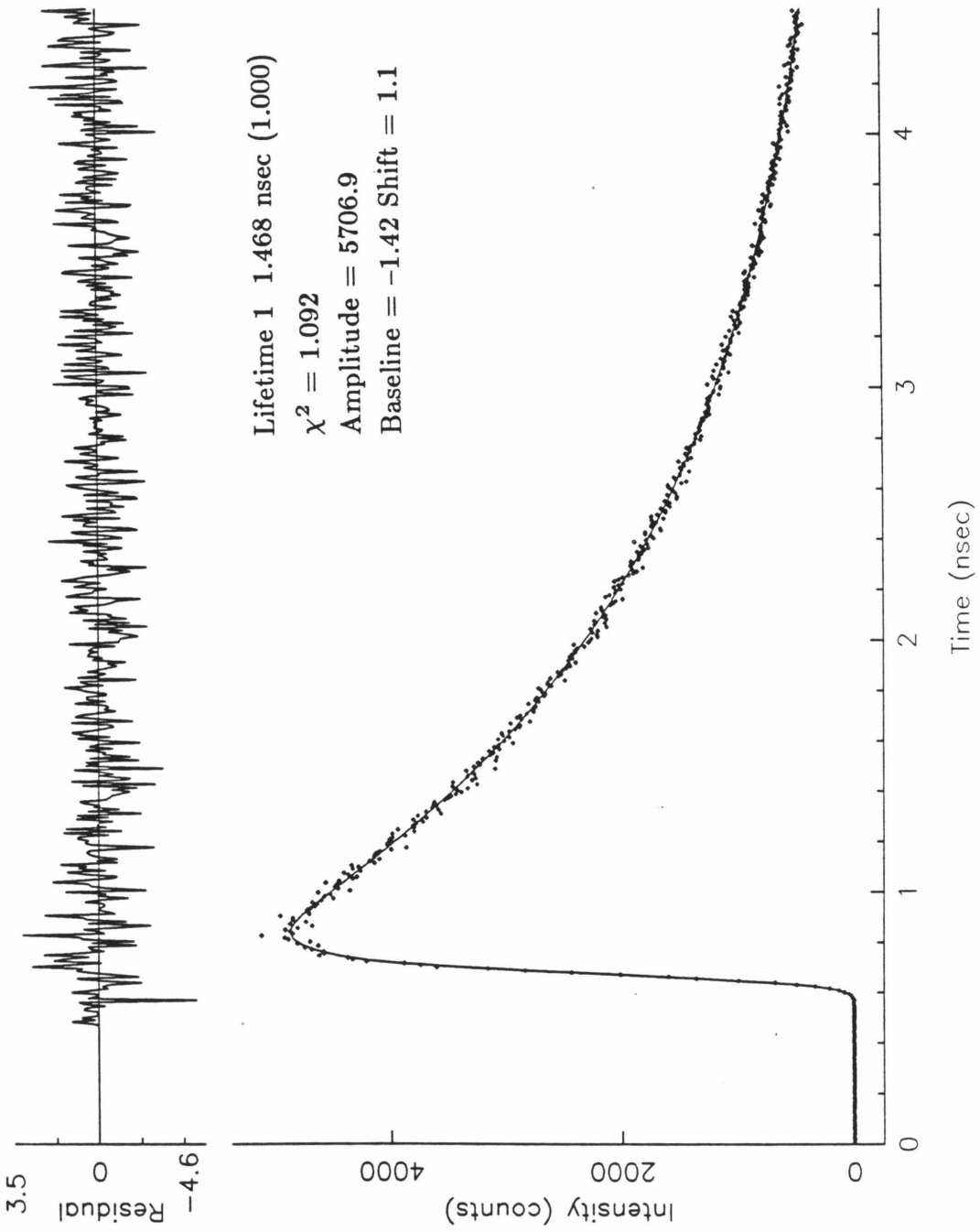

Figure 4. Monoexponential decay analysis of *ZnP2Q* in benzene.

where $k(r)$ is the electron transfer rate at separation distance r, β is the decay constant, and k_o is the electron transfer rate for the donor and acceptor at the contact distance r_o. Although only limits on k_{ET} can be obtained for *ZnP2Q*, and assuming the reorganization energies for *ZnP1Q* and *ZnP2Q* are roughly constant, the ratio of k_{ET} for the two compounds yields $\beta \geq 14$ nm^{-1} ($\alpha \geq 0.7$ Å^{-1}) for propagation across a bicyclo[2.2.2]octyl linker at these redox potentials ($\Delta G^\circ \sim 1$ eV). The assumption of a constant reorganization energy for the two compounds is not rigorously valid since corrections for coloumbic interactions in the charge–separated state are distance dependent, and λ_o has a separation distance component (equation [1.6]). These distance dependencies have led to the astounding prediction that under certain conditions the electron transfer rate at large separation distances may exceed rates for shorter distances.[170] Although only limits can be placed on the electron transfer rate in the bis–linked system, a reasonable estimate for the β decay constant can be obtained. Numerous studies have determined β values for a variety of systems, and values for the decay constant vary from 3–5 nm^{-1} for a fluorescence quenching experiment in which the donors and acceptors were separated by a fatty–acid monolayer,[171] to $\beta \sim 20$ nm^{-1} for reactions between solvated electrons and various acceptors.[172] A review of experimentally determined β values can be found in reference 61. In general, β tends to be <10 nm^{-1} for reactions in which one of the reactants is electronically excited, and the origin of the relatively large value of β determined here for electron transfer from the photoexcited porphyrin to the quinone is discussed below.

A recent theoretical calculation[114] for electron transfer through oligomers of bicyclo[2.2.2]octane determined the decrease in k_{ET} for incremental additions of linkers. The method was refined by the analysis of an inorganic system which incorporated an incremental distance change through a spirocyclobutane framework.[173] The treatment was developed to predict the energy and bridging spacer effects on the distance dependence for nonadiabatic electron–transfer reactions. The tunneling matrix element governing the transfer T_{ab} was considered to be a function of the separation distance between the donor and acceptor, and the energy of the transferring electronic state. Hence, different distance dependencies are predicted depending on the particular reaction under investigation. In particular, as the energy of the transferring state is closer to the highest occupied bonding orbital (HOMO) of the bridge states, "hole transport" is said to dominate the charge–transfer process. Similarly, "electron transport" will dominate for energy levels close in energy to the lowest unoccupied (LUMO) states of the bridge. The problem was formulated in an extended Hückel framework with the neglect of non–nearest neighbor interactions to provide the donor and acceptor wave functions which allow the calculation of T_{ab}. The linker units were considered to provide a periodic potential through which the electron propagates. Considering the carbon backbone only, the distance decay was determined to be independent of linker geometries in both the staggered and eclipsed orientations of adjacent bicyclo[2.2.2]octyl units, as well as staggered and eclipsed geometries between the π–donor (acceptor) system and the bicyclo[2.2.2]octane linker. The distance dependence was shown to depend on the symmetry of the donor and acceptor, how-

ever, and different effects are expected to be observed for σ–symmetry donors than for the π–symmetry donors studied here as a result of the differences in overlap with the bridge orbitals. An interesting prediction from this model is the different distance dependence (β) for the forward transfer ($P^*LQ \rightarrow P^{+\cdot}LQ^{-\cdot}$) in relation to back transfer ($P^{+\cdot}LQ^{-\cdot} \rightarrow PLQ$). This is a consequence of the fact that the energy transferring state is approximately the average of the porphyrin excited singlet energy and the quinone reduction potential, while the back transfer is the average of the energy of the charge–separated state and the porphyrin oxidation potential. Since the latter value is closer to the HOMO of the linker, the decrease of k_{ET} with distance is predicted to be less for the back transfer reaction than the forward transfer. The prediction for the ratio of electron transfer rates in the mono– and bis–linked compounds for the forward transfer step is ~1500, while the ratio of back transfer rates is ~60. This dramatic prediction awaits further experimental conformation. The ratio of the forward rate constants observed here demonstrate a ratio of 500 to $\geq$1700 in accord with these predictions.

Recent work on rigidly linked bichromophoric compounds have investigated incremental distance effects for electron transfer from a photoexcited naphthalene donor transferring an electron to a dicyanoethylene acceptor across a rigid hydrocarbon spacer.[107-109] These results revealed a decrease in k_{ET} of approximately one order of magnitude for the incremental addition of two sigma bonds. The assignment of the exothermicity of the electron transfer was based on the previously discussed Weller treatment, but comparison of the acetonitrile data for which electrochemical values are available indicate an electron transfer rate of $2x10^9 s^{-1}$ s^{-1}

at ΔG° ~1 eV, within an order of magnitude of the rates observed here. The calculated distance decay (β) for these compounds was β ~13–17 nm^{-1}. Although this decay factor is remarkably similar to the estimates for the porphyrin–quinone system discussed above, direct comparison is difficult due to the major differences between the chromophore orientations, nature of the bridging linker units, and energy of the transferring state. The decade decrease in k_{ET} per two σ–bond increment has also been reported for pulse radiolysis studies on intramolecular systems.[174] In contrast, aromatic bridging units have recently been reported which revealed a decrease in k_{ET} of only 22 to 27 per phenyl group (4Å) increment.[119]

Solvent Effects on Electron Transfer Rates

Picosecond fluorescence measurements allow the quantitation of the electron transfer deactivation of the porphyrin excited singlet. The high degree of reproducibility of the lifetime measurements thus allows an extremely sensitive probe for modest changes in the electron transfer rate constant. The study above investigated four solvents of varying polarity. This investigation was broadened in scope to determine if k_{ET} depends critically on solvent. The results of the solvent investigation are tablulated in Table II. A very weak dependence of k_{ET} on the solvent was observed. The electron transfer rate varies by at most a factor of 50 in all of the solvents examined to date. Two control experiments were performed, in which the fluorescence emission was measured in the presence of added electrolyte (TBAP or THAP), *i.e.*, under similar conditions in which the electrochemical measurements were performed. Modest decreases in the calculated k_{ET} values

(~20%) were obtained indicating the presence of the added electrolyte has only a minor effect on the overall rate. The absence of electrochemical measurements in all solvents investigated hamper the determination of the changes in exothermicity which would affect the observed rates. What is reliably determined in this study is the absence of correlation of the electron transfer rate with a number of solvent parameters. Least–squares analyses of the results in Table II revealed poor correlations with the solvent index of refraction n, n^2, $1/n^2$ or the Marcus solvent parameter $(1/n^2 - 1/\epsilon)$.[145] The best correlation appeared to be with the solvent dielectric constant (correlation coefficient 0.9), confirming the qualitative trend of a decrease in k_{ET} with increasing solvent polarity. No correlation of k_{ET} with solvent viscosity was observed. These results contrast with recent reports of a correlation of k_{ET} with the solvent index of refraction for a moderately flexible porphyrin–quinone system linked via a methylene–amide spacer.[85]

Future experiments will investigate the temperature dependence of this compound near the freezing point of various solvent glasses,[175] where more significant changes in viscosity[176] can be investigated to compare with the preliminary results found here. A broader range of viscosities may be required to unequivocally rule out a modulation of the *meso*–phenyl "wobble" frequency with solvent, which could result in the direct modulation of the T_{ab} (and hence k_{ET}) for this compound.

The observed range of rates could be due to shifts in the exothermicity for the reaction, changes in the outer sphere reorganization energy, changes in the coupling to the porphyrin π–system through the *meso*–phenyl substituent, or a combination

Table II. Solvent Effects on k_{ET} for *ZnP1Q*.[a]

compound	solvent	χ^2_R	τ, nsec	k_{ET}, s^{-1} [b]
ZnP^{t}Bu	C_6H_6+2%pyr	1.00	1.60	
ZnP1Q	C_6H_6+2%pyr	1.08	0.051	1.90×10^{10}
ZnP^{t}Bu	*o*–Xyl	1.00	1.53	
ZnP1Q	*o*–Xyl	1.01	0.082	1.15×10^{10}
ZnP^{t}Bu	C_6H_6	1.02	1.47	
ZnP1Q	C_6H_6	1.08	0.076	1.25×10^{10}
ZnP^{t}Bu	C_6H_6+0.1M THAP	1.02	1.48	
ZnP1Q	C_6H_6+0.1M THAP	1.10	0.091	1.03×10^{10}
ZnP^{t}Bu	2MTHF	1.06	1.66	
ZnP1Q	2MTHF	1.02	0.092	1.03×10^{10}
ZnP^{t}Bu	*n*PrCN	0.98	1.59	
ZnP1Q	*n*PrCN	1.01	0.118	7.85×10^{9}
ZnP^{t}Bu	*p*–Dioxane	1.02	1.21	
ZnP1Q	*p*–Dioxane	0.88	0.121	7.44×10^{9}
ZnP^{t}Bu	CH_3CN	1.04	1.64	
ZnP1Q	CH_3CN	0.98	0.178	5.01×10^{9}
ZnP1Q	CH_3CN+0.1M TBAP	1.00	0.203	4.32×10^{9}
ZnP^{t}Bu	DMF	1.07	1.71	
ZnP1Q	DMF	1.01	0.234	3.69×10^{9}

[a] DMF: *N*,*N*–dimethylformamide; *n*PrCN: butyronitrile; *o*–Xyl: *o*–Xylene; THAP: tetra–*n*–hexylammonium perchlorate; pyr: pyridine; TBAP: tetra–*n*–butylammonium perchlorate; 2MTHF: 2–methyltetrahydrofuran.

[b] Calculated from $k_{ET} = 1/\tau - 1/\tau_o$, where τ is the fluroescence lifetime of *ZnP1Q* and τ_o is the fluroescence lifetime of *ZnP^{t}Bu*.

of the above. The small trend in the observed electron transfer rates with solvent polarity is consistent with expectations for a nonadiabatic electron transfer from an initial uncharged state, however.[177] The extent of dielectric relaxation in response to the generated charge–transfer state does not affect the forward transfer rate since the dielectric relaxation occurs largely after the electron transfer has taken place. Significant polarity effects are expected for the back electron transfer in these systems, however, as a result of the large solvent polarization about the charge–separated state.

Low Temperature Fluorescence Studies

The efficient electron transfer pathway observed for the single bicyclo[2.2.2]octyl linked porphyrin–quinone was investigated as a function of temperature. Measurement of *ZnP1Q* and *ZnP1QCl* at room temperature revealed the typical biexponential decay behavior discussed in detail above. Cooling the *same* samples to 77K resulted in a highly nonexponential fluorescence decays. In contrast, the fluorescence decay of ZnP^tBu remained strictly monoexponential under the identical measurement conditions at 77K (τ = 1.83 nsec; χ^2_R = 1.02). A biexponential decay can be expressed as as

$$I(t) = \exp^{-t/\tau_1} + \frac{b_\circ}{a_\circ}\exp^{-t/\tau_2} \qquad [5.5]$$

where *I(t)* is the fluorescence intensity at time t, $b_\circ/a_\circ$ is the ratio of initial fluorescence amplitudes, and τ_1 and τ_2 are the fitted lifetimes. A reasonable biexponential fit could not be obtained for either sample. However, an angle–modulated

biexponential decay[178] expressed as

$$I(t) = \sum_{i=1}^{N} \frac{1}{N} \exp^{-t[\cos^2\theta_i/\tau_1 + 1/\tau_2]} + \frac{b_\circ}{a_\circ} \exp^{-t/\tau_2} \qquad [5.6]$$

where N is the number of dihedral angles, $0° \leq \theta_i \leq 90°$, gave an excellent agreement with the observed decay. The cos θ factor is the approximate overlap of two π–systems as a function of the angle between the planes of the molecules. Since k_{ET} is a function of $| T_{ab} |^2$, $\cos^2\theta$ is the expected modulation of the observed lifetime.

The strict monoexponentiality of the reference *ZnP*^{t}*Bu* porphyrin under identical measurement conditions argues strongly against any "site effects"[179] in the rigid amorphous solvent glass at 77K. Measurements of the visible absorption spectra of *ZnP1Q* at 77K rule out significant aggregation of the molecule which could provide a fluorescence quenching mechanism.[145] Additional control experiments were performed by measuring *ZnP2Q* at 77K, resulting in excellent (unquenched) monoexponential fluorescence decays. Thus, the quenching observed for *ZnP1Q* and *ZnP1QCl* are unique to these compounds and are not due to the presence of the quinone functionality providing a ligand to the porphyrin which could also provide a quenching mechanism. In light of the efficient electron transfer quenching for these compounds at room temperature, the control experiments suggest an efficient electron transfer quenching pathway is also viable in a rigid glass at 77K. The proposed explanation for the nonexponential behavior observed for *ZnP1Q* and *ZnP1QCl* at 77K is that freeezing the sample results in an ensemble of rotational conformations between the porphyrin and quinone. At room temperature,

the quinone is spinning fast enough to effectively average the observed rate. At 77K an ensemble of rotomers are present and the distribution of angles between the porphyrin plane and the quinone planes results in a distribution of k_{ET} values. Thus, the maximum rate would be for an angle $\theta = 0°$, and k_{ET} would fall off approximately as a $\cos^2\theta$ function.

An important point to note is that the results of the low temperature fit (shown in Figures 5 and 6) are consistent with the observed hydroquinone fraction observed in the *same* samples at room temperature. As the angle θ approaches 90°, k_{ET} decreases significantly, and the observed decay would be similar to the reference porphyrin. While it is likely that k_{ET} is not rigorously zero (*e.g.*, at $\theta = 90°$), it suffices to say the rate is significantly slower than the maximum k_{ET} observed at $\theta = 0°$, *i.e.*, in a coplanar arrangement between the porphyrin and quinone. The advantage of the angle–modulated fit is that the low temperature results can be fit *without additional free parameters.* A comparably good fit was obtained for *ZnP1Q* using a triexponential decay analysis (τ_1=0.194, τ_2=0.782, τ_3=1.871 nsec (1:0.38:0.31), χ^2=1.04), but this fit involves two *additional* free parameters compared to the angle–modulated biexponential fit.

If these low temperature results are born out by transient absorption measurements to confirm the production of the porphyrin radical cation, this indicates a dramatic dependence of k_{ET} on the precise geometry of the molecule. If the transfer was adiabatic, a decrease in the matrix element by a factor of 100 would not significantly change the k_{ET} value since the rate is dominated by solvational and other nuclear motions. In the nonadiabatic regime, however, the small value for

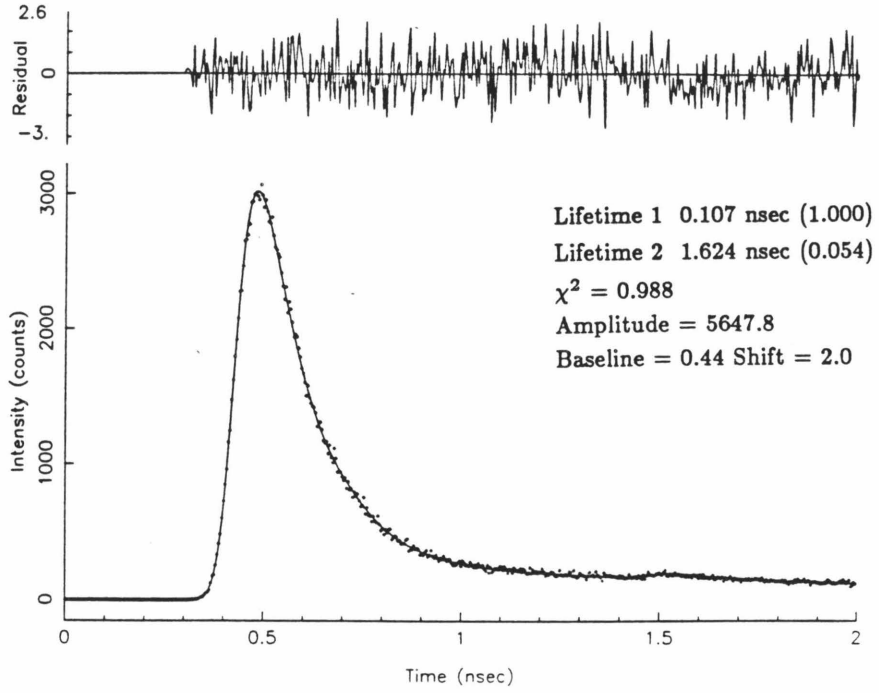

Figure 5a. Biexponential decay analysis of *ZnP1QCl* in MTHF at 298K.

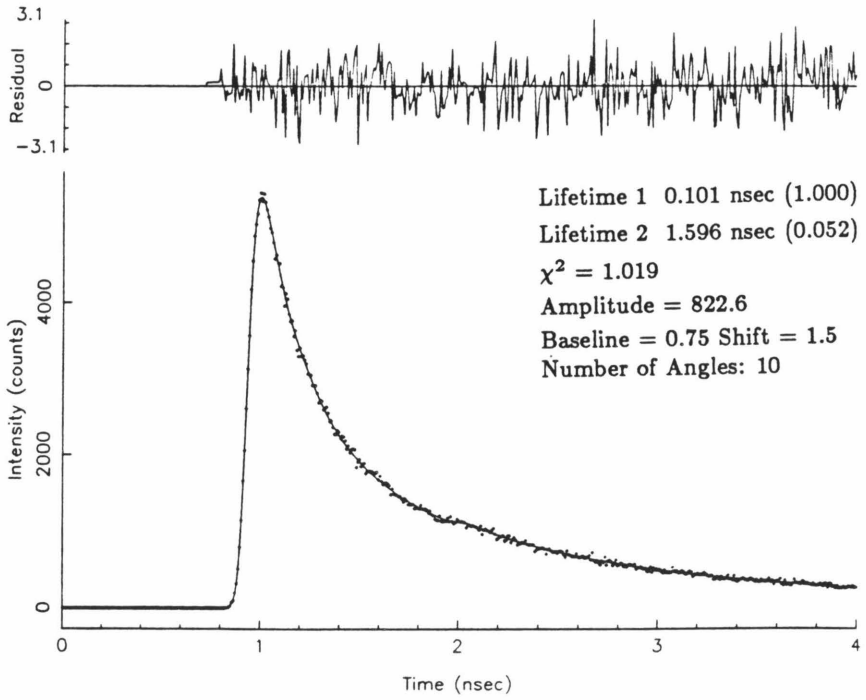

Figure 5b. Angle–modulated decay analysis of *ZnP1QCl* in MTHF at 77K.

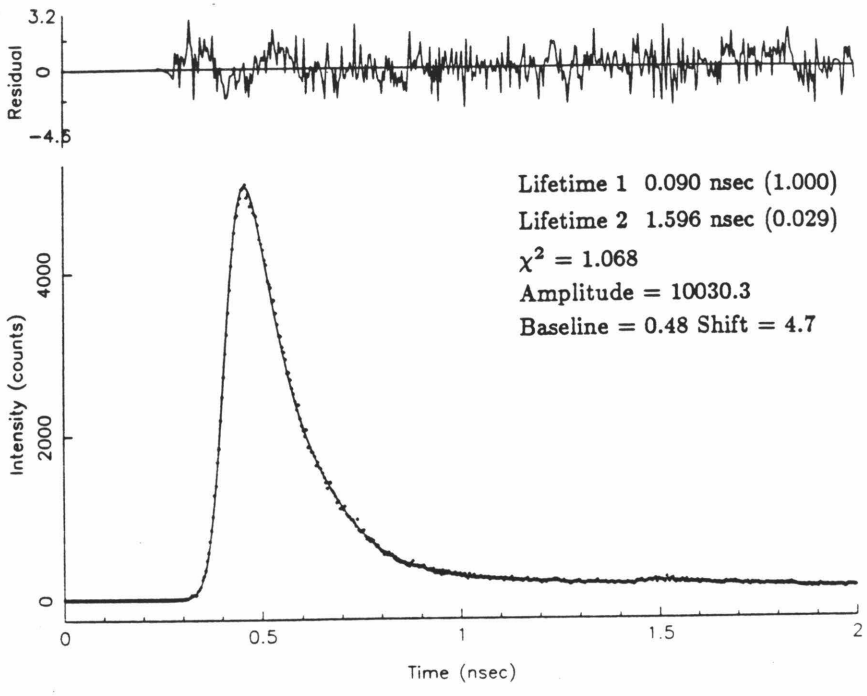

Figure 6a. Biexponential decay analysis of *ZnP1Q* in MTHF at 298K.

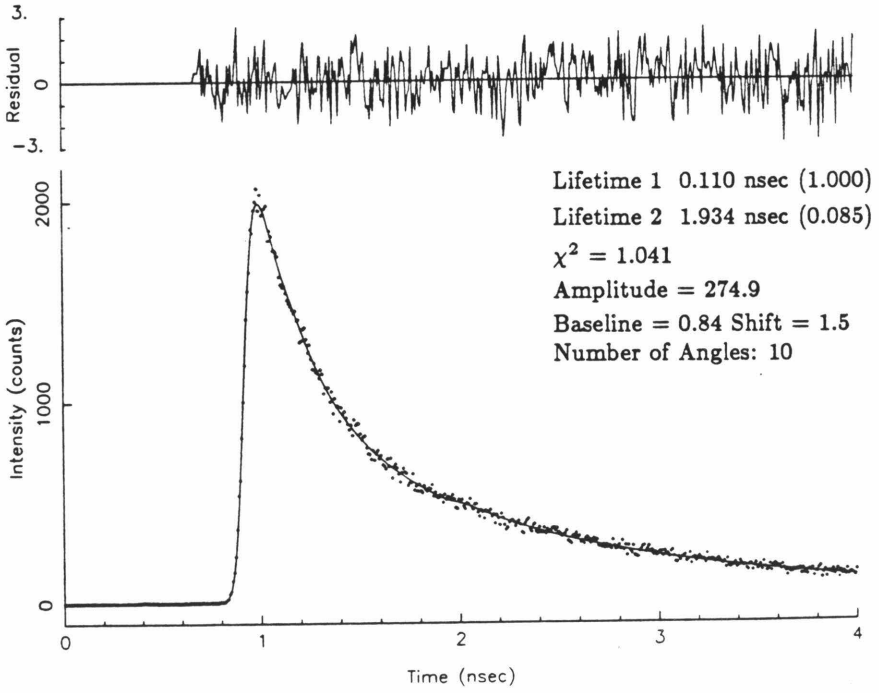

Figure 6b. Angle–modulated decay analysis of *ZnP1Q* in MTHF at 77K.

T_{ab} significantly affects the observed rate when modulated by the cos θ function describing the orientation angle between the planes of the chromophores. The low temperature data argues strongly for the nonadiabatic nature for the electron transfer in these bicyclo[2.2.2]octyl linked systems.

The lifetime obtained in the angle–modulated fit is the maximum rate observed for $\theta = 0°$ (*i.e.*, a coplanar orientation). To compare this lifetime to the rotationally averaged room temperature rate,

$$k_{ET}^{avg} = k_{ET}^{max} \int_0^{2\pi} \frac{1}{\theta} \cos^2\theta d\theta = k_{ET}^{max} \frac{1}{2\pi} \left(\frac{2\pi}{2} + \frac{1}{4} \sin 4\pi \right) \qquad [5.7]$$

$$k_{ET}^{avg} = \frac{1}{2} k_{ET}^{max} \qquad [5.8]$$

where k_{ET}^{max} is the rate obtained from the angle modulated decay analysis and k_{ET}^{avg} is the rate obtained from the biexponential fit. Thus, comparing the results from the room temperature fit for *ZnP1QCl* (τ = 107 psec, $k_{ET}^{avg} = 8.7 \times 10^9 s^{-1}$) with the low temperature data (τ = 101 psec, $k_{ET}^{max} = 9.4 \times 10^9 s^{-1}$, $k_{ET}^{avg} = 4.7 \times 10^9 s^{-1}$) indicates the electron transfer rate has decreased by only a factor of 1.9 at 77K. Similarly, comparisons for *ZnP1Q*, (τ = 90 psec, $k_{ET}^{avg} = 1.0 \times 10^{10} s^{-1}$), with the low temperature data (τ = 110 psec, $k_{ET}^{max} = 8.5 \times 10^9 s^{-1}$, $k_{ET}^{avg} = 4.3 \times 10^9 s^{-1}$) indicate the electron transfer rate has decreased by 2.5 at 77K. The observation of an exceedingly weak dependence of the electron transfer rate with temperature suggests nuclear tunneling may dominate the transfer in these systems over the full temperature range studied.

While no reports exist in the literature of synthetic porphyrin–quinone systems which exhibit fluorescence quenching at 77K, one is left to question the

validity of this proposal. The observation of efficient electron transfer in photosynthetic RCs (Chapter 1) at low temperatures suggests there is reason to expect electron transfer to occur in systems characterized by rigidly fixed chromophores. Efficient ET has also been observed by pulse radiolysis studies of donors and acceptors in rigid glasses at low temperatures.[68] Perhaps the other porphyrin–quinone systems reported in the literature have enough flexibilty to achieve a conformation that insures minimal chromophore interactions at low temperatures. This is the only synthetic porphyrin–quinone system to date capable of reproducing the documented success of photosynthetic RCs at low temperature, and future experiments to directly observe the charge–transfer state will conclusively confirm or refute these findings.

Exothermicity Investigations: Electrochemistry

In an attempt to minimize the ambiguities associated with the calculation[113] of the exothermicity of the electron transfer from the porphyrin to the quinone based on oxidation and reduction potentials for the isolated chromophores in solvents for which electrochemical data is available, an effort was made to directly measure the electrochemistry in the solvents in which the spectroscopic studies were performed. Recent advances in microelectrode techniques[180, 181] suggested the possibility of using this approach for the electrochemical measurements in solvents of low dielectric and high resistivity such as benzene or methyltetrahydrofuran.

Evidence presented elsewhere[145] indicated the linked porphyrin–quinone der-

ivatives can be well approximated by the measurement of the unlinked compounds as model systems. That is, although the chromophores are linked chemically, the individual ends of the molecule act substantially independently in the electrochemical measurements, and the oxidation and reduction potentials are reasonably described by the use of model compounds. The quinone reduction potentials were measured for variously substituted derivatives of *p*–methylbenzoquinone in direct analogy to the porphyrin–quinone derivatives. The methyl, dimethyl, and cyano derivatives were prepared and measured by A.D. Joran.[145] The halogenated derratives were prepared by the identical synthetic method previously discussed (Chapter 3), via the addition of HCl or HBr to *p*–methylbenzoquinone in THF, reoxidation of the resulting hydroquinone to the quinone with PbO_2, and subsequent purification on Grade III alumina. The use of the methyl–benzoquinones as models for the bicyclo[2.2.2]octyl linked quinone derivatives should introduce the error of at most 40 mV[182] due to the differences in reduction potentials for a methyl–benzoquinone versus a tertiary substituted benzoquinone, *e.g.*, the *tert*–butylbenzoquinone reduction potential is observed at more negative potentials.

The first reduction wave for the bromo–, chloro– and dichloro–methylbenzoquinone model compounds as determined by linear sweep voltammetry are shown in Figure 7a–7c in acetonitrile with 0.1 M tetrabutylammonium perchlorate as the added electrolyte. The reduction potentials versus the ferrocene/ferrocenium reference couple[183] are listed with the corresponding data for ZnP^tBu and methyl–benzoquinone model compounds obtained by A.D. Joran[145] in Tables III and IV. To directly compare the data for the four solvents used in the spectroscopic

studies, the assumption was made that the differences between the reduction potential of each of the substituted benzoquinones and methyl–benzoquinone were approximately constant in each solvent. Since the reduction potential for methyl–benzoquinone has been measured in all four solvents under investigation,[145] the electrochemistry on the model quinones in acetonitrile can be used to obtain the relative ranking of the porphyrin–quinone derivatives in each of the four solvents used in the spectroscopic investigations.

The magnitude of specific ion–pairing effects in the different solvents with the concentrations of supporting electrolytes employed is presently unknown. Although no major changes in the observed half–wave potentials were observed over the modest concentration range of supporting electrolyte investigated,[145] ion–pairing effects may dominate the electrochemical measurements in the extremely non–polar solvents investigated. The use of possible ligating perchlorate salts for investigation of the porphyrin oxidation potential could also have a dramatic effect on the observed porphyrin potentials, and future studies should investigate the effect of alternative anions (*e.g.*, BF_4 or PF_6) on the porphyrin oxidation potential to determine the magnitude of this effect. Recent electrochemical investigations may well call into question the use of the "solvent independent" ferrocene/ferrocenium reference couple upon which comparisons between the various solvents is based.[181]

Qualitatively, the data in Table III follow the expected trends in solvent polarity. As the polarity of the solvent is increased, the charge–transfer state is stabilized and the exothermicity of the reaction is increased. There is a com-

Table III. Electrochemical Data for Porphyrins and Quinones[a]

solvent	$E_{1/2}(Q/Q^{-\cdot})$[b]	$E_{1/2}(P/P^{+\cdot})$[c]	W_P[d]	$-\Delta G^{\circ\prime}$	$-\Delta G^{\circ\prime}(R)$
C_6H_6	–1.30V[e]	+0.18V[f]	0.428 eV	0.67 eV[g]	1.10 eV[g]
MTHF	–1.36[e]	–0.14[e]	0.156	0.93	1.08
*n*PrCN	–1.00[h]	+0.16[h]	0.048	0.99	1.04
CH_3CN	–0.95[i]	+0.19[i]	0.026	1.01	1.04

[a] Half–wave potentials were determined by linear sweep voltammetry (or differential pulse voltammetry in acetonitrile due to low solubility of the porphyrin), using a ferrocene/ferrocenium reference. All redox couples are reversible or nearly reversible, *i.e.*, $| E_{3/4} - E_{1/4} |$ = 56–85 mV (n=1). $-\Delta G^{\circ\prime} = W^* - E_{1/2}(P/P^{+\cdot}) + E_{1/2}(Q/Q^{-\cdot})$ where $W^* = 2.15 \pm 0.01$ eV is the singlet excitation energy for the porphyrin. $-\Delta G^{\circ\prime}(R) = -\Delta G^{\circ\prime} + W_P$ is the free energy after correction for Coulombic interactions in the charge–separated state.

[b] *p*–Methylbenzoquinone.

[c] Zinc 5–(*p–tert*–butyl)phenyl–2, 3, 7, 8, 12, 13, 17, 18–octamethylporphyrin.

[d] Correction term for Coulombic interactions in the charge–separated state: $W_p = \frac{1}{4\pi\epsilon\epsilon_o} e^2/R \approx 14.8/\epsilon R$, where ϵ is the solvent dielectric constant and $R(\text{Å}) = 14.8$Å is the center–to–center distance between the porphyrin and quinone for *ZnP1Q*.

[e] 0.3 M tetrahexylammonium perchlorate (THAP); 25μm diameter Pt disk electrode.

[f] 0.1 M THAP; 25μm diameter Pt disk electrode.

[g] Estimated uncertainty is ± 0.05 eV

[h] 0.1 M tetrabutylammonium perchlorate (TBAP); 25μm diameter Pt disk electrode.

[i] 0.2 M TBAP; 1.6–mm diameter Pt disk working electrode.

Table IV. Half-wave potentials for reduction of 2–methyl–1,4–benzoquinone substituted by 5–R_1, 6–R_2[a] groups in acetonitrile.[b]

$-R_1$	$-R_2$	$E_{1/2}(Q/Q^{-\cdot})$ (V)[c]
–Me	–Me	–1.12
–Me	–H	–1.04
–H	–H	–0.95
–Br	–H	–0.91
–Cl	–H	–0.89
–Cl	–Cl	–0.82
–CN	–H	–0.55

[a] 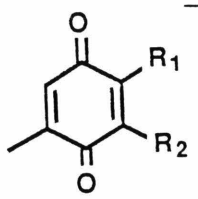

[b] Determined by linear sweep voltametry with 25 or 127μm diameter Pt microelectrode using 0.1M tetrabutylammonium perchlorate (TBAP) as supporting electrolyte; Pt wire auxiliary electrode; ferrocene/ferrocenium reference electrode.

[c] Half-wave potentials are certain to within ±15 mV and are reversible or nearly reversible, *i.e.*, $| E_{3/4} - E_{1/4} | = 55–75$ mV (n=1).

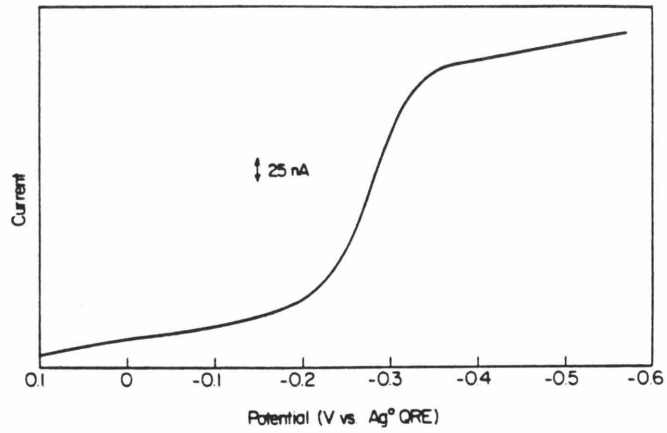

Figure 7a. LSV of 2–methyl–5–bromo–1,4–benzoquinone in CH_3CN (~0.05 M, 0.1 M TBAP).

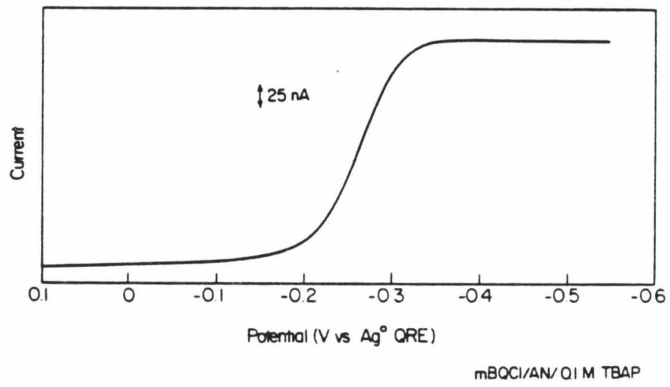

Figure 7b. LSV of 2–methyl–5–chloro–1,4–benzoquinone in CH_3CN (~0.05 M, 0.1 M TBAP).

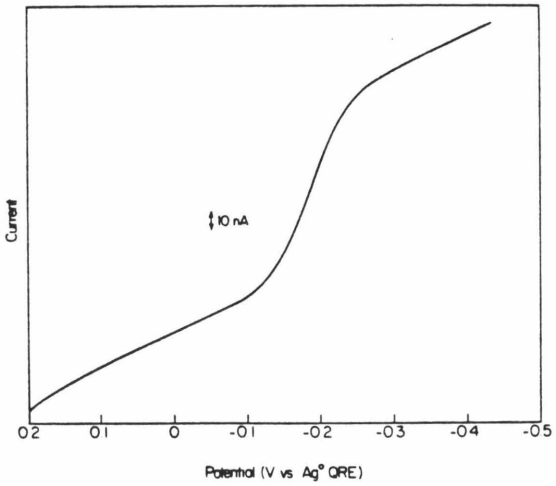

Figure 7c. LSV of 2–methyl–4, 5–dichloro–1,4–benzoquinone in CH_3CN (~0.01 M, 0.1 M TBAP).

pensating effect, however, in that the most non–polar solvents exhibit the least dielectric shielding resulting in a substantial Coulombic correction term for the attraction between the porphyrin cation and quinone anion. This compensating effect is difficult to quantitatively determine. If a simple Coulombic correction applies, this correction term is

$$W_p = \left[\frac{1}{4\pi\epsilon\epsilon_\circ}\right]\frac{e^2}{\mathrm{R}} = \frac{14.38}{\epsilon \mathrm{R}}\ \mathrm{eV} \qquad [5.9]$$

where R is the center–to–center distance between the porphyrin and quinone (14.8 Å) and ϵ is the solvent dielectric constant. This simple expression assumes the charge–transfer state can be reasonably approximated by two point charges at the center–to–center separation distance. The delocalized nature of the two aromatic systems may well call this assumption into question. In addition, shielding effect due to the presence of the bicyclo[2.2.2]octyl unit separating the two charges is difficult to assess quantitatively.

Although substantial effort was invested to quantitatively determine the exothermicity of the reaction between the porphyrin excited singlet and the quinone, the unknown degree of the ion–pairing effects in the electrochemical measurements and the corrections for Coulombic interactions in the charge–separated state suggest the derived values of $\Delta G°$ discussed below for the exothermicity investigations of k_{ET} should be considered accurate in a *relative* order only (and are thus designated as $\Delta G°_{rel}$) and not with regard to absolute scale, particularly in non–polar solvents where these correction terms may be large.

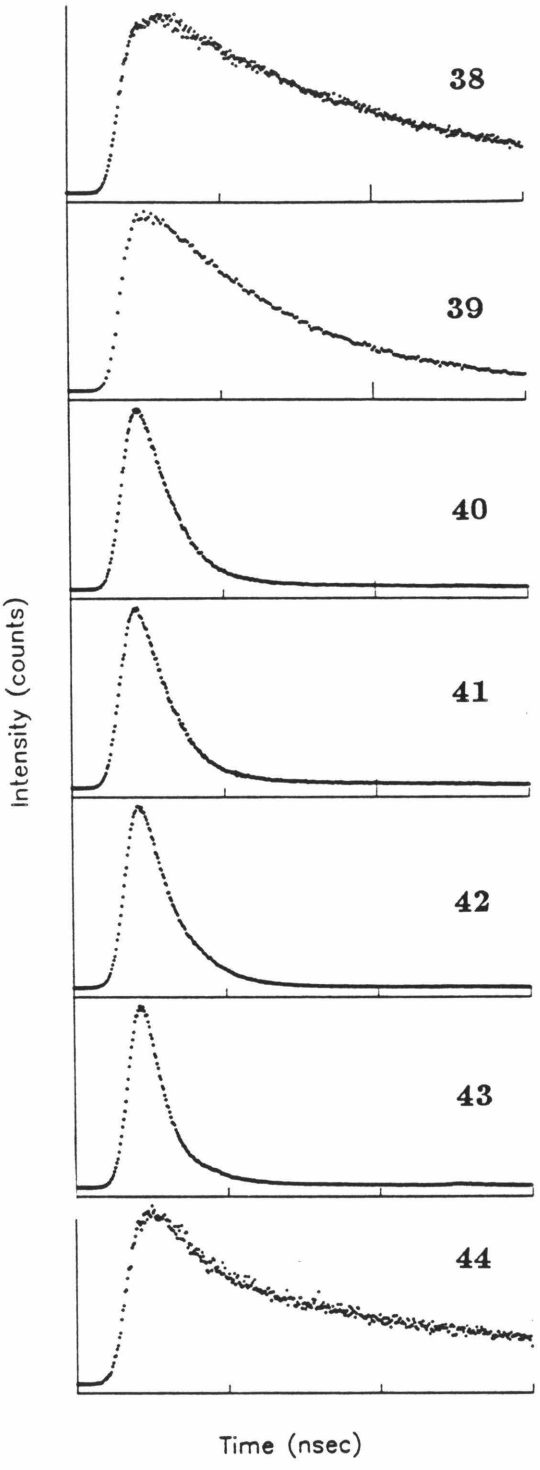

Figure 8. Time–resolved fluorescence decays of compounds **38–44** in benzene at 298K.

Exothermicity Investigations

The seven modified porphyrin–quinones designed to investigate the energy gap dependence on k_{ET} were studied via picosecond fluorescence spectroscopy. The results of this investigation are tabulated in Table V for four solvents of increasing polarity, and representative fluorescence decays for the seven derivatives are shown for comparison in Figure 8. The assignment of the driving force for the reactions from the excited singlet of the porphyrin are based on the singlet excitation energy and the previously discussed electrochemical redox measurements on model compounds such that

$$-\Delta G^{\circ}_{rel} = W^* - E_{1/2}(P/P^{+\cdot}) + E_{1/2}(Q/Q^{-\cdot}) \qquad [5.10]$$

where $W^* = 2.15 \pm 0.01$ eV is the singlet excitation energy and the $E_{1/2}$ values are the oxidation and reduction potentials for the porphyrin and quinone model compounds (see Tables III and IV). This value is uncorrected for Coulombic interactions in the charge separated state. Due to the difficulties in obtaining the electrochemistry in solvents of low dielectric constant, it was assumed that the differences between each of the substituted model quinones and methyl–benzoquinone were approximately constant as discussed above. Thus the reduction potentials for the model quinones in acetonitrile can be used to determine the relative ranking of the porphyrin–quinones in each of the solvents (Table IV) used in the spectroscopic investigations.

Qualitatively, one observes a dramatic increase in k_{ET} over a relatively small range of exothermicity for the dimethyl and monomethyl substituted derivatives.

Table V. Fluorescence Lifetimes for Zinc–porphyrins[a] **38–44**

Compound	Solvent	$-\Delta G^{\circ}_{rel}$ [b]	χ^2_R [c]	τ (nsec)[d]	k_{et} (s^{-1})
–Me,–Me	C_6H_6	0.50	0.913	0.801,1.722(9:1)	5.68×10^{8}
–Me,–H	C_6H_6	0.61	1.080	0.443,1.161(20:1)	1.58×10^{9}
–H,–H	C_6H_6	0.67	1.081	0.076,1.490(71:1)	1.25×10^{10}
–Br,–H	C_6H_6	0.83	0.902	0.075,1.362(50:1)	1.27×10^{10}
–Cl,–H	C_6H_6	0.84	1.103	0.082,1.549(200:1)	1.15×10^{10}
–Cl,–Cl	C_6H_6	0.96	1.063	0.055,1.894(167:1)	1.75×10^{10}
–CN,–H	C_6H_6	1.07	0.990	0.114,1.520(1:2)	8.09×10^{9}
–Me,–Me	MTHF	0.76	0.935	0.594,1.488(7:1)	1.08×10^{9}
–Me,–H	MTHF	0.87	0.997	0.384,1.591(16:1)	2.00×10^{9}
–H,–H	MTHF	0.93	1.017	0.092,1.537(11:1)	1.03×10^{10}
–Br,–H	MTHF	1.09	0.942	0.090,1.611(20:1)	1.05×10^{10}
–Cl,–H	MTHF	1.10	1.118	0.099,1.661(77:1)	9.50×10^{9}
–Cl,–Cl	MTHF	1.22	1.156	0.062,1.629(42:1)	1.55×10^{10}
–CN,–H	MTHF	1.33	1.056	0.236,1.717(2:3)	3.63×10^{9}
–Me,–Me	*n*PrCN	0.82	1.014	0.679,1.798(4:1)	8.44×10^{8}
–Me,–H	*n*PrCN	0.93	1.004	0.448,1.295(7:1)	1.60×10^{9}
–H,–H	*n*PrCN	0.99	1.005	0.118,1.467(20:1)	7.85×10^{9}
–Br,–H	*n*PrCN	1.15	0.953	0.121,1.512(8:1)	7.64×10^{9}
–Cl,–H	*n*PrCN	1.16	0.959	0.132,1.576(25:1)	6.95×10^{9}
–Cl,–Cl	*n*PrCN	1.28	0.965	0.085,1.445(23:1)	1.11×10^{10}
–CN,–H	*n*PrCN	1.39	1.007	0.302,1.811(1:1)	2.68×10^{9}
–Me,–Me	CH_3CN	0.84	1.004	0.829,1.569(2:1)	5.89×10^{8}
–Me,–H	CH_3CN	0.95	0.920	0.617,1.430(6:1)	1.01×10^{9}
–H,–H	CH_3CN	1.01	0.976	0.178,1.601(20:1)	5.00×10^{9}
–Br,–H	CH_3CN	1.17	0.973	0.178,1.513(5:1)	5.00×10^{9}
–Cl,–H	CH_3CN	1.18	1.111	0.215,1.491(2:1)	4.03×10^{9}
–Cl,–Cl	CH_3CN	1.30	1.026	0.121,1.283(24:1)	7.65×10^{9}
–CN,–H	CH_3CN	1.41	1.030	0.335,1.660(1:1)	2.37×10^{9}

[a] Compound designation indicates quinone substitution (see Figure 2, Chapter 3).

[b] $-\Delta G^{\circ}_{rel}$ (eV) = $W^* - E_{1/2}(P/P^{+\cdot}) + E_{1/2}(Q/Q^{-\cdot})$ where $W^* = 2.15\pm0.01$ eV is the singlet excitation energy for the porphyrin, and the $E_{1/2}$ values are the oxidation and reduction potentials for the porphyrin and quinone model compounds.

[c] P.R. Bevington, "Data Reduction and Error Analysis for the Physical Sciences," New York: McGraw-Hill, 1969; p. 202.

[d] Lifetimes tabulated as τ_1, τ_2, and fraction (1:2) for biexponential decay analyses.

With further increases in the driving force, little change in the electron transfer rate constant is observed until the cyano substituted derivative in which a modest decrease in k_{ET} is observed. The data tabulated in Table V are plotted in Figures 9–12. Superimposed on the data are the results of a least–squares fit to a Marcus equation[61] of the form

$$k_{ET} = \frac{2\pi}{\hbar} \mid T_{ab} \mid^2 \frac{1}{\sqrt{4\pi\lambda \mathrm{kT}}} \exp\left(\frac{-(\lambda + \Delta \mathrm{G}^\circ)^2}{4\lambda \mathrm{kT}}\right) \qquad [5.11]$$

The results from the Marcus fit are tabulated in Table VI. Since

$$\lambda = \lambda_i + \lambda_o \qquad [5.12]$$

$$\lambda_o = (\Delta \mathrm{e})^2 \left[\frac{1}{2a_1} + \frac{1}{2a_2} - \frac{1}{\mathrm{r}}\right]\left[\frac{1}{n^2} - \frac{1}{\epsilon_s}\right] \qquad [5.13]$$

with with parameters as defined in Chapter 1, a plot of λ versus the so–called Marcus solvent parameter ($[1/n^2 - 1/\epsilon_s]$) should yield a line of slope $(\Delta \mathrm{e})^2[1/2a_1 + 1/2a_2 - 1/\mathrm{r}]$ and an intercept of λ_i. This plot is shown in Figure 13, and a least–squares analysis results in

$$\lambda = (0.55)\left[\frac{1}{n^2} - \frac{1}{\epsilon_s}\right] + 1.01 \qquad [5.14]$$

with a correlation coefficient of 0.99. The excellent correlation obtained in the fit may well be misleading since the λ obtained in the fits is based on the $\Delta \mathrm{G}^\circ_{\mathrm{rel}}$ values for compounds **38–44**. Strictly speaking, the Coulomb corrected value of $\Delta \mathrm{G}^\circ$ should be used for the compounds in the fits to equation [5.11] (*i.e.*, $\Delta \mathrm{G}^{\circ\prime}(R)$ in Table III), which would result in a significantly decreased correlation. The good correlation observed in the use of $\Delta \mathrm{G}^\circ_{\mathrm{rel}}$ values for the least–squares

Table VI. Marcus Fit Results† for **38–44**.

solvent	T_{ab}, cm^{-1}	λ, eV
C_6H_6	7.4	1.02
MTHF	6.0	1.20
*n*PrCN	5.2	1.26
CH_3CN	4.5	1.32

† Least–squares fit of data in Table V to equation [5.11].

fit may reflect approximately equal and compensating effects of the Coulombic correction for interactions in the charge–transfer state, and ion–paring effects in the electrochemical measurements.

The intercept of the plot in Figure 13 corresponds to the inner sphere reorganization energy (λ_i) coupled to the electron transfer. The λ_i obtained (1.01 eV) is too large based on estimates for porphyrin–quinone systems by ~0.5 eV.[57, 58, 61, 174, 184] Since the exothermicity obtained for the series of compounds is likely only accurate in a relative sense, and not with regard to absolute scale, the λ_i obtained in the fit should be corrected for ion–pairing and Coulombic effects. The undetermined magnitude of these correction terms unfortunately does not allow a straightforward extraction of the absolute λ_i for this series.

Qualitatively, the data appear to follow the expected trend with solvent, *i.e.*, the λ obtained in the least–squares analysis increases with increasing solvent polarity. Presumably, the origin of this effect is the increase in λ_o with increasing dielectric constant. As discussed above, however, comparisons with the Coulomb corrected value of ΔG°_{rel} are more ambiguous. The range of T_{ab} obtained in this

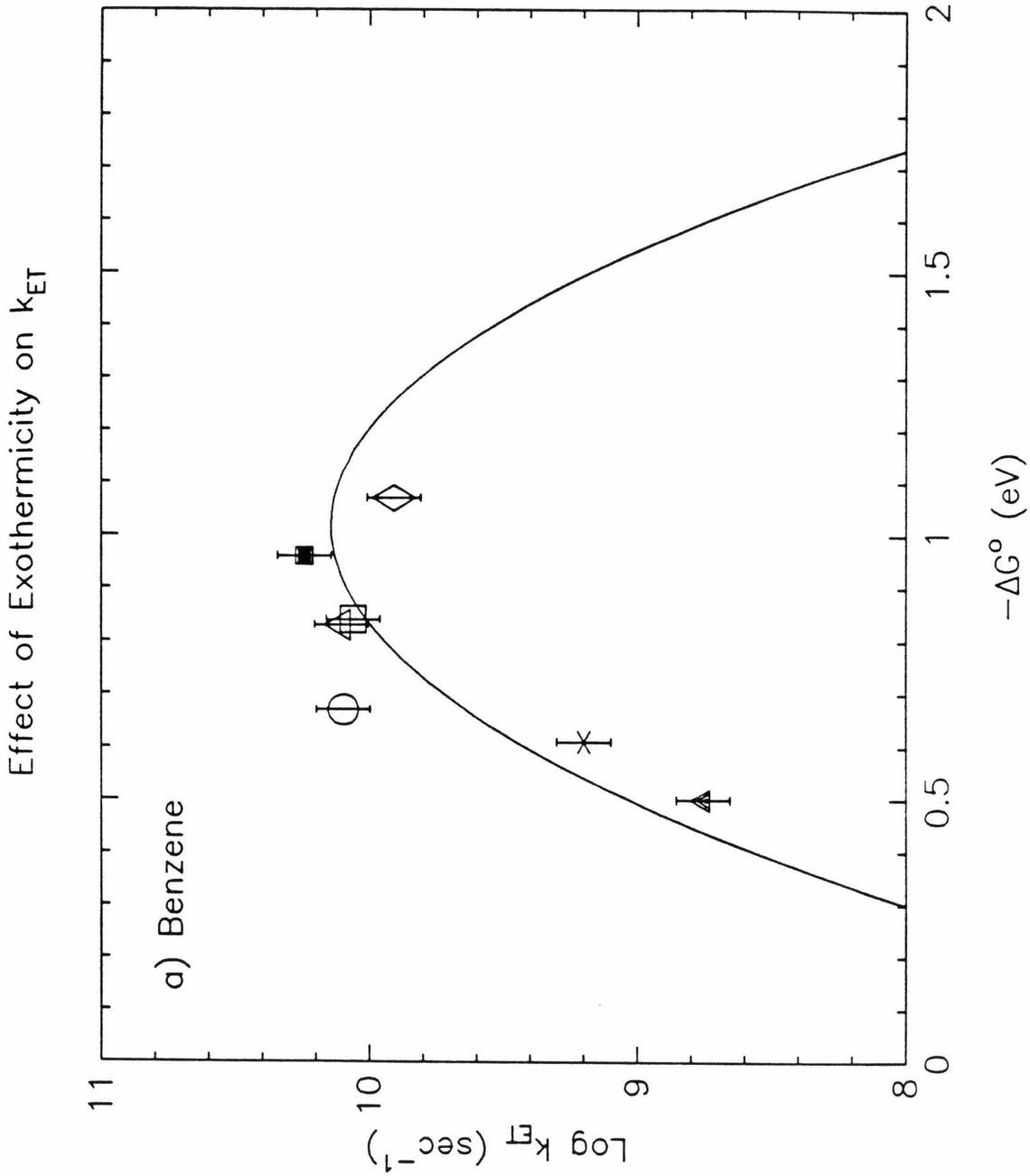

Figure 9. Electron transfer rate constant versus exothermicity for **38–44** in C_6H_6. Solid line is the least–squares fit to equation [5.11].

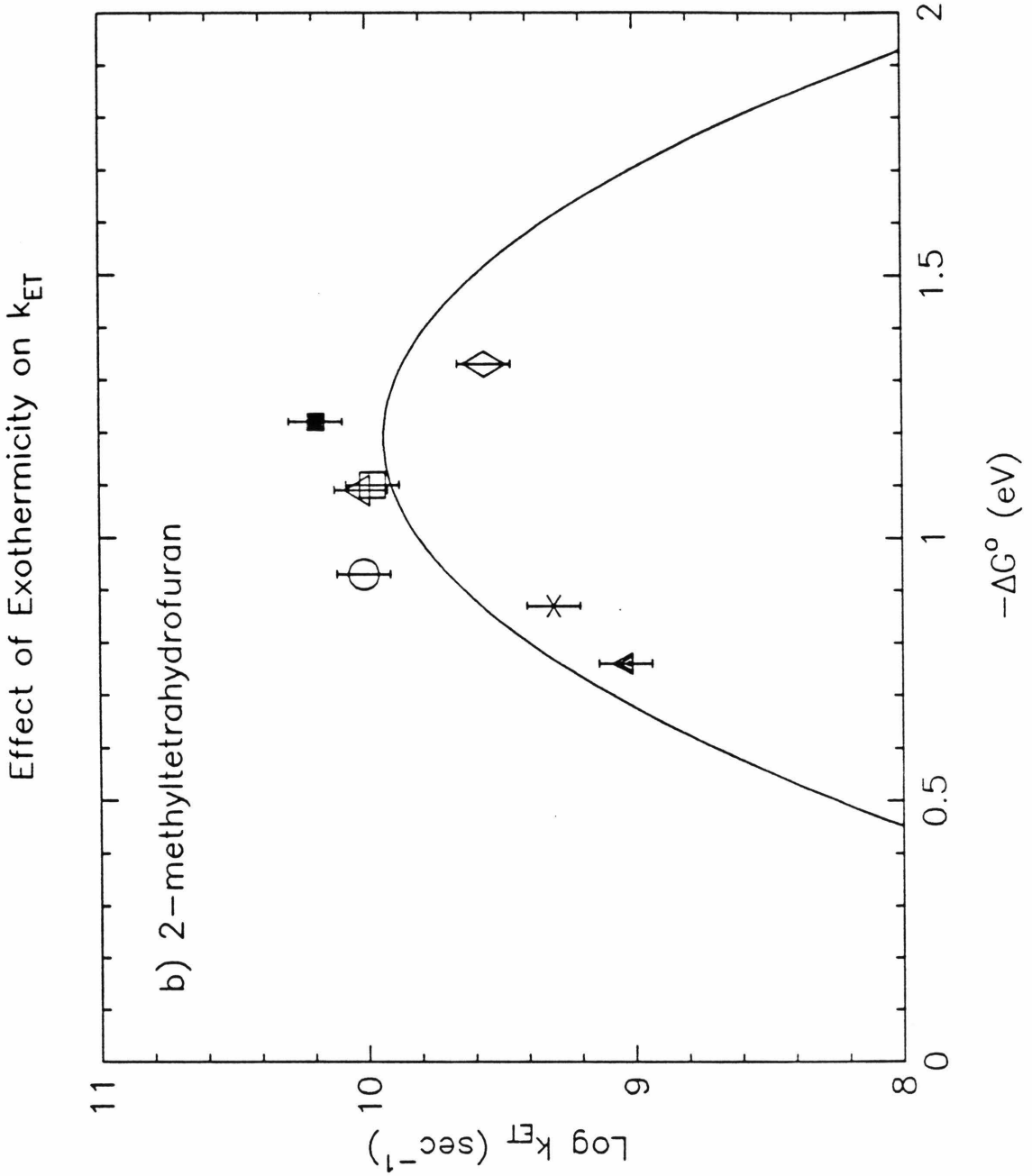

Figure 10. Electron transfer rate constant versus exothermicity for **38–44** in MTHF. Solid line is the least–squares fit to equation [5.11].

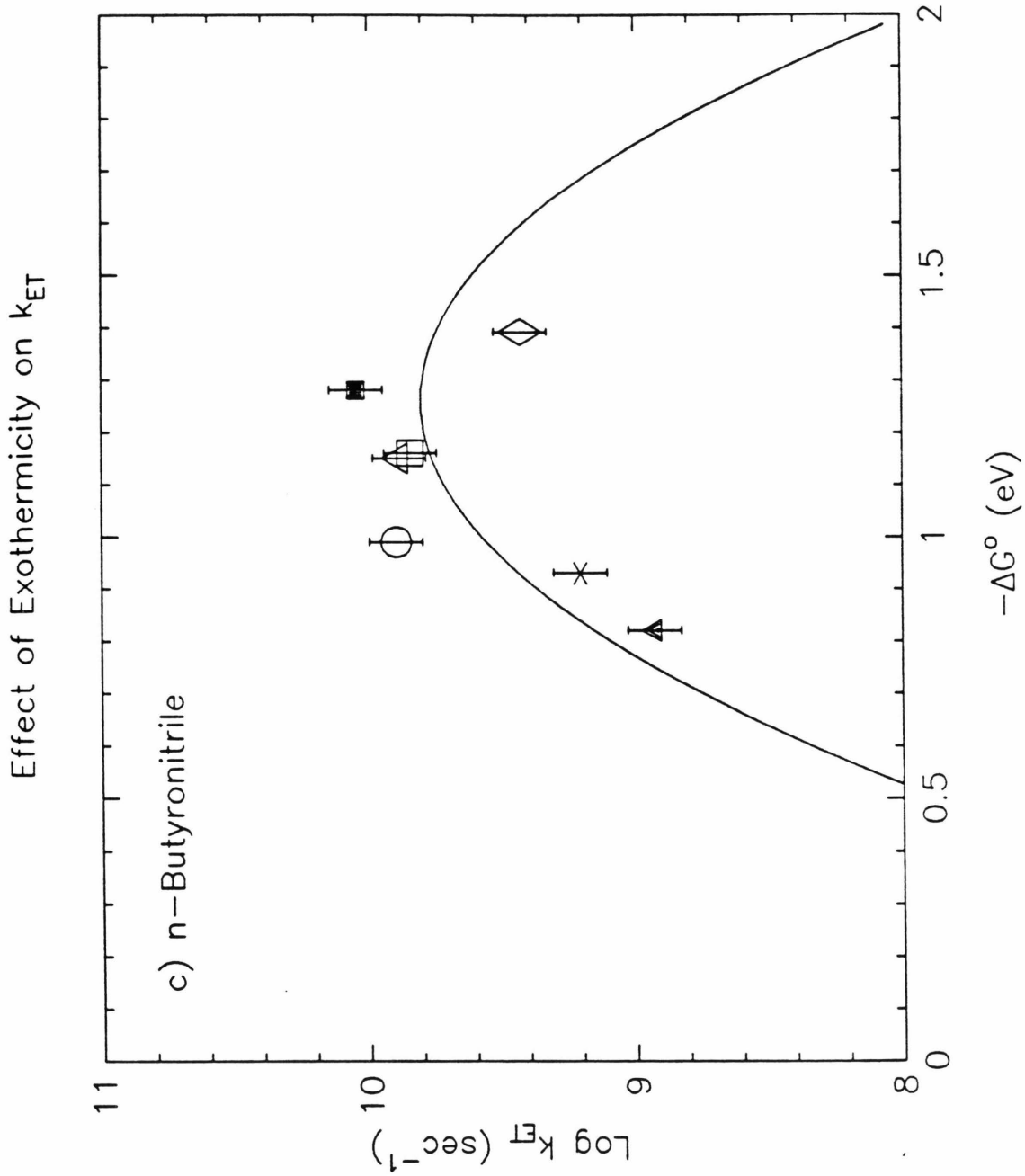

Figure 11. Electron transfer rate constant versus exothermicity for **38–44** in *n*PrCN. Solid line is the least–squares fit to equation [5.11].

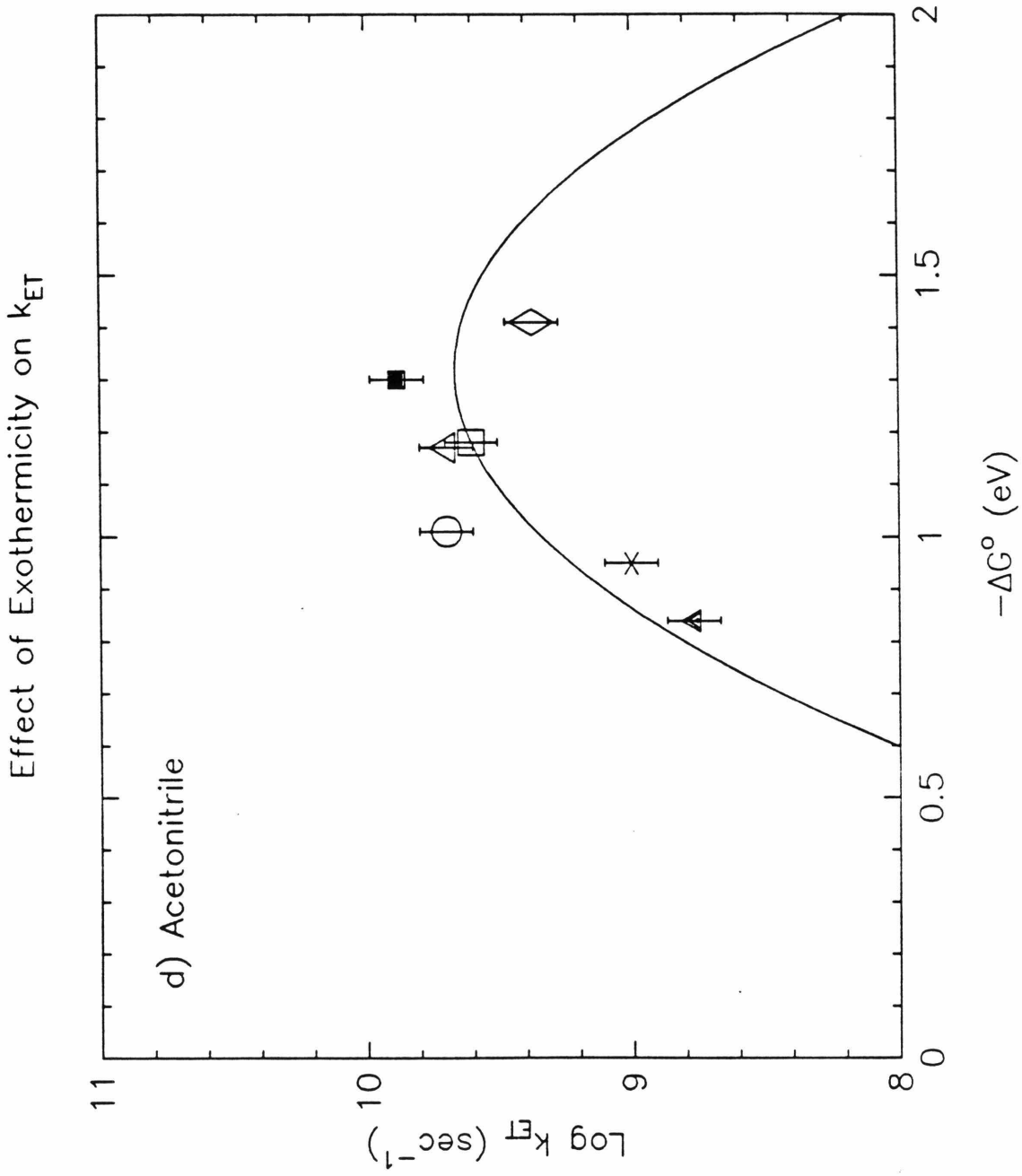

Figure 12. Electron transfer rate constant versus exothermicity for **38–44** in CH_3CN. Solid line is the least–squares fit to equation [5.11].

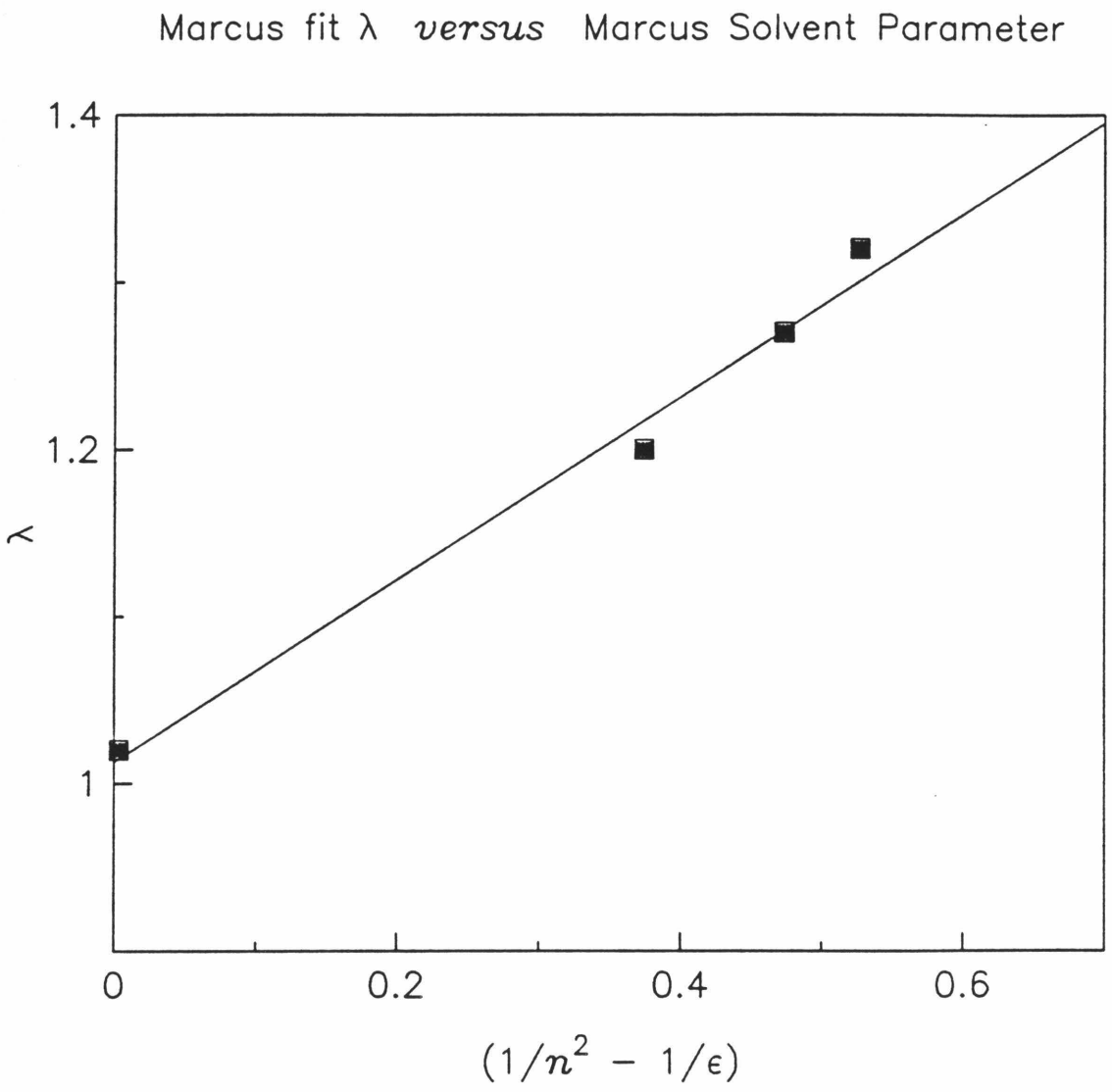

Figure 13. Marcus fit λ term *versus* Marcus solvent parameter.

analysis is interesting. Irrespective of the correction terms which affect the λ term obtained in the fits (see above), the T_{ab} values obtained should be quite accurate. To a first approximation, one would expect a constant T_{ab} given the identical structural basis within the series. The origin of the range of T_{ab} values may be a dependence of the phenyl "wobble" frequency on solvent which could result in a modulation of the coupling to the porphyrin ring. The previously discussed temperature effects would argue against a large modulation, but the small range in T_{ab} observed here suggests this may well be a subtle effect.

Quantitatively, there appears to be some inadequacy in the single mode analysis of equation [5.11]. The fluctuations in the electron transfer rates as obtained from the fluorescence lifetimes appear to be a real effect that is observed in all of the solvents studied. The fluctuations may be due to changes in the distribution of electron density or inequivalence of the carbonyls in the quinones as a result of the introduction of substituents, or other second–order effects. The fast rise in the electron transfer rates over a very limited range of ΔG°_{rel} for the first three compounds in the series is not well described by the expression of equation [5.11]. Other discrepancies such as the observation of relatively temperature insensitive electron transfer rates for *ZnP1Q* and *ZnP1QCl* at 77K also raises some question as to the quantitative applicability of equation [5.11]. Shown in Figure 14 is a plot k_{ET} as a function of ΔG° for 298K and 77K. The predicted dramatic temperature dependence for the first three compounds from equation [5.11] does not seem to be substantiated by the preliminary low temperature data.

One alternative to the classical expression of [5.11] is a semiclassical expression

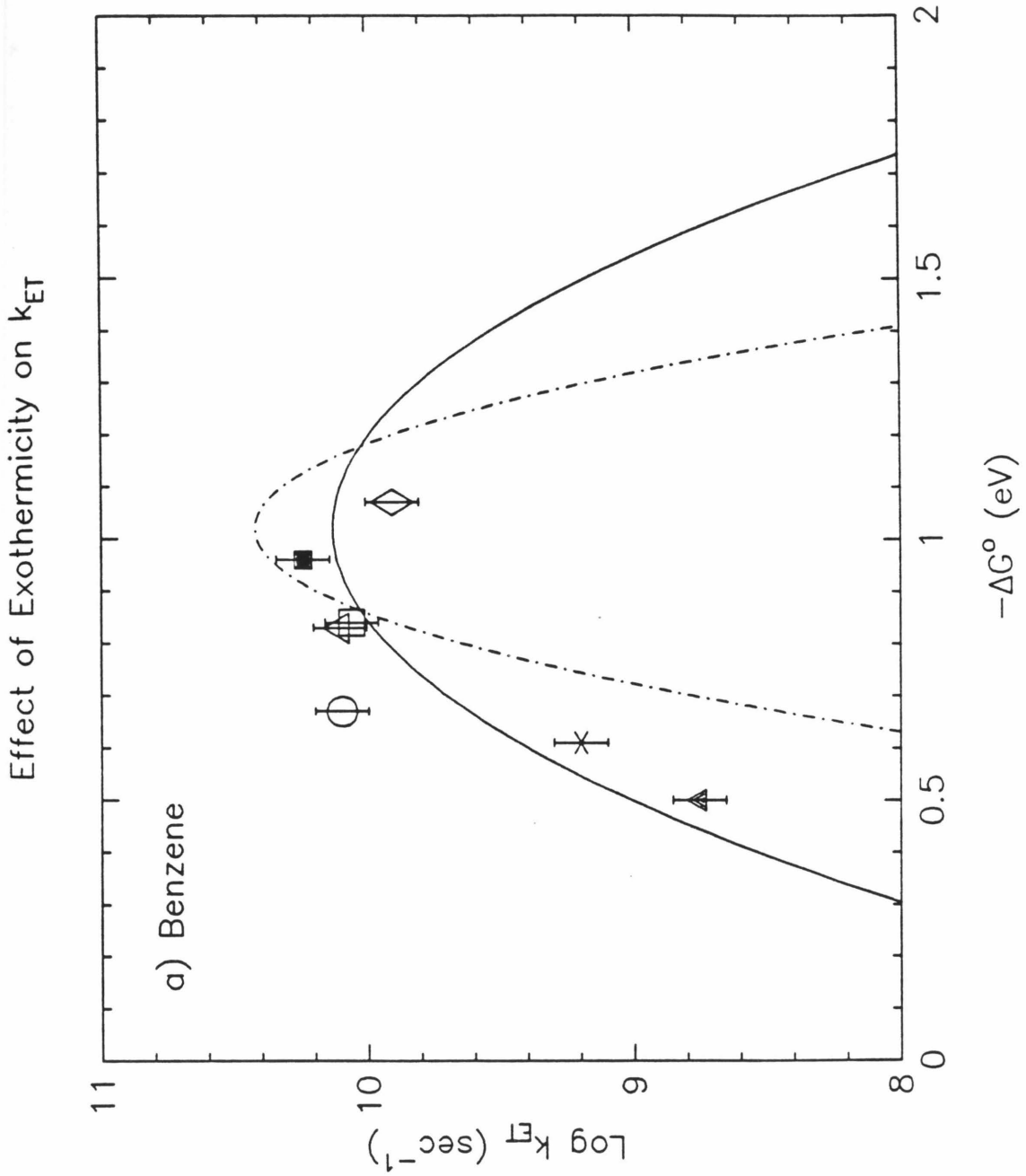

Figure 14. Marcus theory (equation [5.11]) at 298K and 77K.

which treats the solvent classically, assumes the donor is in the vibrational ground state, and quantized vibrational states of the acceptor are specifically included yielding[57, 58, 185, 186]

$$k = \sqrt{\frac{\pi}{\hbar^2 \lambda_s k_B T}} \mid T_{ab} \mid^2 \sum_{m=0}^{\infty} \frac{e^{-S} S^m}{m!} \exp\left[\frac{-(\lambda_s + \Delta G^\circ + mh\nu)^2}{4\lambda_s k_B T}\right] \qquad [5.15]$$

$$S = \frac{\lambda_v}{h\nu} \qquad [5.16]$$

where S is the vibrational–electronic coupling strength, T_{ab} is the coupling matrix element, and λ_s and λ_v are the solvational and vibrational components of the reorganization energy, respectively. As written, this function necessarily is centered at the origin on the absolute ΔG° scale. Due to the aforementioned problems of ion–pairing and Coulombic corrections, an added shift is required to adequately compare this expression with the experimentally determined data, *i.e.*,

$$\Delta G^\circ = \Delta G^\circ_{rel} + \Delta G_{shift} \qquad [5.17]$$

where ΔG°_{rel} is the driving force for the electron transfer reaction as calculated from equation [5.10] and ΔG_{shift} is the added shift. The added shift term would thus correspond to the correction for ion–pairing effects in the electrochemical measurements and for Coulombic interactions in the charge–separated state. The expression of equation [5.15] more adequately describes the fast rise in k_{ET} observed in the first three compounds in the exothermicity series. Additionally, this expression gives a better quantitative agreement with the preliminary low–temperature data discussed above. A comparison of equation [5.15] with the experimental data

for benzene is shown in Figure 16. The parameters used in the fit are: T_{ab} = 9 cm^{-1}, λ_v = 0.3 eV, λ_s = 0.3 eV, hν = 1670 cm^{-1}, and ΔG_{shift} = 0.48 eV.

The effect of ΔG_{shift} is to move the origin of the curve. Hence, $\Delta G°$=0 (*i.e.*, a thermoneutral reaction) would correspond to ΔG°_{rel}=0.48 in Figure 16. This suggests that the exothermicity for the electron transfer reaction in the dimethyl derivative **38** is very close to thermoneutral, or possibly endothermic if the shift correction is slightly larger than 0.48 eV. This implies that repopulation of the excited singlet state of the porphyrin might be possible for this compound in the absence of alternative rapid decay pathways (possibly via the excited triplet state) for the CT state. The rather large fraction of the long lifetime component observed for this compound in benzene (see Table V), and in the preliminary low–temperature data[145] may in fact be a consequence of this singlet repopulation phenomenon, and deserves more detailed investigation. Additional derivatives with a nominal $\Delta G^{\circ}_{rel} \leq$0.48 eV (benzene) could also be prepared to investigate the magnitude of the ΔG_{shift} correction.

A brief discussion of the choice of the parameters used in the comparison of equation [5.15] with the experimental data (Figure 16) is warranted here. The quinone will likely dominate the reorganization energy for the porphyrin–quinones these compounds. This is largely a consequence of the fact that the inner sphere part of the total reorganization energy roughly scales as the inverse of the number of atoms over which the electron is delocalized,[56] hence the contribution of the large porphyrin macrocycle to the total λ will likely be small. One can calculate the approximate value for the reorganization energy for the reduction of a

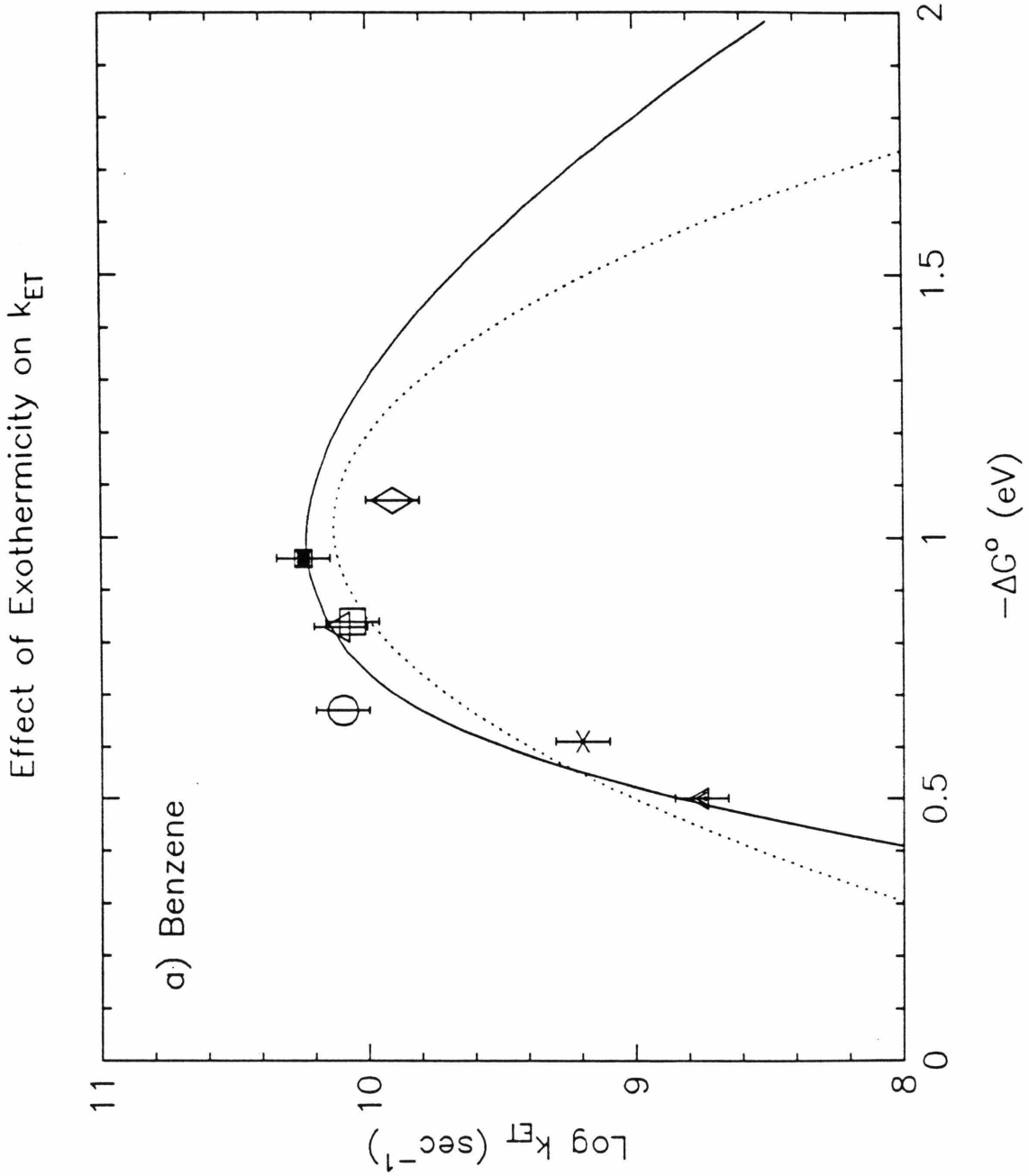

Figure 15. Comparison of classical (eqn. [5.11]) and semiclassical (eqn. [5.15]) rate expressions (see text for parameters).

benzoquinone with the knowledge of the force constants for the critical stretching frequencies (C=O and C–O$^-$), the changes in bond lengths (equation [1.5]), and the fact that two equivalent carbonyl bonds are available. Literature estimates for the force constant of the C=O stretching frequency[187,188] suggest that the force constant can be obtained from the measured infrared frequency for benzoquinone (1669 cm^{-1})[187] and the reduced mass for a carbon and oxygen atom.[189] The bond length for the carbonyl obtained from a crystal structure is 1.23 Å.[187,190] The analogous values for the C–O$^-$ are less well known, but were approximated by a phenolic C–O stretch and an average C–O bond length (~1250 cm^{-1}, and 1.43 Å).[191] These values suggest the reorganization for the fast mode (λ_v) should be on the order of 0.5 eV (equation [1.5]), and hν should be ~1600 cm^{-1}. These calculations assume a totally localized CO vibration (two of which are available), and evidence from EPR studies of semiquinone radical anions[192] suggest that ~40% of the spin is delocalized onto the quinone ring. Thus the calculated value for λ_v of 0.5 eV should be closer to ~0.3 eV. This value of λ_v was used in the comparison of equation [5.11] with the experimental data. In the absence of knowing the precise vibrations coupled to the electron transfer event, the quinone carbonyl frequency was chosen for comparison with the data. If the quinone vibronics are the only contributor to the critical frequency coupled to the electron transfer event, an average frequency of ~1500 cm^{-1} would be more appropriate (see equation [1.5]), however porphyrin vibrations may well be involved which could contribute to the "average" frequency used in this analysis. The contribution of porphyrin vibronics to the transfer could be assessed by comparing the electron transfer rates for

different metallo–porphyrin derivatives of compounds **38–44**.

As observed in Figure 15, the fast rise in k_{ET} is well described by the semiclassical two–mode analysis of equation [5.15]. The homology of the reaction series even within the benzoquinone acceptor structure should be examined in more detail in future investigations. Perhaps the unsubstituted quinone derivative does not belong in the same reaction series, *i.e.*, can the unsubstituted derivative be considered a di–substituted protio benzoquinone, or is the absence of non–proton quinone substituents a significant factor? Alternatively, similar arguments could well be made for the disubstituted derivatives **38** and **43**. Given the limited number of data points available at the present time, all of the compounds are being considered here until further experiments are available to address this ambiguity. Although the series was designed to be *structurally* homologous, there remains the question of whether it should be considered *functionally* homologous as well.

Further differentiation between the classical and semiclassical expressions could be achieved by the synthesis of additional derivatives to investigate the low exothermicity forward transfers. It is these low driving force forward transfer reactions which will be exceedingly important in the transient absorption study of this series, since low exothermic forward transfers are equivalent to highly exothermic transfers when studied in the back transfer reaction (*i.e.*, $-\Delta G^{\circ\,back}_{rel} = W^* + \Delta G^{\circ\,for}_{rel}$, where $W^* = 2.15$ eV), which will be important for probing the inverted region effects.

The plots in Figure 15 suggest a differentiation between the classical and semiclassical treatments could also be achieved by the preparation of compounds

with an exothermicity for the forward transfer of $\geq$1.5 eV. The synthesis of these additional quinone derivatives to probe the more exothermic forward transfers is largely limited by synthetic difficulties in the preparation of these compounds, however. Although a number of benzoquinone derivatives would have the proper reduction potentials to probe forward transfers in this driving force range, the preparation of the materials would be extremely challenging. The severe oxidation procedures that would be required to convert the porphyrin–hydroquinone to the porphyrin–quinone would result in significant porphyrin degradation. This problem was already apparent in the preparation of the cyano derivative[145] and suggests the exothermic limit for the *forward* transfers has been achieved for this series.

A more straightforward experiment would involve the thorough investigation of the temperature dependencies of compounds **38–40**. Preliminary data demonstrated that the electron transfer rate for **40** slows by only a factor of 2.5 in cooling the sample from 298K to 77K. The low temperature data for **38**[145] demonstrated that k_{ET} slows by a factor of 10 over the same temperature range. The classical expression of [5.11] predicts dramatic effects on k_{ET} as a function of temperature for both of these compounds (Figure 14), while the semiclassical expression of [5.15] predicts a larger effect for the dimethyl derivative **38** (Figure 16), consistent with the preliminary low–temperature investigations. The ambiguities involved in comparing room temperature fluid solutions to a frozen glass at 77K should not go unmentioned. Such a dramatic change in medium should have a significant effect on the λ_o term in the classical expression, and may well affect the slow mode (λ_s)

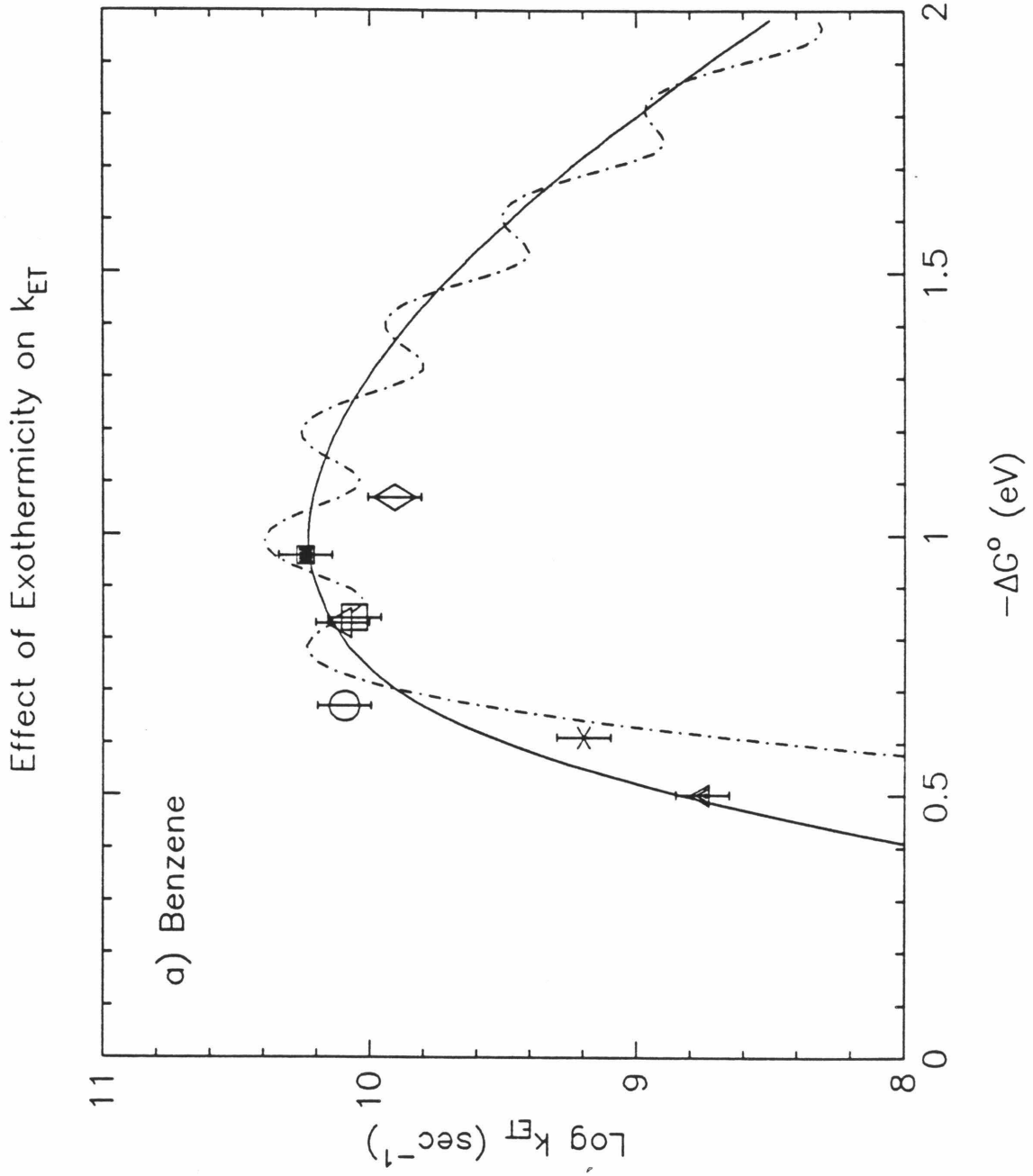

Figure 16. Semiclassical theory (eqn. [5.15]) at 298K and 77K.

in the semiclassical expression. Ideally, the full temperature range from above the melting point of the solvent to temperatures above 298K should be investigated to distinguish between the two theoretical treatments. Such a temperature study may also shed insight on the magnitude of λ_s used in the semiclassical treatment, and may allow determination of enthalpic and entropic contributions to the reaction exothermicity.

Both models may suffer from the use of the continuum model for the solvent. The dielectric unsaturation approximation will likely not be valid for charge–separated states involving very large dipole moments as in these systems. The generation of such a large dipole may well lead to significant ordering of several layers of solvent molecules around the charge–separated state resulting in a breakdown of the continuum model.

Phosphorescence Quenching Investigations

To further investigate the distance dependence of these systems for comparison with theoretical predictions,[114] it is paramount to determine k_{ET} in both the mono– and bis–linked bicyclo[2.2.2]octyl porphyrin–quinone derivatives. The calculation of an absolute T_{ab} value based on molecular structure exceeds the current level of theory, primarily as a result of the paucity of experimental systems of homologous structure to probe the effects of small changes in structure on the matrix element. Work in progress elsewhere may soon shed experimental insights in this regard.[174] As a result, ratios of rates are calculated in this previously discussed theoretical treatment.[114] The very fast rates observed in *ZnP1Q* results in a fast

singlet deactivation pathway which easily competes with the natural deactivation pathways for this porphyrin skeleton. To directly compare the two porphyrin–quinones, one is faced with an exceedingly slow electron transfer pathway for the bis–linked derivative relative to other deactivation pathways, and a very efficient electron transfer pathway in the mono–linked compound.

In an attempt to circumvent these problems and to discover a system which would allow direct comparison with the two compounds, alternative metallo–porphyrins were investigated. The rational was to prepare a metallo–porphyrin derivative that (a) had a long triplet lifetime so as to allow the investigation of a slow electron transfer deactivation and (b) a very high intersystem crossing rate to enhance the triplet yield and to compete effectively with other fast deactivations out of the singlet state. In general, triplet lifetimes are considerably longer than their singlet counterparts,[163] and requirement (a) can be met with virtually any investigation of porphyrin triplets. Requirement (b) is more challenging due to the fast rates observed in the single–linked porphyrin–quinone derivatives (discussed above). Both of these requirements are filled by platinum porphyrins, however. The intersystem crossing for platinum–octaethylporphyrin (*PtOEP*) has been reported to exceed $10^{11}s^{-1}$, resulting in a high yield of the triplet state which exhibits a relatively high phosphorescence quantum yield (~90% at 77K).[193] The triplet lifetime for *PtOEP* has also been reported[194] to be 63 μsec, long enough to probe processes in the $\geq 10^{3}s^{-1}$ range. A possible complication in the triplet study is the limited exothermicity available due to the lower excited triplet energies than their singlet counterparts.[163]

Preparation of platinum porphyrins are slightly more difficult than the zinc metallo derivatives discussed above, but offer some significant advantages. Platinum porphyrins are Class I porphyrins,[141] and are only partially demetallated in concentrated sulfuric acid. In contrast, the zinc derivatives are Class III porphyrins and are easily demetallated in weak acids. The high stability of the platinum derivatives could well be advantagous, although reaction conditions for the metallation are considerably more severe than the zinc derivatives. Conditions that were investigated for the Pt metallation of H_2P^tBu, included metallation in benzonitrile,[195] or DMF.[196] Both methods involve refluxing the porphyrin and a platinum salt (K_2PtCl_4 or $PtCl_2$) in these solvents. Significant degradation of the porphyrin was observed in both cases, and low yields of the Pt–metallated porphyrin were recovered (<5–20%) for metallation of H_2P^tBu. A milder approach was also attempted in which the porphyrin is refluxed in benzene with a soluble Pt salt (bis–benzonitrileplatinous chloride, $Pt(\O CN)_2Cl_2$).[197] Although less porphyrin degradation was observed in this case, the extent of metallation was low and the reaction time was long (>24 hours). Optimum conditions were finally achieved for a sequence in which the porphyrin was refluxed under argon in glacial acetic acid with 20–40 equivalents of K_2PtCl_4,[198] resulting in significantly reduced reaction times (~30 min), excellent metallation conversions, and reduced porphyrin degradation. High yields were obtained for metallation of H_2P^tBu and *H_2P2DMB* (see Chapter 6) under these conditions, suggesting this was the method of choice.

The platinum derivatives are frought with experimental difficulties, however.

Because the intersystem crossing rate is very high the materials do not fluoresce, nor is phosphorescence observable under aerobic conditions due to oxygen quenching.[163] Chromatography (as in the zinc derivatives) must be performed under low light conditions to minimize the formation of singlet oxygen and possible sample degradation. Phosphorescence emission curves obtained for the PtP^tBu and *PtP2DMB* compounds under anaerobic conditions confirmed the presence of other metallo–porphyrin contaminants (likely zinc) due to scavenging of adventitious metals by the free base porphyrin during or prior to platinum metallation. The separation of different metallo-porphyrins is intractable with the current chromatographic purification procedures (Chapter 7). The stability of the Pt porphyrins can be exploited for the removal of these contaminants, however. The Pt porphyrin was dissolved in methylene chloride and 1–2 drops of trifluoracetic acid were added. These highly acidic conditions result in demetallation of any porphyrins of lower stability class than the Pt derivatives. Some degradation is observed here, but the removal of the impurities is critical for unambiguous phosphorescence quenching studies. After neutralization and repurification, emission curves conclusively demonstrated the absence of these minor emissive contaminants.

Attempts to deprotect the *PtP2DMB* derivative using the standard BI_3 conditions resulted in the isolation of an uncharacterized derivative with dramatically altered absorption and NMR spectra, possibly due to the conversion to a Pt(IV) derivative.[199] The alternative approach in which the deprotected derivative (H_2P2QH_2) was metallated resulted in the isolation of a Pt derivative in

exceedingly low yield (<1%) compared to the high yields obtained in the metallation of H_2P^tBu and H_2P2DMB (50–60%) under identical conditions. Perhaps the presence of the quinone/hydroquinone functionality in this oxidizing environment results in significant degradation, or metal coordination. The paucity of material prohibited full characterization of this compound. NMR analysis indicated the material was largely the expected structure, but a number of ambiguous peaks in the spectrum suggest the material is difficult to purify or tends to stack significantly. In general, the solubiltiy of the Pt derivatives are significantly lower than their zinc metallo counterparts. These problems suggest the lifetime results discussed below should be considered as preliminary only, and must await the development of alternative synthetic strategies for protecting the quinone functionality to allow deprotection in the presence of the Pt porphyrin.

The results of phosphorescence lifetime experiments are tabulated in Table VII. The lifetime of the PtP^tBu reference porphyrin was observed to be significantly shorter than the expected ~63 μsec from comparison with literature values for *PtOEP*.[194] While the lifetime was not expected to be identical due to the unknown influence of the *meso*–phenyl substituent, the decrease in the observed phosphorescence lifetime will complicate the investigation of slow deactivation pathways in the quinone derivative of the bis–linked system by a full order of magnitude. The *PtOEP* derivative was also prepared for comparison with the PtP^tBu derivative. The triplet lifetime was observed to be 89 μsec on this apparatus (discussed in Chapter 6), and this value was confirmed by the lifetime measured elsewhere.[200] Determination of the relative phosphorescence quantum

Table VII. Phosphorescence Lifetimes for Platinum Porphyrins[a]

compound[b]	solvent[c]	τ_p (μsec)
PtOEP	MTHF	89.1
PtPØ^{t}Bu	MTHF	1.14
PtPØ^{t}Bu	C_6H_6	1.48
PtP2Q	C_6H_6	1.65

[a] Lifetimes were obtained under rigorous anaerobic conditions. Excitation wavelength was 532 or 355 nm. Sample concentrations were $\sim 10^{-6}$ M.

[b] *PtOEP*: Platinum octaethylporphyrin, *PtPØ^{t}Bu*: [5–(*p–tert*–butyl)phenyl–2, 3, 7, 8, 12, 13, 17, 18–octamethylporphyrinato]platinum(II). *PtP2Q*: see text

[c] Methyltetrahydrofuran was distilled from sodium/benzophenone ketyl under argon. Benzene was HPLC grade and distilled from CaH_2.

yield of *PtP^{t}Bu* relative to *PtOEP* demonstrated a proportionate decrease in Φ_p compared with the ratio of the phosphorescence lifetimes, suggesting the nonradiative internal conversion rate may have increased in the *meso*–phenyl substituted porphyrins.

The oxidation potential of *PtOEP* is estimated to be +0.95 V (vs. SSCE).[201] The methylbenzoquinone reduction potentials presented in Table III when converted to the SSCE scale result in a reduction potential of approximately –0.64 V.[145] The singlet excitation energy for the Pt porphyrin is 2.31 eV (see Chapter 7), and the triplet level is ~0.32 eV below the first excited singlet, based on the onset of the phosphorescence emission (623 nm). The exothermicity is thus estimated to be ~0.4 eV for electron transfer from the first excited triplet state of the platinum porphyrin transferring an electron to the quinone (uncorrected for electrostatic interactions or ion–pairing effects). The ambiguous phosphorescence

lifetimes measured here and the lack of full characterization of the *PtP2Q* cast reasonable doubt on the estimate of k_{ET} in the bis–linked derivative. If these values are correct, however, the preliminary estimate of k_{ET} value for *PtP2Q* is $<10^5$ s^{-1} at these redox potentials.

In the absence of experimental data for k_{ET} in the *PtP1Q* derivative, an estimate for the electron transfer rate can be obtained from the exothermicity study discussed above. If the vibronic coupling in the zinc metallo porphyrin is similar to the platinum porphyrins, the estimated driving force ($-\Delta G^{\circ}_{rel}$ ~0.4 eV) suggests the single linker transfer rate would be ~$8x10^7$ s^{-1} (equation [5.15], and Figure 16) and the ratio of the electron transfer rates is therefore $\geq$800. The predicted rate ratio for the mono– to bis–linked systems at these redox potentials is ~1000.[114] These experimental results are thus in reasonable agreement with theoretical predictions, although the lack of concrete rate data for either compound makes the comparison tentative at best. Future experiments should investigate the phosphorescence lifetime measurements for both *PtP1Q* and *PtP2Q* in more polar solvents since the electrostatic corrections are very large in benzene (see Table IV) used for these preliminary investigations. These correction terms may make the exothermicity for the electron transfer reaction in *PtP2Q* considerably less than the estimated 0.4 eV, and possibly even endothermic, depending on the magnitude of the ΔG_{shift} correction factor discussed above. These preliminary experiments clearly warrant a more thorough experimental determination of k_{ET} in these compounds through the explicit measurement of phosphorescence lifetimes for both *PtP1Q* and *PtP2Q* to adequately assess the quantitative validity of the

theoretical model.

Chapter 6

Conclusions

Conclusions

A series of synthetic porphyrin–quinone molecules has been described which were designed to investigate critical parameters governing electron transfer rates. Only through the precise experimental control of such parameters can further insights be obtained for refinement of theoretical treatments. Synthetic methods for the preparation of these compounds was presented. The compounds allow the investigation of incremental distance effects (6, 10, and 14Å edge–to–edge) on k_{ET} for identical colinear orientations through the introduction of zero, one, or two bicyclo[2.2.2]octyl linker units between the porphyrin donor and the quinone acceptor. A homologous series of porphyrin–quinone compounds was prepared for the investigation of exothermicity effects on the photoinduced electron transfer rate constant. These compounds allow the investigation of electron transfer parameters in the absence of major electronic perturbations. The precise control of donor–acceptor separation distance allows unambiguous analysis of electron transfer rates from time–resolved fluorescence measurements, and are in striking contrast to previous flexibly coupled systems.

- Analysis of a phenyl linked porphyrin–quinone in comparison with a single phenylbicyclo[2.2.2]octyl linked derivative indicates the addition of the first spacer unit decreases k_{ET} by at least one order of magnitude. Addition of a second bicyclo[2.2.2]octyl linker results in a further decrease in k_{ET} by a factor of 500

to $\geq$1700 in accord with recent theoretical predictions for nonadiabatic electron transfer through oligomers of the bicyclo[2.2.2]octyl spacer unit.

- A weak dependence of the photoinduced electron transfer rate constant on solvent was observed. These results are consistent with expectations for a neutral initial state transferring to a charge–separated state. Conversely, dramatic solvent effects are predicted to be observed in the electron transfer from the charge–separated state returning to ground state or triplet products.
- Preliminary investigations at 77K indicate that the electron transfer rates for these compounds are relatively temperature independent. The electron transfer rate was observed to decrease by a factor of approximately two for the temperature change from 298K to 77K in the highly exothermic transfers (R = H, Cl) investigated. The electron transfer rate for the least exothermic case studied (R = Me_2) is more dramatically affected by temperature (one order of magnitude). These results suggest that nuclear tunneling dominates the electron transfer rates in this series.
- Low temperature investigations suggest the nonexponential lifetimes observed at 77K may be due to an ensemble of rotational conformations between the porphyrin donor and the quinone acceptor, indicating dramatic effects of the precise molecular structure on k_{ET}. This behavior confirms the nonadiabatic nature of the electron transfer in these compounds.
- Investigaton of the effect of exothermicity on k_{ET} through the synthesis of a structurally homologous series of porphyrin–benzoquinones revealed a dramatic increase in the electron transfer rate with small increases in the driving force,

followed by a relatively ΔG° insensitive region. Further increases in the exothermicity resulted in a modest decrease in the calculated electron transfer rate (R = CN). These results appear to be well described by a semiclassical theory which treats the solvent classically, and includes specific vibrational modes for the acceptor.

Precise structural definition through the rational synthetic design of donor–acceptor systems can dramatically aid in experimental investigations of electron transfer processes.

Chapter 7

Experimental Procedures

Experimental Procedures

Electronic spectra were recorded with a Varian Associates Cary 219 UV–Visible spectrometer. Infrared spectra were obtained from KBr pellets of the compound of interest and were recorded using a Shimadzu IR–435 Infrared Spectrometer. Proton nuclear magnetic resonance (NMR) spectra were measured using a Varian Associates EM–390 spectrometer, a Varian Associates XL–200 spectrometer, a Japan Electro–Optical Laboratories (JEOL) FX–90Q spectrometer, a JEOL GX–400 NMR spectrometer, or a Bruker WM–500 spectrometer, operating at 90MHz, 200.06MHz, 89.56MHz, 399.65MHz, and 500.13MHz, respectively. Carbon NMR spectra were obtained using broadband proton decoupling techniques on the FX–90Q, or the XL–200 operating at 22.4MHz, and 50.31MHz, respectively. Chemical shifts (δ) are reported in parts per million (ppm) relative to a tetramethylsilane (TMS) internal standard, or a solvent residual peak: $CHCl_3$, 7.24 ppm (^{1}H NMR) and 77.0 ppm (^{13}C NMR); CH_2Cl_2, 5.32 ppm (^{1}H NMR). Mass spectra were obtained from the Midwest Center for Mass Spectrometry (NSF Regional Instrumentation Facility) by applying either electron impact (EI) or fast–atom bombardment (FAB) techniques. Elemental analyses were performed by Spang Microanalytical Laboratory, Eagle Harbor, Michigan. Thin layer chromatography (TLC) was performed with silica gel 60 F–254 (E. Merck; 250μ thick) precoated analytical plates. Melting points were measured with a Thomas–Hoover Capillary

Melting Point Apparatus and are reported uncorrected.

Analytical gas chromatography was carried out using a Hewlett–Packard (HP) 5700A gas chromatograph modified with an inlet splitter (Scientific Glass Eng. Co., GISS–4A) an SE–54 fused silica capillary column (15m × 0.32mm I.D., J&W Scientific 18704A), and a flame ionization detector. Ultra–high purity hydrogen (Big Three Industries) was the carrier gas and nitrogen was the makeup gas. The ouput from the detector was analyzed using an HP 3390A electronic integrator.

Reagents and Solvents. 1,4–Dimethoxybenzene, HI (57% in water), 4–Bromobenzaldehyde, maleic anhydride, *p*–toluenesulfonic acid (TsOH), lead(IV) oxide (PbO_2), and *n*–Butyllithium (1.6 M solution in hexanes) were obtained from Aldrich Chemical Co. and were used without further purification. Boron triiodide (BI_3), bis(triphenylphosphine)nickel(II) chloride ($Ni(P\emptyset_3)_2Cl_2$), nickel(II) chloride, and 1,2–dimethoxyethane were obtained from Alfa Ventron. Cuprous Oxide was obtained from Allied Chemical Co. 1,2–dichloroethane, and quinoline were obtained from Matheson, Coleman, and Bell. 2,2′–dipyridyl was obtained from Polysciences Inc. Hydrogen bromide, hydrogen chloride, ammonia, and boron trifluoride gases were obtained from Matheson Gas Products. All other reagents were obtained from standard commercial sources and were used as received.

Solvents designated as "dry" in the following experimental procedures were purified as below. All other solvents were used without further purification. Tetrahydrofuran, diethyl ether, and 1,2–dimethoxyethane were distilled from sodium/benzophenone ketyl under argon. *N*,*N*–dimethylformamide was distilled from activated Linde 4Å molecular sieves at ~30 mm Hg. Quinoline was distilled from

Zn dust at ~30 mm Hg. Methylene chloride and methanol (HPLC or spectrograde) were dried over activated Linde 4Å molecular sieves. 1,2–Dichloroethane, benzene, and acetonitrile were distilled from CaH_2 under argon. 2–Methyltetrahydrofuran was distilled from CaH_2 and then vacuum transferred or distilled from sodium/benzophenone ketyl under argon. Butyronitrile was distilled from sodium carbonate and potassium permanganate and then redistilled from phosphorous pentoxide under argon.

Preparation of Bibicyclo[2.2.2]octylbenzaldehyde **20**

1,4–Dimethoxy–1,4–cyclohexadiene (5) The general method of Birch and Chamberlain[202] was followed. A three–neck 5 L flask was equipped with a cold–finger condenser cooled to –78°C, outlet tube and mechanical stirrer. Ammonia (~3 L) was condensed into the vessel. Dry tetrahydrofuran (300 mL), distilled *tert*–butanol (500 mL), and 1,4–dimethoxybenzene (130.38 g, 0.944 mol) were added and stirring was commenced. Lithium wire (23.77 g) was added in 0.5–1 inch segments. Addition was initially slow to minimize violent frothing. The reaction mixture was stirred for 1 hour and the blue color was discharged by the dropwise addition of methanol (200 mL). Water was then added (~750 mL), and the reaction mixture was allowed to sit overnight to evaporate excess NH_3. More water was added and the reaction mixture was transferred to a separatory funnel. The mixture was extracted with 3x150 mL petroleum ether (35–60°C), 2x150 mL diethyl ether, and the combined organics were back extracted with 3x100 mL H_2O. The organics were dried over $MgSO_4$ and solvent removed *in vacuo* to yield 117.8

g of white crystals (crude yield, 89%). ^{1}H NMR (90MHz, $CDCl_3$, TMS): δ 4.60 (m, 2H), 3.55 (s, 6H), 2.87 (m, 4H) ppm.

1,4–Dimethoxybicyclo[2.2.2]octane–2,3–dicarboxylic acid anhydride (7) A flask was charged with compound **5** (116.45 g, 0.831 mole), maleic anhydride (Aldrich, 81.50 g, 0.831 mole), and chloroform (150 mL). The mixture was heated to relux for 24 hours. The solvent was removed *in vacuo* to yield 202.4 g of an orange waxy solid. The crude olefin **6** was dissolved in THF and transferred to a 500 mL Parr bottle and hydrogenated (50 psi H_2) in several increments (~40 g each, due to low solubility of the olefin) over Pd on carbon (2%(w/w) of olefin) for 12 hours. A large excess of catalyst was generally employed to circumvent poisoning due to unidentified impurities in the olefin. The hydrogenated material was isolated by filtering off the catalyst and removing the solvent *in vacuo* to yield a green waxy solid (189.2 g total, 0.787 mol, crude yield, 95%). ^{1}H NMR (90MHz, $CDCl_3$, TMS): δ 3.60 (m, 2H), 3.35 (s, 6H), 2.00–1.85 (m, 8H) ppm.

1,4–Dimethoxybicyclo[2.2.2]octane–2,3–dicarboxylic acid (7) *Anhydride* **6** (50.1 g, 0.21mole) was added to 1,2–dimethoxyethane (250 mL) and vigorously stirred. Water (500 mL) was slowly added and the reaction was heated to reflux for 24 hours. The solvent was removed *in vacuo* yielding a tan solid (52.2 g, crude yield 97%). The product can be recrystallized from acetone if desired, but not generally required in this sequence. ^{1}H NMR (90MHz, DMSO–d_6, TMS): δ 3.2 (s, 2H), 3.0 (s, 6H), 2.2 (m, 2H), 1.61 (m, 6H) ppm.

1,4–Dimethoxybicyclo[2.2.2]oct–2–ene (9) The general method of Snow, Degenhardt and Paquette[152] was followed. A flask was charged with *diacid* **8** (20.36 g, 78.8 mmol), cuprous oxide (22.62 g, 158 mmol), 2,2′–dipyridyl (24.63 g, 157 mmol), glass powder (3.0 g), and quinoline (150 mL). The mixture was heated with stirring to 185°C for 48 hours. The black solution was allowed to cool and the volatiles were removed by distillation at reduced pressure (60 Torr) under nitrogen. The distillate was poured into 600 mL 2N HCl, and was extracted with 3x100 mL petroleum ether (35–60°C). The combined organics were washed with 4x30 mL 2N HCl, 4x25 mL saturated $CuSO_4$, 1x25 mL H_2O, and dried over $MgSO_4$. The drying agent was removed by filtration and the solvent was removed *in vacuo* to yield a green oil (9.25 g, crude yield, 70%). ^{1}H NMR (90MHz, $CDCl_3$, TMS): δ 6.20 (s, 2H), 3.28 (s, 6H), 1.60 (m, 8H) ppm.

1,4–Dimethoxybicyclo[2.2.2]octane (10) *Olefin* **9** (14.01 g, 83.3 mmol) was dissolved in THF (250 mL) and added to a 500 mL Parr bottle. Pd on carbon (0.28 g, 2% (w/w) of olefin) was added to the solution and the bottle was pressurized to 50 psi H_2 on a Parr rocker overnight. The catalyst was filtered off, and the solvent removed *in vacuo* to yield a green oil (13.48 g, crude yield, 95%). ^{1}H NMR (90MHz, $CDCl_3$,TMS): δ 3.20 (s, 6H, 2xOCH_3), 1.79 (s, 12H, 6xCH_2) ppm.

1,4–Diiodobicyclo[2.2.2]octane (11) *Dimethoxy* **10** (2.00 g, 11.7 mmol) was added to 57% aqueous HI (21.05 g, 93.8 mmol) in a thick walled glass tube. The contents were frozen in liquid nitrogen and the tube was evacuated. The

tube was then sealed and annealed, and carefully warmed to room temperature (CAUTION! Explosion hazard!). The tubes were placed in a sealed tube oven and heated to 160°C for 48 hours and then allowed to cool. A white crystalline solid was evident in the tube after heating. The contents were again frozen in liquid nitrogen and the tubes were cautiously broken open and allowed to warm to room temperature. A two tube workup is as follows: The contents were poured into 100 mL H_2O and 100 mL CH_2Cl_2 was used to transfer the crystalline solid to the separatory funnel. The aqueous layer was washed with 3x50 mL CH_2Cl_2. The combined organics were washed with 1x50 mL 5% $Na_2S_2O_3$, 1x50 mL H_2O, 1x40 mL saturated NaCl and dried over $MgSO_4$. The drying agent was filtered and the solvent was removed *in vacuo* to yield a slightly tan powder. An unidentified impurity can be removed by washing the solid with a minimum amount of ice cold diethylether to yield a white powder. Typical yield: 70%; mp 242–243°C (lit[143] mp 239–240.5°C). ^{1}H NMR (90MHz, $CDCl_3$, TMS): δ 2.55(s, 12H, 2,3–CH_2) ppm.

4–Iodo–1–bicyclo[2.2.2]octyl Acetate[143] (12) *Diiodide* **11** (9.32 g, 25.7 mmol) was added to 160 mL glacial acetic acid and heated at reflux. Silver acetate (4.65 g, 27.8 mmol) was added to 90 mL of glacial acetic acid and was heated close to the boiling point. The silver acetate suspension was added to the *diiodide* in increments. Silver iodide was observed to precipitate immediately upon addition. When addition was complete, reflux was continued for 1 hour. The condenser was the removed and most of the acetic acid was removed by distillation. Water (100 mL) was added to the remaining residue and the AgI was removed by suction

filtration. The precipitate was washed copiously with Et_2O. The aqueous layer was separated and extracted with 2x100 mL Et_2O and the combined organics were washed with 4x40 mL saturated $NaHCO_3$ and dried over $MgSO_4$. The drying agent was filtered off and the solvent was removed *in vacuo* to yield 7.50 g of a slightly tan solid. Crude isolated yield: 98%. ^{1}H NMR (90MHz, $CDCl_3$, TMS): δ 2.60–2.40 (m, 6H, 3–CH_2), 2.20–2.05 (m, 6H, 2–CH_2), 1.94 (s, 3H, –CO_2CH_3) ppm.

4–Iodo–1–bicyclo[2.2.2]octanol[143] (13) *Iodoacetate* **12** (7.50 g, 25.5 mmol) was added to KOH (6.22 g, 96.4 mmol) in EtOH (95%(v/v), 70 mL). The mixture was heated at reflux for 2.5 hours. The reaction was allowed to cool and poured into H_2O(50 mL). The mixture was extracted with 3x30 mL Et_2O. The combined organics were washed with saturated NaCl and dried over $MgSO_4$. The drying agent was removed by filtration and the solvent was removed *in vacuo* to yield 6.11 g of solid material. Crude yield: 95%. ^{1}H NMR (90MHz, $CDCl_3$, TMS): δ 2.60–2.40 (m, 6H, 3–CH_2), 1.80–1.65 (m, 6H, 2–CH_2), 1.30 (bs, 1H, –OH) ppm.

4–Iodo–1–bicyclo[2.2.2]octyl Methyl Ether[143] (14) *Iodoalcohol* **13** (4.16 g, 16.5 mmol) was added to 45 mL dry dimethoxyethane. Methyl iodide (9.0 mL, 145 mmol) was added with stirring. Sodium hydride dispersion (50% by weight, 3.12 g, 65 mmol) was rinsed clean of mineral oil with hexane and transferred to a solid addition funnel. The apparatus was purged with argon and slow addition of NaH was begun. After the addition was complete, the solution was allowed to stir for an additional two hours. The progress of the reaction was checked by

capillary GC (15m SE–54 column; inj 250°/col 130°/ det 250°C) by quenching an aliquot and injecting the organics (retention times: *iodoalcohol* **13** 4.8 min, *iodomethoxy* **14** 5.4 min). Excess NaH was quenched by cautious addition of 15 mL H_2O. The reaction mixture was poured into H_2O (150 mL) and was extracted with 4x75 mL Et_2O . The combined organics were washed with 1x50 mL 2N HCl, 1x50 mL H_2O and 1x40 mL saturated NaCl. The solution was dried over $MgSO_4$, filtered and the solvent was removed *in vacuo* to yield 4.07 g of material. Crude yield: 93%. The product from two reactions was combined (6.18 g) and flash chromatographed on a 4x15 cm silica gel column. Fraction I was 1.5 L of elutant, then 60 mL fractions were collected. Elution was with 2.5 L hexane; 0.25 L 1%; 0.5 L 4%; 1.5 L 10%; 0.3 L 25%; 0.3 L 50% Et_2O/hexane (v/v), and 2 L Et_2O: Fraction 10–30, 1.15 g *diiodide* **7**, fraction 70–80, 5.39 g *iodomethoxy* **10**, fraction 80–∞, 0.34 g *iodoalcohol* **9**. Yield: 95%; mp 77.5–78.5°C (lit[143] mp 79–79.5°C). ^{1}H NMR (90MHz, $CDCl_3$, TMS): δ 1.65–1.80 (m, 6H, 2–CH_2) 2.45–2.60 (m, 6H, 3–CH_2) 3.10 (s, 3H, –OCH_3) ppm.

4,4′–Dimethoxy–1,1′–bibicyclo[2.2.2]octane [143] (15) A flask containing magnesium turnings (2.00 g, 82 mmol) was flame dried under a stream of argon. Half of the *iodomethoxy* **14** (11.57 g total, 43.5 mmol) in 15 mL dry diethylether was added to the turnings. The Grignard reaction began instantaneously. The remainder of the starting material was dissolved in more dry ether (20 mL) and added to a flame–dried addition funnel. This solution was slowly added to the magnesium turnings to maintain a gentle reflux. Grignard formation was moni-

tored by capillary GC (15 m SE–54; inj 250°/col 130°/det 250°C) by quenching a small aliquot and injecting the organics (retention times: *iodomethoxy* 5.2 min, quenched Grignard 1.3 min). When Grignard formation was complete, oven–dried $NiCl_2$ (6.90 g, 53.2 mmol) was added and reflux was maintained under argon for 15–20 hours. The solution immediately turned black upon addition of $NiCl_2$. A majority of the ether was then removed by distillation under argon. The residual solid was cautiously treated with water, washed with ethanol, and then extensively with Et_2O until only a fine gray–black powder of nickel remained. The aqueous layer was extracted with 3x30 mL Et_2O and the combined organic layers were washed with saturated NaCl, dried over $MgSO_4$ and filtered. The solvent was removed *in vacuo* and the solid was recrystallized from hexane yielding 3.33 g of white crystals (12.0 mmol, yield 55%). Alternatively, the product could be purified by flash chromatography in 25% Et_2O/hexane (R_f 0.20). mp 169–169.5°C (lit[143] mp 168.1–168.5°C). ^{1}H NMR (500MHz, $CDCl_3$, TMS): δ 3.12 (s, 6H, 2xOCH_3), 1.57–1.52 (m, 12H, 6xCH_2), 1.47–1.42 (m, 12H, 6xCH_2) ppm. ^{13}C NMR (22.4MHz, $CDCl_3$, TMS): δ 73.23, 48.99, 33.98, 29.30, 26.05 ppm.

4′–Iodo–1,1′–bibicyclo[2.2.2]octan–4–ol[143] (16) A solution of *dimethoxybislinker* **15** (2.60 g, 9.35 mmol) in 240 mL distilled benzene was added to a 500 mL 3–neck flask equipped with addition funnel, condenser, and mechanical stirrer. The solution was heated to reflux and the hot mixture was slowly treated with 60 mL of 57% HI while vigorously stirring, forming an emulsion. After addition was complete, the mixture was allowed to reflux 1 hour. The solution was poured

onto ice and neutralized with a copious amount of $NaHCO_3$. The aqueous layer was treated with HCl until just acid to litmus, then extracted with ether. The combined organics were washed with 10% $Na_2S_2O_3$, water, saturated NaCl, dried over $MgSO_4$, filtered, and the solvent was removed *in vacuo* to yield 3.7 g of a white solid.

The crude material from two reactions (8.73 g) was loaded onto a 4.5x18 cm silica column and purified by flash chromatography. Elution was with 1.5 L 10%, 0.25 L 25%, 2 L 50% Et_2O/hexane (v/v). Fraction size was 300 mL. Fractions 1–2 contained 0.89 g (9.2%) of 4′–Iodo–1,1′–bibicyclo[2.2.2]oct–4-yl methyl ether, and fractions 5–7 contained 7.05 g (76%) of pure **16**. ^{1}H NMR (500MHz, $CDCl_3$, TMS): δ 2.38 (m, 6H, 3xCH_2), 1.54 (m, 12H, 6xCH_2), 1.42 (m, 6H, 3xCH_2) ppm. ^{13}C NMR (50.3MHz, $CDCl_3$, TMS): δ 69.02 (4–*C*OH), 43.49 (4′–*C*I), 33.92, 31.52 (1,1′–*C*), 40.79, 33.78, 29.12, 26.16 (2,2′,3,3′–CH_2) ppm.

4–Iodo–4′–phenyl–1,1′–bibicyclo[2.2.2]octane (17) *Iodo–bislinker–alcohol* **16** (1.25 g, 3.47 mmol) was added to 200 mL of distilled benzene previously saturated with *p*–toluenesulfonic acid in a 3–neck 300 mL flask equipped with teflon sleeve protected joints. The solution was cooled to 0°C and saturated with BF_3 by slow passage over the stirred solution for 30 min. The solution was then heated to 60°C for 12 hours. The mixture was allowed to cool and was quenched by addition of H_2O. The aqueous layer was neutralized with solid $NaHCO_3$ and the organic layer was separated. The aqueous layer was extracted with 3x50 mL of CH_2Cl_2. The combined organics where dried over $MgSO_4$, filtered, and solvent

removed *in vacuo* to yield 1.40 g of a white solid. Crude yield: 96%.

An analytical sample was prepared by flash chromatography of 0.60 g of the product on a 2.5x16 cm silica column with CH_2Cl_2 as the elutant. Fraction size was 50 mL. Fractions 7–10 gave a total of 0.59 g pure **17** (mp >290°C). IR (KBr): ν_{max} 2930, 2910(sh), 2850, 1495, 1455, 1230, 975, 905, 810, 755, 695, 660, 620, 530 cm^{-1}. ^1H NMR (500MHz, $CDCl_3$, TMS): δ 7.26 (obscured by solvent, 4H), 7.13 (m, 1H), 2.40(m, 6H), 1.73(m, 6H), 1.56(m, 6H), 1.42(m, 6H) ppm. ^{13}C NMR (100.4MHz, $CDCl_3$, TMS): δ 149.70 (1″–*C*), 127.77, 125.25, 125.20 (2″/6″, 3″/5″, 4″–*C*H), 47.31, 35.40, 34.29, 31.96 (1,1′,4,4′–*C*), 41.13, 32.48, 29.45, 25.68 (2, 2′, 3, 3′–*C*H_2) ppm. Mass spectrum (EI, 70eV): *m/z* (relative intensity, %) 294(14), 293 (M^+–I, 55), 213(19), 185(34), 143(36), 129(45), 127(10), 117(30), 105(20), 91(100), 81(48). Exact mass for $C_{22}H_{29}I$: calcd 420.1314, (M^+–I) 293.2269, obsd 293.2266. *Anal.* Calcd for $C_{22}H_{29}I$: 62.86%C, 6.95%H, 30.19%I. Found: 62.98%C, 7.05%H, 30.35%I.

4–Bromo–4′–(4″–bromophenyl)–1,1′–bibicyclo[2.2.2]octane (18)

Phenyl–bislinker–iodide **17** (2.00 g, 4.76 mmol) was added to 300 mL of CCl_4 and the solution was heated to 70°C. Bromine (0.98 g, 6.13 mmol) in 15 mL CCl_4 was added to the solution. The mixture was allowed to stir protected from light until bridgehead exchange was complete (~1.5 hours). Reaction progress was monitored via capillary GC (15m SE–54; inj 350°/col 275°/det 350°C) by quenching a small aliquot with 5% $Na_2S_2O_3$ and injecting the organics. Iron filings (90 mg, 1.6 mmol) were added and the reaction was monitored every 10–15

min. If the reaction had not inititated within ~1 hour, aliquots (0.2–0.5 eq) of iron and bromine were successively added until the product peak was observed in the GC analysis (~4.7 min retention time). Once the product was observed, the reaction was monitored as frequently as possible to avoid dibromination of the phenyl ring. Immediately after the starting material was consumed, the reaction was quenched with 5% $Na_2S_2O_3$. The organics were separated and the aqueous layer was extracted with 3x50 mL CH_2Cl_2. The combined organics were dried over $MgSO_4$, filtered, and solvent removed *in vacuo* to yield 1.05 g of an off–white powder.

An analytical sample was obtained by flash chromatography of the crude product on a 2.5x20 cm silica column. Fraction size was 30 mL. Elution was with 1 L hexane, 50 mL 1%, 50 mL 2%, 50 mL 5%, 50 mL 10%, 20 mL 25%, 1 L 50% $CHCl_3$/hexane (v/v), and 250 mL $CHCl_3$. Fraction 1 was 1.2 L of elutant containing an unidentified hexane–mobile impurity. Fractions 3–35 contained pure *bromophenyl–bislinker–bromide* **18** (0.90 gm, yield: 83%). mp 296°C, decomp. IR (KBr): ν_{max} 2930, 2910(sh), 2850, 1485, 1455, 1230, 1075, 1005, 975, 820, 810(sh), 710, 665, 530 cm^{-1}. ^1H NMR (500MHz, $CDCl_3$, TMS): δ 7.358 ($\frac{1}{2}AA'BB'$ q, 2H, J=8.5Hz), 7.130 ($\frac{1}{2}AA'BB'$ q, 2H, J=8.5Hz), 2.17 (m, 6H, 3xCH_2), 1.68 (m, 6H, 3xCH_2), 1.57 (m, 6H, 3xCH_2), 1.44 (m, 6H, 3xCH_2) ppm. ^{13}C NMR (50.3MHz, $CDCl_3$, TMS): δ 149.10 (1″–C), 131.01, 127.37 (2″/6″, 3″/5″–CH), 119.25 (4″–CBr), 64.68 (4–CBr), 37.82, 32.23, 28.41, 25.42 (2, 2′, 3, 3′–CH_2) 34.82, 33.98, 32.84 (1,1′,4′–C) ppm. Mass spectrum (EI, 70eV): m/z (relative intensity, %) 454 ($M^+ + 4$, 2.3), 452 ($M^+ + 2$, 4.3), 450 (M^+, 2.7), 373 (2.5), 371 (3.4), 211 (10), 208

(13), 129 (100), 107 (12), 91 (13). Exact mass for $C_{22}H_{28}{}^{81}Br_2$: calcd 454.0517, obsd 454.0479; $C_{22}H_{28}{}^{79}Br^{81}Br$: calcd 452.0537, obsd 452.0519; $C_{22}H_{28}{}^{79}Br_2$: calcd 450.0558, obsd 450.0523. *Anal.* Calcd for $C_{22}H_{28}Br_2$: 58.42%C, 6.24%H. Found 58.88%C, 6.66%H.

4–(4‴–Bromophenyl)–4′–(2″,5″–dimethoxyphenyl)–1,1′–bibicyclo[2.2.2]octane (19) *Bromophenyl–bislinker–bromide* **18** (1.00 g, 2.21 mmol), 1,4–dimethoxybenzene (3.05 g, 22.1 mmol, 10 eq), and 150 mL dry 1,2–dichloroethane was added to a flame–dried argon–purged flask equipped with condenser and argon inlet. Aluminum bromide (0.62 g, 2.32 mmol) was added and the solution was heated to reflux for 24 hours. Reaction progress was monitored by quenching a small aliquot and analyzing by TLC (50% $CHCl_3$/hexane, short λ UV detection). Additional $AlBr_3$ aliquots (0.4 eq) were periodically added until the product was observed by TLC (starting material R_f 0.70, product R_f 0.40). After the starting material had largely disappeared, the reaction was quenched with dilute aqueous HBr. The aqueous layer was separated and washed with 4x50 mL CH_2Cl_2. The combined organics were washed with 2x75 mL 10% NaOH, 1x50 mL H_2O, 1x50 mL brine, dried over $MgSO_4$, filtered, and the solvent was removed *in vacuo*. The excess 1,4–dimethoxybenzene was removed by vacuum distillation (Kugelröhr oven, 1mm Hg, 110°C). The crude material (1.06 g, 2.08 mmol, crude yield 94%) was purified by flash chromatography. Elution was with 1 L hexane, 50 mL 2%, 50 mL 5%, 50 mL 10%, 100 mL 25%, 750 mL 50% $CHCl_3$/hexane (v/v). Fraction 1 was 1.1 L of elutant, then 25 mL fractions were collected. Fractions

21–32 contained 0.80 g of pure **19** (1.57 mmol, yield 71%).

A sample was purified for analytical analysis by flash chromatography of 0.40 g of the purified product from above on a 2.5x12 cm silica column with 30% CH_2Cl_2/hexane as the elutant. Fraction size was 5 mL. Fractions 12–15 contained 0.38 g of pure **19**. IR (KBr): ν_{max} 2930, 2910(sh), 2850, 1490, 1455(sh), 1275, 1220(sh), 1040, 995, 815, 720, 535 cm^{-1}. ^1H NMR (500MHz, $CDCl_3$, TMS): δ 7.375, 7.358 ($\frac{1}{2}AA'BB'$ q, 2H, 2‴,6‴/3‴,5‴–C*H*, *J*=8.6Hz), 7.171, 7.153 ($\frac{1}{2}AA'BB'$ q, 2H, 2‴,6‴/3‴,5‴–C*H*, *J*=8.5Hz), 6.76 (d, 1H, *J*= 8.4Hz, 3″–C*H*), 6.76 (d, 1H, *J*= 3.2Hz, 6″–C*H*), 6.65 (dd, 1H, *J*= 8.7, 3.0Hz, 4″–C*H*), 3.76 (s, 3H, –OCH_3), 3.74 (s, 3H, –OCH_3), 1.85–1.89 (m, 6H, 3xCH_2), 1.70–1.74 (m, 6H, 3xCH_2), 1.44–1.52 (m, 12H, 6xCH_2) ppm. ^{13}C NMR (100.4MHz, $CDCl_3$, TMS): δ 152.97, 152.72 (2″, 5″–*C*OCH$_3$), 149.22 (1‴–*C*), 138.82 (1″–*C*), 130.69, 127.19 (2‴/6‴, 3‴/5‴–*C*H), 118.92 (4‴–*C*Br), 114.31, 112.15, 109.54 (3″, 4″, 6″–*C*H), 55.76, 55.71 (2″, 5″–O*C*H$_3$), 35.10, 34.79, 34.51, 34.42 (1,1′,4,4′–*C*), 32.71, 30.07 (3,3′–*C*H$_2$), 25.84, 25.79 (2,2′–*C*H$_2$) ppm. Mass spectrum (EI, 70eV): *m/z* (relative intensity, %) 510 (M^+ + 2, 100), 508 (M^+, 96), 429 (M^+–Br, 3.8), 300 (4), 190 (20), 151 (9), 129 (8). Exact mass for $C_{30}H_{37}{}^{81}BrO_2$: calcd 510.1957, obsd 510.1952; $C_{30}H_{37}{}^{79}BrO_2$: calcd 508.1977, obsd 508.1982. *Anal.* Calcd for $C_{30}H_{37}BrO_2$: 70.72%C, 7.32%H, 15.68%Br. Found: 70.68%C, 7.45%H, 15.74%Br.

4‴–Formyl–2″,5″–dimethoxy– 4,4′–diphenyl–1,1′–bibicyclo[2.2.2]octane (20) was prepared by the general procedure of Jones and Grayshan.[153] Compound **19** (210 mg, 0.41 mmol) was dissolved in dry THF (20 mL) and added

to a flame–dried argon–purged flask and cooled to –78°C. *n*BuLi (550 μL, 1.6 mmol/mL in hexanes, 0.88 mmol, 2.1 eq) was added via syringe over ~10 min at –78°C. The solution was allowed to stir 1 hour at –78°C. Dry DMF (300 μL) in 100 μL dry THF was added to the aryllithium. The reaction was allowed to warm to room temperature for 1 hour. Excess organolithium was quenched by cautious addition of dilute aqueous HCl. The reaction was extracted with 50 mL ether, 3x25 mL CH_2Cl_2, and the combined organics were washed with brine, dried over $MgSO_4$, filtered and the solvent was removed *in vacuo* to yield 200 mg of an off–white powder. The crude material was purified by flash chromatography in 40% hexane/CH_2Cl_2 (R_f= 0.22), yielding 170 mg of pure **20** (0.37 mmol, yield 90%).

An analytical sample was prepared by flash chromatography of 200 mg of impure material on a 2.5x15 cm silica column. The material was dry loaded onto the column, and eluted with 200 mL hexane, 50 mL 2% CH_2Cl_2/hexane, 50 mL 20% CH_2Cl_2/hexane, and 400 mL 60% CH_2Cl_2/hexane. Fraction size was 15 mL. Fractions 31–36 contained 86 mg of pure **20**. Remaining fractions were combined to yield 80 mg of lesser purity **20**. IR (KBr): ν_{max} 2930, 2910(sh), 2850, 2820(sh), 2720(w), 1695, 1610, 1485, 1465, 1275, 1220, 1175, 1060(sh), 1050, 1025, 1005, 860, 825(sh), 820, 795, 725, 535 cm^{-1}. ^1H NMR (500MHz, $CDCl_3$, TMS): δ 9.95(s, 1H, –C*H*O), 7.794, 7.778 ($\frac{1}{2}AA'BB'$ q, 2H, J=8.3Hz), 7.480, 7.463 ($\frac{1}{2}AA'BB'$ q, 2H, J=8.3Hz), 6.78 (d, 1H, J= 3 Hz, 6″–C*H*), 6.77 (d, 1H, J= 8.9 Hz, 3″–C*H*), 6.66 (dd, 1H, J= 8.8, 3.0 Hz, 4″–C*H*), 3.77 (s, 3H, –OCH_3), 3.75 (s, 3H, –OCH_3), 1.92–1.87 (m, 6H, 3xCH_2), 1.82–1.78 (m, 6H, 3xCH_2), 1.56–1.51 (m, 6H,

3xCH_2), 1.51–1.47 (m, 6H, 3xCH_2) ppm. ^{13}C NMR (50.3MHz, $CDCl_3$, TMS): δ 192.03 (4‴–*C*HO), 158.02, 153.34 (2″, 5″–*C*OCH_3), 153.08 (1‴–*C*), 139.04 (1″–*C*), 133.98 (4‴–*C*), 129.55, 126.25 (2‴/6‴, 3‴/5‴–*C*H), 114.48, 112.32, 109.69 (3″, 4″, 6″–*C*H), 55.64, 55.58 (2″, 5″–O*C*H_3), 35.18, 34.99, 34.56, 34.31 (1,1′,4,4′–*C*), 32.37, 29.81 (2,2′–*C*H_2), 25.59, 25.47 (3,3′–*C*H_2) ppm. Mass spectrum (EI, 70eV): *m/z* (relative intensity, %) 459 ($M^+ + 1$, 13), 458 (M^+, 38), 430 (100), 190 (76), 151 (23), 91 (28). Exact mass for $C_{31}H_{38}O_3$: calcd 458.2821, obsd 458.2821 *Anal.* Calcd for $C_{31}H_{38}O_3$: 81.18%C, 8.35%H, found: 81.22%C, 8.46%H.

Preparation of Biphenylaldehyde **24**

1–Bromo–2,5–dimethoxybenzene (21) This compound was prepared by the method of Jurd.[203] 1,4–Dimethoxybenzene (41.05 g, 0.30 mole), KBr (35.73 g, 0.30 mole), H_2O (200 mL), ethanol (400 mL), and sulfuric acid (50 mL) were added to a flask and the solution was heated to a slow relux. Hydrogen peroxide (120 mL) was added to the hot solution over ~15 minutes and the reaction was allowed to reflux an additional 15 minutes. The product was isolated by ether extraction of the cooled reaction mixture. The organics were dried over Na_2SO_4, filtered, and the solvent was removed *in vacuo* to yield a red oil which was purified by vacuum distillation (bp 141–143°C at 17 mm Hg) to yield 43.91 g of a red oil (yield, 67%). ^{1}H NMR (90MHz, $CDCl_3$, TMS): δ 7.14 (m, 1H), 6.82 (m, 2H), 3.78 (s, 3H), 3.87 (s, 3H) ppm.

4–Bromobenzaldehyde ethylene acetal (22) was prepared by the general procedure of Swenton, Blankenship, and Sanitra.[204] 4–Bromobenzaldehyde (19.22 g, 0.104 mmol), ethylene glycol (29.96 g, 0.48 mmol, 4.6 eq), *p*–toluenesulfonic acid (0.2 g), and toluene (300 mL) were heated to reflux with azeotropic removal of H_2O for 12 hours. The reaction was allowed to cool, and the solution was filtered through a fritted funnel filled with silica gel to remove excess glycol. The filtrate was dried over $MgSO_4$, filtered and solvent removed *in vacuo* to yield a light green oil. The product was purified by distillation at reduced pressure (bp 146–147°C at 15mm Hg), distilling as a clear oil which crystallizes upon standing to white needle–like crystals. (19.21 g, yield, 81%). ^{1}H NMR (90MHz, $CDCl_3$, TMS): δ 7.45 (*AA'BB'* q, 4H), 5.80 (s, 1H), 4.05 (m, 4H) ppm.

4′–Formyl–2,5–dimethoxy–1,1′–biphenyl ethylene acetal (23) was prepared by the general procedure of Kumada, *et al.*[154] Magnesium turnings (4.0 g, 0.16 mol) were added to a 250 mL flask equipped with stir bar, condenser, and addition funnel. The entire apparatus was flame–dried under a stream of argon. Dry THF (2 mL) and ~20% of the *bromodimethoxybenzene* **21** (total 11.40 g, 52.5 mmol) were added to the turnings. The remaining *bromodimethoxybenzene* was added to the addition funnel in 60 mL dry THF. This solution was slowly added to the now exothermic Grignard reaction. After complete addition, the reaction was heated to reflux for 1 hour and allowed to cool. Grignard formation was monitored by quenching a small aliquot and analyzing the organics by capillary GC (conditions: 15m SE–54 column, inj 350°/col 150°/det 350°C). The Grignard

reagent was transferred via cannula to the addition funnel of a similar reaction apparatus. The second flask was charged with *bromo–acetal* **22** (10.00 g, 43.7 mmol), $Ni(P\emptyset_3)_2Cl_2$ (0.50 g, 0.76 mmol, 0.2 eq), and dry THF (20 mL). This mixture was cooled to 0°C, and the Grignard solution was slowly added over ~1.5 hours. The solution was then heated to relux for 36 hours under argon and quenched by the cautious addition of H_2O. The reaction was extracted with 3x100 mL ether, 2x75 mL CH_2Cl_2. The combined organics were washed with saturated NaCl, dried over $MgSO_4$, filtered and solvent removed *in vacuo* to yield a brown oil. The material was purified by flash chromatography in CH_2Cl_2 (R_f= 0.30), yielding 2.5 g of the cross–coupled product (yield, 20%). IR (KBr): ν_{max} 2950, 2895, 2820, 1490, 1410, 1290, 1260, 1230, 1200, 1170, 1075, 1050, 1020, 980, 960, 940, 840, 800, 740, 705, 610 cm^{-1}. ^1H NMR (500MHz, $CDCl_3$, TMS): δ 7.534, 7.518 ($\frac{1}{2}AA'BB'$ q, 2H, J=8.2Hz), 7.496, 7.479 ($\frac{1}{2}AA'BB'$ q, 2H, J=8.3Hz), 7.25 (d obscured by solvent, 1H, 6–C*H*), 6.93 (d, 1H, J=8.8Hz, 3–C*H*), 6.85 (dd, 1H, J=8.7, 3.0Hz, 4–C*H*), 5.87 (s, 1H), 4.15 (m, 2H), 4.05 (m, 2H), 3.79 (s, 3H, $-OCH_3$), 3.74 (s, 3H, $-OCH_3$) ppm. ^{13}C NMR (50.3MHz, $CDCl_3$, TMS): δ 153.72, 150.80 (2,5 $-COCH_3$), 139.28, 136.61, 131.32 (1,1′,4′–*C*) 129.45, 126.04 (2′/6′, 3′/5′–*C*H), 116.69, 113.19, 112.81 (3,4,6 –*C*H), 103.65 (acetal –*C*H), 65.29 (acetal $-CH_2$), 56.22, 55.78 (2,5 $-OCH_3$) ppm. Mass spectrum (EI, 70eV): *m/z* (relative intensity, %) 287 (M^+ +1, 19), 286 (M^+, 100), 285 (47), 242 (42), 214 (81), 199 (59), 184 (21), 73 (42). Exact mass for $C_{17}H_{18}O_4$: calcd 286.1205, obsd 286.1204. *Anal.* Calcd for $C_{17}H_{18}O_4$: 71.31%C, 6.34%H, found 71.18%C, 6.21%H.

4′–Formyl–2,5–dimethoxy–1,1′–biphenyl (24) *Biphenyl–acetal* **23** (2.50 g, 8.73 mmol) was stirred with heating for 1 hour in 2N HCl. The reaction mixture was extracted into ether, washed with H_2O, saturated NaCl, dried over $MgSO_4$, filtered, and solvent removed *in vacuo* to yield a light green oil which solidified upon standing. The product was purified by flash chromatograpy in toluene (R_f= 0.18) to remove the acetal starting material (R_f= 0.07). IR (KBr): ν_{max} 2995, 2930, 2820, 2720, 1690, 1600, 1515(sh), 1495, 1455, 1445, 1395, 1385, 1315, 1270, 1235, 1220, 1175, 1045, 1020, 870, 830, 805, 745, 692, 600, 475 cm^{-1}. ^1H NMR (500MHz, CD_2Cl_2, TMS): δ 10.03 (s, 1H), 7.911, 7.894 ($\frac{1}{2}AA'BB'$ q, 2H, J=8.3Hz), 7.718, 7.701 ($\frac{1}{2}AA'BB'$ q, 2H, J=8.2Hz), 6.97 (m, 1H), 6.92 (m, 2H), 3.80 (s, 3H), 3.76 (s, 3H) ppm. ^{13}C NMR (50.3MHz, $CDCl_3$, TMS): δ 191.96 (4′–*C*HO), 153.79, 150.69 (2,5 –*C*OCH_3), 144.80 (1′–*C*), 134.93 (4′–*C*CHO), 130.07, 129.39 (2′/6′, 3′/5′–*C*H), 129.62 (1–*C*), 116.56, 114.13, 112.73 (3,4,6 –*C*H), 56.22, 55.78 (2,5 –O*C*H_3) ppm. Mass spectrum (EI, 70eV): *m/z* (relative intensity, %) 243 (M^+ +1, 17), 242 (M^+, 100), 199 (49), 184 (26), 120 (17), 73 (15), 69 (18), 57 (20). Exact mass for $C_{15}H_{14}O_3$: calcd 242.0943, obsd 242.0940. *Anal.* Calcd for $C_{15}H_{14}O_3$: 74.36%C, 5.83%H, found 74.40%C, 5.93%H.

Preparation of Bicyclo[2.2.2]octylbenzaldehydes **46, 49, 51**

4″–Formyl–4′–bromo–2′,5′–dimethoxy–1,4–diphenylbicyclo[2.2.2]octane (46) was prepared by the method of Podall and Foster.[205] *Aryl aldehyde* **45**[145] (50.2 mg, 0.143 mmol) was dissolved in dry dichloroethane (50 mL) and cooled to 0°C under argon. Bromine (8.8 μL, 3.119 g/mL, 0.17 mmol, 1.2 eq) was

added to 2–3 mL dry dichloroethane in an addition funnel and slowly added to the cooled aldehyde solution over ~4 min. The reaction was allowed to stir at 0°C protected from light for 1 hour and then quenched by addition of 1% $Na_2S_2O_3$. The reaction was washed with water and extracted with 3x25 mL CH_2Cl_2. The combined organics were dried over Na_2SO_4, filtered and solvent removed *in vacuo* to yield an off–white solid. The product was purified by flash chromatography in toluene (2.5x12 cm column, R_f= 0.2, fraction size 10 mL). Fractions 9–15 were combined to yield 53.2 mg of *bromo–aldehyde* product. (0.12 mmol, yield, 87%). ^{1}H NMR (500MHz, CD_2Cl_2, TMS): δ 9.96 (s, 1H, –C*H*O), 7.82, 7.80 ($\frac{1}{2}AA'BB'$ q, 2H, J=8.2Hz), 7.56, 7.54 ($\frac{1}{2}AA'BB'$ q, 2H, J=8.5Hz), 7.05 (s, 1H, 3′ or 6′–C*H*) 6.84 (s, 1H, 3′ or 6′–C*H*) 2.10 (m, 6H, 3xCH_2), 1.97 (m, 6H, 3xCH_2) ppm. ^{13}C NMR (50.3MHz, $CDCl_3$, TMS): δ 192.01 (4″–*C*HO), 157.47, 149.83 (2′,5′–*C*OCH_3), 153.22 (1″–*C*), 137.12 (1′–*C*), 134.14 (4″–*C*), 129.64, 126.23 (2″/6″, 3″/5″–*C*H), 116.82, 112.37, (3′,6′–*C*H), 108.91 (4′–*C*Br) 57.15, 55.86 (2′,5′–O*C*H_3), 35.50, 35.29 (1,4 –*C*), 32.36, 29.82 (2,3 –*C*H_2) ppm. Mass spectrum (EI, 70eV): *m/z* (relative intensity, %) 431 (M^+ [^{81}Br]+1, 21), 430 (M^+ [^{81}Br], 92), 429 (M^+ [^{79}Br]+1, 21), 428 (M^+ [^{81}Br], 87), 387 (26), 385 (24), 270 (79), 268 (78), 73 (54), 71 (51), 69 (92), 57 (100), 55 (83). Exact mass for $C_{23}H_{25}O_3{}^{81}$Br: calcd 430.0967, obsd 430.0946; $C_{23}H_{25}O_3{}^{79}$Br: calcd 428.0987, obsd 428.0968 *Anal.* Calcd for $C_{23}H_{25}O_3$Br: 64.34%C, 5.87%H, 18.61%Br, found: 64.44%C, 5.88%H, 18.54%Br.

4″–Formyl–2′,5′–dihydroxy–1,4–diphenylbicyclo[2.2.2]octane (47) was prepared by the method of Lansinger and Ronald.[206] *Aryl aldehyde* **45**[145]

(105.4 mg, 0.301 mmol) was dissolved in dry CH_2Cl_2 (65 mL), purged with argon and cooled to 0°C. Boron triiodide (0.4142 g) was weighed under argon into a dry flask, and dry CH_2Cl_2 was added (total volume 760 μL). A portion (500 μL, 0.71 mmol, 2.04 eq) of the BI_3 solution was added slowly to the aldehyde solution. The reaction was allowed to stir 20 minutes at 0°C, then quenched by the addition of 2 mL H_2O, followed by 1.5 mL 10% $Na_2S_2O_3$. The reaction was extracted with Et_2O, and the combined organics were washed with 10% $Na_2S_2O_3$, saturated NaCl, dried over $MgSO_4$, and the solvent was removed *in vacuo* . The crude material was purified by flash chromatography (2.5x15 cm column, 35% EtOAc/Hexane, R_f= 0.18, fraction size 5 mL) Fractions 27–35 contained 41.3 mg of pure **47** (yield, 43%). IR (KBr): ν_{max} 3400 (br, –OH), 2930, 2910(sh), 2850, 2710(w), 1680(sh), 1665, 1605, 1565, 1510, 1380, 1220,(sh), 1200, 855, 820, 800, 775 cm^{-1}. ^1H NMR (400MHz, $CDCl_3$, TMS): δ 9.96 (1H, –C*H*O), 7.819, 7.799 ($\frac{1}{2}AA'BB'$ q, 2H, J=7.9Hz), 7.531, 7.510 ($\frac{1}{2}AA'BB'$ q, 2H, J=8.3Hz), 6.70 (m, 1H), 6.53 (m, 2H), 4.6 (br s, –OH), 2.15–2.04 (m, 6H, 3xCH_2), 2.00–1.90 (m, 6H, 3xCH_2) ppm. ^{13}C NMR (50.3MHz, CD_3OD, TMS): δ 194.13 (4″–*C*HO), 159.50 (1″–*C*), 150.73, 150.44 (2′, 5′–*C*OH), 136.80 (1′–*C*), 135.58 (4″–*C*CHO), 130.63, 127.51 (2″/6″, 3″/5″–*C*H), 117.78, 114.99, 113.74 (3′, 4′, 6′–*C*H), 36.53, 36.05 (1,4 –*C*), 33.67, 30.87 (2,3 –CH_2) ppm. ^{13}C NMR (50.3MHz, CD_3CN, TMS): δ 193.23 (4″–*C*HO), 158.72 (1″–*C*), 150.90, 149.59 (2′, 5′–*C*OH), 136.88 (1′–*C*), 135.32 (4″–*C*CHO), 130.29, 127.39 (2″/6″, 3″/5″–*C*H), 117.39(sh), 115.10, 113.68 (3′, 4′, 6′–*C*H), 36.14, 35.73 (1,4 –*C*), 33.12, 30.42 (2,3 –CH_2) ppm. Mass spectrum (EI, 70eV): *m/z* (relative intensity, %) 323 (M^+ + 1, 23), 322 (M^+, 100), 320

(M^+ –2H, 8), 162 (70), 161 (55), 147 (69), 136 (14), 123 (17), 91 (18). Exact mass for $C_{21}H_{20}O_3$: calcd 322.1570, obsd 322.1567.

4″–Formyl–4–(2′,5′–benzoquinonyl)–1–phenylbicyclo[2.2.2]octane (48) *Aryl hydroquinone* **47** (35.5 mg, 0.11 mmol) was dissolved in hot CH_2Cl_2 and transferred to a 25 mL erlenmeyer. A large excess of PbO_2 (1.6 g, 60 eq) was added and the solution was stirred for 7–10 minutes on a warm hot–plate until TLC (35% EtOAc/Hexane, short λ UV detection) demonstrated the reaction had largely gone to completion. The warm solution was concentrated *in vacuo* and loaded onto a Grade III alumina column (2.5x6 cm, fraction size 5 mL) and eluted with 7% CH_3CN/CH_2Cl_2 (v/v). Fractions 6–8 contained pure **48** (24.6 mg, yield: 70%). IR (KBr): ν_{max} 2930, 2910(sh), 2850, 1690, 1650(C=O), 1605, 1585, 1080, 905, 850, 830, 815(sh) cm^{-1}. ^1H NMR (400MHz, CD_2Cl_2, TMS): δ 9.95 (1H, –C*H*O), 7.81, 7.79 ($\frac{1}{2}AA'BB'$ q, 2H, J=8.3Hz), 7.53, 7.51($\frac{1}{2}AA'BB'$ q, 2H, J=8.3Hz), 6.66 (s, 2H), 6.53 (s, 1H), 1.95 (br s, 12H, 6xCH_2) ppm. ^{13}C NMR (50.3MHz, $CDCl_3$): δ 191.97 (4″–*C*HO), 188.02, 187.42 (2′, 5′–*C*=O), 156.60 (1″–*C*), 154.83 (1′–*C*), 134.34 (4″–*C*CHO), 138.76, 134.96, 132.60 (3′, 4′, 6′–*C*H), 129.74, 126.22 (2″/6″, 3″/5″–*C*H), 36.15, 35.34 (1,4 –*C*), 31.81, 29.91 (2,3 –CH_2) ppm. Mass spectrum (EI, 70eV): *m/z* (relative intensity, %) 323 (M^+ + 2H + 1, 21), 322 (M^+ + 2H, 94), 321 (M^+ + 1, 20), 320 (M^+, 83), 188 (54), 185 (62), 184 (74), 171 (66), 162 (88), 161 (62), 147 (94), 136 (71), 115 (51), 91 (100). Exact mass for $C_{21}H_{20}O_3$: calcd 320.1413, obsd 320.1409.

4″–Formyl–4′–chloro–2′,5′–dihydroxy –1,4–diphenylbicyclo[2.2.2]octane (49) *Aryl quinone* **48** (24.6 mg, 0.077 mmol) was dissolved in 10 mL dry THF. The flask was purged with argon and cooled to 0°C. HCl gas was bubbled through the solution for 8 min at 0°C with a slow argon purge. The solution was poured into H_2O and neutralized with $NaHCO_3$, and copiously extracted with Et_2O. The combined organics were washed with H_2O, saturated NaCl, dried over Na_2SO_4, and the solvent was removed *in vacuo* yielding a green oil. A majority of the THF breakdown product was removed by high vacuum treatment (1 Torr) for 4–6 hours. The remaining residue was dissolved in Et_2O and precipitated by addition of hexane. The solid was placed under high vacuum overnight. The material was purified by flash chromatography (2.5x15 cm column, 30% EtOAc/hexane, fraction size 8 mL) Two products were observed to be present by TLC, $R_f = 0.56$, 0.32. The two components were isolated, the faster moving material identified as the *chloroquinone* **50** (8 mg, 0.023 mmol), and the slower component was found to be the *chlorohydroquinone* product **49** (14.9 mg, 0.042 mmol), for a combined yield of 83%. NMR analysis revealed the product to be a mixture of the 4′– (~60%) and 3′–chloro (~40%) derivatives, inseparable with the above chromatography conditions. IR (KBr): ν_{max} 3400(br, –OH) 2930, 2910(sh), 2850, 1680(br), 1605, 1570, 1505, 1270, 1190(br), 1165, 840, 785 cm^{-1}.

4′–chloro isomer: ^1H NMR (400MHz, CD_2Cl_2, TMS): δ 9.96 (1H, –C*H*O), 7.823, 7.802 ($\frac{1}{2}AA'BB'$ q, 2H, J=8.3Hz), 7.559, 7.539 ($\frac{1}{2}AA'BB'$ q, 2H, J=8.3Hz), 6.85 (s, 1H), 6.71 (s, 1H), 4.6 (br s, –OH), 2.18–2.04 (m, 6H, 3xCH_2), 2.02–1.87 (m, 6H, 3xCH_2),ppm. ^{13}C NMR (50.3MHz, CD_3OD, TMS): δ 194.10 (4″–*C*HO),

159.33 (1″–*C*), 150.80, 146.43 (2′, 5′–*C*OH), 136.11 (1′–*C*), 135.62 (4″–*C*CHO), 130.65, 127.51 (2″/6″, 3″/5″–*C*H), 118.26 (4′–*C*Cl), 117.73, 116.40 (3′, 6′–*C*H), 36.48, 36.03 (1,4 –*C*), 33.58, 30.85 (2,3 –CH_2) ppm.

3′–chloro isomer: ^{1}H NMR (400MHz, CD_2Cl_2, TMS): δ 9.96 (1H, –C*H*O), 7.823, 7.802 ($\frac{1}{2}AA'BB'$ q, 2H, J=8.3Hz), 7.559, 7.539($\frac{1}{2}AA'BB'$ q, 2H, J=8.3Hz), 6.74(sh) (d, 1H, J=~3Hz), 6.65 (d, 1H, J=~3Hz), 4.6 (br s, –OH), 2.18–2.04 (m, 6H, 3xCH_2), 2.02–1.87 (m, 6H, 3xCH_2),ppm. ^{13}C NMR (50.3MHz, CD_3OD, TMS): δ 194.10 (4″–*C*HO), 159.33 (1″–*C*), 151.16, 150.37(sh) (2′, 5′–*C*OH), 139.83 (1′–*C*), 135.62 (4″–*C*CHO), 130.65, 127.51 (2″/6″, 3″/5″–*C*H), 126.17 (3′–*C*Cl), 114.39, 114.10 (4′, 6′–*C*H), 36.48, 36.03 (1,4 –*C*), 33.58, 30.85 (2,3 –CH_2) ppm.

Mass spectrum (EI, 70eV): *m/z* (relative intensity, %) 358 (M^+ [^{37}Cl], 30), 357 (M^+ [^{35}Cl] + 1, 22), 356 (M^+ [^{35}Cl], 100), 354 (M^+ [^{35}Cl]–2H, 14), 198 (41), 196 (75), 195 (49), 184 (26), 171 (26), 169 (59), 115 (31), 91 (47). Exact mass for $C_{21}H_{21}O_3{}^{35}Cl$: calcd 356.1179, obsd 356.1167. Exact mass for $C_{21}H_{21}O_3{}^{37}Cl$: calcd 358.1150, obsd 358.1167.

4″–Formyl–4–(4′–chloro–2′,5′–benzoquinonyl)–1–phenylbicyclo[2.2.2]octane (50) *Chlorohydroquinone* **49** (19.8 mg, 0.056 mmol) was dissolved in hot CH_2Cl_2 and transferred to a 25 mL erlenmeyer. A large excess of PbO_2 (0.85 g, 50 eq) was added and the solution was stirred for 10 minutes on a warm hot–plate until TLC (35% EtOAc/Hexane, short λ UV detection) showed the reaction had largely gone to completion. The warm solution was concentrated *in vacuo* and loaded onto a Grade III alumina column (2.5x6 cm, fraction size 5

mL) and eluted with 7% CH_3CN/CH_2Cl_2 (v/v). Fractions 4–8 contained pure **50** (16.2 mg, 0.046 mmol, yield: 65%). NMR analysis revealed the product to be a mixture of the 4′– (~60%) and 3′–chloro (~40%) derivatives. IR (KBr): ν_{max} 2960, 2910(sh), 2860, 2720, 1695, 1660, 1650 (C=O), 1605, 1585, 1385, 1265, 1210, 1095(br), 1010, 915, 815, 795, 535 cm^{-1}.

4′–chloro isomer: ^1H NMR (400MHz, CD_2Cl_2, TMS): δ 9.96 (1H, –C*H*O), 7.824, 7.803 ($\frac{1}{2}AA'BB'$ q, 2H, J=8.3Hz), 7.541, 7.519 ($\frac{1}{2}AA'BB'$ q, 2H, J=8.3Hz), 6.92 (s, 1H), 6.69 (s, 1H) 2.02 (br s, 12H) ppm. ^{13}C NMR (50.3MHz, $CDCl_3$): δ 191.94 (4″–*C*HO), 185.35, 180.14 (2′, 5′–*C*=O), 156.36 (1″–*C*), 155.73 (1′–*C*), 142.56 (4′–*C*Cl), 134.36 (4″–*C*CHO), 135.59, 132.25 (3′, 6′–*C*H), 129.74, 126.18 (2″/6″, 3″/5″–*C*H), 36.38, 35.30 (1,4 –*C*), 31.72, 30.03 (2,3 –CH_2) ppm.

3′–chloro isomer: ^1H NMR (400MHz, CD_2Cl_2, TMS): δ 9.96 (1H, –C*H*O), 7.824, 7.803 ($\frac{1}{2}AA'BB'$ q, 2H, J=8.3Hz), 7.541, 7.519 ($\frac{1}{2}AA'BB'$ q, 2H, J=8.3Hz), 6.67 (d, 1H, J=1.6 Hz), 6.54 (d, 1H, J=1.6 Hz), 2.02 (br s, 12H) ppm. ^{13}C NMR (50.3MHz, $CDCl_3$): δ 191.94 (4″–*C*HO), 185.11, 180.62 (2′, 5′–*C*=O), 156.36 (1″–*C*), 155.00 (1′–*C*), 145.59 (3′–*C*Cl), 134.36 (4″–*C*CHO), 132.93, 132.40(sh) (4′, 6′–*C*H), 129.74, 126.18 (2″/6″, 3″/5″–*C*H), 36.38, 35.30 (1,4 –*C*), 31.72, 30.03 (2,3 –CH_2) ppm.

Mass spectrum (EI, 70eV): *m/z* (relative intensity, %) 356 (M^+ [^{37}Cl], M^+ [^{35}Cl] + 2H, 100), 354 (M^+ [^{35}Cl], 14), 198 (41), 196 (75), 195 (49), 184 (26), 171 (26), 169 (59), 115 (31), 91 (47). Exact mass for $C_{21}H_{19}O_3{}^{35}Cl$: calcd 354.1024, obsd 354.1020.

4″–Formyl–3′,4′–dichloro–2′,5′–dihydroxy –1,4–diphenylbicyclo[2.2.2]octane (51) *Chloroquinone* **50** (13.8 mg, 0.039 mmol) was dissolved in 10 mL dry THF. The flask was purged with argon and cooled to 0°C. HCl gas was bubbled through the solution with a slow argon purge until the yellow color of the quinone solution had disappeared (~10 min at 0°C). The solution was poured into H_2O and neutralized with $NaHCO_3$, and extracted with Et_2O. The combined organics were washed with H_2O, saturated NaCl, dried over Na_2SO_4, and the solvent was removed *in vacuo*. The THF breakdown product was removed by high vacuum treatment (1 Torr) overnight. The remaining residue was dissolved in Et_2O and precipitated by addition of hexane. The crude material was purified by flash chromatography (2.5x15 cm column, 30%EtOAc/hexane, major product R_f= 0.25, fraction size 5 mL) The major component was isolated to yield 9.7 mg of *dichlorohydroquinone* **51** (0.025 mmol, yield: 64%). IR (KBr): ν_{max} 3400(br, –OH), 2950, 2910, 2850, 2750(w), 1675(br), 1605, 1570, 1505, 1455, 1410, 1318(sh), 1290, 1275, 1205(br), 1175, 840, 795, 540 cm^{-1}. ^1H NMR (200MHz, CD_3OD, TMS): δ 9.95 (1H, –C*H*O), 7.872, 7.830 ($\frac{1}{2}AA'BB'$ q, 2H, J=8.4Hz), 7.626, 7.584 ($\frac{1}{2}AA'BB'$ q, 2H, J=8.5Hz), 6.79 (s, 1H, 6′–C*H*), 2.21–2.09 (m, 6H, 3xCH_2), 2.05–1.92 (m, 6H, 3xCH_2) ppm. ^{13}C NMR (50.3MHz, CD_3OD, TMS): δ 194.11 (4″–*C*HO), 159.10 (1″–*C*), 147.98, 146.63 (2′, 5′–*C*OH), 137.55 (1′–*C*), 135.69 (4″–*C*CHO), 130.68, 127.50 (2″/6″, 3″/5″–*C*H), 126,85, 126.23 (3′, 4′–*C*Cl), 114.42 (6′–*C*H), 36.82, 36.48 (1,4 –*C*), 33.51, 30.87 (2,3 –CH_2) ppm. Mass spectrum (EI, 70eV): *m/z* (relative intensity, %) 392 (M^+ [$^{35}Cl^{37}Cl$], 13), 390 (M^+ [$^{35}Cl_2$], 34), 185 (47), 184 (49), 171 (39), 129 (51), 128 (46), 115 (64), 91 (100), 77 (41), 55 (45). Ex-

act mass for $C_{21}H_{20}O_3{}^{35}Cl^{37}Cl$: calcd 392.0760, obsd 392.0766; $C_{21}H_{20}O_3{}^{35}Cl_2$: calcd 390.0791, obsd 390.0774.

Preparation of Porphyrins **1, 3, 41, 42, 43**

5–[4′–(2″,5″–Dimethoxyphenyl)phenyl]– 2,3,7,8,12,13,17,18 –octamethylporphyrin (52) A flask was charged with *ac–biladiene dihydrobromide* **36**[145] (555 mg, 0.957 mmol), *biphenyl–aldehyde* **24** (470 mg, 1.9 mmol, 2.1 eq), anhydrous methanol (150 mL), and freshly prepared HBr saturated acetic acid (15 drops). The mixture was heated to reflux in air but protected from light for 24 hours. The cooled reaction mixture was neutralized with $NaHCO_3$, and filtered. The filtrate was discarded, and the precipitate was dissolved in $CHCl_3$ and filtered. The solvent was removed *in vacuo* in darkness, and the material was purified by flash chromatography in 2% acetone/CH_2Cl_2(v/v). Spectroscopic yield, (ϵ_{404} = 170,000 estd) 20%. UV–Vis($CHCl_3$): λ_{max} 320(sh), 404, 502, 536, 570, 624 nm. ^{1}H NMR (500MHz, $CDCl_3$, TMS): δ 10.12 (s, 2H, 10, 20–C*H*), 9.91 (s, 1H, 15–C*H*), 8.056, 8.040 ($\frac{1}{2}AA'BB'$ q, 2H, J=8.1Hz), 7.914, 7.898 ($\frac{1}{2}AA'BB'$ q, 2H, J=7.8Hz), 7.25 (obscured by solvent, 6″–C*H*), 7.08 (d, 1H, J= 8.9 Hz, 3″–C*H*), 6.96 (dd, 1H, J= 8.9, 3.1 Hz, 4″–C*H*), 3.93 (s, 3H, –OCH_3), 3.91 (s, 3H, –OCH_3), 3.60 (s, 6H, 13,17–CH_3), 3.57 (s, 6H, 12,18–CH_3), 3.52 (s, 6H, 2,8–CH_3), 2.53 (s, 6H, 3,7–CH_3) ppm. Mass spectrum (Fast Atom Bombardment, positive ion, *o*-nitrophenyloctylether matrix): *m/z* (relative intensity, %) Exact mass for $C_{42}H_{42}N_4O_2$: calcd 634.3308, (M^+ + H) 635.3386, obsd 635.3359.

5–[4′–(2″,5″–Dihydroxyphenyl)phenyl]– 2, 3, 7, 8, 12, 13, 17, 18 –octamethylporphyrin (53) A solution of *H_2PØDMB* **52** (20 mg, 0.032 mmol) in dry CH_2Cl_2 was cooled to –78°C in an argon–purged flask protected from light. Boron tribromide (3 mL, 1.0 M in CH_2Cl_2, 3 mmol, 100 eq) was slowly added to the porphyrin solution. The reaction was allowed to stir for 1 hour at –78°C, then warmed to room temperature and allowed to react for 12 hours. The reaction was quenched by the addition of aqueous ammonia. The reaction was poured into $CHCl_3$, washed with water, dried over Na_2SO_4, filtered, and the solvent was removed *in vacuo*. The material was stored as a solid under argon and protected from light. UV–Vis ($CHCl_3$): λ_{max} 320(sh), 404, 502, 535, 571, 624 nm. ^{1}H NMR (500MHz, $CDCl_3$, TMS): δ 10.15 (s, 2H, 10, 20–C*H*), 9.95 (s, 1H, 15–C*H*), 8.169, 8.152 ($\frac{1}{2}AA'BB'$ q, 2H, J=8.1Hz), 7.920, 7.905 ($\frac{1}{2}AA'BB'$ q, 2H, J=7.8Hz), 7.25 (obscured by solvent, 6″–C*H*), 7.04 (d, 1H, J= 10.3 Hz, 3″–C*H*), 6.97 (dd, 1H, J= 10.3, 2.4 Hz, 4″–C*H*), 3.62 (s, 6H, 13,17–CH_3), 3.59 (s, 6H, 12,18–CH_3), 3.53 (s, 6H, 2,8–CH_3), 2.48 (s, 6H, 3,7–CH_3) ppm. Mass spectrum (Fast Atom Bombardment, positive ion, *m*-nitrobenzylalcohol matrix): *m/z* (relative intensity, %) Exact mass for $C_{40}H_{38}N_4O_2$: calcd 606.2995, (M^+ –2H) 604.2838, obsd 604.2824.

5–{ 4′–[4″–(2‴,5‴–Dimethoxy–4‴– bromophenyl)bicyclo[2.2.2]octyl]–phenyl}– 2, 3, 7, 8, 12, 13, 17, 18–octamethylporphyrin (54) *Bromoarylaldehyde* **46** (50 mg, 0.12 mmol), and *ac–biladiene dihydrobromide* **36**[145] (69 mg, 0.12 mmol) were suspended in anhydrous methanol (15 mL). Freshly prepared HBr saturated acetic acid (2 drops) was added, and the reaction was refluxed under

aerobic conditions, but protected from light for 20 hours. The cooled reaction was neutralized with $NaHCO_3$ and dissolved in $CHCl_3$. The organic layer was washed with water, dried over Na_2SO_4, filtered, and the solvent was removed *in vacuo*. The crude material was purified in 4% CH_3CN/CH_2Cl_2 (R_f= 0.56) by flash chromatography. Spectroscopic yield, (ϵ_{404} = 170,000 estd) ~20%. UV–Vis ($CHCl_3$): λ_{max} 402, 501, 534, 570, 623 nm. ^{1}H NMR (500MHz, CD_2Cl_2, TMS): δ 10.17 (s, 2H, 10, 20–C*H*), 9.98 (s, 1H, 15–C*H*), 7.950, 7.934 ($\frac{1}{2}AA'BB'$ q, 2H, J=8.0Hz), 7.759, 7.743 ($\frac{1}{2}AA'BB'$ q, 2H, J=8.0Hz), 7.11 (s, 1H, 3‴ or 6‴–C*H*), 6.96 (s, 1H, 3‴ or 6‴–C*H*), 3.90 (s, 3H, –OCH_3), 3.88 (s, 3H, –OCH_3), 3.63 (s, 6H, 13,17–CH_3), 3.60 (s, 6H, 12,18–CH_3), 3.54 (s, 6H, 2,8–CH_3), 2.45 (s, 6H, 3,7–CH_3), 2.27 (s, 12H, 6xCH_2) ppm. Mass spectrum (Fast Atom Bombardment, positive ion, dithiothreitol/dithioerythritol matrix): *m/z* (relative intensity, %) $C_{50}H_{53}N_4O_2{}^{79}Br$: calcd 820.3352, ($M^+$ + H) 821.3430, obsd 821.3447.

5–{ 4′–[4″–(2‴,5‴–Dihydroxy–4‴– chlorophenyl)bicyclo[2.2.2]octyl]–phenyl}– 2,3,7,8,12,13,17,18 –octamethylporphyrin (55) A flask was charged with *chlorohydroquinone* **49** (16.9 mg, 4.7x10^{-2} mmol), *ac–biladiene dihydrobromide* **36**[145] (27.4 mg, 4.8x10^{-2} mol) and anhydrous methanol (2.1 mL). Freshly prepared HBr saturated acetic acid (1 drop) was added, and the reaction was refluxed under aerobic conditions, but protected from light for 18 hours. The cooled reaction was neutralized with $NaHCO_3$ and dissolved in $CHCl_3$. The organic layer was washed with water, dried over Na_2SO_4, filtered, and the solvent was removed *in vacuo*. Two products were observed by TLC (4% CH_3CN/CH_2Cl_2) to-

have the desired red fluorescence under long wavelength UV irradiation. (R_f~0.6, ~0.1) The corrole side product (R_f~0.4) was separated from the desired free–base porphyrins by flash chromatography in 4% CH_3CN/CH_2Cl_2. The quinone and hydroquinone products were combined for further metallation and oxidation. Spectroscopic yield, (ϵ_{404} = 170,000 estd) ~35%.

5–{ 4′–[4″–(2‴,5‴–Dihydroxy–3‴,4‴–dichlorophenyl)bicyclo[2.2.2]oct–yl]phenyl}– 2,3,7,8,12,13,17,18 –octamethylporphyrin (56) *Dichlorohydroquinone* **51** (10.1 mg, 0.026 mmol), *ac–biladiene dihydrobromide* **36**[145] (14.8 mg, 0.026 mmol) and anhydrous methanol (2.5 mL) were added to a flask. HBr saturated acetic acid (1 drop) was added and the solution was heated to reflux under air but protected from light for 12 hours. The cooled reaction was neutralized with $NaHCO_3$ and dissolved in $CHCl_3$. The organic layer was washed with water, dried over Na_2SO_4, filtered, and the solvent was removed *in vacuo*. The corrole side product was separated by flash chromatography in 3% CH_3CN/CH_2Cl_2. The porphyrin–quinone product from the oxidation of the hydroquinone (PbO_2) was observed to have an R_f= 0.58 in this solvent system. Spectroscopic yield, (ϵ_{404} = 170,000 estd) ~20%. UV–Vis (CH_2Cl_2): λ_{max} 401, 501, 534, 570, 624 nm. ^{1}H NMR (400MHz, CD_2Cl_2, TMS): δ 10.17 (s, 2H, 10, 20–C*H*), 9.98 (s, 1H, 15–C*H*), 7.964, 7.944 ($\frac{1}{2}AA'BB'$ q, 2H, J=8.1Hz), 7.733, 7.713 ($\frac{1}{2}AA'BB'$ q, 2H, J=8.1Hz), 6.85 (s, 1H, 6‴–C*H*), 3.63 (s, 6H, 13,17–CH_3), 3.60 (s, 6H, 12,18–CH_3), 3.53 (s, 6H, 2,8–CH_3), 2.44 (s, 6H, 3,7–CH_3), 2.2 (br s, 12H, 6xCH_2) ppm.

5–{ 4′–[4‴–(2⁗,5⁗–Dimethoxyphenyl)–1″,1‴–bibicyclo[2.2.2]octyl]–phenyl}– 2,3,7,8,12,13,17,18 –octamethylporphyrin (37) *Bislinker–aldehyde* **20** (92 mg, 0.20 mmol), *ac–biladiene dihydrobromide* **36**[145] (100 mg, 0.17 mmol) and anhydrous methanol (30 mL) were added to a flask. HBr saturated acetic acid (5 drops) was added and the solution was heated to reflux under air but protected from light for 24 hours. The cooled reaction was neutralized with $NaHCO_3$ and dissolved in $CHCl_3$. The organic layer was washed with water, dried over Na_2SO_4, filtered, and the solvent was removed *in vacuo*. The product was purified by flash chromatography in 3% CH_3CN/CH_2Cl_2 (R_f=0.30). Spectroscopic yield, (ϵ_{404} = 170,000 estd) ~15%. UV–Vis ($CHCl_3$): λ_{max} 404 (ϵ 175,000 estd), 503 (14,000 estd), 537.5 (6100 estd), 571 (6000 estd), 625 (2100 estd) nm. ^{1}H NMR (400MHz, $CDCl_3$, TMS): δ 10.10 (s, 2H, 10,20–C*H*), 9.90 (s, 1H, 15–C*H*), 7.898, 7.877 ($\frac{1}{2}AA'BB'$ q, 2H, –C*H*,*J*=8.4Hz), 7.642, 7.621 ($\frac{1}{2}AA'BB'$ q, 2H, –C*H*,*J*=8.4Hz), 6.81 (d, 1H, *J*= 2.9 Hz, 6⁗–C*H*), 6.79 (d, 1H, *J*= 9.2 Hz, 3⁗–C*H*), 6.67 (dd, 1H, *J*= 8.8, 2.9 Hz, 4⁗–C*H*), 3.80 (s, 3H, –OCH_3), 3.77 (s, 3H, –OCH_3), 3.59 (s, 6H, 13,17–CH_3), 3.56 (s, 6H, 12,18–CH_3), 3.49 (s, 6H, 2,8–CH_3), 2.40 (s, 6H, 3,7–CH_3), 2.07 (m, 6H, 3xCH_2), 1.94 (m, 6H, 3xCH_2), 1.68 (m, 6H, 3xCH_2), 1.58 (m, 6H, 3xCH_2) ppm. Mass spectrum (Fast Atom Bombardment, positive ion, dithiothreitol/dithioerythritol matrix): *m/z* (relative intensity, %) Exact mass for $C_{58}H_{66}N_4O_2$: calcd 850.5186, (M^+ + H) 851.5264, obsd 851.5270.

5–{ 4′–[4‴–(2⁗,5⁗–Dihydroxyphenyl)–1″,1‴–bibicyclo[2.2.2]octyl]–phenyl}– 2,3,7,8,12,13,17,18 –octamethylporphyrin (57) A solution of *H_2P2DMB* **37** (~25 mg, 0.03 mmol) in dry CH_2Cl_2 was cooled to –78°C in an argon purged flask protected from light. Boron tribromide (3.5 mL, 1.0M in hexanes, 3.5 mmol, 120 eq) was slowly added to the porphyrin solution. The reaction was allowed to stir for 3 hours at –78°C, then warmed to room temperature and allowed to stir an additional 12 hours. The reaction was quenched by the addition of aqueous ammonia. The reaction was poured into $CHCl_3$, washed with water, dried over Na_2SO_4, filtered, and the solvent removed *in vacuo*. The product was purified by flash chromatography in 10% CH_3CN/CH_2Cl_2 (R_f= 0.31). The estimated solubility limit for this compound in $CHCl_3$ (ϵ_{404} = 170,000 estd) is 4x10^{-6}M. UV–Vis ($CHCl_3$): λ_{max} 298(sh), 404, 504, 538, 571, 624 nm.

5–{ 4′–[4‴–(2⁗,5⁗–Benzoquinonyl)–1″,1‴–bibicyclo[2.2.2]octyl]–phenyl}– 2,3,7,8,12,13,17,18 –octamethylporphyrin (58) A saturated solution of *H_2P2QH$_2$* **57** in 100 mL CH_2Cl_2 (~4x10^{-4} mmol) was oxidized with a large excess of PbO_2 (200 mg) on a hot plate over low heat for 30 min protected from light. The solution was filtered, concentrated *in vacuo*, and purified in 10% CH_3CN/CH_2Cl_2 (R_f= 0.75) by flash chromatography. UV–Vis (C_6H_6): λ_{max} 404, 502, 534, 574, 628 nm. (ϵ_{404} = 175,000 estd) ^{1}H NMR (500MHz, $CDCl_3$, TMS): δ 10.10 (s, 2H, 10,20–C*H*), 9.90 (s, 1H, 15–C*H*), 7.897, 7.880 ($\frac{1}{2}AA'BB'$ q, 2H, 2′,6′–C*H*,*J*=8.2Hz), 7.630, 7.615 ($\frac{1}{2}AA'BB'$ q, 2H, 3′,5′–C*H*,*J*=7.6Hz), 6.67 (s, 2H), 6.53 (s, 1H), 3.60 (s, 6H, 13,17–CH_3), 3.57 (s, 6H, 12,18–CH_3), 3.49 (s, 6H, 2,8–CH_3), 2.39 (s, 6H, 3,7–CH_3), 2.07 (m, 6H, 3xCH_2), 1.80 (m, 6H, 3xCH_2), 1.66

(m, 6H, 3xCH_2), 1.58 (m, 6H, 3xCH_2) ppm. Mass spectrum (Fast Atom Bombardment, positive ion, *m*-nitrobenzylalcohol matrix): *m/z* (relative intensity, %) Exact mass for $C_{56}H_{60}N_4O_2$ calcd 820.4716, (M^+ +H) 821.4794, obsd 821.4770.

[5–{ 4′–[4″–(2‴,5‴–Benzoquinonyl)]phenyl}– 2,3,7,8,12,13,17,18–octamethylporphyrinato]zinc(II) (1) A solution of H_2P0QH_2 **53** in 50 mL CH_2Cl_2(~2x10^{-3} mmol) was metallated under standard conditions by the addition of 2 mL of anhydrous methanol saturated with zinc acetate. The solution was allowed to stir for 20–30 min. The mixture was then poured into water and the organic layer was separated and dried over Na_2SO_4. Lead dioxide (~100 mg) was added to the filtered solution and the slurry was stirred for 15 min on a hot plate over low heat. The solution was again filtered and concentrated *in vacuo*, and the product was purified by flash chromatography in CH_2Cl_2 (R_f= 0.42). UV–Vis ($CHCl_3$): λ_{max} 240 (ϵ 40,000 estd), 340(sh) (25,000 estd), 406.5 (375,000 estd), 536 (20,000 estd), 571 (17,000 estd) nm. ^{1}H NMR (400MHz, CD_2Cl_2, TMS): δ 10.17 (s, 2H, 10,20–C*H*), 10.04 (s, 1H, 15–C*H*), 8.17, 8.15, ($\frac{1}{2}AA'BB'$ q, 2H, 2′,6′–C*H*,*J*=7.9Hz), 7.94, 7.92, ($\frac{1}{2}AA'BB'$ q, 2H, 3′,5′–C*H*,*J*=8.2Hz), 7.252 (d, 1H, 6‴–C*H*, *J*=2.4Hz), 7.031 (d, 1H, 3‴–C*H*, *J*=10.1Hz), 6.958 (dd, 1H, 4‴–C*H*, *J*=10.1, 2.1 Hz), 3.63 (s, 6H, 13,17–CH_3), 3.62 (s, 6H, 12,18–CH_3), 3.55 (s, 6H, 2,8–CH_3), 2.50 (s, 6H, 3,7–CH_3) ppm. Mass spectrum (Fast Atom Bombardment, positive ion, dithiothreitol/dithioerythritol matrix): *m/z* (relative intensity, %) Exact mass for $C_{40}H_{35}N_4O_2Zn$: calcd 666.1973, (M^++H) 667.2051, obsd 667.2051.

[5–{ 4′–[4″–(4‴–Bromo–2‴,5‴–benzoquinonyl)bicyclo[2.2.2]oct–yl]phenyl}– 2, 3, 7, 8, 12, 13, 17, 18 –octamethylporphyrinato]zinc(II) (41)

A solution of free–base *H_2P1DMB(Br)* **54** (2.4 mg, 2.9x10^{-3} mmol) in 4 mL dry CH_2Cl_2 was cooled to 0°C in an argon purged flask protected from light. Boron triiodide (90 mg) was weighed into a dry flask under argon, and dissolved in 200 μL of dry CH_2Cl_2. A portion of the BI_3 solution (130 μL, 150 mmol, 50 eq) was added all at once to the porphyrin solution. The reaction was allowed to stir for 10 min at 0°C. The reaction was then quenched by the addition of aqueous ammonia, and was poured into $CHCl_3$. The organics were washed with water, dried over Na_2SO_4, filtered, and the solvent was removed *in vacuo*. The reaction yielded three products by TLC, (4% CH_3CN/CH_2Cl_2, long λ UV detection) R_f= 0.56, 0.30, and 0.15. The fastest and slowest components were found to be the quinone and hydroquinone products, respectively. The mixture was purified by flash chromatography in 4% CH_3CN/CH_2Cl_2 (v/v). The fastest and slowest moving components were combined, and the middle component was isolated. NMR analysis confirmed this material was the monodeprotected product which was retained for future deprotection. A solution of the *porphyrin hydroquinone* (*ca.* 2 mg) in CH_2Cl_2 (20 mL) was metallated by adding 1–2 mL of anhydrous methanol saturated with zinc acetate. This solution was allowed to stir for 20–30 min protected from light. The mixture was then poured into water and the organic layer was separated and dried over Na_2SO_4 and filtered. Lead dioxide (~100 mg) was added and the solution was allowed to stir for 15 min on a hot plate over low heat. The solution was again filtered and concentrated *in vacuo*, and the product was

purified by flash chromatography in CH_2Cl_2 (R_f= 0.75). UV–Vis ($CHCl_3$): λ_{max} 267 (ϵ 20,000 estd), 340(sh) (22,000 estd), 406 (375,000 estd), 536 (18,000 estd), 572 (16,000 estd) nm. ^{1}H NMR (400MHz, CD_2Cl_2, TMS): δ 10.16 (s, 2H, 10,20–C*H*), 10.04 (s, 1H, 15–C*H*), 7.96, 7.94, ($\frac{1}{2}AA'BB'$ q, 2H, 2′,6′–C*H*,*J*=8.2Hz), 7.73, 7.71, ($\frac{1}{2}AA'BB'$ q, 2H, 3′,5′–C*H*,*J*=8.2Hz), 7.26 (s, 1H, 3‴ or 6‴–C*H*), 6.85 (s, 1H, 3‴ or 6‴–C*H*), 3.63 (s, 6H, 13,17–CH_3), 3.62 (s, 6H, 12,18–CH_3), 3.53 (s, 6H, 2,8–CH_3), 2.44 (s, 6H, 3,7–CH_3), 2.26 (m, 6H, 3xCH_2), 2.14 (m, 6H, 3xCH_2) ppm. Mass spectrum (Fast Atom Bombardment, positive ion, *m*-nitrobenzylalcohol matrix): *m/z* (relative intensity, %) Exact mass for $C_{48}H_{45}N_4O_2{}^{79}BrZn$: calcd 852.2017, ($M^+$ +2H) 854.2174, obsd 854.2151.

[5–{ 4′–[4″–(4‴–Chloro–2‴,5‴–benzoquinonyl)bicyclo[2.2.2]octyl]–phenyl}– 2,3,7,8,12,13,17,18 –octamethylporphyrinato]zinc(II) (42) A solution of *H_2P1QH_2Cl* **55** (*ca.* 2 mg) in CH_2Cl_2 (20 mL) was metallated by the standard procedure of adding 1–2 mL of anhydrous methanol saturated with zinc acetate. This solution was allowed to stir for 20–30 min protected from light. The mixture was then poured into water and the organic layer was separated and dried over Na_2SO_4 and filtered. Lead dioxide (~100 mg) was added and the solution was allowed to stir for 15 min on a hot plate over low heat. The solution was again filtered and concentrated *in vacuo*, and the product was purified by flash chromatography in CH_2Cl_2 (R_f= 0.67). NMR analysis indicated the material is a mixture of the 4‴– (~60%) and 3‴–chloro (~40%) isomers. UV–Vis ($CHCl_3$): λ_{max} 262 (ϵ 24,000 estd), 340(sh) (21,000 estd), 406.5 (375,000 estd), 536 (18,000

estd), 572 (16,000 estd) nm.

4‴–chloro isomer: ^{1}H NMR (400MHz, CD_2Cl_2, TMS): δ 10.15 (s, 2H, 10,20–C*H*), 10.02 (s, 1H, 15–C*H*), 7.96, 7.94, ($\frac{1}{2}AA'BB'$ q, 2H, 2′,6′–C*H*,J=8.2Hz), 7.73, 7.71, ($\frac{1}{2}AA'BB'$ q, 2H, 3′,5′–C*H*,J=8.2Hz), 6.98 (s, 1H, 3‴ or 6‴–C*H*), 6.80 (s, 1H, 3‴ or 6‴–C*H*), 3.62 (s, 12H, 12,13,17,18–CH_3), 3.53 (s, 6H, 2,8–CH_3), 2.44 (s, 6H 3,7–CH_3), 2.26 (m, 6H, 3xCH_2), 2.14 (m, 6H, 3xCH_2) ppm.

3‴–chloro isomer: ^{1}H NMR (400MHz, CD_2Cl_2, TMS): δ 10.15 (s, 2H, 10,20–C*H*), 10.02 (s, 1H, 15–C*H*), 7.96, 7.94, ($\frac{1}{2}AA'BB'$ q, 2H, 2′,6′–C*H*,J=8.2Hz), 7.73, 7.71, ($\frac{1}{2}AA'BB'$ q, 2H, 3′,5′–C*H*,J=8.2Hz), 6.80 (d obscured by para–chloro isomer, 1H, 4‴ or 6‴–C*H*), 6.69 (d, 1H, 4‴ or 6‴–C*H*, J=2.4Hz), 3.62 (s, 12H, 12,13,17,18–CH_3), 3.53 (s, 6H, 2,8–CH_3), 2.44 (s, 6H 3,7–CH_3), 2.26 (m, 6H, 3xCH_2), 2.14 (m, 6H, 3xCH_2) ppm.

Mass spectrum (Fast Atom Bombardment, positive ion, *o*-nitrophenyloctyl-ether matrix): *m/z* (relative intensity, %) Exact mass for $C_{48}H_{45}N_4O_2{}^{35}ClZn$: calcd 808.2523, obsd 808.2470.

[5–{ 4′–[4″–(3‴,4‴–Dichloro–2‴,5‴–benzoquinonyl)bicyclo[2.2.2]oct–yl]phenyl}– 2,3,7,8,12,13,17,18 –octamethylporphyrinato]zinc(II) (43)

A solution of *$H_2P1QH_2Cl_2$* **56** (*ca.* 2 mg) in CH_2Cl_2 (20 mL) was metallated by adding 1–2 mL of anhydrous methanol saturated with zinc acetate. This solution was allowed to stir for 20–30 min protected from light. The mixture was then poured into water and the organic layer was separated and dried over Na_2SO_4 and filtered. Lead dioxide (~100 mg) was added and the solution was to stirred

for 15 min on a hot plate over low heat. The solution was again filtered and concentrated *in vacuo*, and the product was purified by flash chromatography in CH_2Cl_2 (R_f= 0.76). UV–Vis ($CHCl_3$): λ_{max} 266 (ϵ 21,000 estd), 340(sh) (22,000 estd), 406.5 (375,000 estd), 536.5 (18,000 estd), 571.5 (16,000 estd) nm. ^{1}H NMR (400MHz, CD_2Cl_2, TMS): δ 10.17 (s, 2H, 10,20–C*H*), 10.06 (s, 1H, 15–C*H*), 7.966, 7.946, ($\frac{1}{2}AA'BB'$ q, 2H, 2′,6′–C*H*,*J*=7.9Hz), 7.734, 7.713, ($\frac{1}{2}AA'BB'$ q, 2H, 3′,5′–C*H*,*J*=8.2Hz), 6.86 (s, 1H, 6″–C*H*), 3.63 (s, 12H, 12,13,17,18–CH_3), 3.54 (s, 6H, 2,8–CH_3), 2.44 (s, 6H 3,7–CH_3), 2.28 (m, 6H, 3xCH_2), 2.15 (m, 6H, 3xCH_2) ppm. Mass spectrum (Fast Atom Bombardment, positive ion, *o*-nitrophenyloctylether matrix): *m/z* (relative intensity, %) Exact mass for $C_{48}H_{44}N_4O_2{}^{35}Cl_2Zn$: calcd 842.2133, obsd 842.2185.

[5–{ 4′–[4‴–(2⁗,5⁗–Benzoquinonyl)–1″,1‴–bibicyclo[2.2.2]octyl]–phenyl}– 2,3,7,8,12,13,17,18 –octamethylporphyrinato]zinc(II) (3) A solution of *H_2P2QH_2* **57** (*ca.* 2 mg) in CH_2Cl_2 (20 mL) was metallated by the addition of 1–2 mL of anhydrous methanol saturated with zinc acetate. This solution was stirred for 20–30 min protected from light. The mixture was then poured into water and the organic layer was separated, dried over Na_2SO_4, and filtered. Lead dioxide (~100 mg) was added and the solution was allowed to stir for 15 min on a hot plate over low heat. The solution was again filtered and concentrated *in vacuo*, and the product was purified by flash chromatography in CH_2Cl_2 (R_f= 0.57). UV–Vis ($CHCl_3$): λ_{max} 248 (ϵ 30,000 estd), 340(sh) (22,000 estd), 406 (375,000 estd), 536 (18,000 estd), 572 (16,000 estd) nm. UV–

Vis (CH_3CN): λ_{max} 242, 336, 408, 538, 574 nm. (ϵ_{408} = 380,000 estd) ^{1}H NMR (400MHz, CD_2Cl_2, TMS): δ 10.18 (s, 2H, 10,20–C*H*), 10.08 (s, 1H, 15–C*H*), 7.92, 7.90, ($\frac{1}{2}AA'BB'$ q, 2H, 2′,6′–C*H*, J=8.6Hz), 7.69, 7.67, ($\frac{1}{2}AA'BB'$ q, 2H, 3′,5′–C*H*, J=8.2Hz), 6.66 (s, 2H, 3′′′′,4′′′′–C*H*), 6.53 (s, 1H, 6′′′′–C*H*), 3.64 (s, 12H, 12,13,17,18–CH_3), 3.53 (s, 6H, 2,8–CH_3), 2.43 (s, 6H 3,7–CH_3), 2.12 (m, 6H, 3xCH_2), 1.85 (m, 6H, 3xCH_2), 1.68 (m, 6H, 3xCH_2), 1.51(sh) (m, 6H, 3xCH_2) ppm. Mass spectrum (Fast Atom Bombardment, positive ion, dithiothreitol/dithioerythritol matrix): *m/z* (relative intensity, %) Exact mass for $C_{56}H_{58}N_4O_2Zn$: calcd (M^+) 882.3851, (M^++H) 883.3929, obsd 883.3929.

Preparation of Platinum Porphyrins **59, 60, 61**

[5–(4′–t–Butylphenyl) –2, 3, 7, 8, 12, 13, 17, 18 –octamethylporphyrinato]platinum(II) (59) A CH_2Cl_2 solution of free–base *t–butylporphyrin*[145] was transferred to a 50 mL flask. The porphyrin concentration was determined (UV–Vis, ϵ_{404} = 175,000 estd, 2.04x10^{-2} mmol) and the solvent was removed *in vacuo*. Glacial acetic acid (10 mL), sodium acetate (170 mg), and K_2PtCl_4 (160 mg, 19 eq) were added and the mixture was heated to reflux under argon and protected from light. After 30 min, 6–7 mL of the acetic acid was distilled off under argon and the concentrated solution was allowed to reflux an additional 15 min. The reaction was allowed to cool for 1 hour. The mixture was then poured into water, and the aqueous layer was extracted with 3x25 mL $CHCl_3$. The combined organics were dried over Na_2SO_4, filtered, and the solvent was removed *in vacuo*. The material was purified by flash chromatography in 40% CH_2Cl_2/hexane (R_f= 0.54). After the

metallo derivative had been collected from the column, the column was flushed with 4% CH_3CN/CH_2Cl_2 to recover unreacted free–base porphyrin ($5.64x10^{-3}$ mmol, 27% of starting material). The purified metallo derivative was obtained in 61% yield ($9.03x10^{-3}$ mmol, ϵ_{384} = 282,000 estd) based on recovered starting material. The product was observed to be contaminated with another metallo derivative based on its emission spectrum. This impurity was removed by dissolving the platinum porphyrin in CH_2Cl_2 (~100 mL), treating with trifluoracetic acid (6 drops) and allowing the solution to stir for 30 min. The solution was neutralized with $NaHCO_3$, washed with water, dried over Na_2SO_4, filtered, concentrated *in vacuo* and repurified by flash chromatography in 40% CH_2Cl_2/hexane. UV–Vis (2–MTHF): λ_{max} 384 (ϵ 282,000 estd), 504 (15,000 estd), 538 (46,000 estd) nm. ^{1}H NMR (400MHz, $CDCl_3$, TMS): δ 9.95 (s, 2H, 10,20–C*H*), 9.90 (s, 1H, 15–C*H*), 7.899, 7.878, ($\frac{1}{2}AA'BB'$ q, 2H, 2′,6′–C*H*,*J*=8.4Hz), 7.721, 7.701, ($\frac{1}{2}AA'BB'$ q, 2H, 3′,5′–C*H*,*J*=8.1Hz), 3.52 (s, 6H, 13,17–CH_3), 3.51 (s, 6H, 12,18–CH_3), 3.41 (s, 6H, 2,8–CH_3), 2.37 (s, 6H 3,7–CH_3), 1.59 (s, 9H, 4′–[C(CH_3)$_3$]) ppm. Mass spectrum (Fast Atom Bombardment, positive ion, *o*-nitrophenyloctylether matrix): *m/z* (relative intensity, %) Exact mass for $C_{38}H_{40}N_4{}^{195}Pt$: calcd 747.2906, obsd 747.2922.

[5–{ 4′–[4‴–(2⁗,5⁗–Dimethoxyphenyl)–1″,1‴–bibicyclo[2.2.2]oct–yl]phenyl}–2,3,7,8,12,13,17,18–octamethylporphyrinato]platinum(II) (60) A $CHCl_3$ solution of free–base *H$_2$P2DMB* **37** was transferred to a 50 mL flask. The porphyrin concentration was determined (UV–Vis, ϵ_{404} = 175,000 estd,

$1.10x10^{-2}$ mmol) and the solvent was removed *in vacuo*. Glacial acetic acid (12 mL), sodium acetate (212 mg), and K_2PtCl_4 (127 mg, 28 eq) were added and the mixture was heated to reflux under argon and protected from light. After 1 hour, 7–8 mL of the acetic acid was distilled off under argon and the concentrated solution was allowed to reflux an additional 30 min. The reaction was allowed to cool for 1 hour. The acetic acid was removed *in vacuo*, and the residue was dissolved in $CHCl_3$ and washed with water. The aqueous layer was back extracted with 3x50 mL $CHCl_3$. The combined organics were dried over Na_2SO_4, filtered, and the solvent was removed *in vacuo*. The material was purified by flash chromatography in 10% hexane/CH_2Cl_2. After the metallo derivative had been collected from the column, the column was flushed with 4% CH_3CN/CH_2Cl_2 to recover unreacted free–base porphyrin ($3.2x10^{-3}$ mmol, 30% of starting material). The purified metallo derivative was obtained in 54% yield ($4.2x10^{-3}$ mmol, ϵ_{384} = 282,000 estd) based on recovered starting material. The product was observed to be contaminated with another metallo from emission spectroscopy. This impurity was removed by dissolving the platinum porphyrin in CH_2Cl_2 (~100 mL), treating with trifluoracetic acid (6 drops) and allowing the solution to stir for 30 minutes. The solution was neutralized with $NaHCO_3$, washed with water, dried over Na_2SO_4, filtered, concentrated *in vacuo* and repurified by flash chromatography in CH_2Cl_2. UV–Vis (2–MTHF): λ_{max} 287 (ϵ 20,000 estd), 383.5 (ϵ 282,000 estd), 504 (14,000 estd), 537 (44,000 estd) nm. ^{1}H NMR (400MHz, $CDCl_3$, TMS): δ 9.97 (s, 2H, 10,20–C*H*), 9.93 (s, 1H, 15–C*H*), 7.875, 7.854, ($\frac{1}{2}AA'BB'$ q, 2H, 2′,6′–C*H*,*J*=8.4Hz), 7.642, 7.621, ($\frac{1}{2}AA'BB'$ q, 2H, 3′,5′–C*H*,*J*=8.4Hz), 6.83 (d,

1H, J= 3.0 Hz), 6.81 (d, 1H, J= 9.1 Hz), 6.70 (dd, 1H, J= 8.9, 3.2 Hz), 3.82 (s, 6H, –OCH_3), 3.79 (s, 6H, –OCH_3), 3.54 (s, 6H, 12, 13, 17, 18–CH_3), 3.42 (s, 6H, 2,8–CH_3), 2.36 (s, 6H 3,7–CH_3), 2.10–2.06 (m, 6H, 3xCH_2), 1.97–1.94 (m, 6H, 3xCH_2), 1.70–1.67 (m, 6H, 3xCH_2), 1.63–1.60 (m, 6H, 3xCH_2) ppm.

[5–{ 4′–[4‴–(2⁗,5⁗–Benzoquinonyl)–1″,1‴–bibicyclo[2.2.2]octyl]phenyl}– 2,3,7,8,12,13,17,18 –octamethylporphyrinato]platinum(II) (61)

A $CHCl_3$ solution of free–base H_2P2QH_2 **57** was transferred to a 50 mL flask. The porphyrin concentration was determined (UV–Vis, ϵ_{404} = 175,000 estd, 1.5x10^{-3} mmol) and the solvent was removed *in vacuo*. Glacial acetic acid (6 mL) was added along with sodium acetate (59 mg), and K_2PtCl_4 (24.2 mg, 40 eq). The mixture was heated to reflux under argon and protected from light. After 1 hour, 3.5 mL of the acetic acid was distilled off under argon and the concentrated solution was allowed to reflux an additional 30 min. The reaction was allowed to cool for 1 hour. The acetic acid was removed *in vacuo*, and the residue was dissolved in $CHCl_3$ and washed with water. The aqueous layer was back extracted with 5x50 mL $CHCl_3$. The combined organics were dried over Na_2SO_4, filtered, and the solvent was removed *in vacuo*. The material was dissolved in ~150 mL $CHCl_3$ and treated with trifluoracetic acid (6 drops) and allowing the solution to stir under argon for 15 minutes. The solution was neutralized with $NaHCO_3$, washed with water, dried over Na_2SO_4, filtered, concentrated *in vacuo*, and purified by flash chromatography in $CHCl_3$ (R_f 0.56). Spectroscopic yield <5% (ϵ_{384} = 282,000 estd). A saturated solution of the quinone in $CHCl_3$ was determined to be

$\sim$8x10^{-6}M (ϵ_{384} 282,000 estd). UV–Vis ($CHCl_3$): λ_{max} 385, 422(sh), 506.5, 539 nm. ^{1}H NMR (400MHz, $CDCl_3/D_2O$ (9:1 v/v), TMS): δ 9.95 (s, 2H, 10,20–C*H*), 9.91 (s, 1H, 15–C*H*), 7.859, 7.837, ($\frac{1}{2}AA'BB'$ q, 2H, 2′,6′–C*H*, J=7.7Hz), 7.613, 7.592, ($\frac{1}{2}AA'BB'$ q, 2H, 3′,5′–C*H*, J=8.1Hz), 6.66 (s, $\sim$2H), 6.52 (s, 1H), 3.51 (s, 12H, 12, 13, 17, 18–CH_3), 3.39 (s, 6H, 2,8–CH_3), 2.33 (s, 6H, 3,7–CH_3), 2.05–2.02 (m, 6H, 3xCH_2), 1.84–1.80 (m, 6H, 3xCH_2), 1.70–1.67(sh) (m, 6H, 3xCH_2), 1.5 (obscured by water peak, 6H, 3xCH_2) ppm.

Electrochemical Measurements

Solvents and Chemicals. Acetonitrile was HPLC grade (Burdick & Jackson), and was distilled from CaH_2 immediately prior to use. Tetra–*n*–butyl ammonium perchlorate (TBAP, Alfa) was dried *in vacuo* at 75°C for 24 hours and stored in an inert atmosphere box.

2–Chloro–5–methyl–1,4–benzoquinone was prepared by the addition of HCl to methyl–*p*–benzoquinone (Aldrich). Methylbenzoquinone was purified by flash chromatography in dichloromethane prior to use. The quinone was then dissolved in tetrahydrofuran previously distilled from sodium/benzophenone ketyl, and HCl was bubbled through the solution until the yellow color of the quinone had disappeared. The resulting 2–chloro–5–methyl–*p*–hydroquinone was oxidized in CH_2Cl_2 (PbO_2) with gentle warming. The quinone was purified on Grade III alumina with 5% CH_3CN/CH_2Cl_2 as the elutant. ^1H NMR (400MHz) of the isolated product confirmed the absence of coupling between the two remaining ring protons, indicating the chlorine was exclusively incorporated *para* to the methyl group. Repeating this procedure on the 2–chloro–5–methyl–*p*–benzoquinone derivative resulted in the isolation of 2,3–dichloro–6–methyl–1,4–benzoquinone. The analogous procedure was used in the preparation of 2–Bromo–5–methyl–*p*–benzoquinone by substituting HBr for HCl. Preparation of the dimethyl–, trimethyl–, and cyano–methyl–substituted quinone model compounds are described elsewhere.[145]

Sample Preparation. The quinones were diluted to $\sim 10^{-2}$ M in acetonitrile and added to a stoppered flask containing an appropriate amount of TBAP, previously weighed out under an inert atmosphere to minimize the absorption of water

by the hygroscopic salts. The supporting electrolyte was present at ~0.1 M concentration. The quinone solutions were transferred to the electrochemical cell and purged with argon for 10–15 min prior to the electrochemical measurements.

Equipment. A complete description of the electrochemical equipment and a discussion of the electrode construction can be found elsewhere.[145]

Steady–State Fluorescence Emission Spectroscopy

Solvents and Chemicals. The porphyrins were purified by chromatography prior to the measurements. Butyronitrile was obtained from Aldrich. Benzene was HPLC grade and was obtained from Burdick & Jackson. Benzene was distilled from CaH_2 prior to use. Butyronitrile was distilled from $KMnO_4/K_2CO_3$, then dried by an additional distillation from phosphorous pentoxide.

Sample preparation. Solutions of the reference porphyrin and the porphyrin–quinones were matched in concentration by dissolving each to the approximate concentration of 10^{-5}–10^{-6} M and adding solvent to the more concentrated solution until the absorbance at the Soret band (~400 nm) were the same (±10%). The measurements were made under aerobic conditions in 1 cm square matched fluorescence cells with teflon caps. Absorption spectra taken before and after the measurements were made to confirm the absence of photochemical degradation.

Equipment. The fluorescence emission spectra were recorded on a custom built apparatus of H.B. Gray's group. The excitation source was a 200 W Hg/Xe lamp. The excitation wavelength was selected with a Spex Minimate monochromator with interchangable fixed slits. The excitation light was modulated by a

beam chopper, further selected by an interference filter, and then focused onto the sample. Sample emission was collected at right angles to the excitation, filtered, collimated, and focused onto the adjustable slits of a Spex monochromator equipped with a motorized wavelength scan drive. The emission was detected with a Hamamatsu R955 photomultiplier tube. The PMT signal was amplified and passed to a Princeton Applied Research (PAR) 186A lock–in amplifier in phase with the beam chopper. The spectra obtained were uncorrected for detector response.

Time–Resolved Emission Studies

Solvents and Chemicals. All sample cells, pipets, syringes, and the Millipore syringe filtration apparatus were copiously rinsed with dry HPLC grade CH_2Cl_2 and were oven dried overnight, or stored in a dessicator. 2–Methyltetrahydrofuran and butyronitrile were obtained from Aldrich. All other solvents used were HPLC grade or better and were obtained from routine commercial sources. *o*–Xylene, toluene, benzene, and acetonitrile, were distilled from CaH_2 prior to use. MTHF was distilled once from CaH_2, and then was either distilled or vacuum transferred from sodium/benzophenone ketyl. *p*–Dioxane was distilled from sodium/benzophenone ketyl. *N,N*–dimethylformamide was distilled from activated Linde 4Å molecular sieves under reduced pressure. Pyridine was distilled from TsCl, and then from CaH_2 and stored over sieves under argon. Butyronitrile was distilled from $KMnO_4/K_2CO_3$.

Sample Preparation. Porphyrin–quinone samples were oxidized (PbO_2) and

flash chromatographed just prior to the picosecond experiments. Purity was assessed by NMR analysis. The samples were prepared to a concentration of 10^{-5}–10^{-7} M in the purified solvents and were Millipore filtered (FH 0.5 μm) into the sample cells. This filtration is paramount for the removal of small particulates which can result in significant laser excitation scatter. The sample cells were configured with 1 cm square fused quartz cells (NSG Cells, type 163) equipped with a side arm bulb to allow sample degassing, Teflon stopcock, and a 24/40 glass joint for connection to the vacuum line. Low–temperature samples were treated in a similar fashion except that the sample cell was a cylindrical quartz tube (Wilmad Glass Co., #701–PQ) equipped with a 14/35 glass joint. Temperature regulation in the 77K measurements was accomplished via immersion of the sample in a silvered, evacuated finger dewar using liquid nitrogen cryogen. Fluorescence samples were degassed by 3–4 freeze–thaw degassing at $\leq 10^{-4}$ torr on a high vacuum line. Phosphorescence samples were degassed by bubbling ultra–high purity argon (Matheson) through the solutions for 20–30 min. UV–Visible spectra were taken before and after the emission studies to confirm the absence of photochemical degradation.

Picosecond Time–Resolved Emission Apparatus

Equipment. The method of time–correlated single photon counting (TSPC)[207] was employed for the measurement of the time–resolved flourescence decays. The method depends on the assumption that individually timing single photon emissions from an ensemble of molecules, and subsequently producing a histogram of

events *vs.* time, results in a faithful reproduction of the fluorescence decay of an "average" molecule in the ensemble. Most of the experimental analyses were conducted by P.M. Felker in the laboratories of A.H. Zewail on an apparatus primarily used to investigate emission in molecular beams. The full details of the apparatus are available elsewhere,[166, 167] and are briefly described herein.

A schematic of the apparatus is shown in Figure 1.[167] The excitation souce is a synchronously pumped, mode–locked, cavity dumped dye laser (Spectra–Physics, Rhodamine 6G dye) tuned to 570 nm. The laser pulses were typically ~15 psec FWHM with an average power of ~20 mW. The excitation pulse is divided, one part furnishes an electrical pulse via a fast photodiode (PD, Hewlett–Packard 5082–4203) which is modified by pulse shaping electronics (PSE), and subsequently starts a timing clock (time–to–amplitude converter, TAC, Ortec 457), and the other portion of the beam is directed at the emissive sample (S). Various optics collect and collimate a portion of the sample emission at a right angle to the excitation pulse. The emission is filtered to limit scatter from the excitation pulse, passed through a monochrometer (0.5M Jarrel–Ashe) and is focused onto a fast photomultiplier tube (PMT, Hammamatsu R2270U, or R1564U). The pulses from the photomultiplier were amplified and sent to a constant fraction discriminator (Ortec 473A, or Tennelec 455) which then provided a stop pulse to the TAC. The time on the clock is then analyzed by the multi–channel analyzer (MCA, Tracor–Northern TN–1706) and the event is stored in a memory slot designating the particular clock time. A typical system response function was ~80 psec FWHM.

The start and stop pulses are constantly screened to discard extraneous events

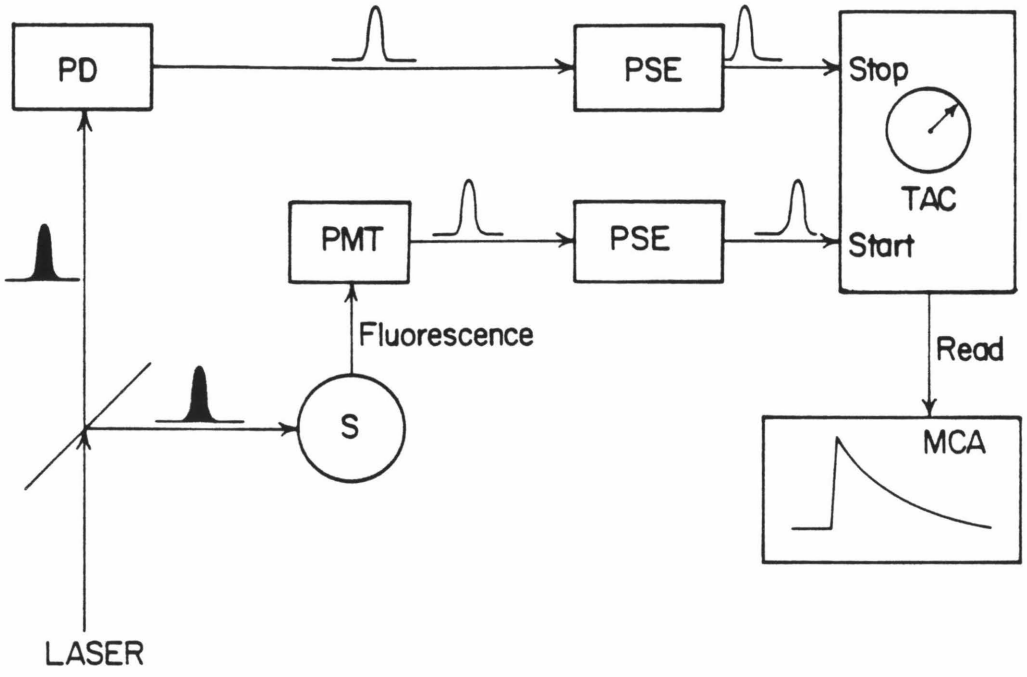

Figure 1. Schematic of picosecond emission apparatus.

such as stop pulses without matching start pulses, and the absence of a stop pulse within a given time period of the start pulse. To limit complications from two or more photons reaching the photocathode an appreciable fraction of the time that single photon events are recorded, the photon counting rate was adjusted to be less than one percent of the excitation source repetition rate (4MHz) via placement of neutral density filters in the excitation beam path. The system apparatus used in these studies was actually run in the reverse sense in which a sample photon provides the start pulse to the TAC, and the delayed pulse from the PD provides the stop pulse. This reversed configuration was employed to enhance the overall detection efficiency of the apparatus.[167]

The observed fluorescence decays $F(t)$ are a convolution of the system response function $R(t)$ and the true decay $I(t)$:[208]

$$F(t) = \int_0^t R(t')I(t-t')dt' \qquad [7.1]$$

The system response function is the decay that would be observed if the true molecular decay were a δ–function in time, and was routinely obtained by measurement of the scattered excitation pulse from a collodial solution placed in the identical configuration and similar counting rate as the sample being analyzed (*i.e.*, response functions for low temperature data were obtained by filling a quartz tube with the colloidal solution and placing it in the finger dewar used for temperature regulation).

The fluorescence decay obtained in these experiments consisted of a 1×N dimensional array of integers, the index of the array representing the clock times,

and the values of the array representing the number of start–stop events recorded for each clock time. The signal to noise in a particular decay is assumed to follow Poisson statistics[165] where the standard deviation of $N(t_i)$ is given by $\sqrt{N(t_i)}$.

The analysis of the measured decay is achieved through an algorithm to the assumed molecular decay function with adjustable parameters using a non–linear least squares fitting algorithm[165] This a procedure uses the sum of the squares of the weighted residuals given by

$$\chi^2 = \sum_i \frac{(N(t_i) - F(t_i))^2}{W(t_i)} \qquad [7.2]$$

where $N(t_i)$ is the number of counts in the ith channel, $F(t_i)$ is the number of counts calculated to be in the ith channel using an assumed decay function, and $W(t_i)$ is the weight for a given data point and in the limit of Poisson statistics is given by $N(t_i)$. The χ^2 value is minimized by the adjustment of parameters used in the calculation of $F(t_i)$, and the goodness of fit was judged by the final value of χ^2.

The picosecond data in this thesis and elsewhere[145] is based on a program for least–squares fitting of emission decays generously supplied by P.M. Felker and S. Baskin, and was modified for use on a Compaq personal computer used for the data analysis. The complete listing of the program source code is available in Appendix A.

Nanosecond Time–Resolved Emission Apparatus

Equipment. Phosphorescence emission decays were conducted by A.W. Axup in the laboratories of H.B. Gray. The apparatus consisted of a Quanta Ray (DCR–1) Nd:YAG laser output to a Quanta Ray HG–1 harmonic generator. The frequency–doubled pulse was filtered through a Quanta Ray PHS–1 prism harmonic separator. The resulting excitation beam was an 8 nsec FWHM 532 nm light pulse of ~50 mJ at the repetition rate of 2 Hz used in these studies. Sample emission was filtered and detected at right angles to the excitation pulse, passed through a monochromator (McPherson, model 270), and detected by the photomultiplier tube (Hamamatsu, R955) The signal was amplified and passed to a waveform recorder (Biomation, model 6500). The recorder was triggered by output from the laser. Laser triggering, recorder arming, and preliminary data analysis were performed by an external computer (PDP11/03–L). Lifetimes were obtained by analysis of the emission decays using a Gray group program written for an IBM–AT.

References

[1] R.R. Alfano, ed., "Biological Events Probed by Ultrafast Laser Spectroscopy," Academic Press, New York, 1982.

[2] C.H. Foyer, "Photosynthesis," John Wiley & Sons, New York, 1984.

[3] R. Hill, and F. Bendall, *Nature (London)*, **186**, 136 (1960).

[4] Govindjee, *Plant Biochem., J.S.M. Sircar Meml. Vol.*, 7 (1980).

[5] B. Kok, *Biochim. Biophys. Acta.*, **22**, 399 (1956).

[6] D. Wong, in reference 1, Chapter 1.

[7] W. Junge, and H.T. Witt, *Z. Naturforsch.*, **23b**, 244 (1968).

[8] P. Mitchell, "Chemiosmotic Coupling in Oxidative and Photosynthetic Phosphorylation," Glynn Research, Bodmin, Cornwall, England, 1966.

[9] D.G. Nicholls, "Bioenergetics: An Introduction to Chemiosmotic Theory," Academic Press, New York, 1982.

[10] A.W. Frenkel, *J. Amer. Chem. Soc.*, **76**, 5568 (1954).

[11] D.I. Arnon, M.B. Allen, and F.K. Whatley, *Nature (London)*, **174**, 394 (1954).

[12] R. Hill, in "Comprehensive Biochemistry," M. Florkin, and G.H. Stotz, eds., Vol. 9, Elsevier, London, pp. 73–97, 1963.

[13] K. Sauer, in "Photosynthesis," G. Akoyunoglu, ed., Vol. III, Structure and Molecular Organization of the Photosynthetic Membrane, Balaban International Science Services, Philadelphia, p. 685–700, 1981.

[14] G. Britton, in "Chemistry and Biochemistry of Plant Pigments," T.W. Goodwin, ed., Academic Press, New York, pp. 262–327, 1976.

[15] H.T. Witt, *Biochim. Biophys. Acta*, **505**, 355 (1979).

[16] L. Bogorad, *Ann. Rev. Plant Physiol.*, **26**, 369 (1975).

[17] K.D. Philipson, V.L. Sato, and K. Sauer, *Biochemistry*, **11**, 4591 (1972).

[18] A.J. Bearden, and R. Malkin, *Q. Rev. Biophys.*, **7**, 131 (1975).

[19] J.J. Katz, J.R. Norris, L.L. Shipman, M.C. Thurnauer, and M.R. Wasielewski, *Annu. Rev. Biophys. Bioenerg.*, **7**, 393 (1978).

[20] M.R. Wasielewski, J.R. Norris, L.L. Shipman, C.P Lin, and W.A. Svec, *Proc. Natl. Acad. Sci. U.S.A.*, **78**, 2957 (1981).

[21] T.L. Netzel, in reference 1, Chapter 4.

[22] G. Feher, and M.Y. Okamura, *Brookhaven Symp. Biol.*, **28**, 183 (1976).

[23] P.L. Dutton, R.C. Price, D.M. Tiede, K.M. Petty, K.J. Kaufmann, T.L. Netzel, and P.M. Rentzepis, *Brookhaven Symp. Biol.*, **28**, 213 (1976).

[24] J.R. Norris, R.A. Uphaus, H.L. Crespi, and J.J. Katz, *Proc. Natl. Acad. Sci. U.S.A.*, **68**, 625 (1971).

[25] J.D. McElroy, G. Feher, and D.C. Mauzerall, *Biochim. Biophys. Acta.*, **267**, 363 (1972).

[26] R.J. Debus, G. Feher, and M.Y. Okamura, *Biochemistry*, **25**, 2276 (1986).

[27] C. Kirmaier, D. Holton, R.J. Debus, G. Feher, and M.Y. Okamura, *Proc. Natl. Acad. Sci., USA*, **83**, 6407 (1986).

[28] D. Holton, M.W. Windsor, W.W. Parson, and J.P. Thornber, *Biochim. Biophys. Acta*, **501**, 112 (1978).

[29] D. DeVault, and B. Chance, *Biophys. J.*, **6**, 825 (1966).

[30] D. DeVault, "Quantum–Mechanical Tunneling in Biological Systems," 2nd ed., Cambridge University Press, New York, 1984 and references therein.

[31] P.L. Dutton, K.J. Kaufmann, B. Chance, and P.M. Rentzepis, *FEBS Letters*, **60**, 275 (1975).

[32] K.J. Kaufmann, K.M. Petty, P.L. Dutton, and P.M. Rentzepis, *Biophys. Res. Commun.*, **70**, 839 (1976).

[33] R.K. Clayton, and H.F. Yau, *Biophys. J.*, **12**, 867 (1972).

[34] P.A. Loach, M.C. Kung, and B.J. Hales, *Ann. N.Y. Acad. Sci.*, **244**, 297 (1975).

[35] B.J. Hales, *Biophys. J.*, **16**, 471 (1976).

[36] D. DeVault, *Q. Rev. Biophys.*, **13**, 4 (1980).

[37] J.D. McElroy, G. Feher, and D.C. Mauzerall, *Biophys. J.*, **10**, 204a (1970).

[38] P.L. Dutton, J.S. Leigh, and M. Seibert, *Biochim. Biophys. Res. Commun.*, **46**, 406 (1972).

[39] W.W. Parsons, R.K. Clayton, and R.J. Cogdell, *Biochim. Biophys. Acta.*, **387**, 265 (1975).

[40] K.J. Kaufmann, P.L. Dutton, T.L. Netzel, J.S. Leigh, and P.M. Rentzepis, *Science*, **188**, 1301 (1975).

[41] P.L. Dutton, K.J. Kaufmann, B. Chance, and P.M. Rentzepis, *FEBS Lett.*, **60**, 275 (1975).

[42] T.L. Netzel, P.L. Dutton, K.M. Petty, E.O. Degenkolb, and P.M. Rentzepis, *Adv. Mol. Relaxation Interact. Processes*, **11**, 217 (1977).

[43] T.L. Netzel, P.M. Rentzepis, and J.S. Leigh, *Science*, **182**, 238 (1973).

[44] M.G. Rockley, M.W. Windsor, R.J. Cogdell, and W.W. Parson, *Proc. Natl. Acad. Sci. U.S.A.*, **72**, 2251 (1975).

[45] J. Fajer, D.C. Brune, M.S. Davis, A. Forman, and L.D. Spaulding, *Proc. Natl. Acad. Sci. U.S.A.*, **72**, 4956 (1975).

[46] C. Kirmaier, D. Holten, and W.W. Parson, *FEBS Lett.*, **185**, 76 (1985).

[47] C. Kirmaier, D. Holten, and W.W. Parson, *Biochim. Biophys. Acta*, **810**, 33 (1985).

[48] C. Kirmaier, D. Holten, and W.W. Parson, *Biochim. Biophys. Acta*, **810**, 49 (1985).

[49] J. Deisenhofer, O. Epp, K. Miki, R. Huber, and H. Michel, *J. Mol. Biol.*, **180**, 385 (1984).

[50] J. Deisenhofer, O. Epp, K. Miki, R. Huber, and H. Michel, *Nature (London)*, **318**, 618 (1985).

[51] W. Zinth, W. Kaiser, and H. Michel, *Biochim. Biophys. Acta*, **723**, 128 (1983).

[52] P. Gast, M.R. Wasielewski, M. Schiffer, and J.R. Norris, *Nature (London)*, **305**, 451 (1983).

[53] G.C. Dismukes, H.A. Frank, R. Friesner, and K. Sauer, *Biochim. Biophys. Acta*, **764**, 253 (1984).

[54] J.P. Allen, G. Feher, T.O. Yeates, D.C. Rees, J. Deisenhofer, H. Michel, and R. Huber, *Proc. Natl. Acad. Sci.*, 1986 *in press.*

[55] C.W. Wraight, and R.K. Clayton, *Biochim. Biophys. Acta*, **333**, 246 (1973).

[56] J.J. Hopfield, *Proc. Natl. Acad. Sci. U.S.A.*, **71**, 3640 (1974).

[57] J. Jortner, *J. Chem. Phys.*, **64**, 4860 (1976).

[58] J. Jortner, *J. Amer. Chem. Soc.*, **102**, 6676 (1980).

[59] M. Bixon, and J. Jortner, *J. Phys. Chem.*, **90**, 3795 (1986).

[60] J. Onuchic, D.N. Beratan, and J.J. Hopfield, *J. Phys. Chem.*, **90**, 3707 (1986).

[61] R.A. Marcus, and N. Sutin, *Biochim. Biophys. Acta*, **811**, 265 (1985).

[62] R.A. Marcus, *J. Chem. Phys.*, **24**, 966 (1956).

[63] R.A. Marcus, *Disc. Faraday Soc.*, **29**, 21 (1960).

[64] R.A. Marcus, *J. Chem. Phys.*, **43**, 679 (1965).

[65] T. Förster, *Naturwissenschaften*, **33**, 166 (1946).

[66] D.L. Dexter, *J. Chem. Phys.*, **21**, 836 (1953).

[67] D. Rehm, and A. Weller, *Isr. J. Chem.*, **8**, 259 (1970).

[68] J.R. Miller, J.V. Beitz, and R.K. Huddleston, *J. Amer. Chem. Soc.*, **106**, 5057 (1984).

[69] J.R. Miller, and J.V. Beitz, *J. Chem. Phys.*, **74**, 6746 (1981).

[70] For example, see (a) N. Mataga, Y. Kanda, and T. Okada, *J. Phys. Chem.*, **90**, 3880 (1986). (b) R. Scheerer and M. Graetzel, *J. Amer. Chem. Soc.*, **99**, 865 (1977). (c) C.R. Brock, T.J. Meyer, and D.G. Whitten, *J. Amer. Chem. Soc.*, **97**, 2909 (1975).

[71] I. Tabushi, N. Koga, and M. Yanagita, *Tett. Lett.*, **3**, 257 (1979).

[72] N. Mataga, A. Karen, T. Okada, S. Nishitani, N. Kurata, Y. Sakata, and S. Misumi, *J. Phys. Chem.*, **88**, 5138 (1984).

[73] A.C. Chan, J. Dalton, and L.R. Milgrom, *J. Chem. Soc., Perkin Trans. II*, 707 (1982).

[74] S. Nishitani, N. Kurata, Y. Sakata, S. Misumi A. Karen, N. Mataga, and T. Okada, *J. Amer. Chem. Soc.*, **105**, 7772 (1983).

[75] M. Migita, T. Okada, N. Mataga, S. Nishitani, N. Kurata, Y. Sakata, and S. Misumi, *Chem. Phys. Lett.*, **84**, 263 (1981).

[76] A.R. McIntosh, A. Siemiarczuk, J.R. Bolton, M. Stillman, T. –F. Ho, and A.C. Weedon, *J. Amer. Chem. Soc.*, **105**, 7215 (1983).

[77] A. Siemiarczuk, A.R. McIntosh, T. –F. Ho, M. Stillman, K.J. Roach, A.C. Weedon, J.R. Bolton, and J.S. Connolly, *J. Amer. Chem. Soc.*, **105**, 7224 (1983).

[78] T. –F. Ho, A.R. McIntosh, and J.R. Bolton, *Nature (London)*, **286**, 254 (1980).

[79] J.L.Y. Kong, K.G. Spears, and P.A. Loach, *Photochem. Photobiol.*, **35**, 545 (1982).

[80] M.A. Bergkamp, J. Dalton, and T.L. Netzel, *J. Amer. Chem. Soc.*, **104**, 253 (1982).

[81] T.L. Netzel, M.A. Bergkamp, C.–K. Chang, and J. Dalton, *J. Photochem.*, **17**, 451 (1981).

[82] A. Harriman, and R.J. Hosie, *J. Photochem.*, **15**, 163 (1981).

[83] J. Dalton, and L.R. Milgrom, *J.C.S. Chem. Comm.*, 609 (1979).

[84] A. Harriman, *Inorg. Chim. Acta*, **88**, 213 (1984).

[85] J.A. Schmidt, A. Siemiarczuk, A.C. Weedon, and J.R. Bolton, *J. Amer. Chem. Soc.*, **107**, 6112 (1985).

[86] J. Weiser, and H.A. Staab, *Tett. Lett.*, **26**, 6059 (1985).

[87] J.S. Lindsey, and D.C. Mauzerall, *J. Amer. Chem. Soc.*, **104**, 4498 (1982).

[88] J.S. Lindsey, D.C. Mauzerall, and H. Linschitz, *J. Amer. Chem. Soc.*, **105**, 6528 (1983).

[89] K.N. Ganesh, J.K.M. Sanders, and J.C. Waterton, *J. Chem. Soc. Perkin Trans. I*, 1617 (1982).

[90] K.N. Ganesh, and J.K.M. Sanders, *J. Chem. Soc. Perkin Trans. I*, 1611 (1982).

[91] M.P. Irvine, R.J. Harrison, G.S. Beddard, P. Leighton, and J.K.M. Sanders, *Chemical Physics*, **104**, 315 (1986).

[92] K.N. Ganesh, *Proc. Indian Acad. Sci.*, **93**, 647 (1984).

[93] R.E. Overfield, A. Scherz, K.J. Kaufmann, and M.R. Wasielewski, *J. Amer. Chem. Soc.*, **105**, 4256 (1983).

[94] R.E. Overfield, A. Scherz, K.J. Kaufmann, and M.R. Wasielewski, *J. Amer. Chem. Soc.*, **105**, 5747 (1983).

[95] T.L. Netzel, M.A. Bergkamp, and C.K. Chang, *J. Amer. Chem. Soc.*, **104**, 1952 (1982).

[96] S.G. Boxer, R.R. Bucks, and C.E.D. Chidsey, *Biophys. J.*, **33**, 172a (1981).

[97] M.R. Wasielewski, W.A. Svec, and B.T. Cope, *J. Amer. Chem. Soc.*, **100**, 1961 (1978).

[98] S.G. Boxer, and G.L. Closs, *J. Amer. Chem. Soc.*, **98**, 5406 (1976).

[99] T.L. Netzel, P. Kroger, C.K. Chang, I. Fujita, and J. Fajer, *Chem. Phys. Lett.*, **67**, 223 (1979).

[100] R.R. Bucks, T.L. Netzel, I. Fujita, and S.G. Boxer, *J. Phys. Chem.*, **86**, 1947 (1982).

[101] M.J. Pellin, K.J. Kaufmann, and M.R. Wasielewski, *Nature (London)*, **278**, 54 (1979).

[102] N. Mataga, A. Karen, T. Okada, S. Nishitani, Y. Sakata, and S. Misumi, *J. Phys. Chem.*, **88**, 4650 (1984).

[103] Y. Sakata, S. Nishitani, S. Misumi, A.R. McIntosh, J.R. Bolton, Y. Kunda, A. Karen, T. Okada, and N. Mataga, *Tett. Lett.*, **26**, 5207 (1985).

[104] P. Pasman, G.F. Mes, N.W. Koper, and J.W. Verhoeven, *J. Amer. Chem. Soc.*, **107**, 5839 (1985).

[105] P. Pasman, N.W. Koper, and J.W. Verhoeven, *Recl. Trav. Chim. Pays-Bas*, **101**, 363 (1982).

[106] L. Onsager, *J. Amer. Chem. Soc.*, **58**, 1486 (1936).

[107] J.W. Verhoeven, *Pure Appl. Chem.*, **58**, 1285 (1986).

[108] J.M. Warman, M.P. de Haas, M.N. Padden–Row, E. Cotsaris, N.S. Hush, H. Oevering, and J.W. Verhoeven, *Nature (London)*, **320**, 615 (1986).

[109] N.S. Hush, M.N. Padden–Row, E. Cotsaris, H. Oevering, J.W. Verhoeven, and M. Heppener, *Chem. Phys. Lett.*, **117**, 8 (1985).

[110] M.R. Wasielewski, M.P. Niemczyk, W.A. Svec, and E.B. Pewitt, *J. Amer. Chem. Soc.*, **107**, 1080 (1985).

[111] M.R. Wasielewski, and M.P. Niemczyk, *J. Amer. Chem. Soc.*, **106**, 5043 (1984).

[112] S.J. Silvers, and A. Tulinsky, *J. Amer. Chem. Soc.*, **86**, 927 (1964).

[113] A. Weller, *Z. Phys. Chem. (Wiesbaden)*, **133**, 93 (1982).

[114] D.N. Beratan, *J. Amer. Chem. Soc.*, **108**, 4321 (1986).

[115] J.R. Miller, L.T. Calcaterra, and G.L. Closs, *J. Amer. Chem. Soc.*, **106**, 3047 (1984).

[116] L.T. Calcaterra, G.L. Closs, and J.R. Miller, *J. Amer. Chem. Soc.*, **105**, 670 (1983).

[117] A.D. Joran, B.A. Leland, G.G. Geller, J.J. Hopfield, and P.B. Dervan, *J. Amer. Chem. Soc.*, **106**, 6090 (1984).

[118] J.R. Bolton, T.–F. Ho, S. Liauw, A. Siemiarczuk, C.S.K. Wan, and A.C. Weedon, *J. Chem. Soc., Chem. Comm.*, 559 (1985).

[119] H. Heitele, and M.E. Michel–Beyerle, *J. Amer. Chem. Soc.*, **107**, 8286 (1985).

[120] C.A. Stein, N.A. Lewis, and G. Seitz, *J. Amer. Chem. Soc.*, **104**, 2596 (1982).

[121] S.S. Isied, and A. Vassilian, *J. Amer. Chem. Soc.*, **106**, 1732 (1984).

[122] S.E. Peterson–Kennedy, J.L. McGourty, and B.M. Hoffman, *J. Amer. Chem. Soc.*, **106**, 5010 (1984).

[123] J.L. McGourty, N.V. Blough, and B.M. Hoffman, *J. Amer. Chem. Soc.*, **105**, 4470 (1983).

[124] K.P. Simolo, G.L. McLendon, M.R. Mauk, and A.G. Mauk, *J. Amer. Chem. Soc.*, **106**, 5012 (1984).

[125] J.R. Winkler, D.G. Nocera, K.M. Yocom, E. Bordignon, and H.B. Gray, *J. Amer. Chem. Soc.*, **104**, 5798 (1982).

[126] D.G. Nocera, J.R. Winkler, K.M. Yocom, E. Bordignon, and H.B. Gray, *J. Amer. Chem. Soc.*, **106**, 5145 (1984).

[127] R.A. Holwerda, D.B. Knaff, and H.B. Gray, *J. Amer. Chem. Soc.*, **102**, 1142 (1980).

[128] A.G. Mauk, R.A. Scott, and H.B. Gray, *J. Amer. Chem. Soc.*, **102**, 4360 (1980).

[129] N. Sailasuta, F.C. Anson, and H.B. Gray, *J. Amer. Chem. Soc.*, **101**, 455 (1979).

[130] S.A. Schichman, and H.B. Gray, *J. Amer. Chem. Soc.*, **103**, 7794 (1981).

[131] S.S. Isied, G. Worsila, and S.J. Atherton, *J. Amer. Chem. Soc.*, **104**, 7659 (1982).

[132] P.A. Liddel, D. Barrett, L.R. Makings, P.J. Pessiki, D. Gust, and T.A. Moore, *J. Amer. Chem. Soc.*, **108**, 5350 (1986).

[133] M.R. Wasielewski, M.P. Niemczyk, W.A. Svec, and E.B. Pewitt, *J. Amer. Chem. Soc.*, **107**, 5562 (1985).

[134] T.A. Moore, D. Gust, P. Mathis, J.C. Mialocq, C. Chachaty, R.V. Bensasson, E.J. Land, D. Doizi, P.A. Liddel, W.R. Lehman, G.A. Nemeth, and A.L. Moore, *Nature (London)*, **307**, 630 (1984).

[135] R.V. Bensasson, T.A. Moore, D. Gust, A.L. Moore A. Joy, T. Tom, G.A. Nemeth, and E.J. Land, in "Porphyrin Tumor Phototherapy," A. Andreoni, and R. Cubedda, eds., Plenum Press, New York, 1984.

[136] P. Mathis, W.L. Butler, and K. Sato, *Photochem. Photobiol.*, **30**, 603 (1979).

[137] R.V. Bensasson, E.J. Land, A.L. Moore, R.L. Crouch, G. Dirks, T.A. Moore, and D. Gust, *Nature (London)*, **290**, 329 (1981).

[138] P. Seta, E. Bienvenue, A.L. Moore, P. Mathis, R.V. Bensasson, P. Liddel, P.J. Pessiki, A. Joy, T.A. Moore, and D. Gust, *Nature (London)*, **316**, 653 (1985).

[139] D. Dolphin ed., "The Porphyrins," Vol. I, Part A, Academic Press, New York, 1978.

[140] For example, see (a) L.O. Spreer, A.C. Maliyackel, S. Holbrook, J.W. Otvos, and M. Calvin, *J. Amer. Chem. Soc.*, **108**, 1949 (1986). (b) J.P. Collman, C.E. Barnes, P.J. Brothers, T.J. Collins, T. Ozawa, J.C. Gallucci, and J.A. Ibers, *J. Amer. Chem. Soc.*, **106**, 5151 (1984).

[141] K.M. Smith, "Porphyrins and Metalloporphyrins," Elsevier Publishing Co., New York, 1975.

[142] H.E. Zimmerman, and R.D. McKelvey, *J. Amer. Chem. Soc.*, **93**, 3638 (1971).

[143] H.E. Zimmerman, T.E. Goldman, T.K. Hirzel, and S.P. Schmidt, *J. Org. Chem.*, **45**, 3933 (1980).

[144] R.A. Beecroft, R.S. Davidson, D. Goodwin, and J.E. Pratt, *Pure Appl. Chem.*, **54**, 1605 (1982).

[145] Full characterization and synthetic details can be found in: A.D. Joran, *Dissertation*, California Institute of Technology, 1986.

[146] J.W. Buchler, K.L. Lay, Y.J. Lee, and W.R. Scheidt, *Angew. Chem. Int. Ed. Engl.*, **21**, 432 (1982).

[147] A.D. Joran, B.A. Leland, G.G. Geller, J.J. Hopfield, and P.B. Dervan, *J. Amer. Chem. Soc.*, **106**, 6090 (1984).

[148] G.L. Closs, personal communication.

[149] D. Harris, A.W. Johnson, and R. Gaete–Holms, *Bioorganic Chem.*, **9**, 63 (1980).

[150] J.–H. Fuhrhop, *Struct. Bonding Berlin*, **18**, 1 (1974).

[151] R.S. Brown, *Can. J. Chem.*, **54**, 805 (1976).

[152] R.A. Snow, C.R. Degenhardt, and L.A. Paquette, *Tett. Lett.*, 4447 (1976).

[153] R.B. Jones and R. Grayshan, *Can. J. Chem.*, **50**, 1414 (1972).

[154] For example, see (a) M. Kumada, *Pure Appl. Chem.*, **52**, 669 (1980). (b) K. Tamao, K. Sumitani, Y. Kiso, M. Zembayashi, A. Fujioka, S. Kodama, I. Nakajima, A. Minato, and M. Kumada, *Bull. Chem. Soc. Jpn.*, **49**, 1958 (1976). (c) T. Hayashi, M. Konishi, K. Yokata, and M. Kumada, *Chem. Lett.*, 767 (1980). (d) K. Tamao, A. Minato, N. Miyake, T. Matsuda, Y. Kiso, and M. Kumada, *Chem. Lett.*, 133 (1975). (e) G. Whitesides, W.F. Fischer, J. San Filippo, R.W. Bashe, and H.O. House, *J. Amer. Chem. Soc.*, **91**, 4871 (1969).

[155] J.B. Paine III, R.B. Woodward, and D. Dolphin, *J. Org. Chem.*, **41**, 2826 (1976).

[156] W.C. Still, M. Kahn, and A. Mitra, *J. Org. Chem.*, **43**, 2923 (1978).

[157] J.M. Lansinger, and R.C. Ronald, *Synth. Comm.*, **9**, 341 (1979).

[158] For example, see (a) M.L. Poutsma, *J. Amer. Chem. Soc.*, **87**, 2161 (1965). (b) M.L. Poutsma, *J. Amer. Chem. Soc.*, **87**, 2172 (1965). (c) F. Dewhurst, and P.K.J. Shah, *J. Chem. Soc., C.*, 1737 (1970). (d) M. Hojo, and R. Masuda, *Syn. Comm.*, **5**, 169 (1975).

[159] For example, see (a) A. Dargelos, J. Migliaccio and M. Chiallet, *Tetrahedron*, **27**, 5673 (1971). (b) J. Cason, R.E. Harman, S. Goodwin, and C. Allen, p. 860, 1950. (c) G. Höfle, *Tetrahedron*, **32**, 1431 (1976). (d) J. Cason, R.E. Harman, S. Goodwin, and C.F. Allen, *J. Org. Chem.*, **15**, 860 (1950). (e) J. Cason, C.F. Allen, and S. Goodwin, *J. Org. Chem.*, **13**, 403 (1948) and references therein.

[160] R.J. Abraham, A.H. Jackson, G.W. Kenner, and D. Warburton, *J. Chem. Soc.*, 853 (1963).

[161] L. Milgrom, *Polyhedron*, **4**, 1279 (1985).

[162] L. Milgrom, *Polyhedron*, **4**, 1661 (1985).

[163] N.J. Turro, "Modern Molecular Photochemistry," Benjamin/Cummings Publishing Co., Menlo Park, CA, 1978.

[164] A.H. Jackson, *Phil. Trans. R. Soc. London, Part A*, **21**, 293 (1979).

[165] P.R. Bevington, "Data Reduction and Error Analysis for the Physical Sciences," McGraw–Hill, New York, 1969.

[166] W.R. Lambert, P.M. Felker, and A.H. Zewail, *J. Chem. Phys.*, **81**, 2217 (1984).

[167] P.M. Felker, *Dissertation*, California Institute of Technology, 1985.

[168] A. Harriman, G. Porter, and A. Wilowska, *J. Chem. Soc., Faraday Trans. 2*, **79**, 807 (1983).

[169] A.T. Gradyushko, and M.P. Tsvirko, *Opt. Spec. R.*, **31**, 291 (1971).

[170] B.S. Brunschwig, S. Ehrenson, and N. Sutin, *J. Amer. Chem. Soc.*, **106**, 6858 (1984).

[171] H. Kuhn, *J. Photochem.*, **10**, 111 (1979).

[172] I.V. Alexandrov, R.F. Khairutdinov, and K.I. Zamaraev, *Chem. Phys.*, **32**, 123 (1978).

[173] D.N. Beratan, and J.J. Hopfield, *J. Amer. Chem. Soc.*, **106**, 1584 (1984).

[174] G.L. Closs, L.T. Calcaterra, N.J. Green, K.W. Penfield, and J.R. Miller, *J. Phys. Chem.*, **90**, 3673 (1986).

[175] J.E. Hanson, California Institute of Technology, work in progress.

[176] G. Fisher, and E. Fisher, *Mol. Photochem.*, **8**, 279 (1977).

[177] J.J. Hopfield, in *Protein Structure: Molecular and Electronic Reactivity*, R.H. Austin, *et al.*, eds., Springer–Verlag, New York, 1986 *in press.*

[178] B.A. Leland, A.D. Joran, P.M. Felker, J.J. Hopfield, A.H. Zewail, and P.B. Dervan, *J. Phys. Chem.*, **89**, 5571 (1985).

[179] V.P. Senthilnathan, and P.S. Platz, *J. Amer. Chem. Soc.*, **102**, 7637 (1980) and references therein.

[180] R. Lines, and V.D. Parker, *Acta Chim. Scand.*, **B31**, 369 (1977).

[181] L. Geng, A.G. Ewing, J.C. Jernigan, and R.W. Murray, *Anal. Chem.*, **58**, 852 (1986).

[182] P.L. Dutton, personal communication.

[183] The ferrocene reference electrode is assumed to provide a solvent–independent potential standard: G. Gritzner and J. Kuta, *Pure and Appl. Chem.*, **56**, 461 (1984).

[184] E. Buhks, J. Jortner, *FEBS Lett.*, **109**, 117 (1980).

[185] J. Ulstrup, J. Jortner, *J. Chem. Phys.*, **63**, 4358 (1975).

[186] R.A. Marcus, *Faraday Discuss. Chem. Soc.*, **74**, 7 (1982).

[187] T. Anno, A. Sadô, *Bull. Chem. Soc. Japan*, **31**, 734 (1958).

[188] M.J. Baudet, G. Berthier, and B. Pullman, *J. chim. phys.*, **54**, 282 (1957).

[189] D.C. Harris, and M.D. Bertolucci, "Symmetry and Spectroscopy," Oxford University Press, New York, 1978.

[190] S.M. Swingle, *J. Amer. Chem. Soc.*, **76**, 1409 (1954).

[191] M.S. Bratoẑ, M.S. Besnaïnou, *J. chim. phys.*, **56**, 555 (1959).

[192] K. Higasi, H. Baba, and A. Rembaum, "Quantum Organic Chemistry," Interscience Publishers, New York, 1965, p. 242.

[193] G. Ponterini, N. Serpone, M.A. Bergkamp, and T.L. Netzel, *J. Amer. Chem. Soc.*, **105**, 4639 (1983).

[194] J.B. Callis, M. Gouterman, Y.M. Jones, and B.H. Henderson, *J. Molec. Spec.*, **39**, 410 (1971).

[195] U. Eisner, and M.J.C. Harding, *J. Chem. Soc.*, 4089 (1964).

[196] L. Edwards, D.H. Dolphin, M. Gouterman, and A.D. Adler, *J. Mol. Spectrosc.*, **38**, 16 (1971).

[197] J. Mercer–Smith, *Dissertation*, Univ. N. Carolina, Chapel Hill, 1978.

[198] reference 141, p. 797.

[199] J.W. Buchler, K.L. Lay, and H. Stoppa, *Z. Naturforsch*, **35b**, 433 (1980).

[200] D.N. Beratan, unpublished results.

[201] The oxidation potential for *PtOEP* is estimated from literature values[199] for the oxidation potential of *PtTPP* corrected for the approximate difference between the OEP skeleton *versus* the TPP ring structure based on electrochemical values[181] for *ZnOEP* and *ZnTPP*. The oxidation potential derived in this manner is moderately different from a literature value for *PtOEP* obtained with more coordinating electrolytes, *e.g.*, A. Stanienda, G. Biebl, *Z. Phys. Chem. Neue Folge*, **52**, 254 (1967).

[202] A.J. Birch, and K.B. Chamberlain, *Org. Syn.*, **57**, 107 (1978).

[203] L. Jurd, *Aust. J. Scien. Res.*, **A2**, 595 (1949).

[204] J.S. Swenton, R.M. Blankenship, and R. Sanitra, *J. Amer. Chem. Soc.*, **97**, 4941 (1975).

[205] H.E. Podall, and W.E. Foster, *J. Org. Chem.*, **23**, 280 (1958).

[206] J.M. Lansinger, and R.C. Ronald, *Syn. Comm.*, **9**, 341 (1979).

[207] For example, see C.C. Lo, B. Leskover, P.R. Harteg, and K. Sauer, *Rev. Sci. Instrum.*, **47**, 107 (1976).

[208] C. Lewis, W.R. Ware, L.J. Doemeny, and T.L. Nemzek, *Rev. Sci. Instrum.*, **44**, 107 (1973).

Appendix A

Emission Fitting Routine

Program SUPERFIT

This program is an iterative non–linear least–squares fitting algorithm used to determine fluorescence lifetimes with deconvolution of the system response function. The program was designed as a menu–driven software package to allow the maximal user control over the fitting routine, and allows interruption of a fit to alter fit parameters prior to convergence. The program also allows display of the data file on screen to allow the user to input the start channel for the fit by inspection of the raw data. If the fit converges, the user can examine the fit and the raw data, as well as the calculated residuals and save the parameters from the fit in a user specified filename for future hardcopy plots (*e.g.*, using GENPLOT on the Chem–VAX).

The decays are fit to an assumed function of the following form

$$\mathrm{I}(t) = \mathrm{I_o}\left[\exp^{-t/\tau_1} + \frac{b_o}{a_o}\exp^{-t/\tau_2} + \frac{c_o}{a_o}\exp^{-t/\tau_3}\right] + \mathrm{B_o}$$

convoluted with the system response function (required) where I(t) is the intensity at time t, I_o is the initial amplitude, $\tau_1, \tau_2,$ and τ_3 are the fluorescence lifetimes, $\frac{b_o}{a_o}$, and $\frac{c_o}{a_o}$ are the amplitude fractions of 2:1 and 3:1, and B_o is the baseline.

The program offers the user the choice of single, double, or triple exponential decay analysis. Additionally, the user can select a biexponential angle–modulated decay analysis of the form

$$\mathrm{I}(t) = \mathrm{I_o}\left[\sum_{i=1}^{N}\frac{1}{N}\exp^{-t[\cos^2\theta_i/\tau_1 + 1/\tau_2]} + \frac{b_o}{a_o}\exp^{-t/\tau_2}\right] + \mathrm{B_o}$$

where N is the number of dihedral angles, $0° \leq \theta_i \leq 90°$ (see Chapter 6).

This program is based on the program CURFIT (P.R. Bevington, "Data Reduction and Error Analysis for the Physical Sciences," McGraw–Hill, New York, 1969, Chapter 11.) and programs obtained from the laboratories of A.H. Zewail courtesy of P.M. Felker and S. Baskin.

The source code was compiled under Microsoft FORTRAN (Copyright IBM Corp, Microsoft Corp, 1982, 1984), version 2.00. The subprogram units were linked under the IBM Personal Computer Linker, version 2.20 (Copyright IBM Corp 1981, 1982, 1983, 1984), and the executable code was run under MD–DOS (version 2.11) on a Compaq Plus personal computer equipped with an 8087 math coprocessor. The executable code was also able to run under MS–DOS (version 3.10) on an IBM–AT personal computer equipped with an 8087 math coprocessor. Similar attempts to run the executable code on an AT&T 6300 personal computer hung the computer following display procedures possibly due to differences in the BIOS interrupts.

Non–standard FORTRAN manipulations

This version of FORTRAN does not support the INQUIRE statements of conventional FORTRAN code and required the use of an ASSEMBLER function STATE (as per the Microsoft FORTRAN manual) to mimic the INQUIRE statement.

Character manipulations are handled ungraciously in this FORTRAN version. Standard FORTRAN allows manipulation of individual elements of a character

string (*e.g.*, CHARVAR(3:3) for the 3rd character in the character string CHARVAR). This FORTRAN version required the use of EQUIVALENCE statments to accomplish the same procedure, *e.g.*,

```
CHARACTER*10 CHARVAR
CHARACTER*1 QCHARVAR(10)
EQUIVALENCE (CHARVAR,QCHARVAR)
```

then QCHARVAR(3) corresponds to the 3rd character in the character string CHARVAR.

Requirements

This program makes heavy use of the ANSI.SYS extended screen and keyboard device driver to allow cursor positioning on the screen and to change screen attributes via control sequences. This driver *must* be installed on the system (*i.e.*, via the CONFIG.SYS file on the IBM compatible personal computers) to obtain the intended program output.

The installation of a math coprocessor to speed floating point arithmetic calculations is suggested, but is not required.

ASSEMBLER Routines Required

STATE(IEND, *filename*): a function which is .TRUE. if *filename* exists and can be opened without error. This function was obtained from the Microsoft FORTRAN user manual, and was used without further changes.

DISP(IFLAG, IXVAL, IYVAL): a subroutine to light (or erase) a pixel at screen location IXVAL,IYVAL on the high resolution graphics screen (640x200) with the home position (0,0) defined as the lower left corner of the screen.

AXES(IFLAG,IX1,IY1,IX2,IY2): a subroutine to draw a horizontal or vertical line from pixel location IX1,IY1 to IX2,IY2. This routine could be replaced with a more general FORTRAN subroutine employing the DISP subroutine described above.

INKEY(ITEST,ISCAN,ANS): a subroutine to read a key entered from the keyboard. This routine is employed heavily in SUPERFIT. The variable ITEST (Integer) is a flag which indicated whether a key has been struck (1=T, 0=F). ISCAN (Integer) is the respective scan code for the key that was entered, and ANS (CHARACTER*1) is the character representation for the key entered.

Expected Data and Response File Formats

The data files analyzed in by SUPERFIT were obtained from a Tracor–Northern digitizer. The file format expected is listed below

ZntBu/o-Xyl/e=5700/o=5800/sl=200u/pol=54.7/nd filter
1000, 7.95

0	1148	54	50	36	68	64	71	81
8	61	67	54	60	61	73	63	68
16	75	54	72	66	58	63	67	62
24	64	78	73	65	64	73	70	52
32	75	65	87	85	65	50	68	62
				.				
				.				
				.				
984	0	0	0	0	0	0	0	0
992	0	0	0	0	0	0	0	0
1000	0	0	0	0	0	0	0	0
1008	0	0	0	0	0	0	0	0
1016	0	0	0	0	0	0	0	

The first line is a comment field not altered by the program but echoed to the user to insure the correct data file is being input. The second line contains an integer value (in the AHZ programs this value corresponded to the number of points in the file, whereas SUPERFIT reads this value, but ignores it and determines the number of data points on the input), and a real value corresponding to the time base for the measurement (psec/channel). The first number in each line is an index, which must be present. In the very first line of data, the number following the index is the ACC (all–clear–channel) which corresponds to the number of seconds of accumulation for the file by the digitizer. The third number

in the first line is the first data point. Each subsequent line contains the index, and eight data points. The file is ordered in decreasing time (*i.e.*, channel 1 is at the bottom of the file). To obtain the time correspondence of each of the intensity values listed in the data file, simply multiply the channel index value by the time base (after inverting the file to obtain the data in an increasing time format).

Array Parameters

The key array in the program is A(8) which contains the parameters used in the fit. Initially the array is loaded with the initial estimates for each of the parameters. Each iteration of the program modifies the parameters to minimize the χ^2 value (*cf.*, Bevington) and outputs a summary to the user to allow examination of the progress of the fit. The elements of the A array correspond as below. Two pointers to the A array are employed, ISTART and ISTOP indicating the range of the A array for the *free* parameters in the fit.

Single exponential decay analysis:

A(1) = unused
A(2) = unused
A(3) = τ_1 lifetime (channels)
ISTART = 3, ISTOP = 6

Double exponential decay analysis:

A(1) = unused
A(2) = τ_1 lifetime (channels)
A(3) = τ_2 lifetime (channels)
ISTART = 2, ISTOP = 7

Triple exponential decay analysis:

A(1) = τ_1 lifetime (channels)
A(2) = τ_2 lifetime (channels)
A(3) = τ_3 lifetime (channels)
ISTART = 1, ISTOP = 8

A(4) = Baseline value
A(5) = Response function shift
A(6) = Initial amplitude
A(7) = Amplitude fraction of τ_2:τ_1
A(8) = Amplitude fraction of τ_3:τ_1

Common Blocks

/FIT/ YFIT(1024)
Calculated Y values based on the current fit parameters
/DATA/ Y(1024)
Input data obtained from file DATFILE
/FILES/ DATROOT, RSPROOT, PLTROOT
Root name of the data, response, and plot files
(type: CHARACTER*12) after stripping off
the path name from the input data file (*e.g.*, if DATFILE
is input as C:\SUBDIR\DATA.DAT then DATROOT is equal to DATA.DAT).
/FLAG/ IOVRFLO
Integer flag indicating if real math overflow is iminent (IOVRFLO=1)
/RES/ A(8) - array containing fit parameters (see above)
CHISQR - χ^2 value from last fit iteration
CHISQ1 - χ^2 value from current fit iteration
ITERNO - iteration cycle number
NTERMS -
/R1/ R(1024) - input response function
RSUM - sum of R array from start channel to end channel
/CHRDAT/ CFIELD - comment field from data file
RSPAVG - 'Y' or 'N' for response function average (not implemented)
BLLMT - 'Y' or 'N' for constrain baseline

ESC – CHAR(27), used for ANSI.SYS control sequences
CLEAR – ANSI sequence for reset screen attributes
REVIDEO – ANSI sequence for inverse video attribute
BOLD – ANSI sequence for bold video attribute
BLINK – ANSI sequence for blinking video attribute
ERASE – ANSI sequence for erase to end of line
/NUMDAT/ NPTS – number of points in data or response files
ITOT – minimum of NPTS(data file) and NPTS(response file)
MINCH – start channel of Y array for fit
MAXCH – end channel of Y array for fit
NSTART – start channel of Y array for fit
NTAUS – number of lifetimes in fit (*i.e.*, single, double or triple)
ISTART – start pointer to free parameters in A array
ISTOP – end pointer to free parameters in A array
ATAU1 – initial estimate of τ_1 (channels)
ATAU2 – initial estimate of τ_2 (channels)
ATAU3 – initial estimate of τ_3 (channels)
FRAC21 – initial estimate of amplitude fraction 2:1
FRAC31 – initial estimate of amplitude fraction 3:1
IFIX1 – number of *fixed* lifetimes
BSLNE – initial estimate of baseline
MINBL – min of range for baseline constraint
MAXBL – max of range for baseline constraint
SHIFT – initial estimate of response function shift
AMPEST – initial amplitude estimate
CTD – Time base (psec/channel)
XMAX – max time in the fit (max channel index times CTD)
YMAX – max intensity (counts) in Y array
IYMAXCH – channel index of YMAX in Y array
NANGS – number of angles in angle modulated decay analysis
IPOS(25) – X position of cursor on screen for each of the
25 lines available in the menu screen

List of Files

File C:SBR_INIT.FOR:
```
  SUBROUTINE INIT(DBGFLG, LOTEMP, DATFILE, QDATFIL,
  $     RSPFILE, QRSPFIL, PLTFILE, QPLTFIL)
  SUBROUTINE HLPMNU
```

File C:SBR_MENU.FOR:
```
  SUBROUTINE MENU(DATFLE, QDATA, RSPFLE, QRESP,
  $     PLTFLE, QPLOT,LOTEMP)
  SUBROUTINE CKRSLT(A, DATFILE, RSPFILE, PLTFILE)
```

File C:FDLOTMP.FOR:
```
  SUBROUTINE FDLOTMP(I, A, DERIV, N)
  SUBROUTINE LNLOTMP(NANGS, NTAUS, A, NPTS, Y, R, RSUM)
```

File C:MENU_SB1.FOR:
```
  SUBROUTINE CHREDT(QTITLE, IMAX, IEND)
  SUBROUTINE RDVAL(XVAL, IXVAL, IFLAG)
```

File C:MENU_SB2.FOR:
```
  SUBROUTINE SETPOS(ICURSOR, IPOS)
  SUBROUTINE CHGVAL(IREAL, XVAL, IXVAL, ICURSOR, IPOS, BOLD,
  $     BLINK, CLEAR, ERASE)
  SUBROUTINE PRTINT(IVALUE)
  SUBROUTINE PRTRL(XVALUE)
  SUBROUTINE CHRALTR(ACHAR, ICURSOR, IPOS, BOLD,
  $     BLINK, CLEAR)
  SUBROUTINE PRTMNU(DATFIL, RSPFIL, PLTFIL, LOTEMP)
  SUBROUTINE CHGXPS(A)
```

File C:SUB1_MNU.FOR:
```
  SUBROUTINE CUNEW(CUABORT, LOTEMP)
  DOUBLE PRECISION FUNCTION FCHNEW(Y, YFIT, NFREE, NPTS, N)
  SUBROUTINE FDNEW(I, A, DERIV, N)
  SUBROUTINE LNNEW(NTAUS, A, NPTS, Y, R, RSUM)
```

File C:SUB2_MNU.FOR:

```
SUBROUTINE MATINV (ARRAY, ISTART, ISTOP, DET)
SUBROUTINE PRNEW(A, CHISQR, CHISQ1, ITERNO, FILE, RSPFIL,
$     IKEEP, LOTEMP)
```

File C:SUB3_MNU.FOR:

```
SUBROUTINE PLTDAT(IDRAW, ISAVE, Y, YFIT,TBASE,NSTART,
$     NPTS,COMMNT)
SUBROUTINE LINE(IFLAG,X1ST,Y1ST,X2ND,Y2ND)
```

Compilation Batch File

```
FOR1 %1,,%1.LST;
FOR2
```

Linking Batch File

```
FORLINK SUPERFIT+SUB1_MNU+SUB2_MNU+SUB3_MNU+
SBR_MENU+MENU_SB1+MENU_SB2+SBR_INIT+DISP+AXES+
INKEY+STATE+FDLOTMP,SUPERFIT,,C:\
```

Source Code for a Program to Create a Data File Header

```
C
C     PROGRAM MAKEFILE.FOR
C
C     creates a file with a comment field ,# of points
C     and time base for use as a data file.....
C     it is presumed this file is run before PC-TALK
C
      CHARACTER*72 CFIELD
C
      WRITE(*,'(1X,2A)') CHAR(27),'[2J'
C
      OPEN (4,FILE='HEADR.DAT',STATUS='NEW',FORM='FORMATTED',
```

```
$         ACCESS='SEQUENTIAL')
      WRITE(*,'(A)') ' Enter the comment field . . . . .'
      WRITE(*,'(A\)') ' >'
      READ(*,'(1A)') CFIELD
      WRITE(4,'(1X,1A)') CFIELD
      WRITE(*,'(A\)') ' Enter the number of data points> '
      READ(*,*) TOTPTS
      WRITE(*,'(A\)') ' Enter the time base (ps/channel)> '
      READ(*,*) TBASE
      NPTS=NINT(TOTPTS)
      WRITE(4,'(1X,I6,A1,F7.2)') NPTS,',',TBASE
C
      CLOSE(4)
      WRITE(*,'(A)') ' Exiting MAKEFILE'
      END
```

Batch File to Initiailize Compaq for Data Transfer

```
ID A:/T
COPY C:\PSEC\PC-TALK.* A:
COPY C:\PSEC\MAKEFILE.EXE A:
COPY C:\PCTALK\PC-TALK.EXE A:
```

This batch file creates a virtual disk and copies the various programs used in data transfer to the virtual disk. Communication protocols are handled by a public domain program, PC-TALK (obtained from Freeware, P.O. Box 862, Tiburon, CA, 94920).

Batch File for Data Transfer

```
A:
MAKEFILE
PC-TALK
COPY HEADR.DAT+TRANS.DAT %1
```

```
COPY %1 C:
DEL %1
DEL HEADR.DAT
DEL TRANS.DAT
C:
ID A:/T
COPY ID A:/T
```

This batch file executes the various programs to transfer a data file from the Tracor–Northern digitizer to the Compaq. The program MAKEFILE creates the header file for the data file. The public domain program PC–TALK is used in the actual data transfer from the digitizer to the Compag Plus computer via the :COM1 serial communication port. An initialized floppy disk is placed in the drive prior to execution of the transfer batch file. A copy of the resulting data file is then copied both to the fixed disk and the floppy (for backup). If the transfer batch file is called TRANS.BAT, the command is

TRANS datafile.dat

Pin Outs for Communication Cable

Compaq Computer		Tracor–Northern
25–pin female		25–pin male
18	⟶	**1**
25	⟶	**25** and **4**

The communication port :COM1 on the Compaq personal computer must be set up in the current–loop configuration.

```
$DEBUG
$NOFLOATCALLS
C    commands to the compiler to
C    invoke the (limited) debug utilities of Microsoft FORTRAN
C    (version 2.00) and maximizes the math coprocessor function
C
C    PROGRAM SUPERFIT.FOR
C
C        Written by B.A. Leland  (3/86)
C
C        Based on the program CURFIT of P.R. Bevington
C        and source code obtained from the AHZ laboratories
C        (progs ANNET,ANNEW,etc)
C
     DIMENSION Y(1024),R(1024),SCR(1024),A(8)
     DOUBLE PRECISION ALPHA(8,8),SIGMAA(8),BETA(8)
     DOUBLE PRECISION CHISQR,CHISQ1,CHISAV
     CHARACTER*1 ANS,QDATFIL(35),QRSPFIL(35),QPLTFIL(35),
      $         ESC,RSPAVG,BLLNT
     CHARACTER*3 ERASE
     CHARACTER*4 REVIDEO,BOLD,BLINK
     CHARACTER*7 CLEAR
     CHARACTER*12 DATROOT,RSPROOT,PLTROOT
     CHARACTER*35 DATFILE,RSPFILE,PLTFILE
     CHARACTER*72 CFIELD
     LOGICAL*2 STATE,CUABORT,DBGFLG,LOTEMP
     EQUIVALENCE (DATFILE,QDATFIL)
     EQUIVALENCE (RSPFILE,QRSPFIL)
     EQUIVALENCE (PLTFILE,QPLTFIL)
     COMMON /DATA/ Y
     COMMON /FIT/ YFIT(1024)
     COMMON /FLAG/ IOVRFLO
     COMMON /FILES/ DATROOT,RSPROOT,PLTROOT
     COMMON /RES/ A,CHISQR,CHISQ1,ITERNO,NTERMS
     COMMON /R1/ R,RSUM
     COMMON /CHRDAT/ CFIELD,RSPAVG,BLLNT,ESC,CLEAR,
      $         REVIDEO,BOLD,BLINK,ERASE
     COMMON /NUMDAT/ NPTS,ITOT,MINCH,MAXCH,NSTART,NTAUS,ISTART,ISTOP,
      $         ATAU1,ATAU2,ATAU3,FRAC21,FRAC31,IFIX1,BSLNE,
      $         MINBL,MAXBL,SHIFT,AMPEST,CTD,XMAX,YMAX,IYMAXCH,
      $         NANGS,IPOS(25)
     COMMON SIGMAA,ALPHA,BETA,FLAMDA
C
     IOVRFLO=0
C
C OPEN LOG FILE OR CREATE IF NECESSARY
C
C              Open log file
     DATFILE='SUPERFIT.LOG'
     LEND=12
     IF (STATE(LEND,DATFILE)) THEN
          OPEN (6,FILE='SUPERFIT.LOG',STATUS='OLD',FORM='FORMATTED',
      $         ACCESS='SEQUENTIAL')
          DO 5 I=1,10000
         READ(6,'(1A)',END=6) ANS
5          CONTINUE
6          CONTINUE
          BACKSPACE 6
     ELSE
          WRITE(*,*) ' Creating log file  . . . . . .'
          OPEN (6,FILE='SUPERFIT.LOG',STATUS='NEW',FORM='FORMATTED',
      $         ACCESS='SEQUENTIAL')
          WRITE(6,'(2A)') '                THIS IS THE LOG FILE FOR ',
      $         'SUPERFIT ANALYSES                    '
           WRITE(6,'(1A)') ' '
          WRITE(6,'(1A)') ' '
     ENDIF
C
C
C  ESTABLISH INITIAL VALUES FOR PARAMETERS A(J)
C
     DO 52 I=1,8
         SIGMAA(I)=0.0D0
         BETA(I)=0.0D0
         A(I)=0.
         DO 51 J=1,8
             ALPHA(I,J)=1.0D0
51         CONTINUE
52     CONTINUE
100    CONTINUE
C
     CALL INIT(DBGFLG,LOTEMP,DATFILE,QDATFIL,RSPFILE,QRSPFIL,
      $         PLTFILE,QPLTFIL)
110    CONTINUE
     CALL MENU(DATFILE,QDATFIL,RSPFILE,QRSPFIL,
      $         PLTFILE,QPLTFIL,LOTEMP)
     WRITE(*,'(1X,2A)') ESC,'[25;30fFitting. . . . . .'
     WRITE(*,'(1A\)') ' '
C
     IF (DBGFLG) THEN
          CALL CKRSLT(A,DATFILE,RSPFILE,PLTFILE)
     ENDIF
C
     CHISQ1 = 1.0D+30
     FLAMDA = 0.001
     RRR = 0.0005
130    CONTINUE
     ITERNO = 0
     ISAVE=0
142    CONTINUE
     ITERNO = ITERNO + 1
     CHISAV = CHISQ1
     CALL CUNEW(CUABORT,LOTEMP)
     CALL PRNEW(A,CHISQR,CHISQ1,ITERNO,
      $                DATROOT,RSPROOT,ISAVE,LOTEMP)
     IF (CUABORT) THEN
         CUABORT=.FALSE.
         ISCAN=59
         ITEST=1
         GO TO 144
     ENDIF
     IF (ITERNO.EQ.20) GO TO 160
     IF (DABS(CHISQ1-CHISQR).LE.DBLE(RRR)) GO TO 190
     CHISQ1 = CHISQR
C
     CALL INKEY(ITEST,ISCAN,ANS)
144    CONTINUE
     IF (ITEST.NE.0) THEN
         IF (ISCAN.NE.59) THEN
         WRITE(*,'(1X,1A\)') BOLD
         WRITE(*,'(1A)') ' '
```

```
      WRITE(*,'(25X,1A)') 'Enter F1 key to interrupt. . .'
      WRITE(*,'(1A)') ' '
      WRITE(*,'(1X,1A\)') CLEAR
      ELSE
C     clear type-ahead buffer
146         CONTINUE
        CALL INKEY(ITEST,ISCAN,ANS)
        IF (ITEST.NE.0) GO TO 146
        WRITE(*,'(1A)') ' '
        WRITE(*,'(8X,5A)') 'Enter ',BOLD,'F2',CLEAR,
     $           ' key to alter initial parameters'
        WRITE(*,'(8X,5A)') '      ',BOLD,'F3',CLEAR,
     $           ' key to save progress in log file'
        WRITE(*,'(8X,5A)') '      ',BOLD,'F4',CLEAR,
     $        ' key to save current results as initial parameters'
        WRITE(*,'(8X,5A)') '      ',BOLD,'F5',CLEAR,
     $        ' key to continue'
        WRITE(*,'(8X,5A)') '      ',BOLD,'F10',CLEAR,
     $        ' key to quit'
      ENDIF
155       CONTINUE
        CALL INKEY(ITEST,ISCAN,ANS)
        IF (ITEST.EQ.0) GO TO 155
        IF ((ISCAN.GE.59).AND.(ISCAN.LE.68)) THEN
            WRITE(*,'(10X,1A)') 'OK. . . . . '
        ELSE
C           invalid key entry
        WRITE(*,'(1A)') ' '
        WRITE(*,'(8X,5A)') 'Enter ',BOLD,'F2',CLEAR,
     $           ' key to alter initial parameters'
        WRITE(*,'(8X,5A)') '      ',BOLD,'F3',CLEAR,
     $           ' key to save progress in log file'
        WRITE(*,'(8X,5A)') '      ',BOLD,'F4',CLEAR,
     $        ' key to save current results as initial parameters'
        WRITE(*,'(8X,5A)') '      ',BOLD,'F5',CLEAR,
     $        ' key to continue'
        WRITE(*,'(8X,5A)') '      ',BOLD,'F10',CLEAR,
     $        ' key to quit'
        GO TO 155
        ENDIF
            IF (ISCAN.EQ.63) THEN
C           > continue <
C        clear type-ahead buffer
158           CONTINUE
                CALL INKEY(ITEST,ISCAN,ANS)
              IF (ITEST.NE.0) GO TO 158
            GO TO 142
        ENDIF
            IF (ISCAN.EQ.60) THEN
C           alter initial conditions
        WRITE(*,'(1X,2A\)') ESC,'[2J'
        CALL PRTMNU(DATFILE,RSPFILE,PLTFILE,LOTEMP)
        CALL MENU(DATFILE,QDATFIL,RSPFILE,QRSPFIL,
     $             PLTFILE,QPLTFIL,LOTEMP)
        CHISQ1 = 1.0D+30
        FLAMDA = 0.001
        RRR = 0.0005
        WRITE(*,'(1X,2A)') ESC,'[25;30fFitting. . . . . '
        WRITE(*,'(1X,1A\)') ' '
        IF (DBGFLG) THEN
            CALL CKRSLT(A,DATFILE,RSPFILE,PLTFILE)
        ENDIF
        GO TO 130
          ENDIF
              IF (ISCAN.EQ.68) GO TO 350
          IF (ISCAN.EQ.61) THEN
C             save progress in log file
        WRITE(6,'(10X,1A)')
     $       '********** Incomplete Results **********'
        IKEEP=1
        CALL PRNEW(A,CHISQR,CHISQ1,
     $             ITERNO,DATROOT,RSPROOT,IKEEP,LOTEMP)
          ENDIF
          IF (ISCAN.EQ.62) THEN
C             change inits to current values
        BSLNE=A(4)
        SHIFT=A(5)
        AMPEST=A(6)
        FRAC21=A(7)
        FRAC31=A(8)
        ATAU1=0.
        ATAU2=0.
        ATAU3=0.
        IF (NTAUS.EQ.1) THEN
            ATAU1=A(3)
        ELSEIF (NTAUS.EQ.2) THEN
            ATAU1=A(2)
            ATAU2=A(3)
        ELSE
            ATAU1=A(1)
            ATAU2=A(2)
            ATAU3=A(3)
        ENDIF
          ENDIF
      GO TO 155
      ENDIF
C
      GO TO 142
160     CONTINUE
      WRITE(*,'(A\)') ' ITERATION LIMIT REACHED - want to continue? '
      READ(*,'(A1)') ANS
      IF ((ANS.EQ.'Y').OR.(ANS.EQ.'y')) GO TO 130
190     IF (IOVRFLO.EQ.0) GO TO 195
      CHISQR = CHISAV
      WRITE(*,192) ' The minimum value of (chi)',CHAR(253),
     $             ' was ',CHISQR
192     FORMAT (3A,F12.5)
C
C  ESTABLISH DOCUMENTATION FORMAT
C
195     CONTINUE
      WRITE(*,200) (SIGMAA(I),I=1,NTERMS)
200     FORMAT(8(F9.4,1X)\)
C
210     CONTINUE
      CALL INKEY(ITEST,ISCAN,ANS)
      IF (ITEST.EQ.0) GO TO 210
      IDRAW=1
      CALL PLTDAT(IDRAW,K,Y,YFIT,CTD,NSTART,NPTS,CFIELD)
      WRITE(*,'(3A\)') CLEAR,ESC,'[2J'
```

```
C        write results to log file and reprint on screen
         WRITE(*,'(1X,1A)') ' '
      IKEEP=1
      CALL PRNEW(A,CHISQR,CHISQ1,ITERNO,
       $                DATROOT,RSPROOT,IKEEP,LOTEMP)
         WRITE(*,'(1X,1A)') ' '
C
      SIG1 = SQRT(SIG1*SNGL(CHISQR))*CTD
      KKKK = 0
220      WRITE(*,'(1A\)') ' Save the fit?? (Y/N): '
      READ(*,225,ERR=255) ANS
225      FORMAT (1A)
240      IF ((ANS.EQ.'Y').OR.(ANS.EQ.'y')) GO TO 260
250      IF ((ANS.EQ.'N').OR.(ANS.EQ.'n')) GO TO 350
255      GO TO 220
C
C  CALL PLOTTING ROUTINE
C
260      CONTINUE
       WRITE(*,'(A\)') ' Enter the name for the output file: '
      READ(*,'(1A)') PLTFILE
      DO 270 I=1,35
          IF (QPLTFIL(I).EQ.' ') THEN
              LOC=I-1
              GO TO 271
          ENDIF
270      CONTINUE
271      CONTINUE
      IF (STATE(LOC,PLTFIL)) THEN
          WRITE(*,*) ' FILE ALREADY EXISTS. . . . .'
          GO TO 260
      ELSE
          OPEN (4,FILE=PLTFIL,STATUS='NEW',FORM='FORMATTED',
       $             ACCESS='SEQUENTIAL')
      ENDIF
      WRITE(4,'(1X,3A)') DATROOT,'/',RSPROOT
      WRITE(4,'(1X,1A)') CFIELD
      WRITE(4,*) NPTS,CTD,NANGS
      WRITE(4,*) XMAX,YMAX,MAXCH,NTAUS,NSTART,ISTART,ISTOP
      WRITE(4,*) (A(I),I=1,8)
      WRITE(4,*) (SIGMAA(I),I=1,8)
      WRITE(4,*) CHISQR
      CLOSE(4)
350      CONTINUE
      WRITE(*,'(1A\)') ' More data analysis? '
      READ(*,'(1A)') ANS
         IF ((ANS.EQ.'Y').OR.(ANS.EQ.'y')) THEN
          WRITE(*,'(1X,2A\)') CHAR(27),'[2J'
          A(4)=BSLNE
          A(5)=SHIFT
          A(6)=AMPEST
          A(7)=FRAC21
          A(8)=FRAC31
          A(1)=0.
          A(2)=0.
          A(3)=0.
          IF (NTAUS.EQ.1) THEN
              A(3)=ATAU1
          ELSEIF (NTAUS.EQ.2) THEN
              A(2)=ATAU1
              A(3)=ATAU2
          ELSE
              A(1)=ATAU1
              A(2)=ATAU2
              A(3)=ATAU3
          ENDIF
          CALL PRTMNU(DATFILE,RSPFILE,PLTFILE,LOTEMP)
          GO TO 110
      ELSE
          CLOSE(6)
          WRITE(*,'(1X,2A)') CHAR(27),'[2J'
      ENDIF
C
800      CONTINUE
      WRITE(*,*) ' Exiting SUPERFIT '
      END
C
C
C
       SUBROUTINE INIT(DBGFLG,LOTEMP,DATFILE,QDATFIL,RSPFILE,QRSPFIL,
       $          PLTFILE,QPLTFIL)
C
C      FUNCTION:
C          PROMPTS THE USER FOR ALL PARAMETERS REQUIRED TO
C          BEGIN A FITTING RUN.  INITIALIZES ALL PARAMETERS
C
      DIMENSION Y(1024),R(1024),SCR(1024),A(8),ISAV(25)
      DOUBLE PRECISION ALPHA(8,8),SIGMAA(8),BETA(8)
      DOUBLE PRECISION CHISQR,CHISQ1,CHISAV
      CHARACTER*1 ANS,QDATFIL(35),QRSPFIL(35),QPLTFIL(35),
       $         QBLINK(4),QREVIDEO(4),QBOLD(4),QCLEAR(7),QERASE(3),
       $      RSPAVG,BLLNT,ESC,QDATROOT(12),QRSPROOT(12),QPLTROOT(12)
      CHARACTER*3 ERASE
      CHARACTER*4 REVIDEO,BOLD,BLINK
      CHARACTER*7 CLEAR
      CHARACTER*35 DATFILE,RSPFILE,PLTFILE
      CHARACTER*72 CFIELD
      CHARACTER*12 LOGDAT,DATROOT,RSPROOT,PLTROOT
      LOGICAL*2 STATE,DBGFLG,LOTEMP
      EQUIVALENCE (DATROOT,QDATROOT),(RSPROOT,QRSPROOT)
      EQUIVALENCE (PLTROOT,QPLTROOT)
          EQUIVALENCE (CLEAR,QCLEAR),(BOLD,QBOLD),(REVIDEO,QREVIDEO),
       $         (BLINK,QBLINK),(ANPTS,QANPTS),(ERASE,QERASE)
C
      COMMON /DATA/ Y
      COMMON /FIT/ YFIT(1024)
      COMMON /FLAG/ IOVRFLO
      COMMON /FILES/ DATROOT,RSPROOT,PLTROOT
      COMMON /RES/ A,CHISQR,CHISQ1,ITERNO,NTERMS
      COMMON /R1/ R,RSUM
      COMMON /CHRDAT/ CFIELD,RSPAVG,BLLNT,ESC,CLEAR,
       $         REVIDEO,BOLD,BLINK,ERASE
      COMMON /NUMDAT/ NPTS,ITOT,MINCH,MAXCH,NSTART,NTAUS,ISTART,ISTOP,
       $         ATAU1,ATAU2,ATAU3,FRAC21,FRAC31,IFIX1,BSLNE,
       $         MINBL,MAXBL,SHIFT,AMPEST,CTD,XMAX,YMAX,IYMAXCH,
       $         NANGS,IPOS(25)
C     DATA IPOS/0,0,0,17,20,45,28,26,0,0,31,27,31,31,31,19,19,
C     $         19,24,25,35,26,26,0,0/
      DATA ISAV/0,0,0,17,20,45,28,0,0,0,31,27,31,31,0,19,0,
       $         19,24,25,0,26,0,0,0/
C
```

```
      IOVRFLO=0
      DO 15 I=1,25
         IPOS(I)=ISAV(I)
15    CONTINUE
      DBGFLG=.FALSE.
      LOTEMP=.FALSE.
      LENGTH=35
      DATFILE='                                   '
      RSPFILE='                                   '
      PLTFILE='                                   '
      DATROOT='            '
      RSPROOT='            '
      PLTROOT='            '
      NANGS=0
      NPTS=1000
      ITOT=0
      MINCH=0
      MAXCH=0
      NSTART=0
      NTAUS=2
      ATAU1=0.
      ATAU2=0.
      ATAU3=0.
      FRAC21=0.
      FRAC31=0.
       IFIX1=0
      ISTART=0
      ISTOP=0
      BSLNE=0.
      MINBL=0
      MAXBL=0
      SHIFT=0.
      AMPEST=0.
      CTD=0.
      YMAX=0.
      IYMAXCH=0
      BLLNT='N'
      RSPAVG='N'
C
C       "CLEAR" CONTAINS ANSI DRIVER CODE FOR ATTRIBUTES OFF,
C        AND BACKGROUND COLOR OF BLACK OR BLUE
C
      ESC=CHAR(27)
C
      QCLEAR(1)=ESC
      QCLEAR(2)='['
      QCLEAR(3)='0'
      QCLEAR(4)=';'
100   CONTINUE
      WRITE(*,*) ' '
      WRITE(*,'(1A\)') ' Is the room dark? '
      READ(*,'(1A)') ANS
      IF ((ANS.EQ.'D').OR.(ANS.EQ.'d')) THEN
          DBGFLG=.TRUE.
          GO TO 100
      ENDIF
      IF ((ANS.EQ.'Y').OR.(ANS.EQ.'y')) THEN
          QCLEAR(5)='4'
          QCLEAR(6)='4'
          QCLEAR(7)='m'
      ELSE
          QCLEAR(5)='4'
          QCLEAR(6)='0'
          QCLEAR(7)='m'
      ENDIF
      WRITE(*,'(1X,3A\)') CLEAR,ESC,'[2J'
C
      QERASE(1)=ESC
      QERASE(2)='['
      QERASE(3)='K'
C
      QBOLD(1)=ESC
      QBOLD(2)='['
      QBOLD(3)='1'
      QBOLD(4)='m'
C
      BLINK=BOLD
      QBLINK(3)='5'
C
      REVIDEO=BOLD
      QREVIDEO(3)='7'
C
      CALL PRTMNU(DATFILE,RSPFILE,PLTFILE,LOTEMP)
C
C
C     Get data and response filenames
      MAXROW=25
      ICURSOR=4
C
      WRITE(*,'(1A\)') BOLD
210     CONTINUE
      CALL SETPOS(ICURSOR,IPOS)
      CALL CHREDT(QDATFIL,LENGTH,IEND)
      CALL SETPOS(ICURSOR,IPOS)
      WRITE(*,'(2A\)') DATFILE,ERASE
      IF (STATE(IEND,QDATFIL)) THEN
          WRITE(*,'(2A\)') ESC,
     $         '[2;20f
          OPEN (4,FILE=DATFILE,STATUS='OLD',FORM='FORMATTED',
     $              ACCESS='SEQUENTIAL')
          DO 220 K=IEND,1,-1
              IF (QDATFIL(K).EQ.'\') GO TO 222
220           CONTINUE
222           CONTINUE
          IPATH=K
          IF (IPATH.NE.0) THEN
              DO 224 J=1,IPATH
                  QRSPFIL(J)=QDATFIL(J)
                  QPLTFIL(J)=QDATFIL(J)
224               CONTINUE
          ENDIF
          K=1
          DO 300 I=(IPATH+1),IEND
              QDATROOT(K)=QDATFIL(I)
              K=K+1
300           CONTINUE
       ELSE
          WRITE(*,'(2A,I2,1A\)') ESC,
     $         '[2;20fFILE DOES NOT EXIST. . . .(',IEND,')'
          GO TO 210
      ENDIF
      READ(4,'(1A)') CFIELD
```

```
      READ(4,*) NPT,CTD
      READ(4,*) K,ACC,(SCR(J), J=1,7)
      DO 320 I=8,1016,8
          READ(4,*,END=330,ERR=330) K,(SCR(J),J=I,I+7)
320     CONTINUE
330     CONTINUE
      ITOTDAT=J-1
      CLOSE(4)
      WRITE(*,'(1A\)') ' '
      WRITE(*,'(1A1,1A5,1A72\)') ESC,'[1;2f',CFIELD
C
      K=ITOTDAT
      DO 360 I=1,ITOTDAT
          Y(I)=SCR(K)
              K=K-1
360     CONTINUE
C
C
      ICURSOR=5
380     CONTINUE
      CALL SETPOS(ICURSOR,IPOS)
      CALL CHREDT(QRSPFIL,LENGTH,IEND)
      CALL SETPOS(ICURSOR,IPOS)
      WRITE(*,'(2A\)') RSPFILE,ERASE
      IF (STATE(IEND,QRSPFIL)) THEN
          WRITE(*,'(2A\)') ESC,
     $         '[2;20f
          OPEN (4,FILE=RSPFILE,STATUS='OLD',FORM='FORMATTED',
     $               ACCESS='SEQUENTIAL')
          DO 400 K=IEND,1,-1
              IF (QRSPFIL(K).EQ.'\') GO TO 410
400           CONTINUE
410           CONTINUE
          IPATH=K
          K=1
          DO 420 I=(IPATH+1),IEND
              QRSPROOT(K)=QRSPFIL(I)
              K=K+1
420           CONTINUE
       ELSE
          WRITE(*,'(2A,I2,1A\)') ESC,
     $         '[2;20fFILE DOES NOT EXIST. . . .(',IEND,')'
          GO TO 380
      ENDIF
C
      READ(4,'(A1)') ANS
      READ(4,*) NPT,CTR
      IF (CTR.NE.CTD) THEN
          WRITE(*,'(1X,2A\)') ESC,
     $         '[2;20f
           WRITE(*,'(2A\)') ESC,
     $               '[2;20fMismatched time bases for data & response'
          CLOSE(4)
          GO TO 380
      ENDIF
      READ(4,*) K,ACC,(SCR(J), J=1,7)
      DO 460 I=8,1016,8
          READ(4,*,END=470,ERR=470) K,(SCR(J),J=I,I+7)
460     CONTINUE
470     CONTINUE
      ITOTRSP=J-1
      CLOSE(4)
      WRITE(*,'(1A\)') ' '
      K=ITOTRSP
      DO 500 I=1,ITOTRSP
          R(I)=SCR(K)
              K=K-1
500     CONTINUE
C
      ITOT=MINO(ITOTDAT,ITOTRSP)
      WRITE(*,'(7A\)') CLEAR,ESC,'[6;5fNumber of data points (100 ',
     $         CHAR(243),' N ',CHAR(243),' '
      CALL PRTINT(ITOT)
          WRITE(*,'(2A\)') '): ',BOLD
      ICURSOR=6
      CALL SETPOS(ICURSOR,IPOS)
      CALL PRTINT(NPTS)
C
C     Get # of points
      IREAL=0
      IPTS=NPTS
      CALL CHGVAL(IREAL,XVAL,IPTS,ICURSOR,IPOS,
     $         BOLD,BLINK,CLEAR,ERASE)
      IF (IPTS.GT.ITOT) THEN
          NPTS=ITOT
      ELSEIF (IPTS.GE.100) THEN
          NPTS=IPTS
      ENDIF
      CALL SETPOS(ICURSOR,IPOS)
      WRITE(*,'(2A\)') ERASE,BOLD
      CALL PRTINT(NPTS)
      WRITE(*,'(1A\)') CLEAR
C
      XMAX = FLOAT(NPTS)*CTD/1000.
      YMAX = 1.
      NTERMS = 8.
      RSUM = 0.
      DO 600 I=1,NPTS
          RSUM = RSUM + R(I)
          IF (Y(I).GT.YMAX) THEN
              YMAX = Y(I)
             IYMAXCH = I
          ELSE
              Y(I) = AMAX1(1.,Y(I))
          ENDIF
600     CONTINUE
C
      WRITE(*,'(4A,F7.2\)') ESC,'[9;15f',BOLD,
     $        'Picoseconds per channel : ',CTD
      WRITE(*,'(3A,F7.0,2X,1A,I4,1A\)') ESC,'[10;15f',
     $         'Ymax = ',YMAX,'Ymax channel = ',IYMAXCH,CLEAR
C
C     channel to start fit
      ICURSOR=11
      CALL SETPOS(ICURSOR,IPOS)
650     CONTINUE
      IREAL=0
      ISAVE=NSTART
      CALL CHGVAL(IREAL,XVAL,NSTART,ICURSOR,IPOS,
     $         BOLD,BLINK,CLEAR,ERASE)
      IF (NSTART.LE.0) THEN
          IDRAW=0
```

```
      CALL PLTDAT(IDRAW,NSTART,Y,YFIT,CTD,NSTART,NPTS,CFIELD)
      WRITE(*,'(1X,3A\)') CLEAR,ESC,'[2J'
      CALL PRTMNU(DATFILE,RSPFILE,PLTFILE,LOTEMP)
      IF (NSTART.LE.0) THEN
          NSTART=0
          GO TO 650
      ENDIF
    ENDIF
C
    CALL CHGXPS(A)
C
    IF (NTAUS.EQ.1) THEN
        ISTART=3
        ISTOP=6
    ELSEIF(NTAUS.EQ.2) THEN
        ISTART=2
        ISTOP=7
    ELSE
        ISTART=1
        ISTOP=8
    ENDIF
    A(4)=BSLNE
    A(5)=SHIFT
    A(6)=AMPEST
    A(7)=FRAC21
    A(8)=FRAC31
C
    RETURN
    END
C
C
C
     SUBROUTINE HLPMNU
C
C    FUNCTION:
C        PRINTS A HELP SCREEN TO REMIND THE USER OF
C        CONTROL KEYS RECOGNIZED BY SUPERFIT
C
    CHARACTER*1 RSPAVG,BLLMT,ESC,ANS
    CHARACTER*3 ERASE
    CHARACTER*4 REVIDEO,BOLD,BLINK
    CHARACTER*7 CLEAR
    CHARACTER*72 CFIELD
    COMMON /CHRDAT/ CFIELD,RSPAVG,BLLMT,ESC,CLEAR,
     $        REVIDEO,BOLD,BLINK,ERASE
C
    WRITE(*,'(4A\)') CLEAR,ESC,'[2J'
    WRITE(*,'(1X,6A\)') ESC,'[10;10f',BOLD,CHAR(24),
     $       CLEAR,'  (keypad #8). . . . . .Move up one line'
    WRITE(*,'(10A\)') ESC,'[11;10f',BOLD,CHAR(25),
     $       CLEAR,'  (keypad #2) or ',BOLD,'RETURN',CLEAR,
     $       '. . .Move down one line'
    WRITE(*,'(6A\)') ESC,'[12;10f',BOLD,
     $       'HOME',CLEAR,'  (keypad #7). . . . . Alter parameter'
    WRITE(*,'(8A\)') ESC,'[13;10f',
     $     'keypad ',BOLD,'+',CLEAR,'. . . . . .',
     $     'Estimate amplitude with current parameters'
    WRITE(*,'(6A\)') ESC,'[14;10f',BOLD,'?',CLEAR,
     $     '. . . . . This help menu'
    WRITE(*,'(6A\)') ESC,'[15;10f',BOLD,
     $       'END',CLEAR,'  (keypad #1). . . . . .Exit change menu'
C   clear keyboard buffer
80    CONTINUE
    CALL INKEY(ITEST,ISCAN,ANS)
    IF (ITEST.NE.0) GO TO 80
C
    WRITE(*,'(5A\)') ESC,'[17;25f',BOLD,
     $       'Type any key to continue',CLEAR
C
100   CONTINUE
    CALL INKEY(ITEST,ISCAN,ANS)
    IF (ITEST.EQ.0) GO TO 100
C
    RETURN
    END
C
C
C
     SUBROUTINE MENU(DATFLE,QDATA,RSPFLE,QRESP,PLTFLE,QPLOT,LOTEMP)
C
C    FUNCTION:
C        PRINTS THE MENU SCREEN AND PROMPTS THE USER FOR
C        INPUT OF INITIAL ESTIMATES FOR THE FIT PARAMETERS
C
    DIMENSION SCR(1024)
    CHARACTER*1 ANS,QDATA(35),QRESP(35),QPLOT(35),RSPAVG,BLLMT,ESC,
     $        QDATROOT(12),QRSPROOT(12),QPLTROOT(12)
    CHARACTER*3 ERASE
    CHARACTER*4 REVIDEO,BOLD,BLINK
    CHARACTER*7 CLEAR
    CHARACTER*12 DATROOT,RSPROOT,PLTROOT
    CHARACTER*35 DATFLE,RSPFLE,PLTFLE
    CHARACTER*72 CFIELD
    LOGICAL*2 STATE,LOTEMP
    EQUIVALENCE (DATROOT,QDATROOT),(RSPROOT,QRSPROOT)
    EQUIVALENCE (PLTROOT,QPLTROOT)
C
    COMMON /DATA/ Y(1024)
    COMMON /RES/ A(8),CHISQR,CHISQ1,ITERNO,NTERMS
    COMMON /R1/ R(1024),RSUM
    COMMON /FILES/ DATROOT,RSPROOT,PLTROOT
    COMMON /CHRDAT/ CFIELD,RSPAVG,BLLMT,ESC,CLEAR,
     $        REVIDEO,BOLD,BLINK,ERASE
    COMMON /NUMDAT/ NPTS,ITOT,MINCH,MAXCH,NSTART,NTAUS,ISTART,ISTOP,
     $        ATAU1,ATAU2,ATAU3,FRAC21,FRAC31,IFIX1,BSLNE,
     $        MINBL,MAXBL,SHIFT,AMPEST,CTD,XMAX,YMAX,IYMAXCH,
     $        NANGS,IPOS(25)
C
C
    MAXROW=25
    LENGTH=35
    ICURSOR=4
    CALL SETPOS(ICURSOR,IPOS)
C
250   CONTINUE
    CALL INKEY(ITEST,ISCAN,ANS)
    IF (ITEST.EQ.0) GO TO 250
C
260   CONTINUE
    IF (ISCAN.EQ.72) THEN
270       CONTINUE
```

```
        ICURSOR=ICURSOR-1
        IF (ICURSOR.LT.1) THEN
            ICURSOR=MAXROW
        ENDIF
        IF (IPOS(ICURSOR).EQ.0) GO TO 270
        CALL SETPOS(ICURSOR,IPOS)
        GO TO 250
    ELSEIF ((ISCAN.EQ.80).OR.(ISCAN.EQ.28)) THEN
280         CONTINUE
        ICURSOR=ICURSOR+1
        IF (ICURSOR.GT.MAXROW) THEN
            ICURSOR=1
        ENDIF
        IF (IPOS(ICURSOR).EQ.0) GO TO 280
        CALL SETPOS(ICURSOR,IPOS)
        GO TO 250
    ELSEIF ((ISCAN.EQ.79).OR.(ISCAN.EQ.1)) THEN
        IF (AMPEST.LE.0) THEN
            GO TO 420
        ELSE
            GO TO 800
        ENDIF
    ELSEIF (ISCAN.EQ.78) THEN
        GO TO 420
    ELSEIF (ISCAN.EQ.71) THEN
        GOTO(250,250,250,310,320,330,340,344,250,250,
     $        350,360,362,364,366,368,370,375,380,390,391,400,410,
     $        250,250)ICURSOR
    ELSEIF (ISCAN.EQ.53) THEN
        CALL HLPMNU
        WRITE(*,'(3A\)') CLEAR,ESC,'[2J'
        CALL PRTMNU(DATFLE,RSPFLE,PLTFLE,LOTEMP)
        GO TO 250
    ELSE
        WRITE(*,'(2A\)') ESC,'[s'
        WRITE(*,'(5A\)') ESC,'[25;35f',BOLD,
     $        'Enter ? for help',CLEAR
        WRITE(*,'(2A\)') ESC,'[u'
        GO TO 250
    ENDIF
    GO TO 250
C
310    CONTINUE
C    data file
    CALL SETPOS(ICURSOR,IPOS)
    WRITE(*,'(2A\)') ERASE,BOLD
    CALL CHREDT(QDATA,LENGTH,IEND)
C$$$$$$$$$$$$$$$$$$$$$$$$$$$$$$$$$$$$$$$$$$$$$$$$$$$$$$$$$$$$$$$$$$$$$$$$$$$$$$$$$$$
    IF (STATE(IEND,QDATA)) THEN
        WRITE(*,'(2A\)') ESC,
     $        '[2;20f
        OPEN (4,FILE=DATFLE,STATUS='OLD',FORM='FORMATTED',
     $             ACCESS='SEQUENTIAL')
        DO 311 K=IEND,1,-1
            IF (QDATA(K).EQ.'\') GO TO 312
311         CONTINUE
312         CONTINUE
        IPATH=K
        IF (IPATH.NE.0) THEN
            DO 313 J=1,IPATH
                QPLOT(J)=QDATA(J)
313             CONTINUE
        ENDIF
        K=1
        DO 314 I=(IPATH+1),IEND
            QDATROOT(K)=QDATA(I)
            K=K+1
314         CONTINUE
      ELSE
        WRITE(*,'(2A,I2,1A\)') ESC,
     $        '[2;20fFILE DOES NOT EXIST. . . .(',IEND,')'
        GO TO 310
    ENDIF
    READ(4,'(1A)') CFIELD
    READ(4,*) NPT,CTD
    READ(4,*) K,ACC,(SCR(J), J=1,7)
    DO 316 I=8,1016,8
        READ(4,*,END=317,ERR=317) K,(SCR(J),J=I,I+7)
316     CONTINUE
317     CONTINUE
    ITOTDAT=J-1
    CLOSE(4)
    WRITE(*,'(1A\)') ' '
    WRITE(*,'(1A1,1A5,1A72\)') ESC,'[1;2f',CFIELD
C
    IYMAXCH=1
    YMAX=1.0
    K=ITOTDAT
    DO 318 I=1,ITOTDAT
        Y(I)=SCR(K)
        IF (Y(I).GT.YMAX) THEN
            YMAX=Y(I)
        IYMAXCH=I
        ELSE
        Y(I)=AMAX1(1.,Y(I))
        ENDIF
            K=K-1
318     CONTINUE
C
C
    WRITE(*,'(1A\)') CLEAR
    ISCAN=80
    GO TO 260
320     CONTINUE
C    response file
    CALL SETPOS(ICURSOR,IPOS)
    WRITE(*,'(2A\)') ERASE,BOLD
    CALL CHREDT(QRESP,LENGTH,IEND)
C$$$$$$$$$$$$$$$$$$$$$$$$$$$$$$$$$$$$$$$$$$$$$$$$$$$$$$$$$$$$$$$$$$$$$$$$$$$$$$$$$$$
    IF (STATE(IEND,QRESP)) THEN
        WRITE(*,'(2A\)') ESC,
     $        '[2;20f
        OPEN (4,FILE=RSPFLE,STATUS='OLD',FORM='FORMATTED',
     $             ACCESS='SEQUENTIAL')
        DO 322 K=IEND,1,-1
            IF (QRESP(K).EQ.'\') GO TO 323
322         CONTINUE
323         CONTINUE
        IPATH=K
        K=1
        DO 324 I=(IPATH+1),IEND
            QRSPROOT(K)=QRESP(I)
```

```
          K=K+1
324       CONTINUE
      ELSE
        WRITE(*,'(2A,I2,1A\)') ESC,
     $       '[2;20fFILE DOES NOT EXIST. . . .(',IEND,')'
        GO TO 320
      ENDIF
C
      READ(4,'(A1)') ANS
      READ(4,*) NPT,CTR
      IF (CTR.NE.CTD) THEN
        WRITE(*,'(1X,2A\)') ESC,
     $       '[2;20f
         WRITE(*,'(2A\)') ESC,
     $            '[2;20fMismatched time bases for data & response'
        CLOSE(4)
        GO TO 320
      ENDIF
      READ(4,*) K,ACC,(SCR(J), J=1,7)
      DO 325 I=8,1016,8
        READ(4,*,END=326,ERR=326) K,(SCR(J),J=I,I+7)
325     CONTINUE
326     CONTINUE
      ITOTRSP=J-1
      CLOSE(4)
      WRITE(*,'(1A\)') ' '
      K=ITOTRSP
      DO 327 I=1,ITOTRSP
        R(I)=SCR(K)
          K=K-1
327     CONTINUE
C
      RSUM = 0.
      DO 328 I=1,NPTS
        RSUM = RSUM + R(I)
328     CONTINUE
C
C$$$$$$$$$$$$$$$$$$$$$$$$$$$$$$$$$$$$$$$$$$$$$$$$$$$$$$$$$$$$$$$$$$$$$$$$$$$$
      WRITE(*,'(1A\)') CLEAR
      ISCAN=80
      GO TO 260
330     CONTINUE
C     # of data points
      IREAL=0
      ISAVE=NPTS
      CALL CHGVAL(IREAL,XVAL,NPTS,ICURSOR,IPOS,
     $       BOLD,BLINK,CLEAR,ERASE)
      IF ((NPTS.LE.99).OR.(NPTS.GT.ITOT)) THEN
        CALL SETPOS(ICURSOR,IPOS)
        WRITE(*,'(2A\)') ERASE,BOLD
        NPTS=ISAVE
        CALL PRTINT(NPTS)
        WRITE(*,'(1A\)') CLEAR
      ENDIF
      XMAX=FLOAT(NPTS)*CTD/1000.
      RSUM = 0.
      DO 335 I=1,NPTS
        RSUM = RSUM + R(I)
335     CONTINUE
      ISCAN=80
      GO TO 260
340     CONTINUE
C       angle modulated decay fitting ON or OFF
      IF (ISCAN.NE.28) THEN
        CALL SETPOS(ICURSOR,IPOS)
        WRITE(*,'(2A\)') ERASE,BOLD
        IF (LOTEMP) THEN
          LOTEMP=.FALSE.
          WRITE(*,'(1A\)') 'Off'
        ELSE
          LOTEMP=.TRUE.
          WRITE(*,'(1A\)') 'On '
        ENDIF
        WRITE(*,'(1A\)') CLEAR
342       CONTINUE
        CALL INKEY(ITEST,ISCAN,ANS)
        IF (ITEST.EQ.0) GO TO 342
        GO TO 340
      ELSE
        CALL SETPOS(ICURSOR,IPOS)
        WRITE(*,'(2A\)') ERASE,REVIDEO
        IF (LOTEMP) THEN
          WRITE(*,'(1A\)') 'On '
          IPOS(8)=26
        ELSE
          WRITE(*,'(1A\)') 'Off'
          IPOS(8)=0
        ENDIF
        WRITE(*,'(1A\)') CLEAR
      ENDIF
344     CONTINUE
      IF (LOTEMP) THEN
        WRITE(*,'(2A\)') ESC,'[8;8fNumber of angles: ',
        IF (NANGS.EQ.0) THEN
          WRITE(*,'(3A\)') REVIDEO,'  ',CLEAR
        ELSE
          WRITE(*,'(1A,I2,1A\)') BOLD,NANGS,CLEAR
        ENDIF
        ICURSOR=8
        IREAL=0
        IXSAVE=NANGS
        CALL CHGVAL(IREAL,XVAL,NANGS,ICURSOR,IPOS,
     $       BOLD,BLINK,CLEAR,ERASE)
        IF ((NANGS.LT.0).OR.(NANGS.GT.30)) THEN
          NANGS=IXSAVE
          CALL SETPOS(ICURSOR,IPOS)
          WRITE(*,'(1A\)') BOLD
          CALL PRTINT(NANGS)
          WRITE(*,'(1A\)') CLEAR
        ENDIF
      ELSE
        WRITE(*,'(3A\)') ESC,'[8;1f',ERASE
      ENDIF
      IF ((LOTEMP).AND.(NANGS.EQ.0)) GO TO 344
C
      ISCAN=80
      GO TO 260
C
C
C
C     response baseline correction
C     CALL CHRALTR(RSPAVG,ICURSOR,IPOS,BOLD,BLINK,CLEAR)
```

```
C341    CONTINUE
C     WRITE(*,'(1A\)') CLEAR
C     IF ((RSPAVG.EQ.'Y').OR.(RSPAVG.EQ.'y')) THEN
C      IPOS(8)=45
C      IF (MINCH.GE.MAXCH) THEN
C         WRITE(*,'(10A\)') ESC,'[8;8fChannel range for average',
C     $    ' (min,max): ',REVIDEO,'    ',CLEAR,',',REVIDEO,'    ',CLEAR
C      ELSE
C         WRITE(*,'(4A\)') ESC,
C     $      '[8;8fChannel range for average',
C     $      ' (min,max): ',BOLD
C        CALL PRTINT(MINCH)
C        WRITE(*,'(3A\)') CLEAR,' , ',BOLD
C        CALL PRTINT(MAXCH)
C        WRITE(*,'(1A\)') CLEAR
C      ENDIF
C
C     Response baseline correction
C     SUM=0.
C     DO 44 I=MINCH,MAXCH
C         SUM=SUM + R(I)
C44    CONTINUE
C      AVG = SUM/FLOAT(MAXCH-MINCH+1)
C     WRITE(*,*) ' AVERAGE =',AVG
C     DO 46 I=1,NPTS
C         R(I) = R(I) - AVG
C46    CONTINUE
C50    CONTINUE
C
C      ICURSOR=8
C      IREAL=0
C      CALL CHGVAL(IREAL,XVAL,MINCH,ICURSOR,IPOS,
C      $         BOLD,BLINK,CLEAR,ERASE)
C      IF ((MINCH.LE.0).OR.(MINCH.GE.NPTS)) THEN
C         MINCH=1
C         CALL SETPOS(ICURSOR,IPOS)
C         WRITE(*,'(2A\)') ERASE,BOLD
C         CALL PRTINT(MINCH)
C      ENDIF
C      WRITE(*,'(2A\)') CLEAR,' , '
C      ISAVE=IPOS(ICURSOR)
C      IPOS(ICURSOR)=ISAVE+7
C      CALL CHGVAL(IREAL,XVAL,MAXCH,ICURSOR,IPOS,
C      $         BOLD,BLINK,CLEAR,ERASE)
C      IPOS(ICURSOR)=ISAVE
C      IF ((MAXCH.LT.0).OR.(MAXCH.GT.NPTS)) THEN
C         MAXCH=0
C      ENDIF
C
C      IF (MINCH.GE.MAXCH) THEN
C           WRITE(*,'(4A\)') ESC,'[8;1f',ESC,'[K'
C         IPOS(8)=0
C         RSPAVG='N'
C         ICURSOR=7
C         CALL SETPOS(ICURSOR,IPOS)
C         WRITE(*,'(3A\)') BOLD,RSPAVG,CLEAR
C      ELSE
C          WRITE(*,'(4A\)') ESC,'[8;8fChannel range for average',
C     $               ' (min,max): ',BOLD
C         WRITE(*,'(1A\)') ERASE
C         CALL PRTINT(MINCH)
C         WRITE(*,'(3A\)') CLEAR,' , ',BOLD
C         CALL PRTINT(MAXCH)
C         WRITE(*,'(1A\)') CLEAR
C      ENDIF
C     ELSEIF ((RSPAVG.NE.'N').OR.(RSPAVG.NE.'n')) THEN
C         RSPAVG='N'
C            IPOS(8)=0
C         WRITE(*,'(3A\)') ESC,'[8;1f',ERASE
C         ICURSOR=7
C         CALL SETPOS(ICURSOR,IPOS)
C         WRITE(*,'(3A\)') BOLD,RSPAVG,CLEAR
C      ENDIF
C      ISCAN=80
C      GO TO 260
C
350    CONTINUE
C     channel to start fit
      IREAL=0
      ISAVE=NSTART
      CALL CHGVAL(IREAL,XVAL,NSTART,ICURSOR,IPOS,
       $         BOLD,BLINK,CLEAR,ERASE)
      IF (NSTART.LE.0) THEN
          IDRAW=0
          CALL PLTDAT(IDRAW,NSTART,Y,YFIT,CTD,NSTART,NPTS,CFIELD)
          WRITE(*,'(1X,3A\)') CLEAR,ESC,'[2J'
          CALL PRTHNU(DATFLE,RSPFLE,PLTFLE,LOTEMP)
          IF (NSTART.LE.0) THEN
              NSTART=0
              GO TO 350
          ENDIF
      ENDIF
      ISCAN=80
      GO TO 260
360    CONTINUE
C     # of components
      CALL CHGXPS(A)
      ISCAN=80
      GO TO 260
362    CONTINUE
C     lifetime #1
      IREAL=1
      XSAVE=ATAU1
      CALL CHGVAL(IREAL,ATAU1,IXVAL,ICURSOR,IPOS,
       $         BOLD,BLINK,CLEAR,ERASE)
      IF (ATAU1.LE.0) THEN
          CALL SETPOS(ICURSOR,IPOS)
          WRITE(*,'(2A\)') ERASE,BOLD
          ATAU1=XSAVE
          CALL PRTRL(ATAU1)
          WRITE(*,'(1A\)') CLEAR
      ENDIF
      ISAVE=IPOS(ICURSOR)
      IPOS(ICURSOR)=ISAVE+8
      CALL SETPOS(ICURSOR,IPOS)
      WRITE(*,'(1A\)') '('
      XTAU=ATAU1*CTD
      CALL PRTRL(XTAU)
      IPOS(ICURSOR)=ISAVE
      WRITE(*,'(1A\)') ' psec)'
      IF (IFIX1.GT.0) THEN
          ISAVE=IPOS(ICURSOR)
```

```
        IPOS(ICURSOR)=ISAVE+27
        CALL SETPOS(ICURSOR,IPOS)
        WRITE(*,'(2A\)') CLEAR,'constrained'
        IPOS(ICURSOR)=ISAVE
      ENDIF
      ISCAN=80
      GO TO 260
364   CONTINUE
C     lifetime #2
      IREAL=1
      XSAVE=ATAU2
      CALL CHGVAL(IREAL,ATAU2,IXVAL,ICURSOR,IPOS,
     $        BOLD,BLINK,CLEAR,ERASE)
      IF (ATAU2.LE.0) THEN
        CALL SETPOS(ICURSOR,IPOS)
        WRITE(*,'(2A\)') ERASE,BOLD
        ATAU2=XSAVE
        CALL PRTRL(ATAU2)
        WRITE(*,'(1A\)') CLEAR
      ENDIF
      ISAVE=IPOS(ICURSOR)
      IPOS(ICURSOR)=ISAVE+8
      CALL SETPOS(ICURSOR,IPOS)
      WRITE(*,'(1A\)') '('
      XTAU=ATAU2*CTD
      CALL PRTRL(XTAU)
      IPOS(ICURSOR)=ISAVE
      WRITE(*,'(1A\)') ' psec)'
      IF (IFIX1.GT.1) THEN
        ISAVE=IPOS(ICURSOR)
        IPOS(ICURSOR)=ISAVE+27
        CALL SETPOS(ICURSOR,IPOS)
        WRITE(*,'(2A\)') CLEAR,'constrained'
        IPOS(ICURSOR)=ISAVE
      ENDIF
      ISCAN=80
      GO TO 260
366   CONTINUE
C     lifetime #3
      IREAL=1
      XSAVE=ATAU3
      CALL CHGVAL(IREAL,ATAU3,IXVAL,ICURSOR,IPOS,
     $        BOLD,BLINK,CLEAR,ERASE)
      IF (ATAU3.LE.0) THEN
        CALL SETPOS(ICURSOR,IPOS)
        WRITE(*,'(2A\)') ERASE,BOLD
        ATAU3=XSAVE
        CALL PRTRL(ATAU3)
        WRITE(*,'(1A\)') CLEAR
      ENDIF
      ISAVE=IPOS(ICURSOR)
      IPOS(ICURSOR)=ISAVE+8
      CALL SETPOS(ICURSOR,IPOS)
      WRITE(*,'(1A\)') '('
      XTAU=ATAU3*CTD
      CALL PRTRL(XTAU)
      WRITE(*,'(1A\)') ' psec)'
      IPOS(ICURSOR)=ISAVE
      ISCAN=80
      GO TO 260
368   CONTINUE
C     fraction 2/1
      WRITE(*,'(2A,F5.2,2A\)') BOLD,BLINK,FRAC21,CLEAR,BOLD
      CALL SETPOS(ICURSOR,IPOS)
      CALL RDVAL(XVAL,IXVAL,IWARN)
      IF ((IWARN.LT.0).OR.(XVAL.LT.0)) THEN
        GO TO 368
      ELSEIF (IWARN.GT.0) THEN
        FRAC21=XVAL
      ENDIF
      CALL SETPOS(ICURSOR,IPOS)
      WRITE(*,'(1A\)') ERASE
      WRITE(*,'(F5.2,1A\)') FRAC21,CLEAR
C
      ISAVE=IPOS(ICURSOR)
      IPOS(ICURSOR)=ISAVE+8
      CALL SETPOS(ICURSOR,IPOS)
      WRITE(*,'(1A\)') '('
      IF (NTAUS.EQ.2) THEN
        XPRCNT=(FRAC21/(FRAC21+1))*100.
        CALL PRTRL(XPRCNT)
        WRITE(*,'(1A\)') '%)'
        IPOS(ICURSOR)=ISAVE
      ELSE
        XPRCNT=(FRAC21/(FRAC21+FRAC31+1))*100.
        CALL PRTRL(XPRCNT)
        WRITE(*,'(1A\)') '%)'
        IPOS(ICURSOR)=ISAVE
C     update FRAC31 percentage also
        ICURSOR=17
        ISAVE=IPOS(ICURSOR)
        IPOS(ICURSOR)=ISAVE+8
        CALL SETPOS(ICURSOR,IPOS)
        WRITE(*,'(1A\)') '('
        XPRCNT=(FRAC31/(FRAC21+FRAC31+1))*100.
        CALL PRTRL(XPRCNT)
        WRITE(*,'(1A\)') '%)'
        IPOS(ICURSOR)=ISAVE
      ENDIF
C
      A(7)=FRAC21
      ISCAN=80
      GO TO 260
370   CONTINUE
C     fraction 3/1
      WRITE(*,'(2A,F5.2,2A\)') BOLD,BLINK,FRAC31,CLEAR,BOLD
      CALL SETPOS(ICURSOR,IPOS)
      CALL RDVAL(XVAL,IXVAL,IWARN)
      IF ((IWARN.LT.0).OR.(XVAL.LT.0)) THEN
        GO TO 370
      ELSEIF (IWARN.GT.0) THEN
        FRAC31=XVAL
      ENDIF
      CALL SETPOS(ICURSOR,IPOS)
      WRITE(*,'(1A\)') ERASE
      WRITE(*,'(F5.2,1A\)') FRAC31,CLEAR
C
      ISAVE=IPOS(ICURSOR)
      IPOS(ICURSOR)=ISAVE+8
      CALL SETPOS(ICURSOR,IPOS)
      WRITE(*,'(1A\)') '('
      XPRCNT=(FRAC31/(FRAC21+FRAC31+1))*100.
```

```
      CALL PRTRL(XPRCNT)
      WRITE(*,'(1A\)') '%)'
      IPOS(ICURSOR)=ISAVE
C           update FRAC21 percentage also
      ICURSOR=16
      ISAVE=IPOS(ICURSOR)
      IPOS(ICURSOR)=ISAVE+8
      CALL SETPOS(ICURSOR,IPOS)
      WRITE(*,'(1A\)') '('
      XPRCNT=(FRAC21/(FRAC21+FRAC31+1))*100.
      CALL PRTRL(XPRCNT)
      WRITE(*,'(1A\)') '%)'
      IPOS(ICURSOR)=ISAVE
C
      A(8)=FRAC31
      ISCAN=80
      GO TO 260
C
C
375     CONTINUE
C     fix lifetime #
      IFIX=IFIX1
      IREAL=0
      CALL CHGVAL(IREAL,XVAL,IFIX,ICURSOR,IPOS,
     $         BOLD,BLINK,CLEAR,ERASE)
      IF ((IFIX.LT.1).OR.(IFIX.GT.3)) THEN
          ICURSOR=13
          DO 377 K=1,3
              ISAVE=IPOS(ICURSOR)
              IPOS(ICURSOR)=ISAVE+27
              CALL SETPOS(ICURSOR,IPOS)
              WRITE(*,'(1A\)') ERASE
              IPOS(ICURSOR)=ISAVE
              ICURSOR=ICURSOR+1
377         CONTINUE
          ICURSOR=18
          CALL SETPOS(ICURSOR,IPOS)
          IFIX1=0
          WRITE(*,'(1A,I1,1A\)') BOLD,IFIX1,CLEAR
      ELSE
C          a valid entry was read
          IF (NTAUS.EQ.2) THEN
              IFIX1=1
              CALL SETPOS(ICURSOR,IPOS)
              WRITE(*,'(1A,I1,1A\)') BOLD,IFIX1,CLEAR
          ELSE
              IF (IFIX.EQ.1) THEN
                  IFIX1=1
                  ICURSOR=14
                  ISAVE=IPOS(ICURSOR)
                  IPOS(ICURSOR)=ISAVE+27
                  CALL SETPOS(ICURSOR,IPOS)
                  WRITE(*,'(1A\)') ERASE
                  IPOS(ICURSOR)=ISAVE
              ELSE
                  IFIX1=2
                  CALL SETPOS(ICURSOR,IPOS)
                  WRITE(*,'(1A,I1,1A\)') BOLD,IFIX1,CLEAR
                  ICURSOR=14
                  ISAVE=IPOS(ICURSOR)
                  IPOS(ICURSOR)=ISAVE+27
                  CALL SETPOS(ICURSOR,IPOS)
                  WRITE(*,'(2A\)') CLEAR,'constrained'
                  IPOS(ICURSOR)=ISAVE
              ENDIF
          ENDIF
          ICURSOR=13
          ISAVE=IPOS(ICURSOR)
          IPOS(ICURSOR)=ISAVE+27
          CALL SETPOS(ICURSOR,IPOS)
          WRITE(*,'(2A\)') CLEAR,'constrained'
          IPOS(ICURSOR)=ISAVE
          ICURSOR=18
          CALL SETPOS(ICURSOR,IPOS)
      ENDIF
      IF (NTAUS.EQ.2) THEN
          IF (IFIX1.GT.0) THEN
              ISTART=3
          ELSE
              ISTART=2
          ENDIF
          ISTOP=7
      ELSE
          IF (IFIX1.EQ.0) THEN
              ISTART=1
          ELSEIF (IFIX1.EQ.1) THEN
              ISTART=2
          ELSE
              ISTART=3
          ENDIF
          ISTOP=8
      ENDIF
      ISCAN=80
      GO TO 260
380     CONTINUE
C     baseline estimate
      IREAL=1
      CALL CHGVAL(IREAL,BSLNE,IXVAL,ICURSOR,IPOS,
     $         BOLD,BLINK,CLEAR,ERASE)
      CALL SETPOS(ICURSOR,IPOS)
      WRITE(*,'(2A\)') ERASE,BOLD
      CALL PRTRL(BSLNE)
      WRITE(*,'(1A\)') CLEAR
      A(4)=BSLNE
      ISCAN=80
      GO TO 260
C
390     CONTINUE
C     constrain baseline???
      CALL CHRALTR(BLLWT,ICURSOR,IPOS,BOLD,BLINK,CLEAR)
391     CONTINUE
      WRITE(*,'(1A\)') CLEAR
      IF ((BLLWT.EQ.'Y').OR.(BLLWT.EQ.'y')) THEN
       IPOS(21)=35
       IF (MINBL.GE.MAXBL) THEN
            WRITE(*,'(10A\)') ESC,'[21;8f',
       $          'Baseline limits (min,max): ',REVIDEO,'     ',CLEAR,
       $          ',',REVIDEO,'     ',CLEAR
       ELSE
          WRITE(*,'(2A\)') ESC,'[21;8fBaseline limits (min,max): '
         WRITE(*,'(1A\)') BOLD
         CALL PRTINT(MINBL)
```

```
      WRITE(*,'(3A\)') CLEAR,' , ',BOLD
      CALL PRTINT(MAXBL)
      WRITE(*,'(1A\)') CLEAR
    ENDIF
    ICURSOR=21
    IREAL=0
    CALL CHGVAL(IREAL,XVAL,MINBL,ICURSOR,IPOS,
    $        BOLD,BLINK,CLEAR,ERASE)
    WRITE(*,'(1A\)') ' , '
    ISAVE=IPOS(ICURSOR)
    IPOS(ICURSOR)=ISAVE+7
    CALL CHGVAL(IREAL,XVAL,MAXBL,ICURSOR,IPOS,
    $        BOLD,BLINK,CLEAR,ERASE)
    IPOS(ICURSOR)=ISAVE
C
    IF (MINBL.GE.MAXBL) THEN
        WRITE(*,'(3A\)') ESC,'[21;1f',ERASE
      IPOS(21)=0
      BLLMT='N'
      ICURSOR=20
      CALL SETPOS(ICURSOR,IPOS)
      WRITE(*,'(3A\)') BOLD,BLLMT,CLEAR
    ELSE
      WRITE(*,'(3A\)') ESC,'[21;1f',ERASE
        WRITE(*,'(2A\)') ESC,'[21;8fBaseline limits (min,max): ',
      WRITE(*,'(1A\)') BOLD
       CALL PRTINT(MINBL)
       WRITE(*,'(3A\)') CLEAR,' , ',BOLD
       CALL PRTINT(MAXBL)
       WRITE(*,'(1A\)') CLEAR
    ENDIF
   ELSEIF ((BLLMT.NE.'N').OR.(BLLMT.NE.'n')) THEN
      BLLMT='N'
        IPOS(21)=0
      WRITE(*,'(3A\)') ESC,'[21;1f',ERASE
      ICURSOR=20
      CALL SETPOS(ICURSOR,IPOS)
      WRITE(*,'(3A\)') BOLD,BLLMT,CLEAR
   ENDIF
   ISCAN=80
   GO TO 260
C
400   CONTINUE
C    lamp-shift estimate
   IREAL=1
   CALL CHGVAL(IREAL,SHIFT,IXVAL,ICURSOR,IPOS,
    $        BOLD,BLINK,CLEAR,ERASE)
   CALL SETPOS(ICURSOR,IPOS)
   WRITE(*,'(2A\)') ERASE,BOLD
   CALL PRTRL(SHIFT)
   WRITE(*,'(1A\)') CLEAR
   A(5)=SHIFT
   ISCAN=80
   GO TO 260
410   CONTINUE
C    estimated amplitude
   IREAL=1
   XSAVE=AMPEST
   CALL CHGVAL(IREAL,XSAVE,IXVAL,ICURSOR,IPOS,
    $        BOLD,BLINK,CLEAR,ERASE)
   IF (XSAVE.LE.0) THEN
      GO TO 410
   ELSE
      CALL SETPOS(ICURSOR,IPOS)
      WRITE(*,'(2A\)') ERASE,BOLD
      AMPEST=XSAVE
      CALL PRTRL(AMPEST)
      WRITE(*,'(1A\)') CLEAR
   ENDIF
   A(6)=AMPEST
   ISCAN=80
   GO TO 260
C
420   CONTINUE
C       estimate amplitude
   WRITE(*,'(4A\)') BOLD,ESC,'[23;5f',
    $       'Estimating amplitude. . . . . '
   IF (LOTEMP) THEN
      CALL LNLOTMP(NANGS,NTAUS,A,NPTS,Y,R,RSUM)
   ELSE
      CALL LNNEW(NTAUS,A,NPTS,Y,R,RSUM)
   ENDIF
    AMPEST=A(6)
   ICURSOR=23
   IPOS(ICURSOR)=26
   WRITE(*,'(4A\)') CLEAR,ESC,'[23;5f',ERASE
   WRITE(*,'(4A\)') ESC,'[23;5f',
    $       'Estimated amplitude: ',BOLD
   CALL PRTRL(AMPEST)
   WRITE(*,'(1A\)') CLEAR
450   CONTINUE
   IREAL=1
   XSAVE=AMPEST
   CALL CHGVAL(IREAL,XSAVE,IXVAL,ICURSOR,IPOS,
    $        BOLD,BLINK,CLEAR,ERASE)
   IF (XSAVE.LE.0) THEN
      GO TO 450
   ELSE
      CALL SETPOS(ICURSOR,IPOS)
      WRITE(*,'(2A\)') ERASE,BOLD
      AMPEST=XSAVE
      CALL PRTRL(AMPEST)
      WRITE(*,'(1A\)') CLEAR
   ENDIF
   A(6)=AMPEST
800   CONTINUE
   IF (NTAUS.EQ.1) THEN
      A(3)=ATAU1
      ISTART=3
      ISTOP=6
   ELSEIF(NTAUS.EQ.2) THEN
      A(2)=ATAU1
      A(3)=ATAU2
      IF (IFIX1.GT.0) THEN
          ISTART=3
      ELSE
          ISTART=2
      ENDIF
      ISTOP=7
   ELSE
      A(1)=ATAU1
      A(2)=ATAU2
```

```
      A(3)=ATAU3
      IF (IFIX1.EQ.0) THEN
          ISTART=1
      ELSEIF (IFIX1.EQ.1) THEN
          ISTART=2
      ELSE
          ISTART=3
      ENDIF
      ISTOP=8
    ENDIF
    A(4)=BSLNE
    A(5)=SHIFT
    A(6)=AMPEST
    A(7)=FRAC21
    A(8)=FRAC31

    RETURN
    END
C
C
C
     SUBROUTINE CKRSLT(A,DATFILE,RSPFILE,PLTFILE)
C
C    FUNCTION:
C        OUTPUTS THE VALUES OF THE VARIOUS ARRAYS AND
C        VALUES OF PARAMETERS IN THE COMMON BLOCKS
C        ONLY CALLED IN SUPERFIT DEBUG MODE
C
    DIMENSION A(8)
    CHARACTER*1 BRTSCR,ANS,RSPAVG,BLLMT,ESC
    CHARACTER*3 ERASE
    CHARACTER*4 REVIDEO,BOLD,BLINK
    CHARACTER*7 CLEAR
    CHARACTER*35 DATFILE,RSPFILE,PLTFILE
    CHARACTER*72 CFIELD
    COMMON /CHRDAT/ CFIELD,RSPAVG,BLLMT,ESC,CLEAR,
     $         REVIDEO,BOLD,BLINK,ERASE
    COMMON /NUMDAT/ NPTS,ITOT,MINCH,MAXCH,NSTART,NTAUS,ISTART,ISTOP,
     $         ATAU1,ATAU2,ATAU3,FRAC21,FRAC31,IFIX1,BSLNE,
     $         MINBL,MAXBL,SHIFT,AMPEST,CTD,XMAX,YMAX,IYMAXCH,
     $         NANGS,IPOS(25)
C
    WRITE(*,'(1X,3A)') CLEAR,ESC,'[2J'
    WRITE(*,*) ' '
    WRITE(*,*) ' '
    WRITE(*,*) NTAUS,ATAU1,ATAU2,ATAU3,FRAC21,FRAC31
    WRITE(*,*) (A(I),I=1,4)
    WRITE(*,*) (A(I),I=5,8)
    WRITE(*,*) ISTART,ISTOP
    WRITE(*,*) ' '
    WRITE(*,*) DATFILE
    WRITE(*,*) RSPFILE
    WRITE(*,*) PLTFILE
    WRITE(*,'(4A)') ' RSPAVG= ',RSPAVG,' BLLMT= ',BLLMT
    WRITE(*,*) MINCH,MAXCH,MINBL,MAXBL
    WRITE(*,*) NSTART,NPTS,ITOT
        WRITE(*,*) IFIX1,IFIX2
    WRITE(*,*) BSLNE,SHIFT,AMPEST,CTD,YMAX,IYMAXCH
    RETURN
    END
C
C
C
     SUBROUTINE FDLOTWP(I,A,DERIV,N)
C
C    FUNCTION:
C        CALUCULATES THE ANALYTICAL DERIVATIVES FOR THE
C        FREE PARAMETERS IN THE ANGLE--MODULATED BIEXPONENTIAL
C        DECAY ANALYSIS
C
    DOUBLE PRECISION DERIV(1)
    DIMENSION A(1),TAU(3),EA(3),DA(3),F(9),
     $         F1(30),F2(30),F3(30),F4(30),CEA(30),XDA(30),CDA(30)
        CHARACTER*1 ESC,RSPAVG,BLLMT
    CHARACTER*3 ERASE
    CHARACTER*4 REVIDEO,BOLD,BLINK
    CHARACTER*7 CLEAR
    CHARACTER*72 CFIELD
    COMMON /R1/ R(1024),RSUM
    COMMON /FIT/ YFIT(1024)
    COMMON /DRV/ R1,R2,R3,F,EA,DA
    COMMON /DRV2/ F1,F2,F3,F4,CEA,CDA,XDA,FF1,FF2,FF3,FF4
    COMMON /CHRDAT/ CFIELD,RSPAVG,BLLMT,ESC,CLEAR,
     $         REVIDEO,BOLD,BLINK,ERASE
    COMMON /NUMDAT/ NPTS,ITOT,MINCH,MAXCH,NSTART,NTAUS,ISTART,ISTOP,
     $         ATAU1,ATAU2,ATAU3,FRAC21,FRAC31,IFIX1,BSLNE,
     $         MINBL,MAXBL,SHIFT,AMPEST,CTD,XMAX,YMAX,IYMAXCH,
     $         NANGS,IPOS(25)
    COMMON /FLAG/ IOVRFLO
    RESP(X)=((1.+AINT(X)-X)*R(INT(X))+(X-AINT(X))*R(INT(X)+1))/RSUM
    PI=3.14159
C
    TMIN=1.
    TMAX=1022.
    IF ((BLLMT.EQ.'Y').OR.(BLLMT.EQ.'y')) THEN
        A(4)=AMAX1(FLOAT(MINBL),A(4))
        A(4)=AMIN1(FLOAT(MAXBL),A(4))
    ENDIF
C
    A(7)=AMAX1(A(7),0.)
C
    DO 70 J=1,8
        DERIV(J)=0.0D0
70    CONTINUE
    DERIV(4)=1.0D0
C
5     CONTINUE
    IF (I-N) 10,10,175
10    CONTINUE
C
    NTAUS=2
    IF (NANGS.EQ.1) THEN
        NANGS=0
    ENDIF
    XANGS=FLOAT(NANGS)
    XANGS=AMAX1(XANGS,1.)
    FF1=0.
    FF2=0.
    FF3=0.
    FF4=0.
    DO 15 J=1,30
        F1(J)=0.
```

```
        F2(J)=0.
        F3(J)=0.
        F4(J)=0.
15    CONTINUE
C
      DO 50 J=1,3
          TAU(J)=0.
          EA(J)=0.
          DA(J)=0.
50    CONTINUE
      DO 60 J=1,9
          F(J)=0.
60    CONTINUE
C
C
      IF (NTAUS.EQ.1) THEN
          TAU(1)=A(3)
      ELSEIF (NTAUS.EQ.2) THEN
          TAU(1)=A(2)
          TAU(2)=A(3)
      ELSE
          TAU(1)=A(1)
          TAU(2)=A(2)
          TAU(3)=A(3)
      ENDIF
C
      DO 120 J=1,NTAUS
          EA(J)=EXP(-1./TAU(J))
          DA(J)=((1./TAU(J))**2)*EA(J)
120   CONTINUE
C
      DO 125 K=1,(NANGS+1)
          RANG=FLOAT(K-1)*PI/(2*XANGS)
          COS2ANG=(COS(RANG))**2
          CEA(K)=EXP(-1*(COS2ANG*(1/TAU(1))+(1/TAU(2))))
C          XDA(K)=((1/TAU(2))**2)*(CEA(K)+EA(2))
          XDA(K)=((1/TAU(2))**2)*CEA(K)
          CDA(K)=((1/TAU(1))**2)*CEA(K)*COS2ANG
125   CONTINUE
C
      TO=A(5)
      TO=AMIN1(TO,TMAX)
      TO=AMAX1(TO,TMIN)
      R1=0.
      R2=0.
      R3=RESP(TO)
      DO 150 J=1,N
          T=FLOAT(J)+A(5)
          T=AMAX1(T,TMIN)
          T=AMIN1(T,TMAX)
          R1=R2
          R2=R3
          R3=RESP(T)
          DR=0.5*(R3-R1)
          DO 140 K=2,NTAUS
              IPT=3*K
              F(IPT-2)=F(IPT-2)*EA(K)+F(IPT-1)*DA(K)
              F(IPT-1)=F(IPT-1)*EA(K)+R2
              F(IPT)=F(IPT)*EA(K)+DR
140           CONTINUE
          FF1=FF1*EA(2) + DA(2)*FF2
          FF2=FF2*EA(2) + R2
          FF4=FF4*EA(2) + DR
          DO 145 K=1,(NANGS+1)
              F1(K)=F1(K)*CEA(K) + F2(K)*XDA(K)
              F3(K)=F3(K)*CEA(K) + F2(K)*CDA(K)
              F2(K)=F2(K)*CEA(K) + R2
              F4(K)=F4(K)*CEA(K) + DR
145           CONTINUE
C
150   CONTINUE
      GO TO 200
175   CONTINUE
      T=FLOAT(I)+A(5)
      T=AMIN1(T,TMAX)
      T=AMAX1(T,TMIN)
      R1=R2
      R2=R3
      R3=RESP(T)
      DR=0.5*(R3-R1)
      DO 180 K=2,NTAUS
          IPT=3*K
          F(IPT-2)=F(IPT-2)*EA(K)+F(IPT-1)*DA(K)
          F(IPT-1)=F(IPT-1)*EA(K)+R2
          F(IPT)=F(IPT)*EA(K)+DR
180   CONTINUE
      FF1=FF1*EA(2) + DA(2)*FF2
      FF2=FF2*EA(2) + R2
      FF4=FF4*EA(2) + DR
      DO 190 K=1,(NANGS+1)
          F1(K)=F1(K)*CEA(K) + F2(K)*XDA(K)
          F3(K)=F3(K)*CEA(K) + F2(K)*CDA(K)
          F2(K)=F2(K)*CEA(K) + R2
          F4(K)=F4(K)*CEA(K) + DR
190   CONTINUE
200   CONTINUE
C
      XANGS=FLOAT(NANGS)
      YFIT(I)=0.
      DO 300 K=1,(NANGS+1)
          SCALE=1.0
          IF (K.EQ.1) SCALE=0.5
          IF (K.EQ.(NANGS+1)) SCALE=0.5
          YFIT(I)=YFIT(I)+A(6)*F2(K)*SCALE
          DERIV(2)=DERIV(2)+DBLE(SCALE*A(6)*F3(K))
          DERIV(3)=DERIV(3)+DBLE(SCALE*A(6)*F1(K))
          DERIV(5)=DERIV(5)+DBLE(SCALE*A(6)*F4(K))
          DERIV(6)=DERIV(6)+DBLE(SCALE*F2(K))
300   CONTINUE
C
      DERIV(3)=DERIV(3)+DBLE(XANGS*A(6)*A(7)*FF1)
      DERIV(5)=DERIV(5)+DBLE(XANGS*A(6)*A(7)*FF4)
      DERIV(6)=DERIV(6)+DBLE(XANGS*A(7)*FF2)
      DERIV(7)=DBLE(XANGS*A(6)*FF2)
C
      YFIT(I)=YFIT(I)+(XANGS*A(6)*A(7)*FF2)+A(4)
C
C     YFIT(I)=A(6)*(F(2)+(A(7)*F(5))+(A(8)*F(8)))+A(4)
C     IF (NTAUS.EQ.1) THEN
C         DERIV(3)=DBLE(A(6)*F(1))
C     ELSEIF (NTAUS.EQ.2) THEN
C         DERIV(2)=DBLE(A(6)*F(1))
```

```
C         DERIV(3)=DBLE(A(6)*A(7)*F(4))
C      ELSE
C         DERIV(1)=DBLE(A(6)*F(1))
C         DERIV(2)=DBLE(A(6)*A(7)*F(4))
C         DERIV(3)=DBLE(A(6)*A(8)*F(7))
C      ENDIF
C      DERIV(5)=DBLE(A(6)*(F(3)+A(7)*F(6)+A(8)*F(9)))
C      DERIV(6)=DBLE(F(2)+A(7)*F(5)+A(8)*F(8))
C      DERIV(7)=DBLE(A(6)*F(5))
C      DERIV(8)=DBLE(A(6)*F(8))
       RETURN
       END
C
C
C
       SUBROUTINE LNLOTMP(NANGS,NTAUS,A,NPTS,Y,R,RSUM)
C
C      FUNCTION:
C           ESTIMATES THE INITIAL AMPLITUDE FOR THE
C           ANGLE--MODULATED DECAY ANALYSIS BASED ON THE
C           INITIAL ESTIMATES OF THE FIT PARAMETERS
C
       DIMENSION A(1),Y(1),R(1)
       DIMENSION F(3),EA(3),TAU(3),SCR1(31),CEA(31)
C
       RESP(T)=((1.+AINT(T)-T)*R(INT(T))+(T-AINT(T))*R(INT(T)+1))/RSUM
C
       PI=3.14159
       XANGS=FLOAT(NANGS)
C
       DO 10 I=1,3
           TAU(I)=0.
           EA(I)=0.
           F(I)=0.
10     CONTINUE
       IF (NTAUS.EQ.1) THEN
           TAU(1)=A(3)
       ELSEIF (NTAUS.EQ.2) THEN
           TAU(1)=A(2)
           TAU(2)=A(3)
       ELSE
           TAU(1)=A(1)
           TAU(2)=A(2)
           TAU(3)=A(3)
       ENDIF
       BL=A(4)
       SHIFT=A(5)
       FRACT1=A(7)
       FRACT2=A(8)
       DO 20 J=1,NTAUS
           EA(J)=EXP(-1./TAU(J))
20     CONTINUE
       DO 40 K=1,(NANGS+1)
           SCR1(K)=0.
           RANG=FLOAT(K-1)*PI/(2*XANGS)
           COS2ANG=(COS(RANG))**2
           CEA(K)=EXP(-1*(COS2ANG*(1/TAU(1))+(1/TAU(2))))
40     CONTINUE
C
C
       FSUM=0.
       S1=0.
       S2=0.
       FF2=0.
       TMAX=1014.
       TMIN=1.
C
       DO 100 I=1,NPTS
           FO=Y(I)-BL
           FSUM=FSUM+FO
           T=FLOAT(I)+SHIFT
           T=AMIN1(T,TMAX)
           T=AMAX1(T,TMIN)
C
           S1=S1 + FO
           FF2=FF2*EA(2) + RESP(T)
           DO 60 K=1,(NANGS+1)
               SCR1(K)=SCR1(K)*CEA(K) + RESP(T)
               SCALE=1.0
               IF (K.EQ.1) SCALE=0.5
               IF (K.EQ.(NANGS+1)) SCALE=0.5
               S2=S2 + SCALE*SCR1(K)
60         CONTINUE
C
           S2=S2 + FRACT1*XANGS*FF2
C
100    CONTINUE
       A(6)=S1/S2
       RETURN
       END
C
C
C
       SUBROUTINE CUNEW(CUABORT,LOTEMP)
C
C      FUNCTION:
C           THIS ROUTINE IS THE HEART OF THE FITTING ROUTINE
C           AND PERFORMS ALL THE CRITICAL CALLS TO SUBROUTINES
C           TO INVERT THE CURVATURE MATRIX AND EVALUATE THE
C           ANALYTICAL DERIVATIVES FOR THE FIT PARAMETERS
C
       DOUBLE PRECISION FCHNEW,ALPHA(8,8),ALPHA1(8,8),DERIV(8),DSCR
       DOUBLE PRECISION BETA(8),BETA1(8),SIGMAA(8)
       DOUBLE PRECISION ARRAY(8,8),DET,CHISQR,CHISQ1
       DIMENSION Y(1024),A(8),YFIT(1024),B(8),F(9),EA(3),DA(3),
      $          F1(30),F2(30),F3(30),F4(30),CEA(30),CDA(30),XDA(30)
       LOGICAL*2 CUABORT,LOTEMP
           CHARACTER*1 ANS,ESC,RSPAVG,BLLNK
       CHARACTER*3 ERASE
       CHARACTER*4 REVIDEO,BOLD,BLINK
       CHARACTER*7 CLEAR
       CHARACTER*12 DATROOT,RSPROOT,PLTROOT
         CHARACTER*72 CFIELD
       COMMON /DATA/ Y
       COMMON /DRV/ R1,R2,R3,F,EA,DA
       COMMON /DRV2/ F1,F2,F3,F4,CEA,CDA,XDA,FF1,FF2,FF3,FF4
       COMMON /FIT/ YFIT
       COMMON /FLAG/ IOVRFLO
       COMMON /FILES/ DATROOT,RSPROOT,PLTROOT
       COMMON /RES/ A,CHISQR,CHISQ1,ITERNO,NTERMS
       COMMON /R1/ R(1024),RSUM
       COMMON SIGMAA,ALPHA,BETA,FLAMDA
```

```
      COMMON /CHRDAT/ CFIELD,RSPAVG,BLLNT,ESC,CLEAR,
     $         REVIDEO,BOLD,BLINK,ERASE
      COMMON /NUMDAT/ NPTS,ITOT,MINCH,MAXCH,NSTART,NTAUS,ISTART,ISTOP,
     $         ATAU1,ATAU2,ATAU3,FRAC21,FRAC31,IFIX1,BSLNE,
     $         MINBL,MAXBL,SHIFT,AMPEST,CTD,XMAX,YMAX,IYMAXCH,
     $         NANGS,IPOS(25)
C
C         initializations
C
C     WRITE(*,*) ' Entering CUNEW '
      CUABORT=.FALSE.
      DERIV(4) = 1.0D0
      NFREE = NPTS - (ISTOP - ISTART) - NSTART
      IF (ITERNO.GT.1) GO TO 40
      DO 20 J=1,NTERMS
          B(J) = A(J)
20     CONTINUE
      GO TO 180
C
C invert modified curvature matrix to find new parameters
C
40     DO 80 J=ISTART+1,ISTOP
         DO 60 K =ISTART,J-1
            DSCR=(ALPHA(J,J)*ALPHA(K,K))
            IF (DSCR.LT.0.0D0) THEN
                WRITE(*,*) ' DO 60 LOOP . .SQRT OF NEG ## IN CUNEW'
            ELSEIF (DSCR.EQ.0.0D0) THEN
                WRITE(*,*) ' DO 60 LOOP . .DIV BY ZERO IN CUNEW'
            ENDIF
            ARRAY(J,K)=ALPHA(J,K)/DSQRT(DSCR)
            ARRAY(K,J)=ARRAY(J,K)
60         CONTINUE
80     CONTINUE
90     CONTINUE
      DO 100 J=ISTART,ISTOP
         ARRAY(J,J)= DBLE(1.+FLAMDA)
         IF (ALPHA(J,J).EQ.0.0D0) THEN
             WRITE(*,*) ' DO 100 LOOP. .DIV BY 0 IN CUNEW'
         ENDIF
         SIGMAA(J) =DSQRT(ARRAY(J,J)/ALPHA(J,J))
100    CONTINUE
C     WRITE(*,*) ' Calling subroutine MATINV . .'
      CALL MATINV(ARRAY,ISTART,ISTOP,DET)
C     WRITE(*,*) ' Returned from subroutine MATINV . .'
      IF ((DABS(DET).LT.1.0D-200).OR.(DABS(DET).GT.1.0D+200)) THEN
         WRITE(*,*) '         CAUTION! OVERFLOW ERROR IMMINENT . . . '
         WRITE(*,*) '         DET= ',DET
         IOVRFLO = 1
      ENDIF
C     CHISQ1 = CHISQR
C     RETURN
C
140     DO 160 J=ISTART,ISTOP
        B(J)=A(J)
        DO 155 K=ISTART,ISTOP
           DSCR=(ALPHA(J,J)*ALPHA(K,K))
           IF (DSCR.LT.0.0D0) THEN
             WRITE(*,*) ' DO 155 LOOP . .SQRT OF NEG ## IN CUNEW'
               ELSEIF (DSCR.EQ.0.0D0) THEN
         WRITE(*,*) ' DO 155 LOOP . .DIV BY 0 IN CUNEW'
             ENDIF
          B(J)=B(J)+SNGL(BETA(K)*(ARRAY(J,K)/DSQRT(DSCR)))
155        CONTINUE
160     CONTINUE
C
C        EVALUATE ALPHA AND BETA MATRICES
C
180     DO 200  J=ISTART,ISTOP
         BETA1(J)=0.
         DO 190 K=ISTART,ISTOP
            ALPHA1(J,K)=0.
190        CONTINUE
200     CONTINUE
      DO 220 L=NSTART,NPTS
         IF (LOTEMP) THEN
            CALL FDLOTMP(L,B,DERIV,NSTART)
         ELSE
            CALL FDNEW(L,B,DERIV,NSTART)
         ENDIF
C
        DO 210 J=ISTART,ISTOP
           BETA1(J)=BETA1(J)+DERIV(J)*DBLE((1./Y(L))*(Y(L)-YFIT(L)))
           DO 205 K=ISTART,J
              ALPHA1(J,K)=ALPHA1(J,K)+DBLE(1./Y(L))*DERIV(J)*DERIV(K)
205           CONTINUE
210        CONTINUE
220     CONTINUE
C     WRITE(*,*) ' Evaluating new chi**2 '
C
C        evaluate chi-square at new point
C
240     CHISQR=FCHNEW(Y,YFIT,NFREE,NPTS,NSTART)
      IF (CHISQ1-CHISQR+0.0015) 260,280,280
C
C        if chi-square increased, increase flamda and retry
C
260     FLAMDA = (10.)*FLAMDA
      WRITE(*,270) ' Searching. . . . . .new chi',
     $                  CHAR(253),' = ',CHISQR
270     FORMAT(3A,F12.3)
271     CONTINUE
      CALL INKEY(ITEST,ISCAN,ANS)
      IF (ITEST.NE.0) THEN
          IF (ANS.EQ.CHAR(27)) THEN
C              clear type-ahead buffer
265              CALL INKEY(ITEST,ISCAN,ANS)
             IF (ITEST.NE.0) GO TO 265
             CUABORT=.TRUE.
             GO TO 360
          ELSE
              GO TO 271
          ENDIF
      ENDIF
      GO TO 90
C
C        evaluate parameters and uncertainties
C
280     CONTINUE
C     WRITE(*,'(1X,1A,8(F8.2,1X))') ' A-> ',(A(J),J=1,8)
C     WRITE(*,'(1X,1A,8(F8.2,1X))') ' B-> ',(B(J),J=1,8)
C     WRITE(*,'(1X,1A,8(F8.2,1X))') ' BETA-> ',(BETA(J),J=1,8)
C     WRITE(*,'(1X,1A,8(F8.2,1X))') ' BETA1-> ',(BETA1(J),J=1,8)
```

```
      DO 310 J=ISTART,ISTOP
       A(J)=B(J)
       BETA(J)=BETA1(J)
        DO 300 K=ISTART,J
           ALPHA(J,K)=ALPHA1(J,K)
300       CONTINUE
       IF (ALPHA(J,J).EQ.0.) ALPHA(J,J) = 1.
310    CONTINUE
    DO 350 I=ISTART,3
       IF (A(I).LE.0.) A(I) = 1.
350    CONTINUE
    FLAMDA=0.01*FLAMDA
    FLAMDA=AMAX1(0.001,FLAMDA)
360    CONTINUE
C    WRITE(*,*) ' Exiting CUNEW '
    RETURN
    END
C
C
C
C
C
    DOUBLE PRECISION FUNCTION FCHNEW(Y,YFIT,NFREE,NPTS,N)
    DOUBLE PRECISION X
    DIMENSION Y(1),YFIT(1)
    X=0.
    DO 100 I=N,NPTS
        X=X+(DBLE(Y(I)-YFIT(I)))**2/DBLE(ABS(Y(I)))
100    CONTINUE
    FCHNEW=X/DBLE(NFREE)
    RETURN
    END
C
C
C
    SUBROUTINE FDNEW(I,A,DERIV,N)
C
C    FUNCTION:
C        CALCULATES THE ANALYTICAL DERIVATIVES FOR EACH OF
C        THE FIT PARAMETERS FOR THE SINGLE, DOUBLE, OR TRIPLE
C        EXPONENTIAL DECAY ANALYSES
C
    DOUBLE PRECISION DERIV(1)
    DIMENSION A(1),TAU(3),EA(3),DA(3),F(9)
        CHARACTER*1 ESC,RSPAVG,BLLMT
    CHARACTER*3 ERASE
    CHARACTER*4 REVIDEO,BOLD,BLINK
    CHARACTER*7 CLEAR
    CHARACTER*72 CFIELD
    COMMON /R1/ R(1024),RSUM
    COMMON /FIT/ YFIT(1024)
    COMMON /DRV/ R1,R2,R3,F,EA,DA
    COMMON /CHRDAT/ CFIELD,RSPAVG,BLLMT,ESC,CLEAR,
     $        REVIDEO,BOLD,BLINK,ERASE
    COMMON /NUMDAT/ NPTS,ITOT,MINCH,MAXCH,NSTART,NTAUS,ISTART,ISTOP,
     $        ATAU1,ATAU2,ATAU3,FRAC21,FRAC31,IFIX1,BSLNE,
     $        MINBL,MAXBL,SHIFT,AMPEST,CTD,XMAX,YMAX,IYMAXCH,
     $        NANGS,IPOS(25)
    COMMON /FLAG/ IOVRFLO
    RESP(X)=((1.+AINT(X)-X)*R(INT(X))+(X-AINT(X))*R(INT(X)+1))/RSUM
C
    TMIN=1.
    TMAX=1022.
    IF ((BLLMT.EQ.'Y').OR.(BLLMT.EQ.'y')) THEN
        A(4)=AMAX1(FLOAT(MINBL),A(4))
        A(4)=AMIN1(FLOAT(MAXBL),A(4))
    ENDIF
5       CONTINUE
    IF (I-N) 10,10,175
10    CONTINUE
    DO 50 J=1,3
        TAU(J)=0.
        EA(J)=0.
        DA(J)=0.
50    CONTINUE
    DO 60 J=1,9
        F(J)=0.
60    CONTINUE
C
    IF (NTAUS.EQ.1) THEN
        DERIV(1)=0.0D0
        DERIV(2)=0.0D0
        TAU(1)=A(3)
    ELSEIF (NTAUS.EQ.2) THEN
        DERIV(1)=0.0D0
        TAU(1)=A(2)
        TAU(2)=A(3)
    ELSE
        TAU(1)=A(1)
        TAU(2)=A(2)
        TAU(3)=A(3)
    ENDIF
C
    DO 120 J=1,NTAUS
        EA(J)=EXP(-1./TAU(J))
        DA(J)=((1./TAU(J))**2)*EA(J)
120    CONTINUE
C
    TO=A(5)
    TO=AMIN1(TO,TMAX)
    TO=AMAX1(TO,TMIN)
    R1=0.
    R2=0.
    R3=RESP(TO)
    DO 150 J=1,N
        T=FLOAT(J)+A(5)
        T=AMAX1(T,TMIN)
        T=AMIN1(T,TMAX)
        R1=R2
        R2=R3
        R3=RESP(T)
        DR=0.5*(R3-R1)
        DO 140 K=1,NTAUS
            IPT=3*K
            F(IPT-2)=F(IPT-2)*EA(K)+F(IPT-1)*DA(K)
            F(IPT-1)=F(IPT-1)*EA(K)+R2
            F(IPT)=F(IPT)*EA(K)+DR
140        CONTINUE
150    CONTINUE
    GO TO 200
175    CONTINUE
    T=FLOAT(I)+A(5)
```

```
      T=AMIN1(T,TMAX)
      T=AMAX1(T,TMIN)
      R1=R2
      R2=R3
      R3=RESP(T)
      DR=0.5*(R3-R1)
      DO 180 K=1,NTAUS
          IPT=3*K
          F(IPT-2)=F(IPT-2)*EA(K)+F(IPT-1)*DA(K)
          F(IPT-1)=F(IPT-1)*EA(K)+R2
          F(IPT)=F(IPT)*EA(K)+DR
180     CONTINUE
200     CONTINUE
      YFIT(I)=A(6)*(F(2)+(A(7)*F(5))+(A(8)*F(8)))+A(4)
      IF (NTAUS.EQ.1) THEN
          DERIV(3)=DBLE(A(6)*F(1))
      ELSEIF (NTAUS.EQ.2) THEN
          DERIV(2)=DBLE(A(6)*F(1))
          DERIV(3)=DBLE(A(6)*A(7)*F(4))
      ELSE
          DERIV(1)=DBLE(A(6)*F(1))
          DERIV(2)=DBLE(A(6)*A(7)*F(4))
          DERIV(3)=DBLE(A(6)*A(8)*F(7))
      ENDIF
      DERIV(5)=DBLE(A(6)*(F(3)+A(7)*F(6)+A(8)*F(9)))
      DERIV(6)=DBLE(F(2)+A(7)*F(5)+A(8)*F(8))
      DERIV(7)=DBLE(A(6)*F(5))
      DERIV(8)=DBLE(A(6)*F(8))
      RETURN
      END
C
C
C
      SUBROUTINE LNNEW(NTAUS,A,NPTS,Y,R,RSUM)
C
C     FUNCTION:
C          CALCULATES AN ESTIMATE FOR THE INITIAL AMPLITUDE
C          BASED ON THE INITIAL PARAMETER ESTIMATES IN THE A ARRAY
C
C
      DIMENSION A(1),Y(1),R(1)
      DIMENSION F(3),EA(3),TAU(3)
C
      RESP(T)=((1.+AINT(T)-T)*R(INT(T))+(T-AINT(T))*R(INT(T)+1))/RSUM
C
      DO 10 I=1,3
          TAU(I)=0.
          EA(I)=0.
          F(I)=0.
10      CONTINUE
      IF (NTAUS.EQ.1) THEN
          TAU(1)=A(3)
      ELSEIF (NTAUS.EQ.2) THEN
          TAU(1)=A(2)
          TAU(2)=A(3)
      ELSE
          TAU(1)=A(1)
          TAU(2)=A(2)
          TAU(3)=A(3)
      ENDIF
      BL=A(4)
      SHIFT=A(5)
      FRACT1=A(7)
      FRACT2=A(8)
      DO 20 J=1,NTAUS
          EA(J)=EXP(-1./TAU(J))
20    CONTINUE
      FSUM=0.
      S1=0.
      TMAX=1014.
      TMIN=1.
C
      DO 100 I=1,NPTS
          FO=Y(I)-BL
          FSUM=FSUM+FO
          T=FLOAT(I)+SHIFT
          T=AMIN1(T,TMAX)
          T=AMAX1(T,TMIN)
          DO 80 J=1,NTAUS
              F(J)=F(J)*EA(J)+RESP(T)
80        CONTINUE
          S1=S1+F(1)+F(2)*FRACT1+F(3)*FRACT2
100     CONTINUE
      A(6)=FSUM/S1
      RETURN
      END
C
C
C
      SUBROUTINE MATINV (ARRAY,ISTART,ISTOP,DET)
C
C         SUBROUTINE MATINV FROM
C         P.R. BEVINGTON'S
C               "DATA REDUCTION AND ERROR ANALYSIS FOR THE
C         PHYSICAL SCIENCES",MCGRAW-HILL,1969,PP301-303.
C
C     FUNCTION:
C         MATRIX INVERSION SUBROUTINE
C
      DOUBLE PRECISION ARRAY,AMAX,SAVE,DET
      DIMENSION ARRAY(8,8),IK(8),JK(8)
C     WRITE(*,*) ' ISTART= ',ISTART,' ISTOP= ',ISTOP
100     DET = 1.0D0
110     DO 1000 K=ISTART,ISTOP
C
C         FIND LARGEST ELEMENT ARRAY(I,J) IN REST OF MATRIX
C
      AMAX=0.0D0
210     DO 305 I=K,ISTOP
          DO 300 J=K,ISTOP
230           IF (DABS(AMAX)-DABS(ARRAY(I,J))) 240,240,300
240           AMAX=ARRAY(I,J)
              IK(K)=I
              JK(K)=J
300         CONTINUE
305     CONTINUE
C
C         INTERCHANGE ROWS AND COLS TO PUT AMAX IN ARRAY(K,K)
C
310     IF (AMAX) 410,320,410
320     DET = 0.0D0
      GO TO 1400
```

```
410     I=IK(K)
    IF (I-K) 210,510,430
430     DO 500 J=ISTART,ISTOP
         SAVE=ARRAY(K,J)
         ARRAY(K,J)=ARRAY(I,J)
            ARRAY(I,J)=-SAVE
500     CONTINUE
510     J=JK(K)
    IF (J-K) 210,610,530
530     DO 600 I=ISTART,ISTOP
         SAVE=ARRAY(I,K)
         ARRAY(I,K)=ARRAY(I,J)
         ARRAY(I,J)=-SAVE
600     CONTINUE
C
C         ACCUMULATE ELEMENTS OF INVERSE MATRIX
C
610     DO 700 I=ISTART,ISTOP
         IF (I-K) 630,700,630
630         ARRAY(I,K)=-ARRAY(I,K)/AMAX
700     CONTINUE
710     DO 805 I=ISTART,ISTOP
         DO 800 J=ISTART,ISTOP
             IF (I-K) 740,760,740
740             IF (J-K) 750,760,750
750             ARRAY(I,J)=ARRAY(I,J)+ARRAY(I,K)*ARRAY(K,J)
760             CONTINUE
800         CONTINUE
805     CONTINUE
810     DO 900 J=ISTART,ISTOP
         IF (J-K) 830,900,830
830         ARRAY(K,J)=ARRAY(K,J)/AMAX
900     CONTINUE
    ARRAY(K,K)=1./AMAX
         DET=DET * AMAX
1000     CONTINUE
C
C         RESTORE ORDERING OF MATRIX
C
1010     DO 1300 L=ISTART,ISTOP
         K=ISTOP - L + 1
         J=IK(K)
         IF (J-K) 1110,1110,1050
1050         DO 1100 I=ISTART,ISTOP
             SAVE=ARRAY(I,K)
             ARRAY(I,K)=-ARRAY(I,J)
             ARRAY(I,J)=SAVE
1100         CONTINUE
1110         I=JK(K)
         IF (I-K) 1300,1300,1130
1130         DO 1200 J=ISTART,ISTOP
             SAVE=ARRAY(K,J)
             ARRAY(K,J)=-ARRAY(I,J)
             ARRAY(I,J)=SAVE
1200         CONTINUE
1300     CONTINUE
1400     RETURN
    END
C
C
C
```

```
    SUBROUTINE PRNEW(A,CHISQR,CHISQ1,ITERNO,
     $        FILE,RSPFIL,IKEEP,LOTEMP)
C
C     FUNCTION:
C         PRINTS THE CURRENT ITERATION FIT RESULTS
C
    DIMENSION A(1)
    DOUBLE PRECISION CHI,CHISQR,CHISQ1
    LOGICAL*2 FINSHD,LOTEMP
    CHARACTER*1 QFILE(35),QRSPFIL(35),RSPAVG,BLLMT,ESC
    CHARACTER*3 ERASE
    CHARACTER*4 REVIDEO,BOLD,BLINK
    CHARACTER*6 XXX
    CHARACTER*7 CLEAR
     CHARACTER*12 FILE,RSPFIL
    CHARACTER*72 CFIELD
    COMMON /CHRDAT/ CFIELD,RSPAVG,BLLMT,ESC,CLEAR,
     $        REVIDEO,BOLD,BLINK,ERASE
    COMMON /NUMDAT/ NPTS,ITOT,MINCH,MAXCH,NSTART,NTAUS,ISTART,ISTOP,
     $        ATAU1,ATAU2,ATAU3,FRAC21,FRAC31,IFIX1,BSLNE,
     $        MINBL,MAXBL,SHIFT,AMPEST,CTD,XMAX,YMAX,IYMAXCH,
     $        NANGS,IPOS(25)
C
C
    FINSHD=.FALSE.
    CHI=CHISQ1-CHISQR
    CON=CTD/1000.
    IF (NTAUS.EQ.1) THEN
        XXX='Single'
    ELSEIF (NTAUS.EQ.2) THEN
        XXX='Double'
    ELSE
        XXX='Triple'
    ENDIF
C
    WRITE(*,*) ' '
    IF (ITERNO.EQ.1) THEN
        WRITE(*,*) 'Initial parameters: '
    ELSEIF (DABS(CHI).LE.0.0015D0) THEN
C
        WRITE(*,*) 'Final parameters: '
        WRITE(*,*) ' '
        WRITE(*,'(3X,1A,I4,1A,I3)') 'Considered ',NPTS,
     $            ' points, fitting from channel ',NSTART
        WRITE(*,'(3X,1A72)') CFIELD
        WRITE(*,*) ' '
C
    ENDIF
    IF (IKEEP.EQ.1) THEN
C     write to log file if save flag is 1
        FINSHD=.TRUE.
        IF (DABS(CHI).LE.0.0015D0) THEN
C
        WRITE(6,*) 'FINAL parameters: '
        WRITE(6,'(3X,1A,I4,1A,I3)') 'Considered ',NPTS,
     $            ' points, fitting from channel ',NSTART
        WRITE(6,'(3X,1A72)') CFIELD
           ELSE
        WRITE(6,*) 'Saved parameters: '
        WRITE(6,'(3X,1A,I4,1A,I3)') 'Considered ',NPTS,
```

```
     $                  ' points, fitting from channel ',NSTART
         WRITE(6,'(3X,1A72)') CFIELD
        ENDIF
      ENDIF
      IF (LOTEMP) THEN
         WRITE(*,210) XXX,FILE,RSPFIL
210     FORMAT(1X,1A6,'-exponential decay for ',1A12,'/',1A12)
         WRITE(*,211) '**** Angle modulated decay analysis  ****'
211     FORMAT(8X,1A)
      ELSE
         WRITE(*,212) XXX,FILE,RSPFIL
212     FORMAT(1X,1A6,'-exponential decay analysis for ',1A12,'/',1A12)
      ENDIF
C
      IF (FINSHD) THEN
          IF (LOTEMP) THEN
         WRITE(6,210) XXX,FILE,RSPFIL
         WRITE(6,211) '**** Angle modulated decay analysis  ****'
          ELSE
         WRITE(6,212) XXX,FILE,RSPFIL
          ENDIF
      ENDIF
C
      IF (NTAUS.EQ.1) THEN
         IF ((BLLNT.EQ.'y').OR.(BLLNT.EQ.'Y')) THEN
         WRITE(*,215) ' Tau','BL:',MINBL,',',MAXBL,
     $              'Shift',' Amp'
         IF (FINSHD) WRITE(6,215) ' Tau','BL:',MINBL,
     $              ',',MAXBL,'Shift',' Amp'
215         FORMAT(5X,1A,7X,1A,I3,1A1,I3,7X,1A,10X,1A)
         ELSE
         WRITE(*,220)
         IF (FINSHD) WRITE(6,220)
220         FORMAT(5X,' Tau',8X,'Baseline',8X,'Shift',10X,' Amp')
         ENDIF
         WRITE(*,230) A(3),(A(I),I=4,6)
         IF (FINSHD) WRITE(6,230) A(3),(A(I),I=4,6)
230         FORMAT(2X,F8.2,7X,F8.2,6X,F8.2,6X,F8.1)
         WRITE(*,235) A(3)*CON
         IF (FINSHD) WRITE(6,235) A(3)*CON
235         FORMAT(1X,F9.3)
       ELSEIF (NTAUS.EQ.2) THEN
         IF ((BLLNT.EQ.'y').OR.(BLLNT.EQ.'Y')) THEN
              IF (LOTEMP) THEN
         WRITE(*,236) 'Tau1','Tau2','Angles','BL:',MINBL,',',
     $              MAXBL,'Shift',' Amp','Fract 2/1'
         IF (FINSHD) WRITE(6,236) 'Tau1','Tau2','Angles','BL:',
     $              MINBL,',',MAXBL,'Shift',' Amp','Fract 2/1'
236         FORMAT(5X,1A,6X,1A,5X,1A,3X,1A,I3,1A1,I3,
     $              4X,1A,6X,1A,4X,1A)
           ELSE
         WRITE(*,238) 'Tau1','Tau2','BL:',MINBL,',',
     $              MAXBL,'Shift',' Amp','Fract 2/1'
         IF (FINSHD) WRITE(6,238) 'Tau1','Tau2','BL:',
     $              MINBL,',',MAXBL,'Shift',' Amp','Fract 2/1'
238         FORMAT(5X,1A,6X,1A,5X,1A,I3,1A1,I3,4X,1A,6X,1A,4X,1A)
           ENDIF
         ELSE
         IF (LOTEMP) THEN
         WRITE(*,239)
         IF (FINSHD) WRITE(6,239)
239          FORMAT(5X,'Tau1',6X,'Tau2',5X,'Angles',3X,'Baseline',5X,
     $              'Shift',6X,'Amp',4X,'Frac 2/1')
         ELSE
         WRITE(*,240)
         IF (FINSHD) WRITE(6,240)
240           FORMAT(5X,'Tau1',6X,'Tau2',6X,'Baseline',5X,'Shift'
     $              6X,' Amp',4X,'Fract 2/1')
         ENDIF
         ENDIF
         IF (LOTEMP) THEN
         WRITE(*,245) A(2),A(3),NANGS,(A(I),I=4,7)
         IF (FINSHD) WRITE(6,245) A(2),A(3),NANGS,(A(I),I=4,7)
245         FORMAT(2X,F8.2,2X,F8.2,6X,I2,5X,F8.2,2X,
     $              F8.2,2X,F8.1,2X,F8.3)
         ELSE
         WRITE(*,250) A(2),A(3),(A(I),I=4,7)
         IF (FINSHD) WRITE(6,250) A(2),A(3),(A(I),I=4,7)
250         FORMAT(2X,F8.2,2X,F8.2,5X,F8.2,3X,F8.2,2X,F8.1,2X,F8.3)
         ENDIF
         WRITE(*,255) A(2)*CON,A(3)*CON
         IF (FINSHD) WRITE(6,255) A(2)*CON,A(3)*CON
255         FORMAT(1X,2(F9.3,1X))
       ELSE
         IF ((BLLNT.EQ.'y').OR.(BLLNT.EQ.'Y')) THEN
         WRITE(*,260) 'Tau1','Tau2','Tau3','BL:',MINBL,',',
     $              MAXBL,'Shift','Amp','Frac 2/1','Frac 3/1'
         IF (FINSHD) WRITE(6,260) 'Tau1','Tau2','Tau3','BL:',
     $              MINBL,',',MAXBL,'Shift','Amp',
     $              'Frac 2/1','Frac 3/1'
260         FORMAT(4X,1A,5X,1A,5X,1A,2X,1A,I3,1A1,I3,
     $                    2X,1A,6X,1A,2X,1A,1X,1A)
         ELSE
         WRITE(*,265)
         IF (FINSHD) WRITE(6,265)
265         FORMAT(4X,'Tau1',5X,'Tau2',5X,'Tau3',3X,'Baseline',3X,
     $              'Shift',6X,'Amp',2X,'Frac 2/1',1X,'Frac 3/1')
         ENDIF
         WRITE(*,270) A(1),A(2),A(3),(A(I),I=4,8)
         IF (FINSHD) WRITE(6,270) A(1),A(2),A(3),(A(I),I=4,8)
270         FORMAT(1X,F8.2,1X,F8.2,1X,F8.2,2X,F8.2,2X,F6.2,2X,
     $              F8.1,1X,F8.3,1X,F8.3)
         WRITE(*,275) A(1)*CON,A(2)*CON,A(3)*CON
         IF (FINSHD) WRITE(6,275) A(1)*CON,A(2)*CON,A(3)*CON
275         FORMAT(3(F9.3,1X))
         ENDIF
      WRITE(*,280) ' Chi',CHAR(253),' = ',CHISQR
280     FORMAT(3A,F11.5)
      IF (FINSHD) WRITE(6,290) ' Chi-squared = ',CHISQR
290     FORMAT(1A,F11.5)
      WRITE(*,*) ' '
      IF (FINSHD) WRITE(6,*) ' '
1000    CONTINUE
      RETURN
      END
C
C
C
      SUBROUTINE PLTDAT(IDRAW,ISAVE,Y,YFIT,TBASE,NSTART,NPTS,COMMNT)
```

```
C
C    FUNCTION:
C        PLOTS RAW DATA FOR INSPECTION AND INPUT OF STARTING
C        CHANNEL FOR THE FIT, OR PLOTS THE DATA AND THE FIT
C
C    IDRAW=0 MEANS PLOT DATA WITH MOVING CURSOR, RETURN CURSOR
C            POSITION IN ISAVE
C    IDRAW=1 MEANS PLOT DATA WITH FIT
C
     CHARACTER*1 ANS
     CHARACTER*60 COMMNT
     DIMENSION Y(1024),YFIT(1024),RESID(1024)
     EXTERNAL AXES,DISP,LINE,INKEY
C
     ISAVE=0
C
     YMAX=Y(1)
     YMIN=Y(1)
     DO 210 J=2,NPTS
         IF (Y(J).GT.YMAX) THEN
             YMAX=Y(J)
         ELSEIF (Y(J).LT.YMIN) THEN
             YMIN=Y(J)
         ENDIF
210         CONTINUE
215     CONTINUE
     XORG=10
     YORG=25
     YSCLE=173
     XSCLE=618
     IFLAG=1
     WRITE(*,'(1X,A1,A4)') CHAR(27),'[=6h'
     CALL AXES(IFLAG,NINT(XSCLE+XORG),NINT(YORG),NINT(XORG),NINT(YORG))
     CALL AXES(IFLAG,NINT(XORG),NINT(YORG),NINT(XORG),NINT(YSCLE+YORG))
     XDIV=XSCLE/10.
     DO 220 I=0,10
         XPOS=XORG+(FLOAT(I)*XDIV)
         CALL AXES(IFLAG,NINT(XPOS),NINT(YORG),NINT(XPOS),NINT(YORG-5))
220     CONTINUE
     XMIN=0.
     XMAX=TBASE*FLOAT(NPTS)/1000.
     DO 230 I=0,4
         IXPOS=2+(15*I)
         XVAL=(XMAX/5.)*FLOAT(I)
         IF (IXPOS.LT.10) THEN
            WRITE(*,225) CHAR(27),'[24;',IXPOS,'f',XVAL
225            FORMAT(1X,A1,1A,I1,A1,F5.2\)
         ELSE
            WRITE(*,226) CHAR(27),'[24;',IXPOS,'f',XVAL
226            FORMAT(1X,A1,1A,I2,A1,F5.2\)
         ENDIF
230     CONTINUE
     WRITE(*,'(1X,A1,1A\)') CHAR(27),'[24;75fnsec'
C
     YRNGE=YMAX-YMIN
     XRNGE=XMAX-XMIN
     IFLAG=1
     DO 240 I=1,NPTS
         XVAL=TBASE*FLOAT(I-1)/1000.
         IYPLT=NINT((ABS((Y(I)-YMIN)/YRNGE)*(YSCLE-2))+YORG)
         IXPLT=NINT((ABS((XVAL-XMIN)/XRNGE)*(XSCLE-2))+XORG)
         CALL DISP(IFLAG,IXPLT,IYPLT)
240     CONTINUE
     IF (IDRAW.GT.0) THEN
C            plot the fit
        XVAL=TBASE*FLOAT(NSTART)/1000.
        XPREV=(ABS((XVAL-XMIN)/XRNGE)*(XSCLE-2))+XORG
        YPREV=(ABS((YFIT(NSTART)-YMIN)/YRNGE)*(YSCLE-2))+YORG
        IFLAG=1
        DO 250 I=1,(NPTS-NSTART)
          XVAL=TBASE*FLOAT(NSTART+I)/1000.
          XPLT=(ABS((XVAL-XMIN)/XRNGE)*(XSCLE-2))+XORG
          YPLT=(ABS((YFIT(NSTART+I)-YMIN)/YRNGE)*(YSCLE-2))+YORG
            CALL LINE(IFLAG,XPREV,YPREV,XPLT,YPLT)
          XPREV=XPLT
          YPREV=YPLT
250       CONTINUE
C           calculate residuals
        RSDMAX=0
        SUM=0
        DO 252 I=NSTART,NPTS
            RESID(I)=Y(I)-YFIT(I)
            SUM=SUM + (RESID(I)*RESID(I)/Y(I))
            RESID(I)=RESID(I)*SQRT(1/Y(I))
            RSDMAX=AMAX1(RSDMAX,ABS(RESID(I)))
252         CONTINUE
        RSDMAX=RSDMAX + (0.05*RSDMAX)
     ENDIF
     XOLD=1
     XNEW=1
     IYST=NINT(YORG+1)
     IYEND=NINT(YSCLE+YORG)
     WRITE(*,'(1X,A1,1A,1A\)') CHAR(27),'[25;2f',COMMNT
     WRITE(*,'(1X,A1,1A\)') CHAR(27),'[25;65fQ to quit'
255     CONTINUE
     CALL INKEY(IFLAG,ISCAN,ANS)
     IF (IFLAG.EQ.0) GO TO 255
     WRITE(*,'(1X,1A,1A,62(1X)\)') CHAR(27),'[25;1f'
     GO TO 262
260     CONTINUE
     CALL INKEY(IFLAG,ISCAN,ANS)
     IF (IFLAG.EQ.0) GO TO 260
262     CONTINUE
     IF (IDRAW.EQ.1) THEN
         IF (ISCAN.EQ.16) THEN
C                time to quit
            GO TO 280
         ELSEIF (ISCAN.EQ.32) THEN
C                a 'D' was entered, plot data
            GO TO 215
         ELSEIF (ISCAN.EQ.19) THEN
C                an 'R' was entered, plot residuals
            XORG=40
            YORG=100
            YSCLE=90
            XSCLE=598
C
             WRITE(*,'(1X,A1,A4\)') CHAR(27),'[=6h'
            PMAX=RSDMAX
C                print max and min
            WRITE(*,'(2A,F3.1\)') CHAR(27),'[2;1f',PMAX
            PMAX=PMAX*(-1)
```

```
          WRITE(*,'(2A,F4.1\)') CHAR(27),'[24;1f',PMAX
          CHISQR=SUM/(NPTS-NSTART-6)
C               print chisqr
          WRITE(*,'(2A,F8.4\)') CHAR(27),'[25;20f',CHISQR
          IFLAG=1
          CALL LINE(IFLAG,XSCLE,YORG,XORG,YORG)
          Y1ST=YORG-90
          Y2ND=YORG+90
          CALL LINE(IFLAG,XORG,Y1ST,XORG,Y2ND)
          MAXJ=NPTS-NSTART+1
          DO 550 I=NSTART,(NPTS-1)
              REALI=FLOAT(I-NSTART)
      XPLOT=((REALI/FLOAT(MAXJ))*(XSCLE-XORG-5))+(XORG+5)
              YPLOT=((RESID(I)/RSDMAX)*YSCLE)+YORG
              CALL LINE(IFLAG,XPLOT,YORG,XPLOT,YPLOT)
550           CONTINUE
          GO TO 260
        ELSE
C               unrecognized key was entered
          GO TO 260
        ENDIF
      ELSE
C       moving cursor mode
        IF (ISCAN.EQ.77) THEN
        IF (XOLD.LT.NPTS) THEN
        XNEW=XOLD+1
        ELSE
        XNEW=1
        ENDIF
      ELSEIF (ISCAN.EQ.75) THEN
        IF (XOLD.GT.1) THEN
        XNEW=XOLD-1
        ELSE
        XNEW=NPTS
        ENDIF
       ELSEIF (ISCAN.EQ.116) THEN
        IF (XOLD.LT.(NPTS-15)) THEN
        XNEW=XOLD+15
        ELSE
        XNEW=(XOLD+15)-NPTS
        ENDIF
      ELSEIF (ISCAN.EQ.115) THEN
        IF (XOLD.GT.15) THEN
        XNEW=XOLD-15
        ELSE
        XNEW=(XOLD-15)+NPTS
        ENDIF
      ELSEIF (ISCAN.EQ.57) THEN
        ISAVE=NINT(XOLD)
        WRITE(*,265) CHAR(27),'[25;5fSTART=',ISAVE,'
265        FORMAT(1X,A1,1A,I5,1A\)
      ELSEIF (ISCAN.EQ.16) THEN
        GO TO 280
      ELSE
        GO TO 260
      ENDIF
C       erase cursor at old location and
C       redraw point at old cursor location
      XVAL=(XOLD-1)*TBASE/1000.
      IXPLOT=NINT((ABS((XVAL-XMIN)/XRNGE)*(XSCLE-2))+XORG)
      IYPLOT=NINT((ABS((Y(INT(XOLD))-YMIN)/YRNGE)*(YSCLE-2))+YORG)
      IFLAG=0
      CALL AXES(IFLAG,IXPLOT,IYST,IXPLOT,IYEND)
      IFLAG=1
      CALL DISP(IFLAG,IXPLOT,IYPLOT)
C       draw cursor at new location
      XVAL=(XNEW-1)*TBASE/1000.
      IXPLOT=NINT((ABS((XVAL-XMIN)/XRNGE)*(XSCLE-2))+XORG)
      CALL AXES(IFLAG,IXPLOT,IYST,IXPLOT,IYEND)
C
      WRITE(*,270) CHAR(27),'[25;29fAmp= ',Y(INT(XNEW)),
     $           'Channel= ',INT(XNEW)
270      FORMAT(1X,A1,1A,F6.0,2X,1A,I5\)
      XOLD=XNEW
      GO TO 260
    ENDIF
C
280    CONTINUE
     WRITE(*,'(1X,A1,A4)') CHAR(27),'[=2h'
    RETURN
    END
C
C
C
    SUBROUTINE LINE(IFLAG,X1ST,Y1ST,X2ND,Y2ND)
C
C    FUNCTION:
C    DRAWS A LINE FROM X1,Y1 TO X2,Y2
C          IF IFLAG=0, ERASE MODE
C       IFLAG=1, DRAW MODE
C
    EXTERNAL DISP
    X1=X1ST
    Y1=Y1ST
    X2=X2ND
    Y2=Y2ND
C
    IF (Y1.GT.Y2) THEN
       INCY=-1
    ELSE
       INCY=1
    ENDIF
    IF (X1.GT.X2) THEN
       INCX=-1
    ELSE
       INCX=1
    ENDIF
    XDIF=ABS(X2-X1)
    YDIF=ABS(Y2-Y1)
    IF (XDIF.EQ.0) THEN
       IX1=NINT(X1)
       IY1=NINT(Y1)
       DO 100 I=1,NINT(ABS(Y2-Y1)+1)
          CALL DISP(IFLAG,IX1,IY1)
          IY1=IY1+INCY
100       CONTINUE
       GO TO 500
    ELSEIF (YDIF.EQ.0) THEN
       IX1=NINT(X1)
       IY1=NINT(Y1)
       DO 200 I=1,NINT(ABS(X2-X1)+1)
          CALL DISP(IFLAG,IX1,IY1)
```

```
            IX1=IX1+INCX
200         CONTINUE
        GO TO 500
    ELSE
        SLOPE=(Y2-Y1)/(X2-X1)
        YINT=Y2-(SLOPE*X2)
         IF (ABS(Y2-Y1).GT.ABS(X2-X1)) THEN
             DO 300 I=1,NINT(ABS(Y2-Y1)+1)
                 IY1=NINT(Y1)
                 IX1=NINT((Y1-YINT)/SLOPE)
                CALL DISP(IFLAG,IX1,IY1)
                 Y1=Y1+FLOAT(INCY)
300             CONTINUE
        ELSE
            DO 400 I=1,NINT(ABS(X2-X1)+1)
                IY1=NINT(SLOPE*X1+YINT)
                IX1=NINT(X1)
                CALL DISP(IFLAG,IX1,IY1)
                X1=X1+FLOAT(INCX)
400             CONTINUE
        ENDIF
    ENDIF
500    CONTINUE
    RETURN
    END
C
C
C
    SUBROUTINE CHREDT(QTITLE,IMAX,IEND)
C       This subroutine requires passage of a character array.
C       It assumes the cursor has been positioned in the
C       proper location. It will then print the string & return
C       the cursor to the first nonblank character. The left
C       and right arrow keys on the keypad are used to position
C       the cursor.  Typing any "noncontrol" key results in
C       replacement at that position in the array and on the
C       display.  Delete (keypad) and backspace work comple-
C       mentarily.  The routine also has an INSERT mode
C       exited by typing another INSERT or a return (to exit)
C       This routine disallows blanks since it was originally
C       used for input and editing of filenames. A return
C       exits the routine.
C  IMAX=# of elements in the array IEND=(returned) position of 1st
C    nonblank character from end
    CHARACTER*1 QTITLE(80),ACHAR
C
    DO 50 K=IMAX,1,-1
        IF (QTITLE(K).NE.' ') GO TO 60
50    CONTINUE
60    CONTINUE
    IF (K.EQ.IMAX) THEN
        IEND=IMAX
        INDEX=IMAX
        DO 65 K=1,IEND
            WRITE(*,'(1A\)') QTITLE(K)
65        CONTINUE
        WRITE(*,'(2A\)') CHAR(27),'[D'
C    ELSEIF (K.EQ.0) THEN
C        INDEX=1
C        IEND=0
    ELSE
        INDEX=K+1
        IEND=K
        DO 70 K=1,IEND
            WRITE(*,'(1A\)') QTITLE(K)
70        CONTINUE
    ENDIF
C
100    CONTINUE
    CALL INKEY(ITEST,ISCAN,ACHAR)
    IF (ITEST.EQ.0) GO TO 100
C
    IF (ISCAN.EQ.75) THEN
C        a left arrow was entered
        IF (INDEX.NE.1) THEN
            WRITE(*,'(2A\)') CHAR(27),'[D'
            INDEX=INDEX-1
        ENDIF
        GO TO 100
    ELSEIF (ISCAN.EQ.77) THEN
C        a right arrow was entered
        IF (INDEX.NE.IMAX) THEN
            WRITE(*,'(2A\)') CHAR(27),'[C'
            INDEX=INDEX+1
        ENDIF
        GO TO 100
    ELSEIF ((ISCAN.EQ.83).OR.(ISCAN.EQ.14)) THEN
C        a delete (keypad) or a backspace was entered
        IF (INDEX.GT.(IEND+1)) THEN
            WRITE(*,'(2A\)') CHAR(27),'[D'
            INDEX=INDEX-1
            GO TO 100
        ELSEIF (INDEX.EQ.(IEND+1)) THEN
            IF (INDEX.EQ.1) THEN
                IF (QTITLE(INDEX).NE.' ') THEN
                    QTITLE(INDEX)=' '
                    WRITE(*,'(1A\)') ' '
                    WRITE(*,'(2A\)') CHAR(27),'[D'
                ENDIF
            ELSE
                QTITLE(IEND)=' '
                IEND=IEND-1
                INDEX=INDEX-1
                WRITE(*,'(2A\)') CHAR(27),'[D'
                WRITE(*,'(1A\)') ' '
                WRITE(*,'(2A\)') CHAR(27),'[D'
            ENDIF
            GO TO 100
        ELSE
            IF (ISCAN.EQ.14) THEN
C           backspace delete
               J=INDEX-1
               DO 190 K=INDEX,IEND
                   QTITLE(J)=QTITLE(K)
                   J=J+1
190            CONTINUE
            IF (INDEX.GT.1) THEN
                WRITE(*,'(2A\)') CHAR(27),'[D'
                INDEX=INDEX-1
            ENDIF
            ELSE
C           delete mode, slightly different than backspace deletion
```

```
            J=INDEX
            DO 200 K=(INDEX+1),IEND
                QTITLE(J)=QTITLE(K)
                J=J+1
200           CONTINUE
            ENDIF
            QTITLE(IEND)=' '
            IF (IEND.GT.1) THEN
            IEND=IEND-1
            ELSE
            IEND=0
            ENDIF
            WRITE(*,'(2A\)') CHAR(27),'[s'
            DO 210 K=INDEX,(IEND+1)
            WRITE(*,'(A1\)') QTITLE(K)
210           CONTINUE
            WRITE(*,'(2A\)') CHAR(27),'[u'
        ENDIF
        GO TO 100
    ELSEIF (ISCAN.EQ.82) THEN
C        insert mode
250       CONTINUE
        CALL INKEY(ITEST,ISCAN,ACHAR)
        IF (ITEST.EQ.0) GO TO 250
C
        IF (ISCAN.EQ.82) GO TO 100
        IF (ISCAN.EQ.28) GO TO 400
        IF (ISCAN.EQ.14) GO TO 250
        IF (ISCAN.GT.54) GO TO 250
        IF (IEND.GT.0) THEN
           J=IEND
           DO 260 K=(IEND+1),(INDEX+1),-1
            IF (K.LE.IMAX) THEN
                QTITLE(K)=QTITLE(J)
            ENDIF
            J=J-1
260           CONTINUE
        ENDIF
        QTITLE(INDEX)=ACHAR
        WRITE(*,'(1A\)') QTITLE(INDEX)
        IF (INDEX.GE.IMAX) THEN
            WRITE(*,'(2A\)') CHAR(27),'[D'
        ENDIF
        IF (INDEX.GT.IEND) THEN
            IEND=INDEX
        ENDIF
        IF (INDEX.LT.IMAX) THEN
            INDEX=INDEX+1
        ELSEIF (INDEX.GE.IMAX) THEN
            INDEX=IMAX
        ENDIF
        IF (IEND.LT.IMAX) THEN
            IEND=IEND+1
        ELSEIF (IEND.GE.IMAX) THEN
            IEND=IMAX
        ENDIF
        DO 280 K=INDEX,IEND
            WRITE(*,'(1A\)') QTITLE(K)
280       CONTINUE
        DO 285 K=1,(IEND-INDEX+1)
            WRITE(*,'(2A\)') CHAR(27),'[D'
285       CONTINUE
        GO TO 250
    ELSEIF (ISCAN.EQ.79) THEN
C        keypad "end" entered
        DO 286 K=INDEX,IEND
            WRITE(*,'(1A\)') ' '
            QTITLE(K)=' '
286       CONTINUE
        DO 288 K=INDEX,IEND
            WRITE(*,'(2A\)') CHAR(27),'[D'
288       CONTINUE
        IF (INDEX.GE.2) THEN
            IEND=INDEX-1
        ELSE
            IEND=0
        ENDIF
        GO TO 100
    ELSEIF (ISCAN.EQ.28) THEN
C        a return was entered
        GO TO 400
    ELSEIF (ISCAN.GT.54) THEN
C        any alphabet or number keys but not spaces,
C        function keys or keypad entries
        GO TO 100
    ELSE
        QTITLE(INDEX)=ACHAR
        WRITE(*,'(A1\)') ACHAR
        IF (INDEX.GT.IEND) THEN
            IEND=INDEX
        ENDIF
        IF (INDEX.LT.IMAX) THEN
            INDEX=INDEX+1
        ELSEIF (INDEX.EQ.IMAX) THEN
            WRITE(*,'(2A\)') CHAR(27),'[D'
        ENDIF
        GO TO 100
    ENDIF
    GO TO 100
400   CONTINUE
    DO 500 K=1,(INDEX-1)
        WRITE(*,'(2A\)') CHAR(27),'[D'
500   CONTINUE
    DO 550 K=1,IEND
        WRITE(*,'(1A\)') QTITLE(K)
550   CONTINUE
C    blank out the rest of the character string
    DO 560 K=(IEND+1), IMAX
        QTITLE(K)=' '
560   CONTINUE
    RETURN
    END
C
C
C
    SUBROUTINE RDVAL(XVAL,IXVAL,IFLAG)
C
C    FUNCTION:
C        READS A NUMBER FROM THE KEYBOARD USING THE INKEY
C        SUBROUTINE AND RETURNS THE VALUE (REAL AND INTEGER)
C
C    Null input IFLAG=0
```

```
C     Input error IFLAG=-1
C     Input OK, IFLAG=1
C
      EXTERNAL INKEY
      CHARACTER*1 QSTRNG(8),ACHAR
C
      IFLAG=1
      XVAL=0.
      IXVAL=0
      ISIGN=1
      IPERIOD=0
      DO 80 I=1,8
         QSTRNG(I)=' '
80    CONTINUE
C
      K=1
100   CONTINUE
      CALL INKEY(ITEST,ISCAN,ACHAR)
      IF ((ITEST.EQ.0).OR.(ISCAN.EQ.57)) THEN
          GO TO 100
      ELSEIF (ISCAN.EQ.28) THEN
C          a return was entered
          GO TO 150
      ELSEIF (ISCAN.EQ.14) THEN
C          a backspace was entered
          GO TO 115
      ELSEIF (ISCAN.EQ.12) THEN
C          a minus sign was entered
          GO TO 120
      ELSEIF (ISCAN.EQ.52) THEN
C          a period was entered
          GO TO 110
      ELSEIF ((ISCAN.LT.2).OR.(ISCAN.GT.11)) THEN
C          something other than a digit was entered
          GO TO 130
      ENDIF
         WRITE(*,'(1A\)') ACHAR
      IF (K.LE.8) THEN
          QSTRNG(K)=ACHAR
      ENDIF
      K=K+1
      GO TO 100
110   CONTINUE
      IF (IPERIOD.EQ.0) THEN
             WRITE(*,'(1A\)') ACHAR
          IF (K.LE.8) THEN
              IPERIOD=K
              QSTRNG(K)=ACHAR
          ENDIF
          K=K+1
      ENDIF
      GO TO 100
115   CONTINUE
      IF (K.EQ.1) THEN
          IF (ISIGN.LT.0) THEN
              ISIGN=1
              WRITE(*,'(1A\)') ' '
              WRITE(*,'(2A\)') CHAR(27),'[D'
              WRITE(*,'(2A\)') CHAR(27),'[D'
          ENDIF
          WRITE(*,'(1A\)') ' '
          WRITE(*,'(2A\)') CHAR(27),'[D'
      ELSE
          K=K-1
          IF (K.EQ.IPERIOD) THEN
              IPERIOD=0
          ENDIF
          WRITE(*,'(1A\)') ' '
          WRITE(*,'(2A\)') CHAR(27),'[D'
          WRITE(*,'(2A\)') CHAR(27),'[D'
      ENDIF
      GO TO 100
120   CONTINUE
      IF ((K.EQ.1).AND.(ISIGN.GT.0)) THEN
             WRITE(*,'(1A\)') ACHAR
          ISIGN=-1
      ENDIF
      GO TO 100
130   CONTINUE
      IFLAG=-1
      GO TO 300
150   CONTINUE
      IEND=K-1
      IF (IEND.EQ.0) THEN
          IFLAG=0
          GO TO 300
      ELSEIF (IEND.GT.8) THEN
          IEND=8
      ENDIF
C
      IF (IPERIOD.EQ.IEND) THEN
          IEND=IEND-1
          IPERIOD=0
      ENDIF
      IF (IPERIOD.NE.0) THEN
          XMULT=1./(10**(IEND-IPERIOD))
            DO 200 J=IEND,(IPERIOD+1),-1
                 XVAL=XVAL+(XMULT*(FLOAT(ICHAR(QSTRNG(J))-48)))
              XMULT=XMULT*10.
200         CONTINUE
      ENDIF
C
      IF (IPERIOD.EQ.0) THEN
          ISTART=IEND
      ELSE
          ISTART=(IPERIOD-1)
      ENDIF
C
      IMULT=1
      DO 250 J=ISTART,1,-1
             IXVAL=IXVAL+(IMULT*(ICHAR(QSTRNG(J))-48))
          IMULT=IMULT*10.
250   CONTINUE
C
      XVAL=(FLOAT(IXVAL)+XVAL)*FLOAT(ISIGN)
      IXVAL=IXVAL*ISIGN
300   CONTINUE
      RETURN
      END
C
C
C
```

```
      SUBROUTINE SETPOS(ICURSOR,IPOS)
C
C     FUNCTION:
C          POSITIONS THE CURSOR AT (IPOS(ICURSOR), ICURSOR)
C          USING ANSI.SYS ESCAPE SEQUENCES
C
      DIMENSION IPOS(25)
      CHARACTER*1 ESC
C
      ESC=CHAR(27)
      IF (ICURSOR.LT.10) THEN
         WRITE(*,'(2A,I1,1A,I2,1A\)') ESC,'[',
     $              ICURSOR,';',IPOS(ICURSOR),'f'
      ELSE
         WRITE(*,'(2A,I2,1A,I2,1A\)') ESC,'[',
     $              ICURSOR,';',IPOS(ICURSOR),'f'
      ENDIF
      RETURN
      END
C
C
C
      SUBROUTINE CHGVAL(IREAL,XVAL,IXVAL,ICURSOR,IPOS,BOLD,BLINK,
     $         CLEAR,ERASE)
C
C     FUNCTION:
C          ALTERS A REAL OR INTEGER VALUE IN THE MENU SCREEN
C          BY FIRST PRINTING THE VALUE IN HIGH INTENSITY BLINKING
C          BOLD ATTRIBUTE, AND READS A NUMBER FROM THE KEYBOARD
C          (SUBROUTINE RDVAL)
C
      DIMENSION IPOS(25)
      CHARACTER*3 ERASE
      CHARACTER*4 BOLD,BLINK
      CHARACTER*7 CLEAR
C
100     CONTINUE
      WRITE(*,'(2A\)') BOLD,BLINK
      CALL SETPOS(ICURSOR,IPOS)
      IF (IREAL.EQ.1) THEN
          CALL PRTRL(XVAL)
      ELSE
          CALL PRTINT(IXVAL)
      ENDIF
      WRITE(*,'(2A\)') CLEAR,BOLD
      CALL SETPOS(ICURSOR,IPOS)
      CALL RDVAL(X,IX,IWARN)
      IF (IWARN.LT.0) THEN
          GO TO 100
      ELSEIF (IWARN.GT.0) THEN
          XVAL=X
          IXVAL=IX
      ENDIF
      CALL SETPOS(ICURSOR,IPOS)
      WRITE(*,'(2A\)') ERASE,BOLD
      IF (IREAL.EQ.1) THEN
          CALL PRTRL(XVAL)
      ELSE
          CALL PRTINT(IXVAL)
      ENDIF
      WRITE(*,'(1A\)') CLEAR
      RETURN
      END
C
C
C
      SUBROUTINE PRTINT(IVALUE)
C
C     FUNCTION:
C          SELECTS THE PROPER FORMAT TO OUTPUT AN INTEGER VALUE
C          BASED ON THE MAGNITUDE OF IVALUE
C
      IF (IABS(IVALUE).LT.10) THEN
          IF (IVALUE.LT.0) THEN
             WRITE(*,'(I2\)') IVALUE
          ELSE
             WRITE(*,'(I1\)') IVALUE
          ENDIF
      ELSEIF (IABS(IVALUE).LT.100) THEN
          IF (IVALUE.LT.0) THEN
             WRITE(*,'(I3\)') IVALUE
          ELSE
             WRITE(*,'(I2\)') IVALUE
          ENDIF
      ELSEIF (IABS(IVALUE).LT.1000) THEN
          IF (IVALUE.LT.0) THEN
             WRITE(*,'(I4\)') IVALUE
          ELSE
             WRITE(*,'(I3\)') IVALUE
          ENDIF
      ELSEIF (IABS(IVALUE).LT.10000) THEN
          IF (IVALUE.LT.0) THEN
             WRITE(*,'(I5\)') IVALUE
          ELSE
             WRITE(*,'(I4\)') IVALUE
          ENDIF
      ELSE
          IF (IVALUE.LT.0) THEN
             WRITE(*,'(I6\)') IVALUE
          ELSE
             WRITE(*,'(I5\)') IVALUE
          ENDIF
      ENDIF
      RETURN
      END
C
C
C
      SUBROUTINE PRTRL(XVALUE)
C
C     FUNCTION:
C          SELECTS THE PROPER FORMAT TO OUTPUT A REAL VALUE
C          BASED ON THE MAGNITUDE OF XVALUE
C
      IF (ABS(XVALUE).LT.10) THEN
          IF (XVALUE.LT.0) THEN
             WRITE(*,'(F4.1\)') XVALUE
          ELSE
             WRITE(*,'(F3.1\)') XVALUE
          ENDIF
      ELSEIF (ABS(XVALUE).LT.100) THEN
          IF (XVALUE.LT.0) THEN
             WRITE(*,'(F5.1\)') XVALUE
```

```
        ELSE
           WRITE(*,'(F4.1\)') XVALUE
        ENDIF
     ELSEIF (ABS(XVALUE).LT.1000) THEN
        IF (XVALUE.LT.0) THEN
           WRITE(*,'(F6.1\)') XVALUE
        ELSE
           WRITE(*,'(F5.1\)') XVALUE
        ENDIF
     ELSEIF (ABS(XVALUE).LT.10000) THEN
        IF (XVALUE.LT.0) THEN
           WRITE(*,'(F7.1\)') XVALUE
        ELSE
           WRITE(*,'(F6.1\)') XVALUE
        ENDIF
     ELSEIF (ABS(XVALUE).LT.100000) THEN
        IF (XVALUE.LT.0) THEN
           WRITE(*,'(F8.1\)') XVALUE
        ELSE
           WRITE(*,'(F7.1\)') XVALUE
        ENDIF
     ELSE
        IF (XVALUE.LT.0) THEN
           WRITE(*,'(F9.1\)') XVALUE
        ELSE
           WRITE(*,'(F8.1\)') XVALUE
        ENDIF
     ENDIF
     RETURN
     END
C
C
C
     SUBROUTINE CHRALTR(ACHAR,ICURSOR,IPOS,BOLD,BLINK,CLEAR)
C
C     FUNCTION:
C          ALTERS A CHARACTER VALUE IN THE MENU SCREEN
C          BY FIRST PRINTING THE VALUE IN HIGH INTENSITY BLINKING
C          BOLD ATTRIBUTE, AND READS A CHARACTER FROM THE KEYBOARD
C
     EXTERNAL INKEY
     DIMENSION IPOS(25)
     CHARACTER*1 ANS,ACHAR,ESC
     CHARACTER*4 BOLD,BLINK
     CHARACTER*7 CLEAR
C
     ESC=CHAR(27)
C
     CALL SETPOS(ICURSOR,IPOS)
     WRITE(*,'(5A\)') BOLD,BLINK,ACHAR,CLEAR,BOLD
100     CONTINUE
     CALL SETPOS(ICURSOR,IPOS)
200     CONTINUE
     CALL INKEY(ITEST,ISCAN,ANS)
     IF (ITEST.EQ.0) GO TO 200
     IF (ISCAN.EQ.28) GO TO 300
     ACHAR=ANS
     WRITE(*,'(A1\)') ACHAR
     GO TO 100
300     CONTINUE
     WRITE(*,'(1A\)') CLEAR
     RETURN
     END
C
C
C
     SUBROUTINE PRTMNU(DATFIL,RSPFIL,PLTFIL,LOTEMP)
C
C     FUNCTION:
C          OUTPUTS THE MENU SCREEN
C
     LOGICAL*2 LOTEMP
     CHARACTER*1 RSPAVG,BLLMT,ESC
     CHARACTER*3 ERASE
     CHARACTER*4 REVIDEO,BOLD,BLINK
     CHARACTER*5 ANPTS
     CHARACTER*7 CLEAR
      CHARACTER*35 DATFIL,RSPFIL,PLTFIL,BLANK
     CHARACTER*72 CFIELD
     COMMON /CHRDAT/ CFIELD,RSPAVG,BLLMT,ESC,CLEAR,
     $         REVIDEO,BOLD,BLINK,ERASE
     COMMON /NUMDAT/ NPTS,ITOT,MINCH,MAXCH,NSTART,NTAUS,ISTART,ISTOP,
     $         ATAU1,ATAU2,ATAU3,FRAC21,FRAC31,IFIX1,BSLNE,
     $         MINBL,MAXBL,SHIFT,AMPEST,CTD,XMAX,YMAX,IYMAXCH,
     $         NANGS,IPOS(25)
C
     BLANK='                                   '
     IF (DATFIL.GT.BLANK) THEN
          WRITE(*,'(5A\)') ESC,'[4;5fDecay file: ',
     $       BOLD,DATFIL,CLEAR
          WRITE(*,'(A1,2A,A72,1A\)') ESC,'[1;2f',BOLD,CFIELD,CLEAR
     ELSE
          WRITE(*,'(5A\)') ESC,'[4;5fDecay file: ',
     $       REVIDEO,DATFIL,CLEAR
     ENDIF
     IF (RSPFIL.GT.BLANK) THEN
          WRITE(*,'(5A\)') ESC,'[5;5fResponse file: ',
     $       BOLD,RSPFIL,CLEAR
     ELSE
          WRITE(*,'(5A\)') ESC,'[5;5fResponse file: ',
     $       REVIDEO,RSPFIL,CLEAR
     ENDIF
     IF (ITOT.GT.0) THEN
         WRITE(*,'(6A\)') ESC,'[6;5fNumber of data points (100 ',
     $        CHAR(243),' N ',CHAR(243),' '
         CALL PRTINT(ITOT)
             WRITE(*,'(2A\)') '): ',BOLD
         ICURSOR=6
         CALL SETPOS(ICURSOR,IPOS)
         CALL PRTINT(NPTS)
     ENDIF
C
     WRITE(*,'(1A\)') CLEAR
     IF (LOTEMP) THEN
          WRITE(*,'(5A\)') ESC,'[7;5fAngle modulated decay: ',
     $       REVIDEO,'On ',CLEAR
          WRITE(*,'(3A,I2,1A\)') ESC,'[8;8fNumber of angles: ',
     $            BOLD,NANGS,CLEAR
     ELSE
          WRITE(*,'(5A\)') ESC,'[7;5fAngle modulated decay: ',
     $       REVIDEO,'Off',CLEAR
```

```
      ENDIF
C     WRITE(*,'(5A\)') ESC,'[7;5fResponse baseline correction: ',
C     $   BOLD,RSPAVG,CLEAR
C     IF ((RSPAVG.EQ.'Y').OR.(RSPAVG.EQ.'y')) THEN
C      IF (MINCH.GE.MAXCH) THEN
C        WRITE(*,'(10A\)') ESC,'[8;8fChannel range for average',
C     $    ' (min,max): ',REVIDEO,'    ',CLEAR,',',REVIDEO,'    ',CLEAR
C      ELSE
C        WRITE(*,'(4A,I4,3A,I4,1A\)') ESC,
C     $      '[8;8fChannel range for average',
C     $      ' (min,max): ',BOLD,MINCH,CLEAR,',',BOLD,MAXCH,CLEAR
C      ENDIF
C     ENDIF
      IF (CTD.GT.0) THEN
          WRITE(*,'(4A,F7.2,1A\)') ESC,'[9;15f',BOLD,
     $       'Picoseconds per channel : ',CTD,CLEAR
          WRITE(*,'(4A,F7.0,2X,1A,I3,1A\)') ESC,'[10;15f',BOLD,
     $         'Ymax = ',YMAX,'Ymax channel = ',IYMAXCH,CLEAR
      ENDIF
      WRITE(*,'(4A\)') ESC,'[11;5f',
     $  'Channel to start fitting: ',BOLD
      CALL PRTINT(NSTART)
      WRITE(*,'(1A\)') CLEAR
C
      WRITE(*,'(4A,I1,1A\)') ESC,'[12;5f',
     $  'Number of components: ',BOLD,NTAUS,CLEAR
      IF (ATAU1.GT.0.) THEN
          WRITE(*,'(4A\)') ESC,'[13;5f',
     $          'Lifetime 1 estimate (Ch): ',BOLD
          CALL PRTRL(ATAU1)
          WRITE(*,'(1A\)') CLEAR
      ELSE
          WRITE(*,'(6A\)') ESC,'[13;5f',
     $          'Lifetime 1 estimate (Ch): ',REVIDEO,'       ',CLEAR
      ENDIF
      IF ((ATAU2.GT.0.).AND.(NTAUS.GT.1)) THEN
          WRITE(*,'(4A\)') ESC,'[14;5f',
     $          'Lifetime 2 estimate (Ch): ',BOLD
          CALL PRTRL(ATAU2)
          WRITE(*,'(1A\)') CLEAR
      ELSEIF (NTAUS.GT.1) THEN
          WRITE(*,'(6A\)') ESC,'[14;5f',
     $          'Lifetime 2 estimate (Ch): ',REVIDEO,'       ',CLEAR
      ENDIF
      IF ((ATAU3.GT.0.).AND.(NTAUS.GT.2)) THEN
          WRITE(*,'(4A\)') ESC,'[15;5f',
     $          'Lifetime 3 estimate (Ch): ',BOLD
          CALL PRTRL(ATAU3)
          WRITE(*,'(1A\)') CLEAR
      ELSEIF (NTAUS.GT.2) THEN
          WRITE(*,'(6A\)') ESC,'[13;5f',
     $          'Lifetime 3 estimate (Ch): ',REVIDEO,'       ',CLEAR
      ENDIF
      IF ((FRAC21.GT.0.).AND.(NTAUS.GT.1)) THEN
          WRITE(*,'(4A\)') ESC,'[16;5f',
     $          'Fraction 2/1: ',BOLD
          CALL PRTRL(FRAC21)
          WRITE(*,'(1A\)') CLEAR
      ELSEIF (NTAUS.GT.1) THEN
          WRITE(*,'(6A\)') ESC,'[16;5f',
     $          'Fraction 2/1: ',REVIDEO,'       ',CLEAR
      ENDIF
      IF ((FRAC31.GT.0.).AND.(NTAUS.GT.2)) THEN
          WRITE(*,'(4A\)') ESC,'[17;5f',
     $          'Fraction 3/1: ',BOLD
          CALL PRTRL(FRAC31)
          WRITE(*,'(1A\)') CLEAR
      ELSEIF (NTAUS.GT.2) THEN
          WRITE(*,'(6A\)') ESC,'[17;5f',
     $          'Fraction 3/1: ',REVIDEO,'       ',CLEAR
      ENDIF
C
      WRITE(*,'(4A,I1,1A\)') ESC,'[18;5f',
     $          'Fix lifetime: ',BOLD,IFIX1,CLEAR
C
      WRITE(*,'(4A\)') ESC,'[19;5f',
     $  'Baseline estimate: ',BOLD
      CALL PRTRL(BSLNE)
      WRITE(*,'(1A\)') CLEAR
C
      WRITE(*,'(6A\)') ESC,'[20;5f',
     $  'Constrain baseline: ',BOLD,BLLMT,CLEAR
      IF ((BLLMT.EQ.'Y').OR.(BLLMT.EQ.'y')) THEN
          IF (MINBL.GE.MAXBL) THEN
              WRITE(*,'(10A\)') ESC,'[21;8f',
     $          'Baseline limits (min,max): ',REVIDEO,'    ',CLEAR,
     $          ',',REVIDEO,'    ',CLEAR
          ELSE
              WRITE(*,'(4A,I4,3A,I4,1A\)') ESC,'[21;8f',
     $          'Baseline limits (min,max): ',BOLD,MINBL,CLEAR,
     $          ',',BOLD,MAXBL,CLEAR
          ENDIF
      ENDIF
      WRITE(*,'(4A\)') ESC,'[22;5f',
     $  'Lamp-shift estimate: ',BOLD
      CALL PRTRL(SHIFT)
      WRITE(*,'(1A\)') CLEAR
C
      IF (AMPEST.GT.0) THEN
          WRITE(*,'(4A\)') ESC,'[23;5f',
     $      'Estimated amplitude: ',BOLD
          CALL PRTRL(AMPEST)
          WRITE(*,'(1A\)') CLEAR
      ENDIF
C
      RETURN
      END
C
C
C
      SUBROUTINE CHGXPS(A)
C
C     FUNCTION:
C         UPDATES ALL THE PARAMETERS REQUIRED FOR THE CHANGE
C         FROM SINGLE TO DOUBLE TO TRIPLE EXPONENTIAL DECAY
C         ANALYSES
C
      DIMENSION A(8)
      CHARACTER*1 RSPAVG,BLLMT,ESC
      CHARACTER*3 ERASE
      CHARACTER*4 REVIDEO,BOLD,BLINK
```

```
      CHARACTER*7 CLEAR
      CHARACTER*72 CFIELD
      COMMON /CHRDAT/ CFIELD,RSPAVG,BLLMT,ESC,CLEAR,
     $        REVIDEO,BOLD,BLINK,ERASE
      COMMON /NUMDAT/ NPTS,ITOT,MINCH,MAXCH,NSTART,NTAUS,ISTART,ISTOP,
     $        ATAU1,ATAU2,ATAU3,FRAC21,FRAC31,IFIX1,BSLNE,
     $        MINBL,MAXBL,SHIFT,AMPEST,CTD,XMAX,YMAX,IYMAXCH,
     $        NANGS,IPOS(25)
C
30     CONTINUE
      ICURSOR=12
      CALL SETPOS(ICURSOR,IPOS)
      CALL CHGVAL(IREAL,XVAL,NTAUS,ICURSOR,IPOS,BOLD,BLINK,
     $        CLEAR,ERASE)
      IF (NTAUS.LT.1) THEN
          NTAUS=1
          CALL SETPOS(ICURSOR,IPOS)
          WRITE(*,'(2A\)') ERASE,BOLD
          CALL PRTINT(NTAUS)
          WRITE(*,'(1A\)') CLEAR
      ELSEIF (NTAUS.GT.3) THEN
          NTAUS=3
          CALL SETPOS(ICURSOR,IPOS)
          WRITE(*,'(2A\)') ERASE,BOLD
          CALL PRTINT(NTAUS)
          WRITE(*,'(1A\)') CLEAR
      ENDIF
C
      IF (NTAUS.EQ.1) THEN
          DO 36 I=14,18
             WRITE(*,'(2A,I2,2A\)') ESC,'[',I,';1f',ERASE
             IPOS(I)=0
36        CONTINUE
          WRITE(*,'(1A\)') BOLD
          ICURSOR=13
          IF (ATAU1.EQ.0.) THEN
39          CONTINUE
          CALL SETPOS(ICURSOR,IPOS)
          CALL RDVAL(ATAU1,IXVAL,IWARN)
          IF ((IWARN.LT.0).OR.(ATAU1.LE.0)) GO TO 39
          ENDIF
          CALL SETPOS(ICURSOR,IPOS)
          WRITE(*,'(2A\)') ERASE,BOLD
          CALL PRTRL(ATAU1)
          WRITE(*,'(1A\)') CLEAR
          ISAVE=IPOS(ICURSOR)
          IPOS(ICURSOR)=ISAVE+8
          CALL SETPOS(ICURSOR,IPOS)
          WRITE(*,'(1A\)') '('
          XTAU=ATAU1*CTD
          CALL PRTRL(XTAU)
          WRITE(*,'(1A\)') ' psec)'
          IPOS(ICURSOR)=ISAVE
          IFIX1=0
          IFIX2=0
          A(3)=ATAU1
          ISTART=3
          ISTOP=6
      ELSEIF (NTAUS.EQ.2) THEN
          IPOS(14)=31
          IPOS(16)=19
          IPOS(18)=19
          WRITE(*,'(3A\)') ESC,'[15;1f',ERASE
          IPOS(15)=0
          WRITE(*,'(3A\)') ESC,'[17;1f',ERASE
          IPOS(17)=0
          WRITE(*,'(1A\)') BOLD
          ICURSOR=13
          IF (ATAU1.EQ.0.) THEN
37          CONTINUE
          CALL SETPOS(ICURSOR,IPOS)
          CALL RDVAL(ATAU1,IXVAL,IWARN)
          IF ((IWARN.LT.0).OR.(ATAU1.LE.0)) GO TO 37
      ENDIF
      CALL SETPOS(ICURSOR,IPOS)
      WRITE(*,'(2A\)') ERASE,BOLD
      CALL PRTRL(ATAU1)
      WRITE(*,'(1A\)') CLEAR
      ISAVE=IPOS(ICURSOR)
      IPOS(ICURSOR)=ISAVE+8
      CALL SETPOS(ICURSOR,IPOS)
      WRITE(*,'(1A\)') '('
      XTAU=ATAU1*CTD
      CALL PRTRL(XTAU)
          WRITE(*,'(1A\)') ' psec)'
      IPOS(ICURSOR)=ISAVE
C
      ICURSOR=14
      IF (ATAU2.GT.0.) THEN
         WRITE(*,'(4A\)') ESC,'[14;5f',
     $            'Lifetime 2 estimate (Ch): ',BOLD
          CALL PRTRL(ATAU2)
         WRITE(*,'(1A\)') CLEAR
      ELSE
         WRITE(*,'(6A\)') ESC,'[14;5f',
     $            'Lifetime 2 estimate (Ch): ',REVIDEO,'      ',CLEAR
         WRITE(*,'(1A\)') BOLD
40         CONTINUE
         CALL SETPOS(ICURSOR,IPOS)
         CALL RDVAL(ATAU2,IXVAL,IWARN)
         IF ((IWARN.LT.0).OR.(ATAU2.LE.0)) GO TO 40
         CALL SETPOS(ICURSOR,IPOS)
         WRITE(*,'(2A\)') ERASE,BOLD
         CALL PRTRL(ATAU2)
         WRITE(*,'(1A\)') CLEAR
      ENDIF
      ISAVE=IPOS(ICURSOR)
      IPOS(ICURSOR)=ISAVE+8
      CALL SETPOS(ICURSOR,IPOS)
      WRITE(*,'(1A\)') '('
      XTAU=ATAU2*CTD
      CALL PRTRL(XTAU)
      WRITE(*,'(1A\)') ' psec)'
      IPOS(ICURSOR)=ISAVE
C
      ICURSOR=16
      IF (FRAC21.GT.0.) THEN
         WRITE(*,'(4A,F5.2,2A\)') ESC,'[16;5f',
     $            'Fraction 2/1: ',BOLD,FRAC21,ERASE,CLEAR
      ELSE
         WRITE(*,'(6A\)') ESC,'[16;5f',
     $            'Fraction 2/1: ',REVIDEO,'      ',CLEAR
```

```
          WRITE(*,'(1A\)') BOLD
41          CONTINUE
          CALL SETPOS(ICURSOR,IPOS)
          CALL RDVAL(FRAC21,IXVAL,IWARN)
          IF ((IWARN.LT.0).OR.(FRAC21.LE.0)) GO TO 41
          CALL SETPOS(ICURSOR,IPOS)
          WRITE(*,'(1A,F5.2,2A\)') BOLD,FRAC21,ERASE,CLEAR
       ENDIF
       ISAVE=IPOS(ICURSOR)
       IPOS(ICURSOR)=ISAVE+8
       CALL SETPOS(ICURSOR,IPOS)
       WRITE(*,'(1A\)') '('
       XPRCNT=(FRAC21/(FRAC21+1))*100.
       CALL PRTRL(XPRCNT)
       WRITE(*,'(1A\)') '%)'
       IPOS(ICURSOR)=ISAVE
       IFIX1=0
       IFIX2=0
       WRITE(*,'(4A,I1,1A\)') ESC,'[18;5f',
     $            'Fix lifetime: ',BOLD,IFIX1,CLEAR
           A(2)=ATAU1
           A(3)=ATAU2
           ISTART=2
    ELSE
       WRITE(*,'(1A\)') CLEAR
       IPOS(14)=31
       IPOS(15)=31
       IPOS(16)=19
       IPOS(17)=19
       IPOS(18)=19
       WRITE(*,'(1A\)') BOLD
           IF (ATAU1.EQ.0.) THEN
42           CONTINUE
           CALL SETPOS(ICURSOR,IPOS)
           CALL RDVAL(ATAU1,IXVAL,IWARN)
           IF ((IWARN.LT.0).OR.(ATAU1.LE.0)) GO TO 42
           ENDIF
       ICURSOR=13
       CALL SETPOS(ICURSOR,IPOS)
       WRITE(*,'(2A\)') ERASE,BOLD
       CALL PRTRL(ATAU1)
       WRITE(*,'(1A\)') CLEAR
       ISAVE=IPOS(ICURSOR)
       IPOS(ICURSOR)=ISAVE+8
       CALL SETPOS(ICURSOR,IPOS)
       WRITE(*,'(1A\)') '('
       XTAU=ATAU1*CTD
       CALL PRTRL(XTAU)
       WRITE(*,'(1A\)') ' psec)'
       IPOS(ICURSOR)=ISAVE
C
       ICURSOR=14
       IF (ATAU2.GT.0.) THEN
          WRITE(*,'(4A\)') ESC,'[14;5f',
     $            'Lifetime 2 estimate (Ch): ',BOLD
           CALL PRTRL(ATAU2)
          WRITE(*,'(1A\)') CLEAR
       ELSE
          WRITE(*,'(6A\)') ESC,'[14;5f',
     $            'Lifetime 2 estimate (Ch): ',REVIDEO,'      ',CLEAR
          WRITE(*,'(1A\)') BOLD
44          CONTINUE
          CALL SETPOS(ICURSOR,IPOS)
          CALL RDVAL(ATAU2,IXVAL,IWARN)
          IF ((IWARN.LT.0).OR.(ATAU2.LE.0)) GO TO 44
          CALL SETPOS(ICURSOR,IPOS)
          WRITE(*,'(2A\)') ERASE,BOLD
          CALL PRTRL(ATAU2)
          WRITE(*,'(1A\)') CLEAR
       ENDIF
       ISAVE=IPOS(ICURSOR)
       IPOS(ICURSOR)=ISAVE+8
       CALL SETPOS(ICURSOR,IPOS)
       WRITE(*,'(1A\)') '('
       XTAU=ATAU2*CTD
       CALL PRTRL(XTAU)
       WRITE(*,'(1A\)') ' psec)'
       IPOS(ICURSOR)=ISAVE
C
       ICURSOR=15
       IF (ATAU3.GT.0.) THEN
          WRITE(*,'(4A\)') ESC,'[15;5f',
     $            'Lifetime 3 estimate (Ch): ',BOLD
           CALL PRTRL(ATAU3)
          WRITE(*,'(1A\)') CLEAR
       ELSE
          WRITE(*,'(6A\)') ESC,'[15;5f',
     $            'Lifetime 3 estimate (Ch): ',REVIDEO,'      ',CLEAR
          WRITE(*,'(1A\)') BOLD
46          CONTINUE
          CALL SETPOS(ICURSOR,IPOS)
          CALL RDVAL(ATAU3,IXVAL,IWARN)
          IF ((IWARN.LT.0).OR.(ATAU3.LE.0)) GO TO 46
          CALL SETPOS(ICURSOR,IPOS)
          WRITE(*,'(2A\)') ERASE,BOLD
          CALL PRTRL(ATAU3)
          WRITE(*,'(1A\)') CLEAR
       ENDIF
       ISAVE=IPOS(ICURSOR)
       IPOS(ICURSOR)=ISAVE+8
       CALL SETPOS(ICURSOR,IPOS)
       WRITE(*,'(1A\)') '('
       XTAU=ATAU3*CTD
       CALL PRTRL(XTAU)
       WRITE(*,'(1A\)') ' psec)'
       IPOS(ICURSOR)=ISAVE
C
       ICURSOR=16
       IF (FRAC21.GT.0.) THEN
          WRITE(*,'(4A,F4.2,2A\)') ESC,'[16;5f',
     $            'Fraction 2/1: ',BOLD,FRAC21,ERASE,CLEAR
       ELSE
          WRITE(*,'(6A\)') ESC,'[16;5f',
     $            'Fraction 2/1: ',REVIDEO,'      ',CLEAR
          WRITE(*,'(1A\)') BOLD
48          CONTINUE
          CALL SETPOS(ICURSOR,IPOS)
          CALL RDVAL(FRAC21,IXVAL,IWARN)
          IF ((IWARN.LT.0).OR.(FRAC21.LE.0)) GO TO 48
          CALL SETPOS(ICURSOR,IPOS)
          WRITE(*,'(1A,F5.2,2A\)') BOLD,FRAC21,ERASE,CLEAR
       ENDIF
```

```
C
      ICURSOR=17
      IF (FRAC31.GT.0.) THEN
         WRITE(*,'(4A,F4.2,2A\)') ESC,'[17;5f',
     $              'Fraction 3/1: ',BOLD,FRAC31,ERASE,CLEAR
      ELSE
         WRITE(*,'(6A\)') ESC,'[17;5f',
     $              'Fraction 3/1: ',REVIDEO,'      ',CLEAR
         WRITE(*,'(1A\)') BOLD
50         CONTINUE
         CALL SETPOS(ICURSOR,IPOS)
         CALL RDVAL(FRAC31,IXVAL,IWARN)
         IF ((IWARN.LT.0).OR.(FRAC31.LE.0)) GO TO 50
         CALL SETPOS(ICURSOR,IPOS)
         WRITE(*,'(1A,F5.2,2A\)') BOLD,FRAC31,ERASE,CLEAR
      ENDIF
C
      ICURSOR=16
      ISAVE=IPOS(ICURSOR)
      IPOS(ICURSOR)=ISAVE+7
      CALL SETPOS(ICURSOR,IPOS)
      WRITE(*,'(1A\)') '('
      XPRCNT=(FRAC21/(FRAC21+FRAC31+1))*100.
      CALL PRTRL(XPRCNT)
      WRITE(*,'(1A\)') '%)'
      IPOS(ICURSOR)=ISAVE
C
      ICURSOR=17
      ISAVE=IPOS(ICURSOR)
      IPOS(ICURSOR)=ISAVE+7
      CALL SETPOS(ICURSOR,IPOS)
      WRITE(*,'(1A\)') '('
      XPRCNT=(FRAC31/(FRAC21+FRAC31+1))*100.
      CALL PRTRL(XPRCNT)
      WRITE(*,'(1A\)') '%)'
      IPOS(ICURSOR)=ISAVE
C
      IFIX1=0
      IFIX2=0
      WRITE(*,'(4A,I1,1A\)') ESC,'[18;5f',
     $              'Fix lifetime: ',BOLD,IFIX1,CLEAR
      WRITE(*,'(1A\)') BOLD
      A(1)=ATAU1
      A(2)=ATAU2
      A(3)=ATAU3
      A(7)=FRAC21
      A(8)=FRAC31
      ISTART=1
      ISTOP=8
   ENDIF
   ICURSOR=12
   CALL SETPOS(ICURSOR,IPOS)
   RETURN
   END
C
C
C
C
```

Appendix B

ASSEMBLER Routines

```
;               Subroutine DISP
;       assembler subroutine to display or erase a pixel at
;       location IXPLT,IYPLT
;
;       FORTRAN call:
;               CALL DISP (IFLAG,IXPLT,IYPLT)
;
;       where
;               IFLAG=0 erase mode, IFLAG=1 display mode
;               IXPLT,IYPLT screen pixel location (INTEGER values only)
;
;       requirements:
;               IFLAG,IXPLT,IYPLT   INTEGER*2 variables
;
;       written by B. Leland 5/6/85
;
PAGE    ,80
FRAME   STRUC
SAVEDS      DW    ?                 ;COPY OF DS REGISTER
SAVEBP      DW    ?                 ;COPY OF BP REGISTER
RETADDR     DD    ?                 ;4 BYTE RETURN ADDRESS
YVAL_ADDR   DD    ?                 ;4 BYTE LOC OF Y VALUE
XVAL_ADDR   DD    ?                 ;4 BYTE LOC OF X VALUE
IFLG_ADDR   DD    ?                 ;4 BYTE LOC OF FLAG
FRAME   ENDS
DGROUP  GROUPDATA
DATA    SEGMENT   PUBLICDATA'
        ASSUME DS:DGROUP
        ROW     DW    ?       ;Y VALUE
        COL     DW    ?       ;X VALUE
DATA    ENDS
;
;
    FSMODE    EQU   0     ;BIOS FUNCTION=SET MODE
    FLOCATE   EQU   2     :BIOS FUNCTION=LOCATE
    FSCROLL   EQU   6     ;BIOS FUNCTION=SCROLL
```

```
        FWRITE      EQU   10      ;BIOS FUNCTION=WRITE CHARACTER
        FPLOT       EQU   12      ;BIOS FUNCTION=PLOT POINT
        WHITE       EQU   7       ;ATTRIBUTE WHITE ON BLACK
        BLACK       EQU   0       ;BLACK ON BLACK BKG-ERASE
        MAXY        EQU   199     ;MAX Y OF SCREEN
;
;
BIOSCALL MACRO FUNCTION
        MOV         AH,FUNCTION
        INT         10H           ;CALL BIOS VIDEO FUNCTION
        ENDM
;
PLOT MACRO XVAL,YVAL ;ASSUMES ATTRIBUTE IN AL,
        MOV         DX,MAXY ; ROW(Y) IN DX, COL(X) IN CX
        SUB         DX,YVAL
        MOV         CX,XVAL
        BIOSCALL FPLOT
        ENDM
;
MYSEG       SEGMENT 'CODE'
            ASSUME      CS:MYSEG,DS:DGROUP,SS:DGROUP
PUBLIC      DISP
DISP        PROC  FAR
        PUSH        BP                  ;SAVE BP REGISTER
        PUSH        DS                  ;SAVE DS REGISTER
        MOV         BP,SP               ;POINT BP AT THE FRAME
        LES         BX,[BP].XVAL_ADDR ;LOAD ADDR OF XVAL
        MOV         AX,WORD PTR ES:[BX]       ;STORE IN COL
        MOV         COL,AX
        LES   BX,[BP].YVAL_ADDR ;LOAD ADDR OF YVAL
        MOV   AX,WORD PTR ES:[BX]
        MOV         ROW,AX      ;STORE IN ROW
        LES   BX,[BP].IFLG_ADDR  ;LOAD ADDR OF YVAL
        MOV   AX,WORD PTR ES:[BX]
        CMP         AL,0
        JNE         IF1
```

```
        MOV         AL,BLACK
        JMP         $$ENDIF
$$IF1:  MOV   AL,WHITE
$$ENDIF:
        PLOT        COL,ROW     ;PLOT POINTS
;
        POP         DS                  ;RESTORE DS
        POP         BP                  ;RESTORE BP
        RET         12
DISP    ENDP
MYSEG   ENDS
        END
```

```
;       Subroutine INKEY
;       assembler subroutine to read a key from the keyboard
;
;       FORTRAN call:
;               CALL INKEY(IFLAG,ISCAN,ANS)
;       where
;               IFLAG=0 means no key available in keyboard buffer
;               IFLAG=1 key is available and was read
;               ISCAN=? scan code for the key that was read (integer)
;               ANS=? character that was read
;
;       Requirements:
;               IFLAG           INTEGER*2 variables
;               ISCAN
;               ANS             CHARACTER*1 variable
;       Notes:
;               scan code can be used to ignore upper or lower case
;               values of the key that was entered since they both have
;               the same scan code
;
;       written by B. Leland 5/6/85
;
PAGE            ,80
FRAME           STRUC
SAVEDS          DW      ?                       ;COPY OF DS REGISTER
SAVEBP          DW      ?                       ;COPY OF BP REGISTER
RETADDR         DD      ?                       ;4 BYTE RETURN ADDRESS
CHAR_ADDR       DD      ?                       ;4 BYTE LOC OF CHAR
ISCN_ADDR       DD      ?                       ;4 BYTE LOC OF ISCAN
IFLG_ADDR       DD      ?                       ;4 BYTE LOC OF IFLAG
FRAME           ENDS
DGROUP          GROUP           DATA
DATA            SEGMENT PUBLIC 'DATA'
                ASSUME          DS:DGROUP
DATA            ENDS
;
```

```
;
        FINQRE      EQU   1       ;KEYBOARD INQUIRY MODE
        FRETRVE     EQU   0       ;RETRIEVE KEYBOARD ENTRY
;
;
MYSEG       SEGMENT 'CODE'
            ASSUME      CS:MYSEG,DS:DGROUP,SS:DGROUP
PUBLIC      INKEY
INKEY PROC  FAR
        PUSH  BP                  ;SAVE BP REGISTER
        PUSH  DS                  ;SAVE DS REGISTER
        MOV   BP,SP               ;POINT BP AT THE FRAME
;
        MOV   AH,FINQRE           ;IS THERE DATA TO READ?
        INT   16H                 ;CALL BIOS KEYBOARD FNCTN
        JNZ   $$IF1               ;CHECK Z FLAG
        MOV   AX,0000H      ;ZERO OUT AX,NO DATA READY
        LES   BX,[BP].IFLG_ADDR  ;LOAD ADDR OF IFLAG
        MOV   WORD PTR ES:[BX],AX ;STORE IN ACCUMULATOR
        JMP   DONE
$$IF1:
        MOV   AH,FRETRVE          ;DATA AVAIL,RETRIEVE
        INT   16H                 ;CALL BIOS KEYBOARD FNCTN
        LES   BX,[BP].CHAR_ADDR ;LOAD ADDR OF CHAR
        MOV   BYTE PTR ES:[BX],AL       ;PUT CHARACTER IN CHAR
        MOV   AL,AH
        MOV   AH,00H
        LES   BX,[BP].ISCN_ADDR  ;LOAD ADDR OF ISCAN
        MOV   WORD PTR ES:[BX],AX       ;PUT SCAN CODE IN ISCAN
        MOV   AX,1                ;LOAD FLAG VALUE INTO AX
        LES   BX,[BP].IFLG_ADDR  ;LOAD ADDR OF IFLAG
        MOV   WORD PTR ES:[BX],AX       ;TOGGLE IFLAG VALUE TO 1
DONE:
        POP   DS                  ;RESTORE DS
        POP   BP                  ;RESTORE BP
        RET   12
```

```
INKEY       ENDP
MYSEG       ENDS
            END
```

```
;       Subroutine DISPPRO
;       assembler subroutine to display or erase a pixel at
;               location IXPLT,IYPLT
;
;       FORTRAN call:
;               CALL DISPPRO (IFLAG,IXPLT,IYPLT)
;
;       where
;               IFLAG=0 erase mode, IFLAG=1 display mode
;               IXPLT,IYPLT screen pixel location (INTEGER values only)
;
;       Requirements:
;               IFLAG           INTEGER*2 variables
;               IXPLT
;               IYPLT
;
;       Written by B. Leland 5/6/85
;       Modified by B. Leland 11/1/86
;               to run under PROFESSIONAL FORTRAN
;
;       Known bugs:
;               Appears to confuse default I/O writes after call, i.e.,
;               WRITE(*,*) after displaying points gives PROFORT
;               error 2023 (unit not connected). Can be remedied by
;               OPEN (UNIT=2, FILE='CON')
;               after points are plotted to write something to screen.
;
;
PAGE            ,80
FRAME           STRUC
IFLG_ADDR       DD      ?                       ;4 BYTE LOC OF FLAG
XVAL_ADDR       DD      ?                       ;4 BYTE LOC OF X VALUE
YVAL_ADDR       DD      ?                       ;4 BYTE LOC OF Y VALUE
FRAME           ENDS
LA@DIS          SEGMENT 'DATA'
                DB      'DISP '
```

```
SP_SAVE     DW    0           ;COPY OF SP
            DD    DISP
            DD    0
            ROW   DW    ?     ;Y VALUE
            COL   DW    ?     ;X VALUE
LA@DIS      ENDS
;
;
      FSMODE      EQU   0     ;BIOS FUNCTION=SET MODE
      FLOCATE     EQU   2     :BIOS FUNCTION=LOCATE
      FSCROLL     EQU   6     ;BIOS FUNCTION=SCROLL
      FWRITE      EQU   10    ;BIOS FUNCTION=WRITE CHARACTER
      FPLOT       EQU   12    ;BIOS FUNCTION=PLOT POINT
      WHITE       EQU   7     ;ATTRIBUTE WHITE ON BLACK
      BLACK       EQU   0     ;BLACK ON BLACK BKG-ERASE
      MAXY        EQU   199   ;MAX Y OF SCREEN
;
;
BIOSCALL MACRO FUNCTION
      MOV   AH,FUNCTION
      INT   10H           ;CALL BIOS VIDEO FUNCTION
      ENDM
;
PLOT MACRO XVAL,YVAL   ;ASSUMES ATTRIBUTE IN AL,
      MOV   DX,MAXY    ;ROW(Y) IN DX, COL(X) IN CX
      SUB   DX,YVAL
      MOV   CX,XVAL
      BIOSCALL FPLOT
      ENDM
;
;
P@DIS SEGMENT 'CODE'
      ASSUME      CS:P@DIS,DS:LA@DIS
      DW    SEG LA@DIS
DISP        PROC  FAR
      PUBLIC      DISP
```

```
        MOV   AX,LA@DIS
        MOV   DS,AX
        MOV   SP_SAVE,SP
;
        LDS   SI,ES:XVAL_ADDR[BX]       ;LOAD ADDR OF XVAL
        MOV   AX,[SI]
        MOV   COL,AX                    ;STORE IN COL
        LDS   SI,ES:YVAL_ADDR[BX]       ;LOAD ADDR OF YVAL
        MOV   AX,[SI]
        MOV   ROW,AX                    ;STORE IN ROW
        LDS   SI,ES:IFLG_ADDR[BX]       ;LOAD ADDR OF IFLAG
        MOV   AX,[SI]               ;MOVE TO ACCUMULATOR
        CMP   AL,0                  ;ERASE OR DRAW MODE?
        JNE   $$IF1
        MOV   AL,BLACK
        JMP   $$ENDIF
$$IF1:  MOV   AL,WHITE
$$ENDIF:
        PLOT  COL,ROW               ;PLOT POINTS
;
        RET
DISP    ENDP
P@DIS   ENDS
        END
```

```
;       Subroutine INKEYPRO
;       assembler subroutine to read a key from the keyboard
;
;       FORTRAN call:
;               CALL INKEYPRO(IFLAG,ISCAN,IANS)
;       where
;               IFLAG=0 means no key available in keyboard buffer
;               IFLAG=1 key is available and was read
;               ISCAN=? scan code for the key that was read (integer)
;               IANS=? CHAR(IANS) is the character that was read
;
;       Requirements:
;               IFLAG INTEGER*2 variables
;               ISCAN
;               IANS
;       Notes:
;               scan code can be used to ignore upper or lower case
;               values of the key that was entered since they both have
;               the same scan code
;
;       Written by B. Leland 5/6/85
;       Modified by B. Leland 11/1/86
;               to run under PROFESSIONAL FORTRAN
;
PAGE        ,80
FRAME       STRUC
IFLG_ADDR   DD    ?                 ;4 BYTE LOC OF IFLAG
ISCN_ADDR   DD    ?                 ;4 BYTE LOC OF ISCAN
IANS_ADDR   DD    ?                 ;4 BYTE LOC OF IANS
FRAME       ENDS
LA@KEY      SEGMENT 'DATA'
            DB    'INKEY '
SP_SAVE     DW    0 ;COPY OF SP
            DD    INKEY
            DD    0
LA@KEY      ENDS
```

```
;
;
;       FINQRE      EQU   1       ;KEYBOARD INQUIRY MODE
;       FRETRVE     EQU   0       ;RETRIEVE KEYBOARD ENTRY
;
;
P@KEY       SEGMENT 'CODE'
        ASSUME      CS:P@KEY,DS:LA@KEY
        DW    SEG LA@KEY
INKEY       PROC  FAR
PUBLIC      INKEY
        MOV   AX,LA@KEY
        MOV   DS,AX
        MOV   SP_SAVE,SP
;
;
        MOV   AH,1                  ;IS THERE DATA TO READ?
        INT   16H                   ;CALL BIOS KEYBOARD FNCTN
        JNZ   $$IF1                 ;CHECK Z FLAG
        MOV   AX,0000H      ;ZERO OUT AX,NO DATA READY
        LDS   SI,ES:IFLG_ADDR[BX]       ;LOAD ADDR OF IFLAG
        MOV   [SI],AX       ;SET FLAG=0
        JMP   DONE ;FINISHED
$$IF1:
        MOV   AH,0                  ;DATA AVAIL,RETRIEVE
        INT   16H                   ;CALL BIOS KEYBOARD FNCTN
        MOV   DX,AX                 ;AL CONTAINS CHAR CODE
                                    ;AH CONTAINS SCAN CODE
        LDS   SI,ES:IANS_ADDR[BX]       ;LOAD ADDR OF IANS
        MOV   AH,00H
        MOV   [SI],AX               ;SAVE AL IN IANS
        MOV   AX,DX                 ;RESTORE RESULTS
        MOV   AL,AH
        MOV   AH,00H
        LDS   SI,ES:ISCN_ADDR[BX]       ;LOAD ADDR OF ISCAN
        MOV   [SI],AX               ;PUT SCAN CODE IN ISCAN
```

```
        MOV   AX,1                  ;LOAD 1 (DATA READ) INTO ACCUM
        LDS   SI,ES:IFLG_ADDR[BX]       ;LOAD ADDR OF IFLAG
        MOV   [SI],AX               ;TOGGLE IFLAG VALUE TO 1
DONE:
        RET
INKEY   ENDP
P@KEY   ENDS
        END
```

```
;       Function STATE
;       from Microsoft FORTRAN manual (version 2.00)
;
;       usage:
;
;       LOGICAL*2 STATE
;
;       IF (STATE(IEND,FILENAME)) THEN ···
;
;       A function designed to mimic the INQUIRE statement
;       of conventional FORTRAN
;       IEND is an integer variable which is a pointer to
;       the last nonblank character in FILENAME
;       If FILENAME exists and can be opened without error,
;       the STATE variable is returned as .TRUE.
;
PAGE        ,80
.RADIX      16
CHMOD       EQU   43
GETATTR     EQU   0
DOSFUNC     EQU   21
FRAME       STRUC
SAVEDS      DW    ?       ;SAVED COPY OF DS REGISTER
SAVEBP      DW    ?       ;SAVED COPY OF BP REGISTER
RETADDR     DD    ?       ;4 BYTE RETURN ADDRESS
FNADDR      DD    ?       ;4 BYTE ADDRESS OF FILENAME
LENADDR     DD    ?       ;4 BYTE ADDRESS OF FILENAME LENGTH
FRAME       ENDS
DATA        SEGMENT PUBLIC 'DATA'
DATA        ENDS
DGROUP      GROUP       DATA
MYSEG       SEGMENT 'CODE'
            ASSUME CS:MYSEG,DS:DGROUP,SS:DGROUP
PUBLIC      STATE
STATE       PROC  FAR
      PUSH        BP    ;SAVE BP REGISTER
```

```
        PUSH    DS      ;SAVE DS REGISTER
        MOV     BP,SP   ;POINT BP AT FRAME
        LES     BX,[BP].LENADDR
                        ;LOAD ADDR OF FILENAME LENGTH
        MOV     AX,WORD PTR ES:[BX]
                        ;LOAD FILENAME LENGTH
;
        MOV     BX,SS   ;SETUP ES REGISTER FOR MOVE
        MOV     ES,BX
        MOV     CX,AX ;SETUP COUNT REGISTER
        INC     AX      ;ALLOW ROOM FOR HEX 00 (END CHARACTER)
        SUB     SP,AX   ;ALLOW ROOM ON STACK FOR FILENAME
        MOV     DI,SP   ;SETUP DI REGISTER FOR MOVE
        MOV     DX,SP   ;DX POINTS TO FILENAME ON STACK
        LDS     SI,[BP].FNADDR
        CLD             ;SET DIRECTION FLAG TO INCREMENT
;
        REP MOVSB       ;MOVE THE STRING
        MOV     BYTE PTR ES:[DI],00H
                                ;MOVE THE BYTE OF ZEROS
                                ;INTO PLACE
        PUSH    AX      ;PUT SIZE OF FILENAME ON THE STACK
;
        MOV     AX,(CHMOD*256D)+GETATTR
                        ;SPECIFY CHMOD FUNCTION AND GET ATTRIB
        INT     DOSFUNC
        JC      ERROR   ;FOUND AN ERROR JUMP
        MOV     AL,1    ;NO ERROR, SET AL=1 (.TRUE.)
        JMP     SHORT NOERROR
ERROR:
        XOR     AL,AL ;ERROR, SET AL=0 (.FALSE.)
NOERROR:
        POP     CX      ;GET SIZE OF FILENAME ON THE STACK
        ADD     SP,CX   ;DEALLOCATE FILENAME ON THE STACK
        POP     DS      ;RESTORE DS
        POP     BP      ;RESTORE BP
```

```
        RET         8       ;RETURN AND CLEAN UP STACK
STATE   ENDP
MYSEG   ENDS
        END
```

```
;       Subroutine AXES
;       assembler subroutine to draw horizontal or vertical (only)
;               lines on the screen. . . . . for interfacing with
;               FORTRAN programs to allow display capabilities.
;               Originally designed for scales, etc.
;
;       Fortran call:
;               CALL AXES (IFLAG,IX1,IY1,IX2,IY2)
;       where
;               IFLAG=0 erase mode, IFLAG=1 draw mode
;
;               Subroutine connects (or erases) IX1,IY2 and IX2,IY2
;               where IX1,IY1,IX2,IY2 are INTEGER values of the desired
;               screen pixel locations.
;
;       requirements:
;               IFLAG,IX1,IY1,IX2,IY2       INTEGER*2 variables
;
;       written by B. Leland 5/6/85
;
PAGE        ,80
FRAME       STRUC
SAVEDS      DW    ?                 ;COPY OF DS REGISTER
SAVEBP      DW    ?                 ;COPY OF BP REGISTER
RETADDR     DD    ?                 ;4 BYTE RETURN ADDRESS
Y2VAL_ADDR  DD    ?                 ;4 BYTE LOC OF Y2 VALUE
X2VAL_ADDR  DD    ?                 ;4 BYTE LOC OF X2 VALUE
Y1VAL_ADDR  DD    ?                 ;4 BYTE LOC OF Y1 VALUE
X1VAL_ADDR  DD    ?                 ;4 BYTE LOC OF X1 VALUE
IFLAG_ADDR  DD    ?                 ;4 BYTE LOC OF IFLAG VALUE
FRAME       ENDS
DGROUP      GROUP       DATA
DATA        SEGMENT PUBLIC 'DATA'
        ASSUME      DS:DGROUP
        X1VAL       DW    ?         ;X1 VALUE
        X2VAL       DW    ?         ;Y1 VALUE
```

```
        Y1VAL       DW    ?           ;X2 VALUE
        Y2VAL       DW    ?           ;Y2 VALUE
DATA        ENDS
;
;
        MAXVAL      EQU   199         ;MAX X OF SCREEN
        FPLOT       EQU   12          ;BIOS FUNCTION=PLOT POINT
        WHITE       EQU   7           ;ATTRIBUTE WHITE ON BLACK
        BLACK       EQU   0           ;ATTRIBUTE BLACK ON BLACK
        PIX_SKP     EQU   2           ;PIXEL SKIP FOR HOR LINES
;
;
;
PLOT    MACRO       XVAL,YVAL   ;ASSUME ATTRIBUTE IN AL,
        MOV   DX,MAXVAL  ; ROW IN DX, COL IN CX
        SUB   DX,YVAL    ;INVERT SO 0,0 IN LOWER LEFT
        MOV   CX,XVAL
        MOV   AH,FPLOT
        INT   10H        ;CALL BIOS VIDEO FUNCTION
        ENDM
;
MYSEG       SEGMENT 'CODE'
        ASSUME      CS:MYSEG,DS:DGROUP,SS:DGROUP
PUBLIC      AXES
AXES    PROC  FAR
        PUSH  BP                ;SAVE BP REGISTER
        PUSH  DS                ;SAVE DS REGISTER
        MOV   BP,SP             ;POINT BP AT THE FRAME
;
        LES   BX,[BP].X1VAL_ADDR        ;LOAD ADDR OF X1
        MOV   AX,WORD PTR ES:[BX]       ;STORE IN X1VAL
        MOV   X1VAL,AX
        LES   BX,[BP].X2VAL_ADDR        ;LOAD ADDR OF X2
        MOV   AX,WORD PTR ES:[BX]       ;STORE IN X2VAL
        MOV   X2VAL,AX
        LES   BX,[BP].Y1VAL_ADDR        ;LOAD ADDR OF Y1
```

```
        MOV   AX,WORD PTR ES:[BX]       ;STORE IN Y1VAL
        MOV   Y1VAL,AX
        LES   BX,[BP].Y2VAL_ADDR        ;LOAD ADDR OF Y2
        MOV   AX,WORD PTR ES:[BX]       ;STORE IN Y2VAL
        MOV   Y2VAL,AX
;
;
        MOV   AX,Y2VAL
        SUB   AX,Y1VAL
        CMP   AX,0
;       $IF   E
        JNE   $$IF5
        MOV   AX,X1VAL                  ;HORIZONTAL LINE
        CMP   AX,X2VAL
;       $IF   G
        JNG   $$IF1
        MOV   BX,X2VAL                  ;PUT XMIN IN X1VAL
        MOV   X1VAL,BX
        MOV   X2VAL,AX
;       $ENDIF
$$IF1:
        LES   BX,[BP].IFLAG_ADDR        ;LOAD ADDR OF IFLAG
        MOV   AX,WORD PTR ES:[BX]
        CMP   AL,0
        JNE   $$IF2
        MOV   AL,BLACK    ;ERASE MODE
        JMP   $$ENDIF2
$$IF2:  MOV   AL,WHITE    ;DRAW MODE
$$ENDIF2:
        MOV   CX,X2VAL
        SUB   CX,X1VAL
        INC   CX          ;LOAD COUNTER W/ X2-X1+1
;       $DO
$$DO6:
        PUSH  CX          ;SAVE COUNTER
        PLOT  X1VAL,Y1VAL
```

```
        ADD   X1VAL,PIX_SKP
        POP   CX            ;RESTORE COUNTER
        DEC   CX            ;BECAUSE WERE SKIPPING 1 PIXEL
        CMP   CX,1          ;TO COMPENSATE FOR ASPECT RATIO
        JGE   $$PASS
        MOV   CX,1          ;MAKE SURE WE DON'T MISS ZERO
$$PASS:
;       $ENDDO LOOP
        LOOP  $$DO6
        JMP   DONE
;       $ENDIF
$$IF5:
        MOV   AX,Y1VAL      ;MUST BE VERTICAL
        CMP   AX,Y2VAL
;       $IF   G
        JNG   $$IF3
        MOV   BX,Y2VAL      ;PUT YMIN IN Y1VAL
        MOV   Y1VAL,BX
        MOV   Y2VAL,AX
;       $ENDIF
$$IF3:
;
        MOV   AX,X2VAL
        SUB   AX,X1VAL
        CMP   AX,0
;       $IF   E
        JNE   $$IF9         ;DOUBLE CHECK ITS VERTICAL
        MOV   CX,Y2VAL
        SUB   CX,Y1VAL
        INC   CX            ;LOAD COUNTER W/ Y2-Y1+1
        LES   BX,[BP].IFLAG_ADDR        ;LOAD ADDR OF IFLAG
        MOV   AX,WORD PTR ES:[BX]
        CMP   AL,0
        JNE   $$IF4
        MOV   AL,BLACK      ;ERASE MODE
        JMP   $$ENDIF4
```

```
$$IF4:  MOV   AL,WHITE     ;DRAW MODE
$$ENDIF4:
;       $DO
$$DO10:
        PUSH  CX           ;SAVE COUNTER
        PLOT  X1VAL,Y1VAL
        INC   Y1VAL
        POP   CX           ;RESTORE COUNTER
;       $ENDDO LOOP
        LOOP  $$DO10
        JMP   DONE
;       $ENDIF
$$IF9:
DONE:
;
        POP   DS                ;RESTORE DS
        POP   BP                ;RESTORE BP
        RET   20
AXES    ENDP
MYSEG   ENDS
        END
```